Western Graduate&PostdoctoralStudies

Western University
Scholarship@Western

Electronic Thesis and Dissertation Repository

12-3-2018 1:10 PM

The Role of TBX3 In Early Breast Cancer Progression

Milica Krstic
The University of Western Ontario

Supervisor
Tuck, Alan B.
The University of Western Ontario Joint Supervisor
Chambers, Ann F.
The University of Western Ontario

Graduate Program in Pathology and Laboratory Medicine
A thesis submitted in partial fulfillment of the requirements for the degree in Doctor of Philosophy
© Milica Krstic 2018

Follow this and additional works at: https://ir.lib.uwo.ca/etd

 Part of the Neoplasms Commons, Pathology Commons, and the Translational Medical Research Commons

Recommended Citation

Krstic, Milica, "The Role of TBX3 In Early Breast Cancer Progression" (2018). *Electronic Thesis and Dissertation Repository*. 5971.
https://ir.lib.uwo.ca/etd/5971

This Dissertation/Thesis is brought to you for free and open access by Scholarship@Western. It has been accepted for inclusion in Electronic Thesis and Dissertation Repository by an authorized administrator of Scholarship@Western. For more information, please contact wlswadmin@uwo.ca.

Abstract

TBX3 is a transcriptional regulator involved in embryonic development and in tumorigenesis of several cancer types. There are two isoforms of TBX3 (TBX3iso1 and TBX3iso2) with different DNA binding domains. The large-scale functional roles of TBX3iso1 and TBX3iso2 were characterized in a breast cancer context. Both TBX3 isoforms induced invasiveness and an epithelial-to-mesenchymal (EMT) phenotype. Coupling data from genome-wide ChIP-array and RNA-Seq studies provided a novel list of genes regulated by each isoform. Both TBX3 isoforms regulate expression of several EMT-related genes, including SLUG and TWIST1. Importantly, TBX3 is a direct regulator of SLUG, and SLUG expression is required for TBX3-induced migration and invasion.

Assessing TBX3 expression in early stage breast cancers by immunohistochemistry (IHC) revealed high expression in low-grade lesions. Within a second non-high-grade cohort, there was an association between TBX3 expression in the pre-invasive ductal carcinoma *in situ* (DCIS) and size of the invasive focus. Additionally, there was a positive correlation between TBX3/SLUG, and TBX3/TWIST1 expression by IHC in the invasive carcinoma. Pathway analysis of transcriptomics data revealed altered expression of several proteases and their inhibitors, consistent with the ability of tumor cells to degrade basement membrane. These findings strongly suggest the involvement of TBX3 in the promotion of invasiveness and progression of early stage pre-invasive DCIS to invasive carcinoma through the low-grade molecular pathway.

Interestingly, only TBX3iso1 overexpressing cells exhibited increased tumorigenic potential in mouse xenograft experiments. Transcriptomics data and functional studies revealed that TBX3iso1 overexpression promotes angiogenesis and secretion of cancer-associated cytokines (including osteopontin) which is able to induce tubule formation by endothelial cells *in vitro*. Tumorigenic TBX3iso1 overexpressing cells also had elevated hyaluronan synthase 2 (HAS2) levels and high levels of hyaluronan retention. These factors may contribute to the survival of cells and promote angiogenesis, allowing the formation of primary tumors *in vivo*.

In conclusion, I have found evidence for a role of TBX3iso1 and TBX3iso2 in direct modulation of EMT and invasiveness, and a role for TBX3iso1 in inducing angiogenesis. Together these, along with previous work showing anti-senescence and pro-proliferative activities of TBX3, suggest multiple potential activities for promotion of malignancy of breast cancer.

Keywords

Breast cancer

Breast cancer progression

Transcriptional regulation

Alternative splicing

DCIS (ductal carcinoma in situ)

IDC (invasive ductal carcinoma)

EMT (epithelial-mesenchymal transition)

Angiogenesis

T-box 3 (TBX3)

SLUG (SNAI2)

Osteopontin (OPN)

Hyaluronan synthase 2 (HAS2)

Co-Authorship Statement

Chapter 2 in this dissertation has been published (Krstic et al. 2016, BMC Cancer). The experiments were conceived and designed by myself and a previous graduate student within the laboratory, Connor MacMillan, with input from my supervisors Dr. Alan Tuck and Dr. Ann Chambers. Connor and I performed the experiments, acquired, and interpreted the data. Specifically, Connor MacMillan, Hon Leong, Allen Clifford, and Lesley Souter were involved in generating the TBX3 expression vectors used for TBX3 overexpression studies, along with generation of lentiviral particles for TBX3 knockdown prior to me joining the lab. I performed the 3D Matrigel cultures, immunofluorescence, migration and invasion assays, and qRT-PCR experiments (including the arrays). David Dales and Carl Postenka conducted the immunohistochemistry of the 21T cell pellets. The manuscript was written by myself, Connor MacMillan, and Alan Tuck.

Chapter 3 in this dissertation is under review. The experiments were conceived and designed by myself, with input from my supervisors Dr. Alan Tuck and Dr. Ann Chambers. I performed the experiments, acquired, and interpreted the data with the help of my supervisors. Joseph Andrews conducted sequencing alignments for RNA-Seq and ChIP-array data, along with helping to generate gene lists for downstream analysis. Bart Kolendowski helped with bioinformatics analyses, including assessment of conserved T-box binding sites in the SLUG (*SNAI2*) gene, integration and analysis of ENCODE data, and integration of grade information for the TCGA BRCA cohort. Haider Hassan conducted a portion of the western blots in SLUG knockdown cell lines. Connor MacMillan aided in development of methodology for *in vivo* invadopodia formation assays. Karla Williams conducted *in vitro* invadopodia formation assays. Hon Leong provided us with CAM models. The manuscript was written by myself, with support from Alan Tuck, Bart Kolendowski, and Joseph Torchia.

Chapter 4 in this dissertation will be submitted for publication. The experiments were conceived and designed by myself, with input from my supervisors Dr. Alan Tuck and Dr. Ann Chambers. I performed the experiments, acquired, and interpreted the data with the help of my supervisors. Nicole Hague conducted the mammary fat pad injections and mouse dissections for the xenograft experiment. Carl Postenka processed the mouse tissues and conducted immunohistochemical staining for OPN and human mitochondria. Pieter Anborgh conducted the OPN ELISA. Haider Hassan generated the heat map and PCA plot of differentially expressed genes between TBX3 isoforms from RNA-Seq data. Bart Kolendowski aided in bioinformatics analyses of TBX3 isoform expression in TCGA and GTEx datasets. The manuscript was written by myself, with support from Alan Tuck.

Dedication

Ово је за моју породицу.

Не бих могла да завршим сав овај напоран рад без моје мајке и оца.

Волим вас.

Acknowledgements

I have learned so much over the past five years of my PhD journey, and have grown so much personally and scientifically. I know all of the skills that I have gained will be instrumental in my path forward, and my supervisors, Dr. Alan Tuck and Dr. Ann Chambers deserve a very big thank you for their support and encouragement in getting me here. Thank you for the hours spent proof-reading my applications and papers, the numerous one-on-one meetings, and providing valuable advice when I had difficulties. Thank you for always being available to help and advise me scientifically, but also giving me the freedom to explore on my own.

To my advisory committee members: Within the first few weeks of starting grad school, I asked Dr. Joe Mymryk to serve as one of my advisors. He has been extremely helpful right from the beginning, and was always available to speak with me whenever I needed help on any topic. To Dr. David Rodenhiser, a newer advisor – thank you for coming to my rescue towards the end of my PhD, and being there to oversee my completion. I'm thankful for both of your kind gestures, and especially for telling me to relax when I put together a paper with nearly 100 figure panels. I really needed that.

Thank you to the Department of Pathology, which I am very happy I chose to do my PhD work in. Every single staff and faculty member that I have come in contact with has been extremely knowledgeable and caring – particularly Tracey Koning, Dr. Zia Khan, and Dr. Chandan Chakraborty. You guys are all wonderful and your work does not go unnoticed.

My lab members, including David Dales, Carl Postenka, Joe Andrews, Pieter Anborgh, have been great as well. I'm glad that I made those outings with the "old man's club", where I could listen to Carl talk about more ridiculous things and always have a few laughs.

I would like to thank Dr. Joe Torchia for his openness to me transitioning into their lab during the end of my PhD work, along with his kindness and willingness to help me with my writing and publishing. I would also like to thank the members of the Torchia lab, which I am happy to call my second home. Going out for coffee with Majdina Isovic, Haider Hassan and Bart Kolendowski was one of my favourite past-times between experiments and writing. They have all been extremely helpful towards me and I am happy to call them my friends.

The friends that I've met throughout grad school have become some of my closest friends. In particular I would like to acknowledge Cecilia Kwok, Kate Cousteils and Amber Harnett. Thank you to my best friend since grade school, Tijana Lozo, who has been there for me from day one.

Lastly, I would like to give the biggest thank you of all to my family for their continuous love and support. I know both my parents, Olivera and Sretko Krstic, are very excited and happy for all of my studies to be coming to an end. All of your visits and phone calls have been appreciated. The same goes to my lovely sister, Marija Krstic.

Table of Contents

List of Abbreviations

ADH	atypical ductal hyperplasia
AKT	protein kinase B
ALH	atypical lobular hyperplasia
ANOVA	analysis of variance
AR	androgen receptor
B-RAF	B-Raf proto-oncogene
BCL2	B-cell lymphoma 2
BRCA1	breast cancer 1, early onset
BRCA2	breast cancer 2, early onset
BSA	bovine serum albumin
CAM	chorioallantoic membrane
CCC	columnar cell change
CCH	columnar cell hyperplasia
CCL	columnar cell lesion
CCLE	Cancer Cell Line Encyclopedia (database)
CCND1	cyclin D1
CCNE1	cyclin E1
CD	cluster of differentiation
CD31	CD31 antigen, platelet and endothelial cell adhesion molecule
CD44	CD44 antigen, cell-surface glycoprotein
CDC25A	cell division cycle 25 homolog A
CDH1	E-cadherin
CDH2	N-cadherin
CDK	cyclin dependent kinase
CDKN2A	cyclin-dependent kinase inhibitor 2A (encodes $p14^{ARF}$ and $p16^{INK4A}$)
CGH	comparative genomic hybridization
ChIA-PET	chromatin interaction analysis by paired-end tag sequencing
ChIP	chromatin immunoprecipitation
CK	cytokeratin
CMFDA	5-chloromethylfluorescein diacetate (green fluorescent dye)
COX	cyclooxygenase
CSC	cancer stem cell
CST6	cystatin E/M
CTCF	CCCTC-binding factor
dbEMT	EMT database
DCIS	ductal carcinoma *in situ*
DHS	DNase I hypersensitivity
DNMT	DNA methyltransferase
DOC	deoxycholic acid
dTTP	deoxythymidine triphosphate
dUTP	deoxyuridine triphosphate
E2F	E2F transcription factor
ECL	enhanced chemiluminescence
ECM	extracellular matrix
EDTA	ethylenediaminetetraacetic acid
EGFR	epidermal growth factor receptor
EGTA	ethylene glycol tetraacetic acid
ELISA	enzyme-linked immunosorbent assay
EMSA	electromobility shift assay
EMT	epithelial-mesenchymal transition

ENCODE	Encyclopedia of DNA Elements (database)
ER	estrogen receptor
EV	empty vector
FBS	fetal bovine serum
FDR	false discovery rate
FEA	flat epithelial atypia
FGF	fibroblast growth factor
FGFR	fibroblast growth factor receptor
FISH	fluorescence *in situ* hybridization
FN1	fibronectin 1
FOXA1	forkhead box protein A1
G418	Geneticin
GAPDH	glyceraldehyde-3-phosphate dehydrogenase
GATA	GATA binding protein
GEO	Gene Expression Omnibus (database)
GJA1	gap junction protein alpha 1 (connexin 43)
GO	gene ontology
GRO-Seq	global run-on sequencing
GST	glutathione S-transferase
GTEx	Genotype Tissue Expression (database)
H&E	hematoxylin and eosin histological stains
H2A	histone 2A
HA	hyaluronan
HAS2	hyaluronan synthase 2
HAse	hyaluronidase
HCC	hepatocellular carcinoma
HDAC	histone deacetylase
HDMEC	human dermal microvascular endothelial cells
HEPES	4-(2-hydroxyethyl)-1-piperazineethanesulfonic acid
HER2	human epidermal growth factor receptor 2
HG	high grade
HIF1α	hypoxia-inducible factor 1 alpha
HNSCC	head and neck squamous cell carcinoma
HPA	Human Protein Atlas (database)
HPF	high power field
HRAS	H-Ras proto-oncogene
hrOPN	human recombinant osteopontin
HRP	horseradish peroxidase
ICGC	International Cancer Genome Consortium (database)
IDC	invasive ductal carcinoma
IG	intermediate grade
IgG	immunoglobulin G
IGV	Interactive Gene Viewer (software)
IHC	immunohistochemistry
IL1RN	interleukin 1 receptor antagonist
IL6	Interleukin 6
ILC	invasive lobular carcinoma
IMC	invasive mammary carcinoma
IP	immunoprecipitation
IPA	Ingenuity Pathway Analysis (software)
ITGA	integrin alpha subunit
ITGB	integrin beta subunit

IV	intravenous
JDP2	jun dimerization protein 2
JUN	jun proto-oncogene, AP-1 transcription factor subunit
KRT8	keratin 8, type II
LCIS	lobular carcinoma *in situ*
LEF1	lymphoid enhancer binding factor 1
LG	low grade
LN	lymph node
LOH	loss of heterozygosity
LUC	luciferase
MALDI-TOF-MS	matrix assisted laser desorption/ionization time of flight mass spectrometry
MAPK	mitogen-activated protein kinase
MDM2	mouse double minute 2 proto-oncogene
MET	mesenchymal-epithelial transition
MKI67	marker of proliferation Ki67
MLH1	MutL homolog 1, colon cancer, nonpolyposis type 2
MMP	matrix metallopeptidase
MMTV	mouse mammary tumor virus
MYC	MYC proto-oncogene, BHLH transcription factor
Nanog	homeobox transcription factor Nanog
NBF	neutral buffered formalin
Nkx2-5	NK2 homeobox 5
NF_KB	nuclear factor kappa light chain enhancer of activated B cells
NLS	nuclear localization sequence
NMD	nonsense-mediated mRNA decay
NOD/SCID	non-obese diabetic severe combined immunodeficiency
Nppa	natriuretic peptide A
NR3C1	nuclear receptor subfamily 3, group C, member 1 glucocorticoid receptor
NSCLC	non-small-cell lung cancer
OPN	osteopontin
$p14^{ARF}$	p14 alternative reading frame tumor suppressor
$p16^{INK4A}$	p16 inhibitor of cyclin-dependent kinase 4 tumor suppressor
$p21^{CIP1}$	p21 cyclin dependent kinase inhibitor protein 1
p53	p53 tumor suppressor protein
p63	p63 tumor protein
PBS	phosphate-buffered saline
PCA	principal component analysis
PDB	Protein Data Bank (database)
PDGF	platelet derived growth factor
PGS	Partek Genomic Suites (software)
PI3K	phosphoinositide 3-kinase
PIK3CA	phosphatidylinositol-3-kinase catalytic subunit alpha
PKC	protein kinase C
PLAU	plasminogen activator, urokinase (uPa)
PLCε	phospholipase C epsilon
Pol II	RNA polymerase II
POLR2A	RNA polymerase II A
PR	progesterone receptor
PRDM2	PR domain zinc finger protein 2
PTEN	phosphatase and tensin homolog
PVDF	polyvinylidene difluoride
qRT-PCR	quantitative reverse transcriptase polymerase chain reaction

Ras	Ras proto-oncogene, GTPase
Rb	retinoblastoma
RGD	arginine-glycine-aspartate integrin binding domain
RHAMM	receptor for hyaluronan-mediated motility
RIPA	radioimmunoprecipitation assay buffer
RPKM	reads per kilobase of transcript per million mapped reads
RPLP0	ribosomal protein lateral stalk subunit P0
RTK	receptor tyrosine kinase
SBR	Scarff-Bloom-Richardson
SCC	squamous cell carcinoma
SCR	scramble (control)
SDS-PAGE	sodium dodecyl sulfate polyacrylamide gel electrophoresis
SERPINE1	serpin peptidase inhibitor, clade E, member 1
SFN	stratifin
shRNA	short hairpin RNA
SLUG	Snail family transcriptional repressor 2
SMAD	suppressor of mothers against decapentaplegic
SNAI1	snail family transcriptional repressor 1 (encodes SNAIL protein)
SNAI2	snail family transcriptional repressor 2 (encodes SLUG protein)
SPP1	secreted phosphoprotein 1 (encodes OPN protein)
SRC	Src proto-oncogene
TBE	T-box element
TBS	tris-buffered saline
TBX	T-box
TBX3	T-box 3, with two isoforms: TBX3iso1 and TBX3iso2
TCF	T-cell specific transcription factor
TCGA	The Cancer Genome Atlas (database)
TDLU	terminal duct lobular units
TET2	ten-eleven translocase methylcytosine dioxygenase 2
TGF-ß	transforming growth factor beta
TNM	staging system; T = tumor size, N = positive lymph nodes, M = metastasis
TSS	transcription start site
TWIST1	twist family BHLH transcription factor 1
UMS	ulnar-mammary syndrome
UTR	untranslated region
VEGF	vascular endothelial growth factor
VEGFR	vascular endothelial growth factor receptor
VIM	vimentin
Wnt	wingless/integrated
ZEB1/2	zinc finger E-box binding homeobox

List of Tables

List of Figures

CHAPTER 1 – Introduction

CHAPTER 2 – Examination of functional and phenotypic changes associated with modulation of TBX3 levels at various stages of breast cancer progression

CHAPTER 3 – TBX3 promotes progression of pre-invasive breast cancer cells by inducing EMT and directly up-regulating SLUG

CHAPTER 4 – Isoform-specific promotion of breast cancer tumorigenicity by TBX3 involves induction of angiogenesis

CHAPTER 5 – General Discussion

List of Appendices

Chapter 1

Introduction

1.1 **Breast Cancer**

Recent statistics from the Canadian Cancer Society has revealed that 1 in 2 Canadians will develop cancer in their lifetime, and 1 in 4 Canadians will die of cancer (Canadian Cancer Society, 2017). Leading the list of cancer prevalence for Canadian women is breast cancer, with 1 in 8 women expected to develop breast cancer in their lifetime (Canadian Cancer Society, 2017). This accounted for 10,100 diagnoses of breast cancer in 2017, of which 1,900 succumbed to the disease (Canadian Cancer Society, 2017). While breast cancer incidence rates rose in the 1990s (likely due to increased opportunistic mammography screenings), mortality rates have been declining at a rate of approximately 2.3% per year between 1992 and 2012 (Canadian Cancer Society, 2017). This decline is likely due to a combination of screening mammograms and more effective adjuvant systemic therapies (Canadian Cancer Society, 2017). Similar reductions in mortality rates have been observed in the United States, United Kingdom, and Australia (Bray et al., 2004).

The current public health strategy for breast cancer is one of early detection; at this early stage, treatment generally has a high success rate compared to metastatic diagnosis. In addition to surgical management, treatment for patients with early-stage breast cancer can include systemic therapy, such as chemotherapy (i.e. taxanes, anthracyclines) and/or hormone therapy (i.e. tamoxifen, aromatase inhibitors), which are tailored to the characteristics of the tumour (Esteva and Hortobagyi, 2004). Once the cancer has spread to distant organs, however, survival is greatly reduced.

Molecular profiling of breast cancers has revealed the presence of distinct breast cancer subtypes with different clinical outcomes, including luminal A, luminal B, basal-like and human epidermal growth factor receptor 2 (HER2)-enriched (Perou et al., 2000). In general, age-standardized survival rates for breast cancers are 97% (1-year), 91% (3-year), 86% (5-year) and 82% (10-year) for the specified number of years post-diagnosis (Canadian Cancer Society, 2017), although basal-like and HER2-enriched breast cancers are associated with lower survival rates (Sørlie et al., 2001). Additional prognostic factors that may help predict patient outcome include tumor size, lymph node status, and nuclear and histologic grade of the tumor (Esteva and Hortobagyi, 2004).

1.1.1 **Histopathology of breast cancer progression**

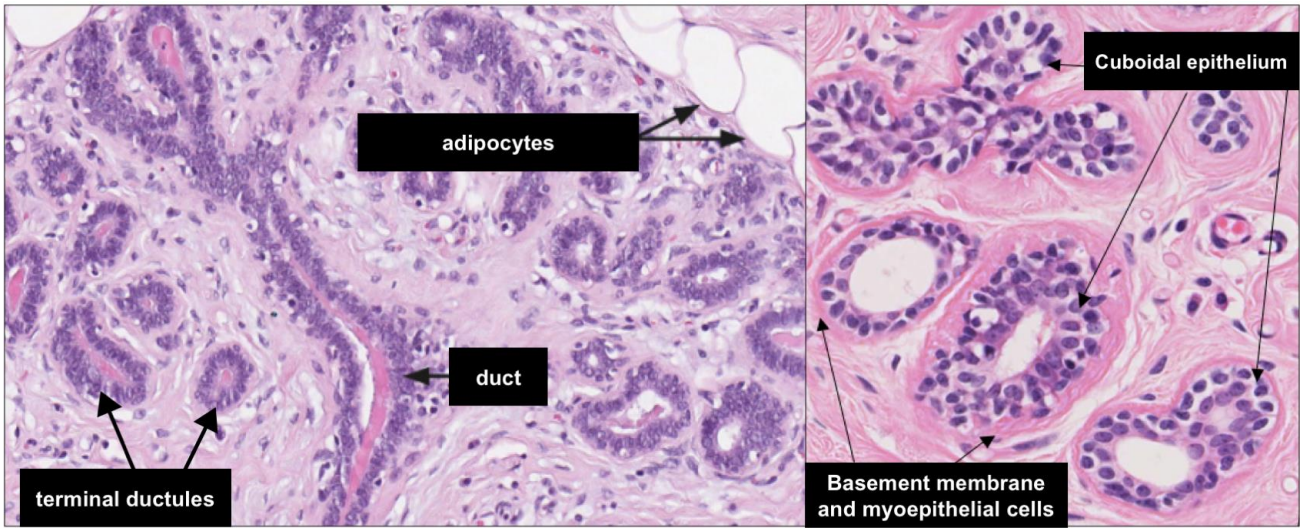

Figure 1.1.1 – Histology of normal breast epithelium.
Obtained from breast histology slides in The Human Protein Atlas, available at www.proteinatlas.org/learn/dictionary/normal/breast

Normal breast histology (depicted in **Figure 1.1.1**) must be appreciated in order to diagnose pathological conditions. Histologically, the breast is made up of several ductal-lobular structures. The lactiferous duct is located beneath the nipple, and branches out into several progressively smaller ductal structures, eventually terminating at the terminal ductules and lobules (Mills, 2007). The epithelium within these ductal-lobular structures consists of two distinct cell layers. The inner (luminal) layer is composed of cuboidal to columnar epithelial cells, with an outer (basal) layer composed of flattened myoepithelial cells (Mills, 2007). The terminal ducts and their corresponding lobules are collectively referred to as the terminal duct lobular unit (TDLU), and represents the structural and functional unit of the breast (Mills, 2007). A layer of type IV collagen and laminin surrounds the ductal-lobular structures, separating them from the surrounding stroma (Mills, 2007). The stroma immediately adjacent to the mammary glands is composed of loose fibrovascular tissue, with dense interlobular stroma composed of collagen, fibroblasts, and adipose tissue surrounding the aforementioned structures (Mills, 2007).

Most breast pathologies, including atypical ductal hyperplasia (ADH), ductal carcinoma *in situ* (DCIS), and invasive breast carcinoma, originate in the TDLUs (Mills, 2007).

The two most common histological subtypes of invasive breast cancer include infiltrating ductal carcinoma (IDC) and infiltrating lobular carcinoma (ILC). While both arise from the TDLUs, they present quite different histologically (Wellings and Jensen, 1973, Wellings et al., 1975). A majority of breast cancers have the morphology of ductal epithelial cells (DCIS, IDC), representing approximately 80% of diagnoses (Kumar et al., 2013). Lobular morphologies, including atypical lobular hyperplasia (ALH), lobular carcinoma *in situ* (LCIS), and invasive lobular carcinoma (ILC), are less common than their ductal counterparts (Kumar et al., 2013). The more common pathways, related to IDC, are discussed below.

The IDC breast cancer progression model is often simplified into a series of phenotypic histological stages, beginning with benign epithelial cells and sometimes transitioning to columnar cell lesions including flat epithelial atypia (FEA), atypical ductal hyperplasia (ADH), ductal carcinoma *in situ* (DCIS), and ultimately invasive and metastatic breast carcinoma (Burstein et al., 2004, Bombonati and Sgroi, 2011). FEA, ADH and DCIS are considered to be non-obligate precursors for the development of invasive breast cancer, meaning that not all cases exhibiting the aforementioned precursor lesions will progress to invasive carcinoma (Bombonati and Sgroi, 2011). Epidemiological, histological, immunohistochemical, loss of heterozygosity (LOH), comparative genomic hybridization (CGH), and later high-throughput mutational studies have shed light on the intricacies of this process, and highlighted the presence of divergent low-grade and high-grade pathways (Thorat et al., 2007, Formenti et al., 2011, Bombonati and Sgroi, 2011, Sagara et al., 2015).

Low-grade (LG) breast lesions usually contain near-diploid chromosomal content, with frequent loss of 16q and gain of 1q (Bombonati and Sgroi, 2011). High-grade (HG) breast lesions are typically aneuploid and associated with a collection of more complex mutational alterations including recurrent loss of 8p, 11q, 13q, 1p and 18q, and recurrent gain of 8q, 17q, 20q and 16p (Buerger et al., 1999, Roylance et al., 1999, Bombonati and Sgroi, 2011). Intermediate grade (IG) breast lesions possess a combination of LG and HG genetic alterations (Buerger et al., 2001). When loss of 16q is observed in HG lesions, the remaining underlying genetic alterations are distinct; while LG lesions demonstrate physical loss of 16q, HG lesions are missing small regions of 16q and undergo mitotic recombination, leading to shuffling of these genetic components (Cleton-Jansen et al., 2004, Abdel-Fatah et al., 2008).

These findings suggest that high-grade breast cancers (basal-like and HER2-enriched) do not arise from low-grade breast cancers (Bombonati and Sgroi, 2011).

Immunohistochemical studies of FEA, ADH and LG DCIS has revealed high expression levels of estrogen receptor (ER) and progesterone receptor (PR), along with lack of HER2 expression (Buerger et al., 2001). Additionally, these precursor lesions frequently express high levels of the proliferation marker Ki67, luminal cytokeratins CK8/18/19, B-cell lymphoma 2 (Bcl2), cyclin D1, and are negative for basal cytokeratins CK5/6 (Schnitt, 2003, Abdel-Fatah et al., 2008, Ahmad, 2013). Genetic analysis of FEA, ADH and LG DCIS has revealed comparable loss of 16q, which is an early hallmark genetic change in LG lesions; the degree of genomic instability, however, increases with further progression (O'Connell et al., 1998, Moinfar et al., 2000, Simpson et al., 2005, Larson et al., 2006, Gao et al., 2009). Genes which may function as tumor suppressors that are subsequently lost with 16q deletions have been assessed, and include E-cadherin (*CDH1*) and CCCTC-binding factor (*CTCF*), with reduced expression reported in LG lesions, as assayed by PCR and immunohistochemistry (Bürger et al., 2013). The detailed breast cancer progression pathways of the LG and HG molecular pathways is depicted in **Figure 1.1.2**.

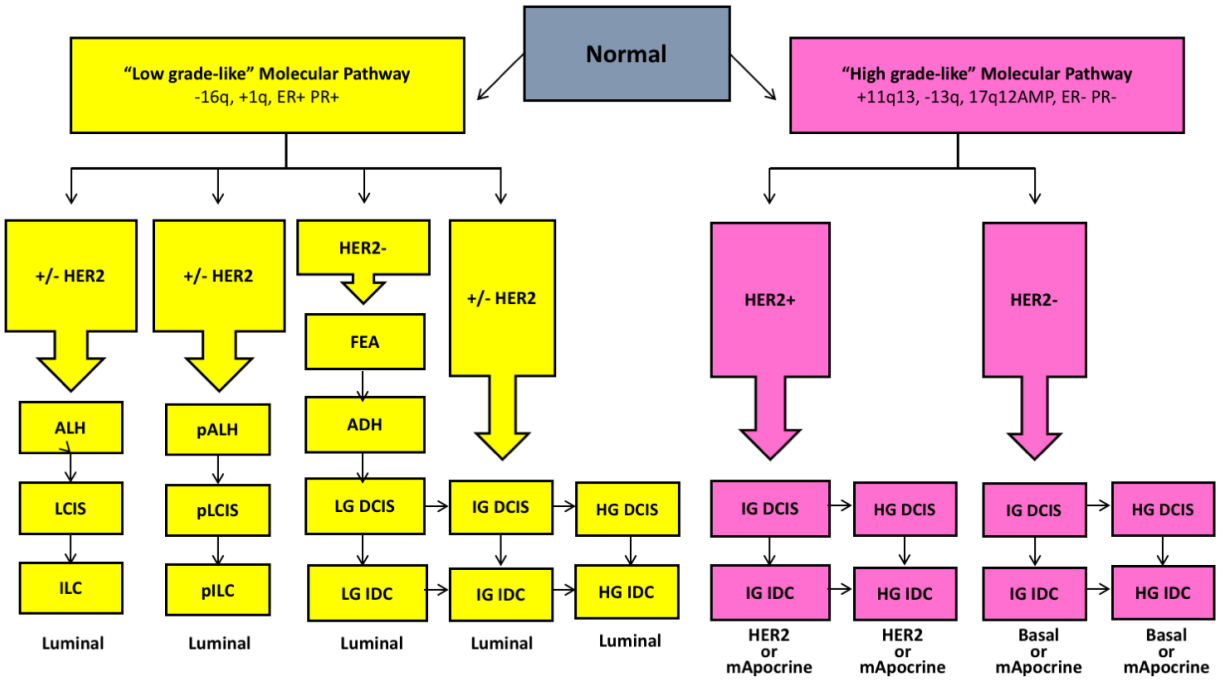

Figure 1.1.2 – Detailed breast cancer progression pathway of LG and HG breast cancers. Adapted from Bombonati & Sgroi, 2011.

1.1.2 **Columnar cell lesions (CCLs)**

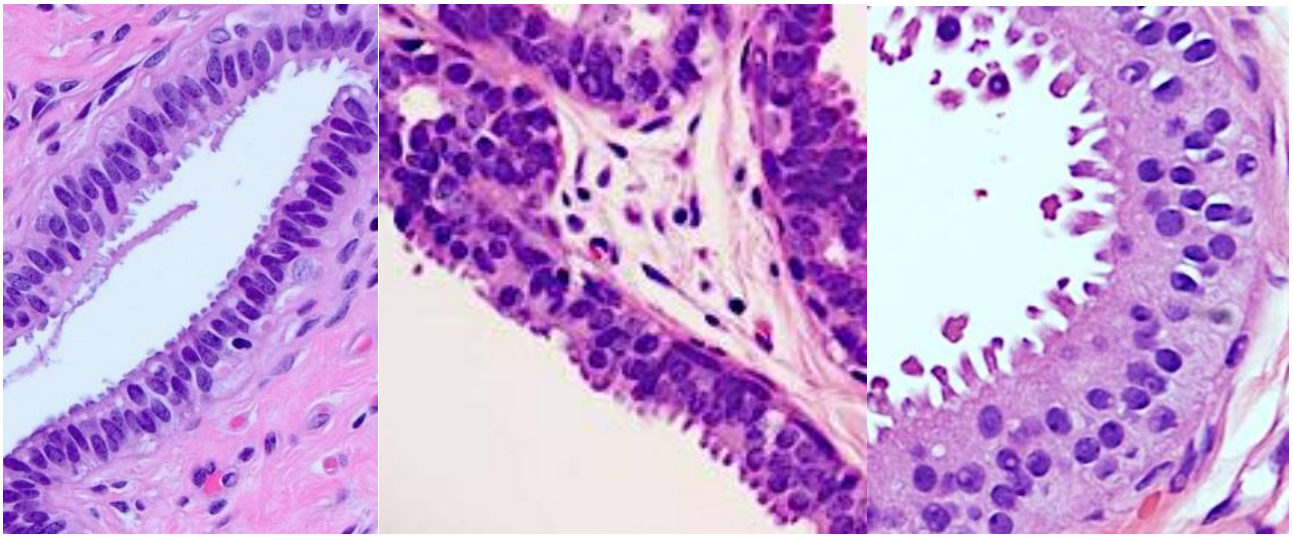

Figure 1.1.3 – Columnar cell lesions (CCLs) of the breast.
Columnar cell change (CCC), columnar cell hyperplasia (CCH), and flat epithelial atypia (FEA) of the breast (left to right).

Columnar cell lesions (CCLs) are among the most common abnormalities observed in breast biopsies (Turashvili et al., 2008). CCLs are generally divided into columnar cell change (CCC) and columnar cell hyperplasia (CCH), consisting of one or several layers of pseudostratified ductal epithelial cells, respectively, which have taken on a columnar phenotype (depicted in **Figure 1.1.3**) (Dabbs et al., 2006). CCLs present with frequent exaggerated apical blebs or snouts, often resulting in intraluminal secretions that can calcify, and are thus often detected as abnormalities on mammographic screening (Lerwill, 2008). CCC and CCH with the aforementioned histological patterns can be further subdivided, depending on the presence or absence of atypia (Turashvili et al., 2008, Go et al., 2012).

Genetic analysis of CCLs without atypia has revealed infrequent mutations relative to the background of normal ductal epithelial cells (Dabbs et al., 2006), although more recently, phosphatidylinositol-3-kinase catalytic subunit alpha (*PIK3CA*) mutations have been documented in CCLs with or without atypia (Troxell et al., 2012). The atypical CCL variant FEA is often considered to be the earliest neoplastic lesion within the breast (Dabbs et al., 2006, Turashvili et al., 2008). FEA lesions show slightly enlarged columnar epithelial cells, frequently consisting of several layers, and low-grade cytologic atypia (Turashvili et al.,

2008). Interestingly, CCLs with HG atypia tend to progress to comedo DCIS (associated with necrosis and higher rates of invasive recurrence), whereas FEA with LG cytologic atypia is thought to progress to LG DCIS (Azzopardi et al., 1979), further providing evidence for the divergent LG and HG progression pathways. Additionally, CCLs were reported to coexist in 76% of LG and 10% of HG breast cancers (Abdel-Fatah et al., 2008). Coexisting CCLs, ADH and DCIS lesions often exhibit near identical cytological morphologies, with the differences typically being size and architecture-related (Go et al., 2012).

Little is known regarding the clinical significance of the presence of CCLs and FEA in a biopsy. The risk of invasive recurrence for patients with FEA is unclear – some studies suggest that the associated risk is slightly increased relative to that of the general population, up to a risk similar to ADH (4-5 fold) (Schnitt, 2003, Kunju and Kleer, 2007, Martel et al., 2007, Lerwill, 2008, Ahmad, 2013). Longitudinal studies examining rates of invasive recurrence revealed that 7.4% of patients with CCLs without atypia, and 18.3% of patients with CCLs with atypia (diagnosed as FEA) developed invasive breast cancer over a period of 5 years (Guerra-Wallace et al., 2004). Upon analysis of 1,000 FEA lesions, it was reported that 7% and 26% of cases had coexisting invasive carcinoma and lobular neoplasia, respectively (Bratthauer and Tavassoli, 2004). The presence of FEA in a biopsy should therefore prompt for potential identification of coexisting precursor lesions and invasive carcinoma (Lerwill, 2008). Although these studies demonstrate that the risk of progression to invasive carcinoma after FEA diagnosis by biopsy is higher than the general population, the relative risk of invasive recurrence is quite low. Clinical management of patients with FEA on biopsy usually consists of close follow-up with repeat mammograms to detect cases of occult carcinoma within the vicinity that were missed by biopsy (Turashvili et al., 2008), or surgical excision if there is any residual abnormality (i.e. indeterminate calcifications) (Calhoun et al., 2015). Larger studies with extended follow-up times are required for critical evaluation of long-term risk of progression to invasive cancer for these patients, as well as time course for progression (Lerwill, 2008). A more thorough understanding of clinicopathologic characteristics would allow for optimal management of patients with CCL lesions, including the FEA variant.

1.1.3 **Atypical ductal hyperplasia (ADH)**

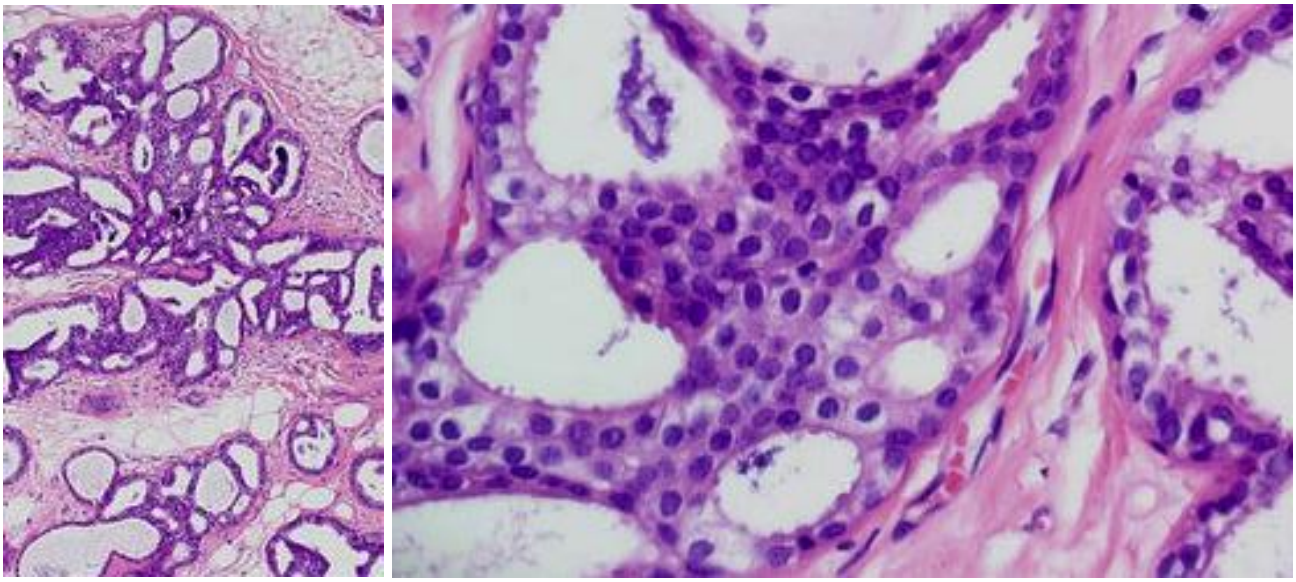

Figure 1.1.4 – Atypical ductal hyperplasia (ADH) of the breast.

Normal breast ductal epithelial cells are lined by two layers of cells consisting of a luminal and myoepithelial cell layer (Kumar et al., 2013). The presence of hyperplasia signifies an excess of two layers of epithelial cells, and can range from mild to florid ductal epithelial hyperplasia without atypia, to atypical ductal hyperplasia (ADH) (Kumar et al., 2013). The pattern observed in ADH is consistent with the presence of two different cell populations: a low-grade neoplastic cell population and a benign ductal epithelial cell population, observed within the same duct cross-section (Kumar et al., 2013). The non-neoplastic cell population contains cells showing random placement and streaming patterns, with nuclei of varying shape and size (Pinder and Ellis, 2003). Conversely, the atypical (LG neoplastic) cells contain enlarged, hyperchromatic nuclei, with uniformity in shape and size and even cell placement, suggestive of a clonal population (Pinder and Ellis, 2003). The atypical cells are often arranged in various architectural patterns, including solid, cribriform, papillary or micropapillary (Kader et al., 2018). Cribriform pattern ADH is shown in **Figure 1.1.4**.

ADH is frequently described as having some but not all features of DCIS (Fitzgibbons et al., 1998). ADH and DCIS are distinguished from each other by the degree of atypia and the extent of atypical epithelial proliferation (Tavassoli and Norris, 1990, Page and Rogers,

1992, Ahmad, 2013). Additionally, ADH is usually small and focal, measuring less than 2 mm; if larger and more extensive, a diagnosis of DCIS is typically made (Pinder and Ellis, 2003). LOH and CGH-based studies of ADH have revealed frequent loss of the 16q chromosomal region (Lakhani et al., 1995, O'Connell et al., 1998, Amari et al., 1999). Additionally, microsatellite analysis has revealed that 60% of IDC and DCIS showed concurrent ADH that was clonal in origin (Larson et al., 2006), with copy number alterations and documented at early stages of ADH (Crissman et al., 1990, Eriksson et al., 1992, Stomper et al., 1992, Ruiz et al., 1999, Niu et al., 2013, Kader et al., 2018).

Marked transcriptional changes have been identified at the ADH stage relative to adjacent benign ductal epithelium (Ma et al., 2003), including up-regulation of several oncogenes such as FOXA1 and GATA3 (Brunner et al., 2014). Several studies have therefore proposed that alteration in expression of genes at the early stages of progression, including ADH and DCIS, may be critical for progression to invasive breast cancer, as expression of several transcripts is maintained throughout progression (van de Vijver et al., 2002, Paik et al., 2004). In fact, transcriptional studies have shown that ADH and LG DCIS possess near-identical gene expression profiles (Bombonati and Sgroi, 2011).

Epidemiological studies estimate that an ADH diagnosis is associated with a 4-5 fold increased risk of developing invasive breast cancer relative to the general population (Page et al., 1985, Page and Dupont, 1993, Fitzgibbons et al., 1998). If an immediate family member has previously been diagnosed with breast cancer, the risk of upgrade from an ADH diagnosis becomes about 10-fold (Page et al., 1985, Tavassoli and Norris, 1990, Page and Dupont, 1992, Pinder and Ellis, 2003). A recent study showed that approximately 20% (142/698) of women with ADH lesions had an upgrade in diagnosis (typically to DCIS) without surgical intervention (Hartmann et al., 2015). Clinical management of patients with ADH upon needle core biopsy thus includes surgical excision to rule out concomitant malignancy (Morrow et al., 2015, Rageth et al., 2016).

1.1.4 **Ductal carcinoma *in situ* (DCIS)**

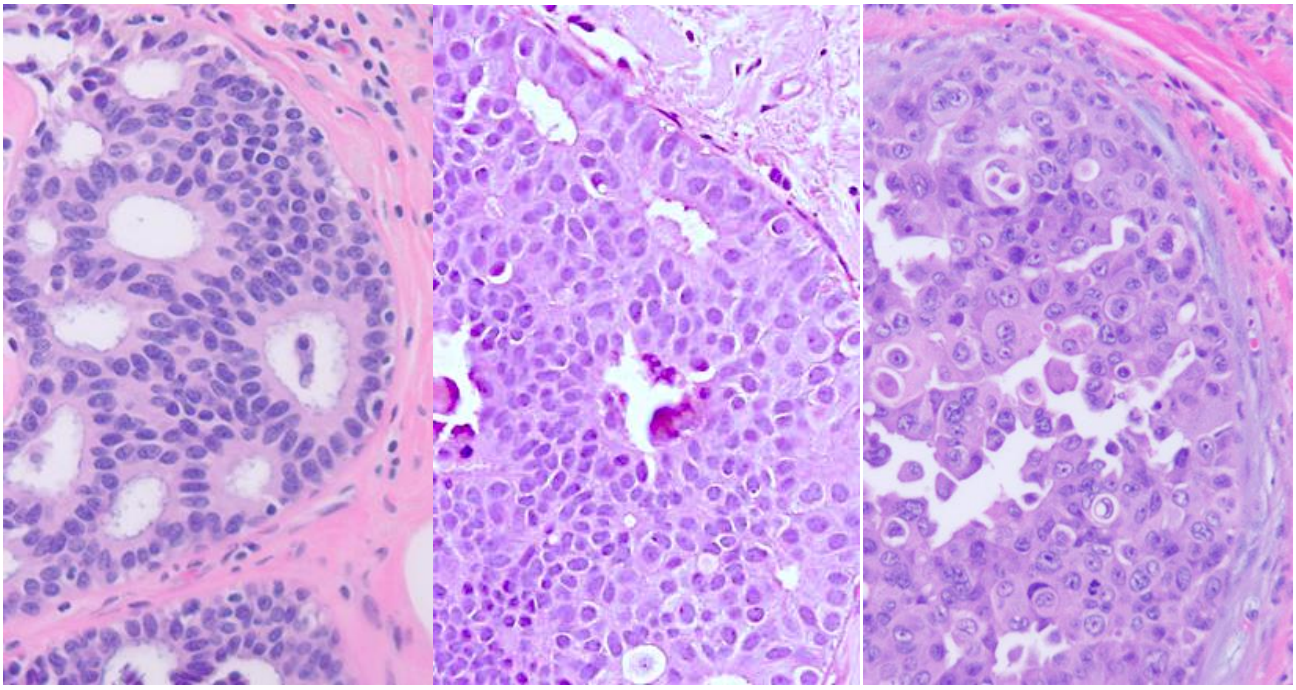

Figure 1.1.5 – Ductal carcinoma *in situ* (DCIS) of the breast.
Low-grade DCIS, intermediate-grade DCIS, and high-grade DCIS (left to right); all neoplastic cells of the DCIS are confined to the duct and possess an intact basement membrane.

1.1.4.1 **Histopathology of DCIS**

The presence of pure ductal carcinoma *in situ* (DCIS) is observed in approximately 15-20% of breast biopsies, compared to 5% before the introduction of mammography screening (van Dongen et al., 1989, Lagios, 1990, Faverly et al., 1994). DCIS is referred to as “Stage 0” breast cancer, with the cancer cells located within the confines of the basement membrane. Relative to ADH, DCIS contains further expansion of tumor volume through the ductal system, along with elevated histological and biological diversity (Allred et al., 2008). Clinically significant parameters which are reported for DCIS include nuclear grade, size, architecture, positive margins, and presence or absence of comedo necrosis (presence of necrosis is an independent prognostic indicator for invasive recurrence) (Lester et al., 2009).

The expanded volume of cells within DCIS can exhibit a wide spectrum of histological patterns (Allred et al., 2001). LG DCIS is composed of small uniform cells, with nuclei subtly

larger than those of adjacent normal epithelial cells (**Figure 1.1.5**, left panel) (Pinder and Ellis, 2003). HG DCIS is associated with an increase in the nuclei to cytoplasm ratio, coarse chromatin, prominent nucleoli, loss of polarization, frequent mitoses, and pleomorphism from cell to cell (**Figure 1.1.5**, right panel) (Lester et al., 2009). The architecture is variable (i.e. solid, cribriform, micropapillary, and/or papillary), although solid is frequently observed, often with central zone necrosis which may undergo calcification (Pinder and Ellis, 2003). The diagnosis of IG DCIS is quite subjective, and is made if nuclear pleomorphism exhibits an intermediate between LG and HG DCIS with some degree of polarization (Pinder and Ellis, 2003). On this note, a recent study using integrative bioinformatic analysis of the Cancer Genome Atlas (TCGA) breast cancer cohort reported that patients with IG IDC could be re-classified into LG-like and HG-like IDC based on a 22 gene tumor aggressiveness classifier (Aswad et al., 2015), suggesting that this subgroup consists of both LG and HG lesions (Bombonati and Sgroi, 2011).

The distinguishing factor between DCIS and IDC is the dissolution of the myoepithelial cell layer in IDC, with neoplastic cells invading beyond the basement membrane and into the adjacent stroma. Previous studies have shown that myoepithelial cells possess tumor-suppressor functions through their secretion of protease inhibitors and continuous synthesis and maintenance of the basement membrane (Barsky and Karlin, 2005, Polyak and Hu, 2005, Hu et al., 2008). During progression of DCIS to IDC, the myoepithelial cell layer gradually disappears, and their associated tumor suppressive function is thus lost (Hu et al., 2008). This can be tracked immunohistochemically using molecular markers such as smooth muscle myosin heavy chain (cytoplasmic) and/or p63 (nuclear), which are characteristically expressed by myoepithelial cells. Staining for these markers is lost with dissolution of the myoepithelial layer. This event results in loss of organization and polarity of breast epithelial cells, paving the way for tumor progression to invasion (Hu et al., 2008).

1.1.4.2 **Clinical Management of DCIS**

It is estimated that 25-50% of DCIS (depending on the DCIS characteristics) will progress to invasive carcinoma during the lifetime of the patient, generating potentially life-threatening disease (Page and Dupont, 1993, Fitzgibbons et al., 1998, Sanders et al., 2005, Ahmad, 2013, Sagara et al., 2015). Local recurrence rates for patients with DCIS are 5-25% with lumpectomy (Fisher et al., 1993, Warneke et al., 1995, Ernster et al., 1996, Fowble et al., 1997, Habel et al., 1998, Boyages et al., 1999, Hetelekidis et al., 1999), and 1-2% for mastectomy in the absence of radiation therapy (Silverstein et al., 1995a, Warneke et al., 1995, Boyages et al., 1999). This risk of non-invasive or invasive recurrence further depends on characteristics of the DCIS, including the nuclear grade, extent and presence or absence of necrosis.

The natural history of DCIS is for the most part unknown since routine treatment includes surgical excision (Bartlett et al., 2014). Prior to the 1980s, most patients with DCIS underwent a mastectomy (Waldman et al., 2000). Such radical surgical practices have been replaced by breast-conserving surgery (lumpectomy), often combined with radiation therapy, regardless of grade (Waldman et al., 2000, Mokbel and Cutuli, 2006). The higher rates of local recurrence for DCIS patients treated with lumpectomy suggest that the recurrent DCIS arises from residual tumor cells missed by surgery (Waldman et al., 2000). Work by Waldman et al. reported that recurrent DCIS lesions exhibited the same histologic architecture as the initial DCIS, and CGH analysis revealed that the initial and recurrent DCIS were clonally related (Waldman et al., 2000).

In a retrospective longitudinal cohort study examining 57,222 patients with documented DCIS and surgery status, Sagara et al. reported a significant survival benefit when comparing the surgery vs. non-surgery arm of patients with IG and HG DCIS (Sagara et al., 2015). In contrast, there was no survival benefit for patients with LG DCIS that underwent surgical excision (Sagara et al., 2015). In the only existing study assessing the natural history of LG DCIS, however, Sanders et al. identified 28 women in which DCIS was not initially diagnosed upon biopsy, but was detected upon examination of archival samples (Sanders et al., 2005). In their median follow-up time of 31 years, 11/29 (39.3%) women developed IDC, and 5/28 (17.9%) died of metastatic breast cancer (Sanders et al., 2005).

They noted that the risk of invasive recurrence is greatest within the first fifteen years after diagnosis (Sanders et al., 2005). Omission of surgical excision for patients with LG DCIS therefore leaves a percentage of women at risk for recurrence.

Randomized control trials have concluded that the addition of radiation therapy to lumpectomy reduces recurrence rates for early breast cancers by approximately 50%, similar to that of mastectomy (Fisher et al., 1998, Bijker et al., 2001, Fisher et al., 2001, Fisher et al., 2002, Bijker et al., 2006, Holmberg et al., 2008, Correa et al., 2010, Cuzick et al., 2011, Wapnir et al., 2011). Clinical records, however, show that only half of women treated by lumpectomy receive radiation therapy (Baxter et al., 2004, Jackson et al., 2008, Hughes et al., 2009). Several studies have also reported that approximately 30% of patients do not receive any significant benefit from radiation therapy (Lagios et al., 1989, Schwartz et al., 1992, Zafrani et al., 1994, Silverstein et al., 1995b, Silverstein et al., 1996).

DCIS represents a heterogeneous spectrum of lesions with several treatment approaches. Some DCIS may require local surgical excision, while others require radiation therapy or mastectomy. While the benefit of lumpectomy and radiation therapy results in great survival benefits to early breast cancer patients as a whole, we are unable to identify which patients are over-treated and do not benefit from these interventions (Bartlett et al., 2014). Paradoxically, we are uncertain of which DCIS lesions have an intrinsically higher propensity to progress to invasive cancer, such that some patients may be under-treated (Bartlett et al., 2014). Most patients therefore receive identical treatment, even though the risk, particularly of over-diagnosis and treatment, is well-recognized (Miller et al., 2014). The exception to this is patients with small, localized, non-high grade DCIS, for whom surgery without radiation is sometimes considered (Hetelekidis et al., 1999, Wong et al., 2014). Due to this important clinical problem, the 2009 National Institutes of Health State-of-the-Science Conference recommended that a focus on development and validation of risk stratification models and/or biomarkers is vital in order to optimize treatment strategies based on the underlying biology of each patient’s DCIS (Allegra et al., 2010).

1.1.5 **Biomarkers for progression to invasive carcinoma**

Breast cancers are now being diagnosed earlier, but this lead-time has not resulted in significant reductions in diagnosis of invasive carcinoma after DCIS (Kerlikowske, 2010, Miller et al., 2014). While up to 50% of DCIS lesions are expected to progress to IDC in the lifetime of the patient (Sagara et al., 2015), there is a high degree of variability in terms of latency (Muggerud et al., 2010). Indeed, some patients with DCIS progress to invasion quickly, while others remains relatively unchanged over 20 years (Porter et al., 2003, Schuetz et al., 2006). Previous studies have reported that traditional clinical and pathologic criteria are not sufficient to consistently and accurately define DCIS risk groups (Porter et al., 2003, Solin et al., 2013, Rakovitch et al., 2015). Conventional markers which are routinely assessed by immunohistochemistry in invasive breast cancers (ER, PR) are also of limited value in DCIS (Bartlett et al., 2014). The lack of reliable markers for risk stratification of patients diagnosed with DCIS results in identical treatment for almost all patients (Bartlett et al., 2014). There is therefore a pressing need for the development of novel diagnostic approaches for risk stratifications of patients with DCIS in order to optimize treatment strategies.

The majority of examined IDCs possess non-invasive DCIS components; histological analysis of both lesion types in these instances has revealed near identical histological and biological features (Allred et al., 2008). A more thorough understanding of molecular alterations within precursor lesions has been made possible through the use of tissue microdissection technologies and high throughput genomic analyses. Diversity has been shown to emerge at the DCIS stage, with very similar histology and transcriptional profiles in the IDC portions within the same patient (Perou et al., 2000, Ma et al., 2003, Porter et al., 2003, Schuetz et al., 2006, Allred et al., 2008). Analysis of pure DCIS, IDC, and mixed DCIS and IDC has revealed that by conducting hierarchical clustering based on the most variably expressed genes, DCIS cluster by “intrinsic subtype” and not by diagnosis (DCIS vs. IDC) (Muggerud et al., 2010). This suggests that genes that confer the ability to invade are active in some pre-invasive lesions (Muggerud et al., 2010). Additionally, they showed that not all HG DCIS exhibit the potential for invasion (Muggerud et al., 2010). Importantly, several studies have demonstrated that most gene expression changes characteristic of invasive breast cancers, including genes which confer invasive growth, are already present at the pre-invasive stage (ADH, DCIS, and persist in IDC) (Ma et al., 2003, Porter et al., 2003, Abba et

al., 2015). These findings are consistent with early LOH and CGH-based studies showing that similar genetic abnormalities associated with DCIS and IDC are already present at the ADH stage (Zhuang et al., 1995, Deng et al., 1996, O'Connell et al., 1998, Allred et al., 2001).

Van't Veer et al. established a poor-prognosis signature associated with a 28-fold increased risk for the development of metastasis over a 5-year period (van 't Veer et al., 2002). Based on their 70-gene approach, they concluded that even small primary tumors displaying a poor prognosis signature are already programmed for a metastatic phenotype (van 't Veer et al., 2002). Taken together, these studies suggest that since DCIS and IDC possess very similar transcriptional profiles, and a poor prognosis signature can be established from the primary IDC, the same may hold true for DCIS.

The assessment of biomarkers for DCIS is still in its infancy. As highlighted by Bartlett et al., 60 DCIS biomarker studies were published during the 2004-2014 period, with 90% of the published studies regarded as statistically under-powered (Bartlett et al., 2014). Additionally, several of these studies remain un-validated (Bartlett et al., 2014).

One DCIS biomarker that has been validated by several groups, however, is HER2 expression (as assessed by immunohistochemistry (IHC) and fluorescence *in situ* hybridization (FISH)). High HER2 expression in DCIS is associated with non-invasive recurrence (Provenzano et al., 2003, Kepple et al., 2006, Nofech-Mozes et al., 2008, Holmes et al., 2011, Ringberg et al., 2001, Han et al., 2012). Additionally, joint assessment of HER2 and Ki67 expression in DCIS was associated with a 3.22-fold increased risk of non-invasive recurrence (Rakovitch et al., 2012). Kerlikowske et al. reported that patients with DCIS which are ER- and HER2+ with high expression of Ki67 possess the greatest risk (Kerlikowske et al., 2010). The conclusions regarding HER2 expression and invasive recurrence post-lumpectomy are variable. This discrepancy was discussed by Kerlikowske et al. and Rakovitch et al., where they suggested this outcome was dependent on subtype (Kerlikowske et al., 2010, Rakovitch et al., 2012, Bartlett et al., 2014).

Biomarkers which have been assessed by immunohistochemistry include HER2, ER, PR, Ki67, cyclooxygenase 2 (COX2), p16 and p53 (Kerlikowske et al., 2010, Rakovitch et al., 2012, Bartlett et al., 2014). Noteworthy examples include studies examining the co-expression of p16, COX2 and Ki67. High expression of p16 and COX2 in the absence of the

proliferation marker Ki67 is indicative of a normal stress response, and protective against progression of DCIS (Gauthier et al., 2007). High p16, and COX2 with elevated Ki67 expression, however, is associated with a 2-fold higher rate of invasive recurrence (Gauthier et al., 2007, Kerlikowske et al., 2010).

The usage of one biomarker for risk stratification will likely result in limited predictive power, so multiple markers are likely needed (van 't Veer et al., 2002). Multi-parameter gene expression approaches for risk stratification of patients with DCIS has also been reported in the literature. Oncotype Dx, a qRT-PCR based assay consisting of a panel of 16 breast-cancer related genes and 5 housekeeping genes, possesses significant prognostic value in predicting recurrence of patients with early-stage, node-negative invasive breast cancers treated with adjuvant tamoxifen (Paik et al., 2004). The Oncotype Dx assay was adapted for assessment of DCIS recurrence risk after treatment by surgical excision without radiation therapy, and referred to as the DCIS Score (Solin et al., 2013). The DCIS Score is calculated through assessment of a 12-gene panel (including the previously-used 5 housekeeping genes), with an emphasis on genes involved in proliferation (Solin et al., 2013). The DCIS score of low, intermediate, and high-risk was associated with a 10.6% (*3.7%*), 26.7% (*12.3%*), and 25.9% (*19.2%*) risk of non-invasive (*and invasive*) recurrence over 10-years in the absence of radiation therapy (Solin et al., 2013). Interestingly, the DCIS Score was not associated with existing clinical or pathologic factors (Solin et al., 2013). These findings have been validated in an independent cohort of 718 patients, with 12.7% (low-risk), 33.0% (intermediate-risk), 27.8% (high-risk) local recurrence rates for the specified risk group over a 10-year follow-up period (Rakovitch et al., 2015). These findings may therefore be used to provide predictive information in order to determine which patients may be spared radiation therapy due to their low intrinsic risk of developing invasive breast cancer.

1.1.6 **Experimental Models of Breast Cancer Progression**

The development of breast cancer is a multi-step process, and our understanding of the underlying molecular events has been hindered due to a lack of suitable models of progression (Liu et al., 1994). Previous studies have demonstrated that mouse-derived pre-malignant lesions are histologically different from those of humans, particularly in transgenic mouse models where the cellular origin of hyperplastic lesions is more often associated with the promoter rather than the transgenes used (Cardiff et al., 2000). The standard method used to determine malignant potential of cells within precursor lesions is transplantation (Cardiff et al., 2000). As described by Cardiff et al., this is similar to “Koch’s Postulates” of tumor biology, including “identification [of cells representing the precursor stage], isolation, transplantation and characterization” (Cardiff et al., 2000). Most human cells lines representing pre-malignant stages do not form any discernible histologic lesions in nude mice, and the majority of existing cell lines used for xenograft assays are of metastatic origin (Band et al., 1990, Miller, 2000). Importantly, only the 21T, HMT-3522, and MCF10AT breast epithelial cell line series have been reported to recapitulate the various histological characteristics of human breast carcinoma within a xenograft model (Santner et al., 2001, Rizki et al., 2008, Souter et al., 2010).

The 21T series cell lines were isolated from a single patient with invasive ductal carcinoma through selective trypsinization and expanding of polygonal tumor-like cells from spindle-shaped epithelial cells and fibroblasts (Band et al., 1989, Band et al., 1990). The 21PT and 21NT cells were isolated from the primary tumor, and 21MT-1 cells were isolated from a pleural effusion (Band and Sager, 1989, Band et al., 1989, Souter et al., 2010). Importantly, the isolated cell lines represent distinct stages of progression: 21PT cells mimic ADH (non-tumorigenic), 21NT cells mimic DCIS (tumorigenic, non-metastatic), and 21MT-1 mimic IDC (tumorigenic, metastatic) when injected into the mammary fat pad of nude mice (Band et al., 1990, Souter et al., 2010). Karyotyping of the 21T series cell lines has previously been conducted by our laboratory (Xu et al., 2008), indicating that all three cell lines have common chromosomal aberrations, potentially reflecting a common origin within the same tumor (Xu et al., 2008). Additionally, these cells are weakly ER and PR positive, HER2 amplified, and possess a mutated form of p53 (Band et al., 1990, Liu et al., 1994, Biswas et al., 1998, Biswas et al., 2001).

The HMT-3522 human breast epithelial cell lines were derived from a reduction mammoplasty, with the S1 cells isolated from a sample with fibrocystic breast disease (Madsen et al., 1992, Rizki et al., 2008). The S2, S3(A-B) and T4-2 cell lines were established through sub-culturing of cells (in 2D or 3D Matrigel), isolation of colonies with distinct phenotypes characteristic of aggressiveness, along with inoculation of cells into mice and passaging of xenograft cells for T4-2 cells (Madsen et al., 1992, Rizki et al., 2008). The cells represent a model of spontaneous transition and exhibit differential growth patterns and phenotypes in 3D Matrigel, along with varying tumorigenicity in nude mouse xenograft assays (Rizki et al., 2008). The S3 cell lines represent the pre-invasive stage of the human breast cancer progression series, but give rise to a metaplastic phenotype (Rizki et al., 2008). Human metaplastic breast cancers are rare, but also extremely aggressive, sharing similar clinical behavior and markers with basal-like breast carcinomas (Kenny et al., 2007, Rizki et al., 2008).

There are several variants of the MCF10A cell line, all previously isolated from a sample consisting of fibrocystic breast disease, most notably the pre-malignant MCF10AT and malignant MCF10CA variants both of which are Ras transformed (Miller, 2000, Miller et al., 2000). In mouse xenograft assays, MCF10AT cells initially form simple ducts and lead to a wide spectrum of pre-malignant lesions, including ADH and DCIS, with approximately 25% of mice developing invasive carcinoma (Miller, 2000). Lesions formed by MCF10AT cells are highly heterogeneous, giving rise to several different and distinct histological subtypes as well as differential immunoreactivity (Strickland et al., 2000, Santner et al., 2001). Additionally, these cells are able to give rise to a myoepithelial cell layer (Tait et al., 1996), indicating the presence of precursor stem cells and likely explaining the unstable and heterogeneous phenotype (Miller, 2000). The MCF10DCIS.com cell variants were isolated from a xenograft lesion formed by MCF10AT cells (Miller et al., 2000). The MCF10DCIS.com cells are highly proliferative and form comedo DCIS (high nuclear grade with zonal necrosis) *in vivo* (Miller, 2000). These cells have high rates of spontaneous progression to invasive carcinoma, although the DCIS component is retained (Miller et al., 2000). The MCF10CA cell line was isolated through serial transplantation of spontaneous tumors formed by MCF10AT cells, and is malignant and highly metastatic (Miller, 2000, Santner et al., 2001). The

tumorigenic MCF10AT cell line variants are ER and PR positive, and possess wildtype p53 (Shekhar et al., 1998, Miller, 2000, Hevir et al., 2011).

A major advantage of utilizing a series of cell lines derived from a single patient to study progression is the minimal genetic variability. This allows for the mining of biologically relevant driver mutations and gene expression changes directly related to a subset of genetic alterations, independent of individual variability. Genetic manipulation of cell lines representing various stages of progression can be used to examine the relative functional impacts of genes on transitions between distinct stages (ADH, DCIS, IDC) (Souter et al., 2010). This can often be done through the use of *in vitro* techniques, which can be modified for high-throughput screens for identification of genes important in functional and phenotypic transitions, or for identification of therapeutically effective chemical agents in preclinical screens (Miller, 2000). Souter et al. described a 3D *in vitro* Matrigel culture in which cells were seeded on Matrigel and the resultant colonies were phenotypically assessed (Souter et al., 2010). Through the use of this 3D culture system, the 21PT, 21NT and 21MT-1 cells were shown to exhibit differential phenotypes and display features of distinct stages of the breast cancer progression pathway (Souter et al., 2010). Less aggressive cell lines (including the 21PT cells) typically show more polarized cells and higher rates of lumen formation, along with more spherical colonies and a lower frequency of single, dispersed cells (Souter et al., 2010) (depicted in **Figure 1.1.6**).

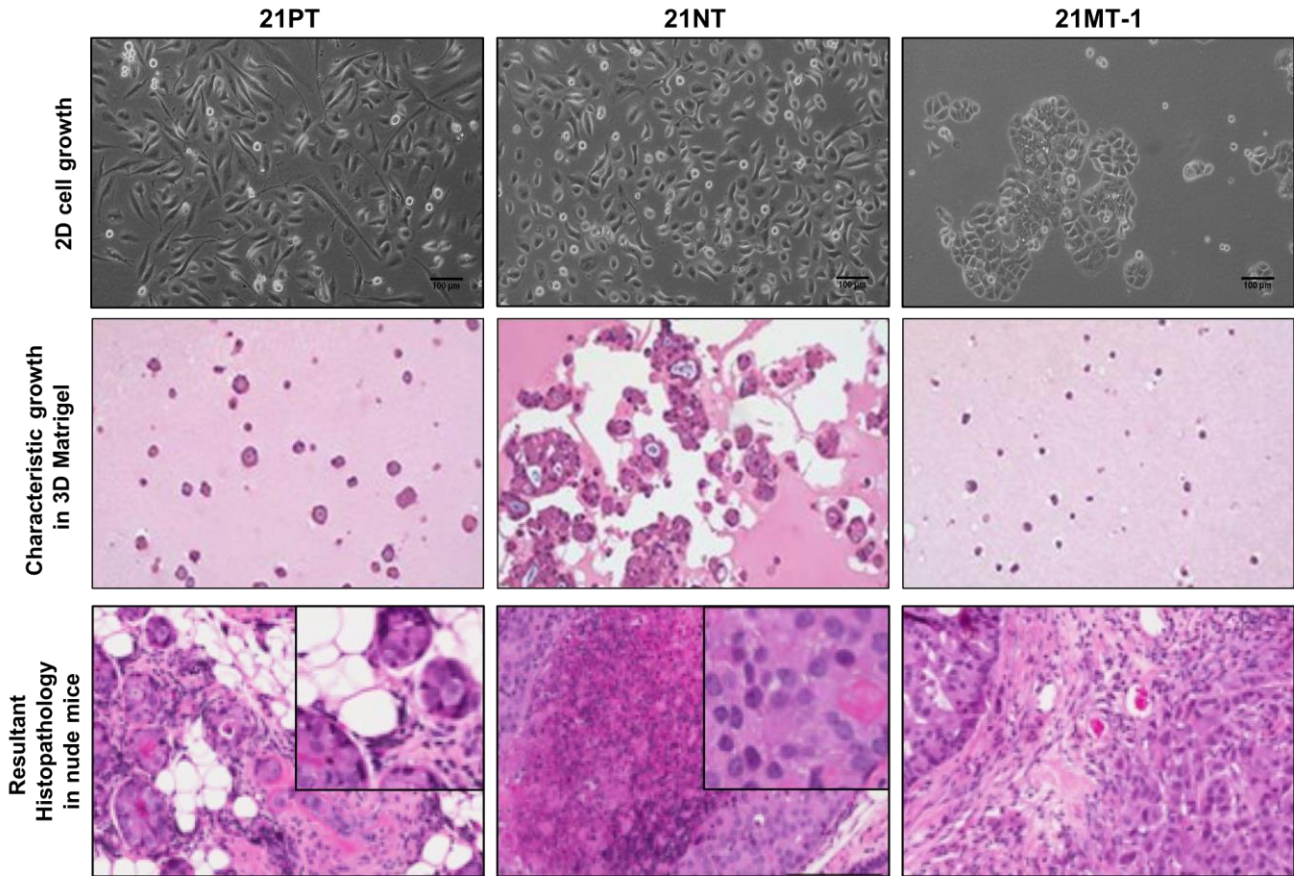

Figure 1.1.6 – Characteristic growth patterns of 21T cell lines in 2D, 3D, and in mouse xenografts.

H&E images were obtained from Souter et al., 2010.

1.2 **TBX3**

TBX3 is a member of the highly conserved family of T-box transcription factors. The 18 T-box genes within mammals are believed to have evolved from tandem duplication of a primordial gene, followed by cluster dispersion (Agulnik et al., 1996, DeBenedittis and Jiao, 2011). Several of the T-box genes are expressed throughout development, with tight temporal and spatial regulation (DeBenedittis and Jiao, 2011). The identification of T-box family members generally occurred through experiments designed to identify genes involved in embryonic development, with lack of expression resulting in developmental defects (Bollag et al., 1994, Bamshad et al., 1999).

The first T-box transcription factor identified was the Brachyury (*TBXT*) gene (Gruneberg, 1958). In mice, homozygous mutations in Brachyury are embryonic lethal due to insufficient formation of mesodermal cells in the developing embryo, while heterozygous mutations result in a variable short tail phenotype (Gluecksohn-Schoenheimer, 1938, Gruneberg, 1958, Yanagisawa et al., 1981, Stott et al., 1993). Several decades later, TBX3 was discovered by Bollag et al., who postulated its role in development after observing highly specific patterns of expression in the developing mouse embryo (Bollag et al., 1994). It was later discovered that TBX3 plays an important role in limb, heart, and mammary gland development (Wilson and Conlon, 2002). In mice, homozygous *TBX3* mutations are embryonic lethal, and most embryos die by E12.5 due to yolk sac defects (Davenport et al., 2003). Limb defects, along with lack of mammary glands was also documented (Davenport et al., 2003), similar to the conditions observed in human patients. In humans, mutations or haploinsufficiency of *TBX3* results in Ulnar-Mammary Syndrome (UMS, OMIM 181450). UMS is fully penetrant although it presents with highly variable clinical characteristics, mainly consisting of mammary gland hypoplasia, apocrine gland, dental, and genital defects (Bamshad et al., 1997, Bamshad et al., 1999, Davenport et al., 2003). These observed phenotypes are consistent with the broad expression profile of TBX3 (**Figure 1.2.2**). Complete loss of *TBX3* expression is predicted to be fatal, as patients lacking both copies of *TBX3* have not been identified (Rowley et al., 2004).

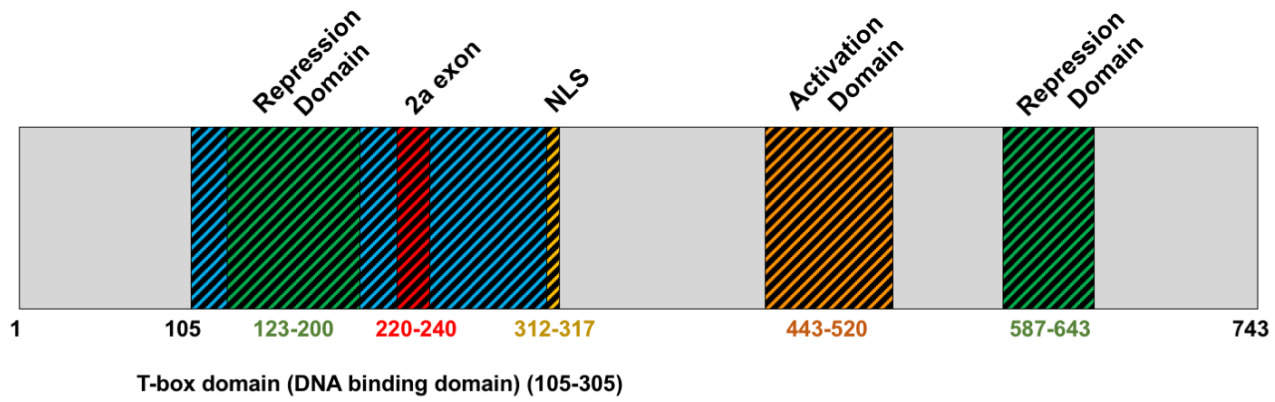

Figure 1.2.1 – Full-length TBX3 protein structure. Adapted from Willmer et al., 2017.

The full-length TBX3 protein is 743 residues in length, containing the T-box domain (residues 105-305), nuclear localization sequence (NLS; residues 312-317), activation domain (residues 443-520) and repression domains (residues 123-200, 587-643) (Smith, 1999, Carlson et al., 2001, Papaioannou, 2001, Willmer et al., 2017) (**Figure 1.2.1**). Two TBX3 isoforms exist through alternative splicing: TBX3iso1 and TBX3iso2 (which contains the 2a exon). TBX3 isoforms are described in **Section 2.3.1**.

All T-box transcription factors possess the highly conserved DNA binding domain known as the T-box domain which shares no sequence similarity to other known DNA binding motifs (Wilson and Conlon, 2002). Most of the described T-box domains are approximately 180 amino acids in length (Coll et al., 2002). T-box transcription factors bind to DNA sequences containing the T-box element (TBE) (Wilson and Conlon, 2002). To date, all T-box transcription factors examined are able to bind to the TBE consisting of bases TCACACCT (Wilson and Conlon, 2002). Coll et al. have proposed a less stringent consensus sequence (5'-xTxxCACxx'-3'; x signifies a less conserved base) for identification of new T-box binding sites (Coll et al., 2002).

T-box proteins function as transcriptional activators or repressors depending on the promoter context (Wilson and Conlon, 2002, Lu et al., 2010). TBX2 is the most closely related T-box gene to TBX3, sharing ~95% sequence homology in the T-box domain and ~70% homology in the repression domain (Bamshad et al., 1999). Interestingly, TBX2 and TBX3 are the only T-box transcription factors that function as transcriptional repressors (Carlson et al., 2001, Lu et al., 2010). Sequence analysis of the repression domain of TBX2 and TBX3 revealed no conserved sequence or motifs shared with other known repression domains (Lu

et al., 2010). While TBX2 and TBX3 exhibit overlapping and complementary expression patterns in the developing mouse embryo, they were found to have non-redundant roles in developmental processes (Rowley et al., 2004).

TBX3 possesses both activation and repression domains. Most of the existing cancer-related literature focuses on transcriptional repression of target genes by TBX3, while transcriptional activation of target genes has been further characterized in heart development (Boogerd et al., 2011, Lu et al., 2011). The effect of TBX3 on transcription likely depends on interacting partners and target genes (Willmer et al., 2017). Several domains which facilitate protein-protein interaction likely reside outside of the T-box domain, since this area has undergone rapid diversification between T-box genes (Bamshad et al., 1999, Coll et al., 2002). The effect of TBX3 on transcription of downstream target genes as they relate to the process of tumorigenesis is discussed in the next section.

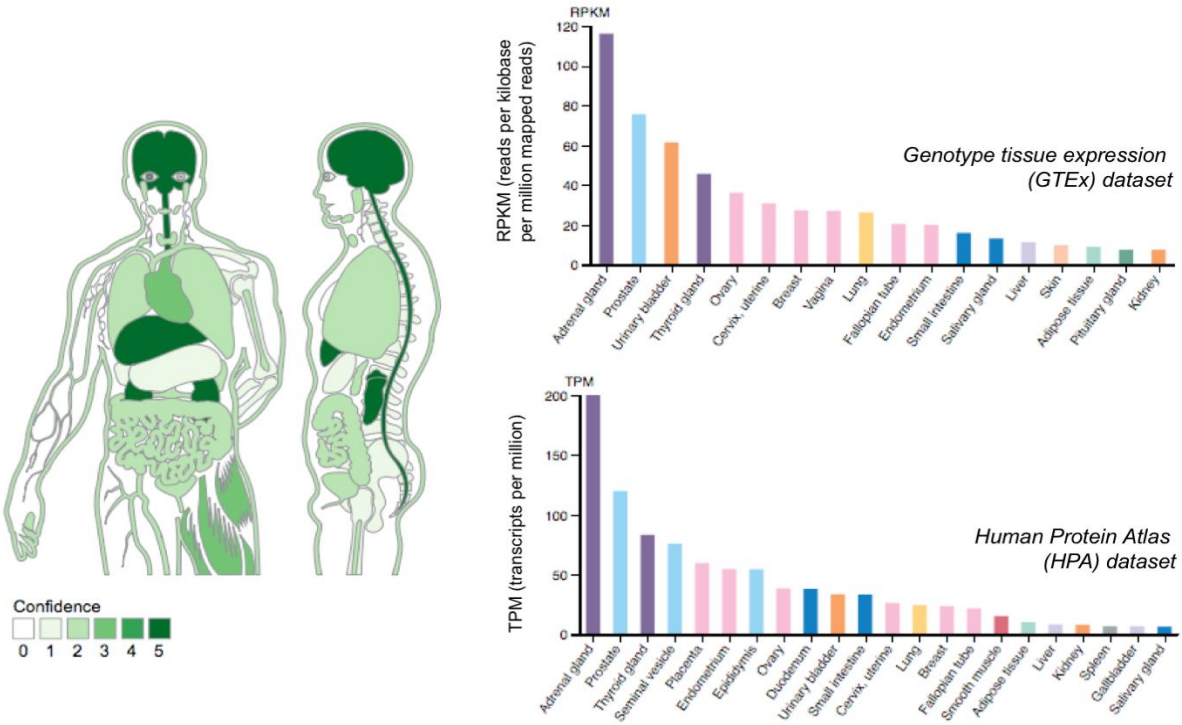

Figure 1.2.2 – TBX3 mRNA expression by tissue type.

Graphical representation of TBX3 mRNA expression across tissue types was obtained from Jensen TISSUES database (tissues.jensenlab.org), depicting Genotype Tissue Expression (GTEx) dataset (histogram plot on upper right). TBX3 mRNA expression in normal tissue is also shown from the Human Protein Atlas (HPA) dataset.

1.2.1 Mechanisms of transcriptional regulation by TBX3

TBX3 is able to bind several target genes through recognition of the conserved TBE sequence by the DNA binding domain (Wilson and Conlon, 2002). X-ray crystallography studies of TBX3 and Brachyury indicate that there are only two specific contacts within the DNA binding domain per TBE (Müller and Herrmann, 1997, Coll et al., 2002). The binding of TBX3 to the phosphatase and tensin homolog (PTEN) promoter, however, occurs in the absence of a TBE sequence (Burgucu et al., 2012), thereby suggesting that the binding of TBX3 to target sites is likely dependent on: i) DNA specificity and binding to a conserved TBE, ii) interaction with specific DNA binding proteins, iii) interaction with chromatin determinants (Lingbeek et al., 2002, Rodriguez et al., 2008). TBX3 is able to interact with chromatin, and directly binds to histone H2A (Kumar P et al., 2014b), histone deacetylases (HDACs), and DNA methyltransferases (DNMTs) (Yarosh et al., 2008, Dan et al., 2013), leading to transcriptional up-regulation or down-regulation of target genes. Additionally, TBX2, TBX4, TBX5 and TBX6 are able to bind to histone H3 N-terminal tails (Demay et al., 2007), the primary location of histone post-translational modifications (Mersfelder and Parthun, 2006).

Acetylation of histones is associated with active chromatin (Lewin et al., 2011). Histone deacetylases (HDACs) are involved in the removal of acetyl groups from histones, which results in tighter histone-DNA interactions and reduced levels of transcription (Yarosh et al., 2008). As HDACs do not contain a DNA binding domain, they are recruited by DNA-binding transcription factors (Cress and Seto, 2000). TBX3 is able to recruit and directly interact with histone deacetylases (HDACs) in order to epigenetically silence gene promoters (Willmer et al., 2017). This includes direct interaction with HDAC1, HDAC2, HDAC3, and HDAC5 to transcriptionally repress $p14^{ARF}$ in MCF7 cells (Yarosh et al., 2008). HDACs are often overexpressed in breast cancers (Zhang et al., 2005, Glozak and Seto, 2007), and it is suggested that each HDAC plays a specific role in the process of breast tumorigenesis (Puri et al., 2001, Dokmanovic and Marks, 2005, Glozak et al., 2005). The association between TBX3 and HDACs may therefore play an important role in breast cancer progression (Yarosh et al., 2008). Additionally, in a recent study in hepatocellular carcinoma (HCC), TBX3 was found to directly interact with HDAC5, resulting in down-regulation of E-cadherin;

administration of HDAC inhibitor was able to block TBX3-induced repression of E-cadherin and TBX3-induced migration in HCC cell lines (Dong et al., 2018).

DNA methylation is associated with transcriptionally inactive DNA (Lewin et al., 2011). ChIP-Seq analysis revealed that TBX3 binds upstream of the DNA methyltransferases *DNMT3A* and *DNMT3B* genes, leading to their transcriptional repression (Han et al., 2010). TBX3 overexpression results in a reduction in the global DNA methylation levels, likely through down-regulation of DNMT3B (involved in DNA methylation) and up-regulation of TET2 (involved in DNA de-methylation) (Dan et al., 2013).

Not only is TBX3 able to modify epigenetic profile of target genes, the physical interaction of TBX3 with several RNA-binding proteins and splice factors has revealed that TBX3 is also able to bind to TBEs within mRNA transcripts and directly regulate splicing (Kumar P et al., 2014b). These studies show that not only does TBX3 regulate gene expression through activation/repression of genes through various means including alterations of histone modifications, but is also able to modulate splicing of target mRNA sequences. In fact, there is an over-representation of TBEs in sequences flanking alternative exons (Kumar P et al., 2014b). Alternative splicing is an important post-transcriptional mechanism of gene regulation, and changes in alternative splicing profiles has been observed in several cancers (Venables, 2004, Pajares et al., 2007, Venables et al., 2008, Shapiro et al., 2011, Oltean and Bates, 2014). The study by Kumar et al. sheds light on other potential mechanisms in which TBX3 overexpression in several cancer types may lead to tumorigenesis (Kumar P et al., 2014b).

1.2.2 **TBX3 in Cancer**

TBX3 levels are up-regulated in several cancers, including breast (Fan et al., 2004, Lomnytska et al., 2006, Yarosh et al., 2008, Souter et al., 2010), melanoma (Rodriguez et al., 2008), pancreatic (Hansel et al., 2004, Cavard et al., 2009, Begum and Papaioannou, 2011), cervical (Lyng et al., 2006), ovarian (Lomnytska et al., 2006), gastric (Miao et al., 2016), and prostate cancers (Gudmundsson et al., 2010, Witte, 2010). TBX3 expression levels in normal tissues, tumor tissues, and plasma samples have been assessed in several studies described below, using methods ranging from IHC, microarray analysis, qRT-PCR, western blot, and 2D gel electrophoresis coupled to mass spectrometry.

TBX3 PROTEIN IN CANCERS – Assessment of TBX3 expression in pancreatic cancer by IHC revealed that elevated TBX3 expression within tumor samples was an independent prognostic factor for reduced overall survival (Wang et al., 2015). In gastric cancers, elevated TBX3 expression by IHC was significantly associated with advanced TNM (tumor, node, metastasis) stage and higher incidence of relapse (Miao et al., 2016). In colorectal cancer, elevated TBX3 expression by IHC was an independent predictor of poor outcome, and was correlated with tumor size, differentiation, TNM stage and lymph node metastasis (Shan et al., 2015).

Lomnytska et al. assessed differential protein expression within plasma samples of breast and ovarian cancer patients through the use of 2D gel electrophoresis coupled to matrix-assisted laser desorption/ionization time of flight mass spectrometry (MALDI-TOF-MS) (Lomnytska et al., 2006). This study revealed significantly higher levels of TBX3 in plasma of both early stage and advanced stage breast cancer and ovarian cancer patients relative to healthy control patients (Lomnytska et al., 2006).

Examination of TBX3 expression by western blot in a diverse subset of cell lines representing normal human fibroblasts, transformed fibroblasts, and several soft tissue and bone sarcoma cell lines reported high levels of TBX3 in transformed fibroblasts and sarcoma cell lines relative to normal human fibroblast controls (Willmer et al., 2016a). Willmer et al. suggested clinical assessment of TBX3 expression to differentiate benign soft tissue masses from sarcomas (Willmer et al., 2016a).

TBX3 mRNA IN CANCERS – TBX3 is overexpressed in a variety of different cancer types (**Figure 1.2.3**). Microarray analysis revealed that elevated TBX3 mRNA expression was associated with advanced tumor stage, chemo-resistance and an unfavorable prognosis in patients with hepatoblastoma (Renard et al., 2007). Assessment of TBX3 expression by qRT-PCR and western blot in non-small cell lung cancer (NSCLC) patient samples revealed that overexpression of TBX3 was associated with tumor size, TNM stage, differentiation, and recurrence, and was an independent prognostic marker for overall survival (Wu et al., 2017). Additionally, up-regulation of TBX3 has been documented with chronic exposure to carcinogens, including a positive correlation with tobacco smoking status (Wu et al., 2017) and exposure to the environmental toxin DE-71 and liver tumorigenesis (Shimbo et al., 2017).

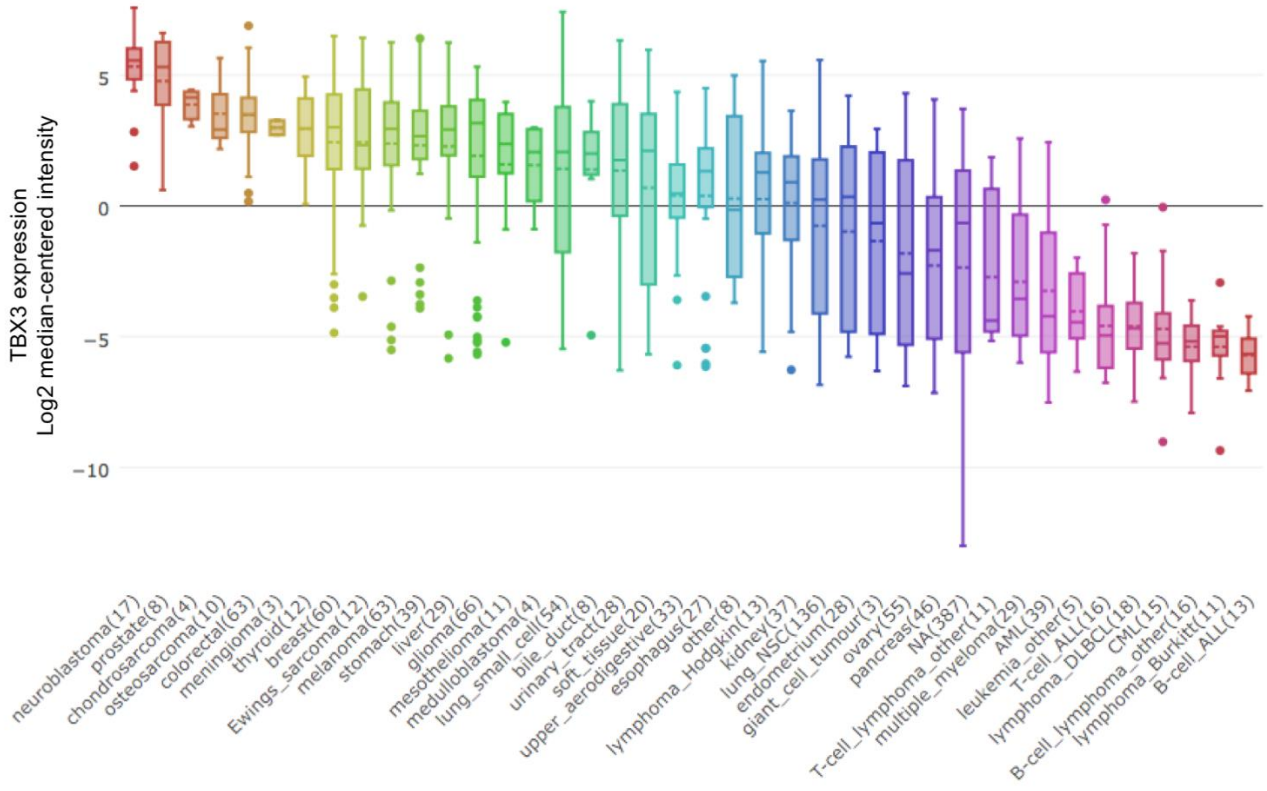

Figure 1.2.3 – TBX3 mRNA expression by cancer type.

Graphic obtained from CCLE (Cancer Cell Line Encyclopedia).

The single published transgenic TBX3-inducible mouse model used a doxycycline-inducible TBX3iso2 expression system under the control of the mouse mammary tumor virus (MMTV) promoter (Liu et al., 2011). Their results showed that overexpression of TBX3iso2 in murine mammary glands resulted in mild focal hyperplasia and importantly no tumor formation (Liu et al., 2011). The effect of inducible overexpression of TBX3iso1 was not examined. Few xenograft studies have been conducted overexpressing either TBX3iso1 or TBX3iso2 (or knockdown of total TBX3 levels) in various cell line backgrounds in order to assess resultant tumorigenicity. TBX3iso1 was overexpressed in SWI1353 chondrosarcoma cells and exhibited enhanced tumor growth (Willmer et al., 2016a). Injection of TBX3-overexpressing non-tumorigenic WM1650 melanoma cells into the flank of nude mice resulted in 6/6 of mice forming tumors compared to 0/6 in the parental control cells (Peres and Prince, 2013). Overexpression of TBX3 in pancreatic cancer cell lines resulted in significantly larger tumors than controls (Perkhofer et al., 2016). The latter two examples did not state which TBX3 isoform was overexpressed. The shRNA-mediated knockdown of TBX3 in tumorigenic ME1402 melanoma cells abolished their ability to form tumors when injected into the flank of nude mice (Peres et al., 2010).

The use of TBX3 as a potential biomarker in various cancer subtypes has been examined through the use of several methodologies, as has its role in chemically-induced carcinogenesis. In all documented cancer cases aside from fibrosarcoma, overexpression of TBX3 has led to increased migration and invasion (Rodriguez et al., 2008, Peres et al., 2010, Krstic et al., 2016, Willmer et al., 2016a). Although the contribution of TBX3 in tumorigenesis is not fully understood, accumulating evidence suggests that several pathways may be involved (summarized in **Figure 1.2.4**). More research is needed for further identification of upstream activators of TBX3 signaling, its target genes, along with co-factors required for its proper functioning (Willmer et al., 2017). Some of the cancer-associated pathways in which TBX3 is involved are described in the next sections.

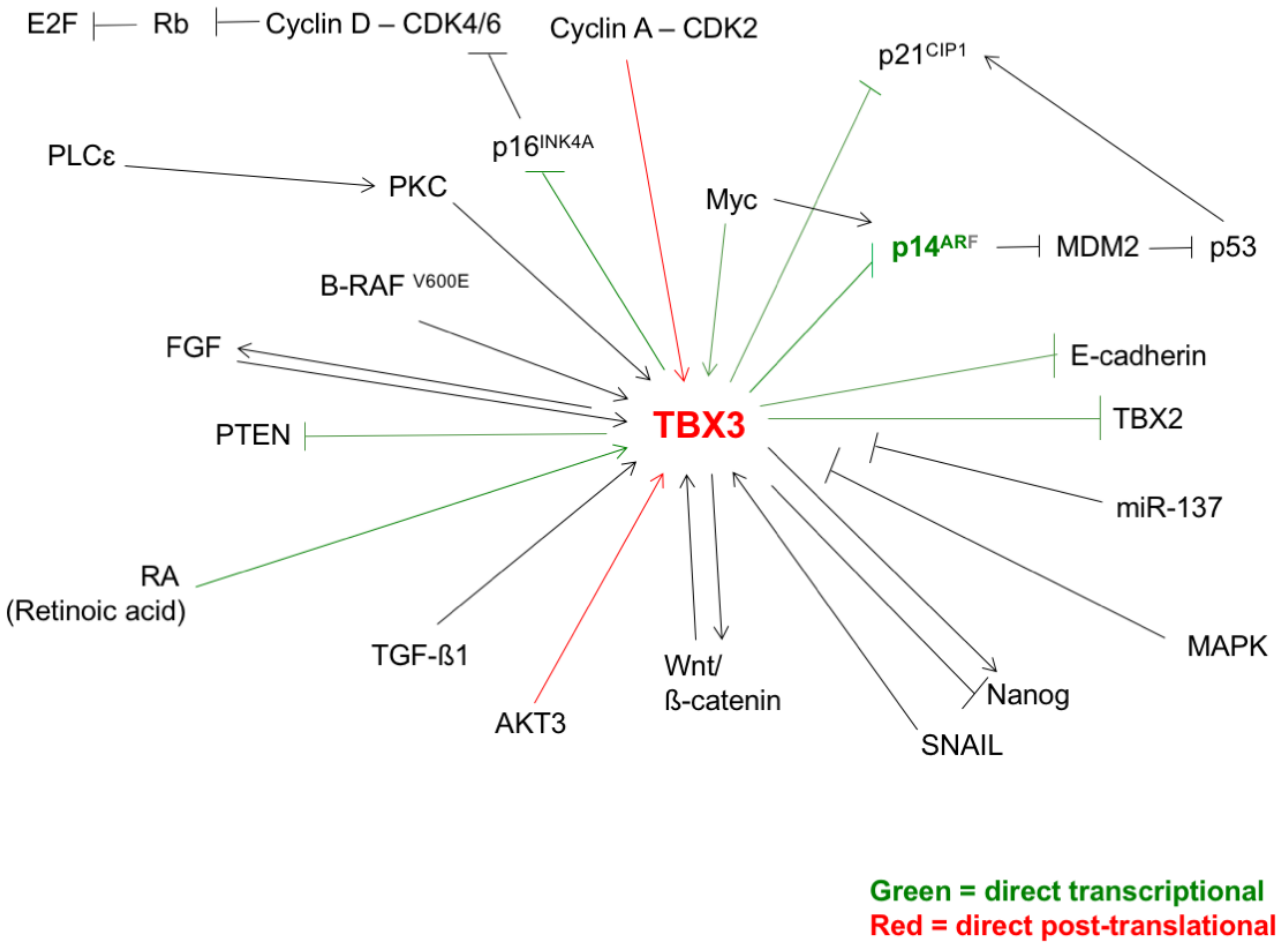

Figure 1.2.4 – Cancer-related TBX3 signaling pathways.

Green lines represent direct transcriptional interactions, while red lines represent direct post-translational interactions.

1.2.3 **TBX3 and Cellular Senescence – p14^{ARF} / p53 / p21^{CIP1} Pathway**

The cyclin-dependent kinase inhibitor 2A (CDKN2A) gene encodes the p16^{INK4A} and p14^{ARF} proteins in humans, with differential promoters and partially overlapping reading frames (Ruas and Peters, 1998). Both proteins act as tumor suppressors and are important regulators of cellular senescence (Ruas and Peters, 1998). While p14^{ARF} is primarily involved in stabilization of p53, p16^{INK4A} inhibits the enzymatic activity of cyclin-dependent kinases 4 and 6 (CDK4/6) (Rayess et al., 2012). CDK4/6 binds cyclin D, which then phosphorylates the Retinoblastoma (Rb) protein, resulting in dissociation of Rb and the E2F transcription factor, thereby promoting the G1 to S phase transition (Rayess et al., 2012).

Cellular senescence is a protective mechanism of irreversible growth-arrest resulting in permanent exit from the cell cycle. Senescence can be induced by cellular stresses (accelerated senescence) or telomere shortening (replicative senescence) (Lu et al., 2010). One of the most well described pathways of accelerated senescence is through activation of p14^{ARF}, whereby p14^{ARF} binds to and sequesters mouse double minute 2 (MDM2), preventing MDM2 from targeting p53 for destruction (Tao and Levine, 1999). High expression of p14^{ARF} thus stabilizes p53, leading to expression of p53 target genes (Lu et al., 2010). Early studies reported that TBX3 overexpression leads to impaired functioning of the p53-pathway, suppression of apoptosis and facilitation of cell transformation (Carlson et al., 2002). TBX3 was later identified in a senescence screen and described as a potent inhibitor of senescence through inhibition of p14^{ARF} (and p19^{ARF} mouse ortholog), explaining the previously reported effect on p53 (Brummelkamp et al., 2002). After this initial identification of the powerful anti-senescence effect of TBX3, both TBX3 and TBX2 have been shown to bind to a variant TBE in the human p14^{ARF} promoter matching 13 of 20 nucleotides within the consensus TBE (Lingbeek et al., 2002). Specifically, TBX3 is able to interact with HDACs 1, 2, 3 and 5, leading to local changes in histone acetylation and subsequent down-regulation of p14^{ARF} expression in breast cancer cell lines (Yarosh et al., 2008).

Overexpression of several oncogenes and activation of mitogenic signaling pathways induces p14^{ARF} expression, and subsequent p53-dependent cell cycle arrest (Rowley et al., 2004). Overexpression of MYC or oncogenic H-Ras^{Val17} with TBX3 (but not by themselves), however, protects cells from apoptosis through inhibition of p14^{ARF} (Carlson et al., 2002). On a similar note, knockdown of TBX3 was shown to sensitize cells to doxorubicin in rat bladder

carcinoma and human colorectal cancer, later attributed to activation of the $p14^{ARF}$ / p53 pathway (Renard et al., 2007, Zhang et al., 2011a).

The cyclin-dependent kinase inhibitor $p21^{CIP1}$ is essential for p53-induced cellular senescence (Waldman et al., 1995). TBX3 was shown to directly bind to the $p21^{CIP1}$ promoter and repress gene transcription in a dose-dependent manner in melanoma cell lines (Hoogaars et al., 2008, Willmer et al., 2016b). This was shown by electromobility shift assays (EMSA), luciferase assays, and ChIP qRT-PCR validation (Hoogaars et al., 2008, Willmer et al., 2016b). Repression of both $p14^{ARF}$ and $p21^{CIP1}$ by TBX3 produces a powerful synergistic effect, leading to a strong inhibition of senescence (Lu et al., 2010).

Lastly, TBX3 is also able to bypass senescence through down-regulation of $p16^{INK4A}$ through formation of a co-repressor complex, leading to destabilization of $p16^{INK4A}$ and inhibition of the Rb pathway (Kumar P et al., 2014a).

1.2.4 **TBX3 and the TGF-ß Pathway**

The transforming growth factor beta (TGF-ß) signaling pathway is involved in development, along with the processes of homeostasis, proliferation and differentiation in adult tissues (Massagué, 2012). TGF-ß proteins bind their cognate receptors, and the signal is mediated through the canonical suppressor of mothers against decapentaplegic (SMAD) proteins that control the expression of hundreds of genes (Massagué, 2012). The TGF-ß signaling pathway is constitutively activated in several breast cancers, leading to a promotion of migration but inhibition of proliferation of cancer cells (Tian et al., 2003, Moses and Barcellos-Hoff, 2011). Treatment of epithelial cell lines with TGF-ß results in up-regulation of TBX3 (Kang et al., 2003). Later it was discovered that TGF-ß1 is able to up-regulate TBX3 through cooperative binding of Smad3/4 and JunB in the TBX3 promoter, with subsequent TBX3-dependent repression of the pro-proliferative family member TBX2 in melanoma cell lines (Li et al., 2013, Li et al., 2014). While overexpression of TBX3 results in an increased proliferation rate in several cell lines, TBX3 has an anti-proliferative effect in melanoma cell lines while still maintaining its pro-tumorigenic properties (Peres et al., 2010). TBX3 was therefore proposed to mediate the anti-proliferative, pro-migratory effect associated with TGF-ß signaling in melanoma cells (Li et al., 2013, Li et al., 2014).

1.2.5 **TBX3 and the FGF Pathway**

The fibroblast growth factor (FGF) signaling pathway is comprised of a group of developmentally-important secreted signaling proteins. Binding of FGF ligands to their signaling receptors (FGFRs) results in activation of their intracellular tyrosine kinase domain, which can activate several intracellular signaling pathways involved in maintenance, repair, regeneration and metabolism of adult tissues (Ornitz and Itoh, 2015).

During development in the mouse, TBX3 is initially expressed in the mammary lineage prior to mammary bud formation at E10.25, which is followed by the first signs of the mammary gland at E10.5 to E11, and expression of several Wnts and FGF ligands (Eblaghie et al., 2004). Eblaghie et al. soaked beads in various FGF proteins, and implanted them into the flank of mice in order to assess expression of downstream genes of interest (Eblaghie et al., 2004). They reported that FGF8 induces expression of TBX3 in an FGFR1-dependent manner (Eblaghie et al., 2004). These early studies showed that TBX3 and FGF ligands are able to interact and influence expression of one another within a developmental context (Eblaghie et al., 2004). Several other studies have reported autoregulation of expression between T-box and FGF family members (Isaacs et al., 1994, Schulte-Merker and Smith, 1995, Casey et al., 1998, Eblaghie et al., 2004).

In a breast cancer context, Fillmore et al. reported that estrogen leads to an expansion of breast cancer stem cells (CSCs) through the FGF and TBX3-mediated signaling pathways (Fillmore et al., 2010). The binding of estrogen to the estrogen receptor results in transcriptional up-regulation of FGF proteins (Fillmore et al., 2010). Specifically, FGF9 binds to FGFR3, which induces TBX3 expression (Fillmore et al., 2010). Elevated TBX3 expression is important for further production of FGF proteins and signal propagation, eventually resulting in an increase in an expansion of the breast CSC population (Fillmore et al., 2010). It was therefore shown that due to this TBX3-mediated expansion of CSCs in MCF7 cells treated with estrogen, TBX3 overexpression resulted in a 100-fold increase in tumor initiation rates in ovariectomized NOD/SCID mice (Fillmore et al., 2010).

1.2.6 **TBX3 and the Wnt / ß-Catenin Pathway**

The Wingless (Wnt) signaling pathway is involved in cellular proliferation and differentiation, and plays a crucial role in development and tissue homeostasis (Giles et al., 2003). Several Wnt proteins are overexpressed in breast cancer cell lines, leading to activation of the canonical Wnt/ß-catenin signaling pathway (Howard and Ashworth, 2006). ß-catenin directly binds to the TBX3 promoter through a T-cell specific (TCF)-binding site, leading to increased proliferation and survival of liver cancer cells (Renard et al., 2007).

TBX3 and Wnt signaling have been extensively studied in the processes of development. Within the developing mammary gland, TBX3 is required for the induction of Wnt signaling, as homozygous TBX3 mutant transgenic mice showed an inability to initiate mammary gland development and lack expression of the earliest markers of this developmental process (Lef1 and Wnt10b) (Davenport et al., 2003, Rowley et al., 2004). Additionally, induction of TBX3 expression in the developing mammary gland requires Wnt signaling (Eblaghie et al., 2004, Douglas and Papaioannou, 2013), suggesting the presence of a feedback loop (Davenport et al., 2003, Eblaghie et al., 2004, Cho et al., 2012). TBX3 overexpression in mammary epithelial cells was additionally reported to coordinate expansion of progenitor cells through induction of Wnt signaling (Arendt et al., 2014).

1.2.7 **TBX3 and the PTEN / PI3K / AKT Pathway**

The phosphoinositide 3-kinase (PI3K) and protein kinase B (AKT) signaling pathway has been described as an upstream mediator of TBX3 expression in mouse embryonic stem cells (Niwa et al., 2009), melanoma, and head and neck squamous cell carcinoma (HNSCC) (Burgucu et al., 2012, Boyd et al., 2013, Peres et al., 2015). The PI3K/AKT pathway promotes proliferation and cell survival in response to binding of growth factors, cytokines and/or hormone ligands to receptor tyrosine kinases (RTKs) (Cantley and Neel, 1999).

AKT3, the predominant AKT isoform expressed in melanomas, was shown to phosphorylate TBX3 at residue Ser-720 *in vitro*, leading to increased protein stability and nuclear localization (Peres et al., 2015). This phosphorylation event resulted in enhanced

repression of E-cadherin by TBX3, and increased migration and invasion of melanoma cell lines (Peres et al., 2015).

There is also evidence that TBX3 may function upstream of the PI3K/AKT pathway through repression of the tumor suppressor PTEN. PTEN is the main negative regulator of PI3K, thus functioning as a tumor suppressor through its PI3K-dependent inhibition of AKT (Cantley and Neel, 1999). There is an inverse correlation between TBX3 and PTEN expression in HNSCC (Burgucu et al., 2012). TBX3 is able to repress both basal and induced expression of PTEN in HNSCC cell lines, through binding a non-canonical TBX3 binding site in the PTEN promoter (Burgucu et al., 2012). TBX3 was not able to repress PTEN in muscle cells, however, suggesting context-dependent repressive functions (Zhu et al., 2016).

1.2.8 **Regulation of TBX3 by miRNAs**

MicroRNAs (miRNAs) are non-coding RNAs which are able to modulate gene expression by binding to complementary nucleotides in the 3' untranslated region (UTR) of target genes (Bartel, 2004). The 3' UTR of TBX3 extends 1,587 bp beyond the termination codon (Bamshad et al., 1999). Binding sites for several microRNAs have been found in the 3' UTR of TBX3, including miR-25, miR-32, miR-92, miR-93 (validated), miR-137 (validated), miR-206 (validated), miR-363, and miR-367 (Zhang et al., 2011b, Humtsoe et al., 2012, Jiang et al., 2013, Cioffi et al., 2015, Amir et al., 2016).

Most of the *in vitro* studies assessing miRNA regulation of TBX3 have been conducted with miR-137 (Jiang et al., 2013, Peres et al., 2017). The miR-137 is an important regulator of differentiation in embryonic stem cells (Szulwach et al., 2010, Sun et al., 2011, Jiang et al., 2013), and inhibits anchorage-independent growth and migration of malignant melanoma cells (Peres et al., 2017). Expression of miR-137 is down-regulated in several cancers, with epigenetic silencing of miR-137 representing an early event in colorectal cancer (Silber et al., 2008, Balaguer et al., 2010, Chen et al., 2010, Jiang et al., 2013, Peres et al., 2017).

1.3 **Alternative Splicing in normal and neoplastic cells**

Gene expression changes, on their own, cannot fully account for changes in gene functions and cellular phenotype (Venables, 2004). It is estimated that over 90% of human genes are alternatively spliced, adding an enhanced layer of complexity and diversification to genes encoded in the genome (Matlin et al., 2005, DeBenedittis and Jiao, 2011). Cancer cells are able to exploit the process of alternative splicing to produce isoform switches, resulting in enhanced survival, proliferation and invasiveness (Oltean and Bates, 2014, Shen et al., 2016).

Genes are transcribed into pre-mRNA, containing long intervening segments called introns, and protein-coding segments called exons. Alternative splicing refers to the “cutting” of intron-exon boundaries in pre-mRNA and joining the exons together in highly specific arrangements, producing structurally and functionally distinct mRNA and protein variants (Blencowe, 2006). The majority of alternative splicing events occur simultaneously with transcription, with the emergence of pre-mRNA from RNA polymerase II (Bentley, 2005, Blencowe, 2006). Additionally, modifiers of chromatin structure, including histone modifications and nucleosome positioning, affect transcription kinetics and thus alternative splicing decisions (Kornblihtt et al., 2013). This global post-transcriptional mechanism thus allows for cell-specific, stage-specific and stimuli-specific responses (Pajares et al., 2007).

After transcription and pre-RNA processing is completed, mature mRNA is exported from the nucleus to the cytoplasm where it is translated into protein. As a precautionary quality control mechanism, the nonsense-mediated mRNA decay (NMD) pathway leads to cytoplasmic degradation of inappropriately expressed transcripts (Pajares et al., 2007). Sometimes an aberrant transcript is not detected by the NMD pathway and is translated into protein; this is observed in several diseases including cancers (Pajares et al., 2007).

Each hallmark of cancer has been associated with changes in alternative splicing (Oltean and Bates, 2014). Mutations in cis-regulatory elements (i.e. splicing enhancers and silencers), near intron-exon junctions (i.e. creating or disrupting splice sites), or trans-acting splicing factors (i.e. involved in assembly of spliceosome) can lead to aberrant splicing (Pajares et al., 2007). Additionally, changes in concentration, localization, activity, and/or

composition of trans-acting splice factors (even in the absence of mutations) has also been documented to alter splicing patterns (Pajares et al., 2007). The documented splicing machinery changes during oncogenesis result in cancer-specific patterns of alternative splicing, leading to the emergence of previously non-existent transcripts and/or aberrant isoform ratios expressed within tumors relative to normal tissues (Pino et al., 2003, Venables, 2004, Ladomery et al., 2007, Pajares et al., 2007).

There are numerous examples of alternatively spliced transcripts having diverse and antagonistic functions (Pajares et al., 2007). A prominent example includes alternative splicing of vascular endothelial growth factor (VEGF); most splice variants are actively pro-angiogenic (Ladomery et al., 2007). Interestingly, the VEGFb splice variant is actively anti-angiogenic, and contains only 6 different amino acids relative to its most similar isoform (Ladomery et al., 2007). A splicing switch from the anti-angiogenic to pro-angiogenic variant is observed both in cancer progression, as well as in diseases such as proliferative diabetic retinopathy (Blencowe, 2006, Ladomery et al., 2007, Pajares et al., 2007). As such, differential expression of VEGF isoforms is associated with significant differences in survival for patients with node-positive breast cancer (Konecny et al., 2004).

Recent studies have shown that alternative-splicing based analyses consistently outperform gene expression-based survival predictors (Shen et al., 2016, Klinck et al., 2008). Shen et al. have reported distinct cancer-associated alternative splicing patterns across 6 different cancer types in the TCGA datasets (Shen et al., 2016). Various strategies are currently being employed in an attempt to exploit alternative splicing in diagnosis, prognosis and treatment of cancer (Yamaguchi et al., 1998, Venables, 2004). The large number of genes encoded in the human genome, along with the many subtypes of cancer in which alternative splicing changes have been documented suggests that the current knowledge is only the beginning in our understanding of the cause and effect of alternative splicing events in cancer, as well as how this knowledge may be used clinically.

1.3.1 **Alternative Splicing of T-box genes**

Most of the T-box family members encode a single transcript and few examples of alternative splicing have been documented (Wilson and Conlon, 2002, DeBenedittis and Jiao, 2011). While TBX3, TBX5 and TBX21 undergo alternative splicing, only TBX3 and TBX21 contain an insertion in their T-box domain (DeBenedittis and Jiao, 2011). Alternative splicing of TBX3 leads to two distinct transcripts; TBX3iso2 contains an additional 20 amino acid sequence in the DNA binding region attributed to the 2a exon, while TBX3iso1 does not (Bamshad et al., 1999). Alternative splicing of TBX21 leads to a three amino acid insertion in the DNA binding domain corresponding to the exon 2a insertion site in TBX3 (DeBenedittis and Jiao, 2011). While alternative splicing of TBX3 in particular is highly conserved within mammals (Hoogaars et al., 2008), the functional significance of the 2a exon remains unclear. These alternative splicing events may therefore provide a potentially critical differential role for TBX3 isoforms in development and tumorigenesis (DeBenedittis and Jiao, 2011).

Previous studies have reported that isoforms of T-box proteins can differ in subcellular localization, expression, protein-protein interaction, and functionality (Wilson and Conlon, 2002, DeBenedittis and Jiao, 2011). For example, alternative splicing of TBX5 leads to two protein products, TBX5a and TBX5b (DeBenedittis and Jiao, 2011). While only TBX5a can bind to the natriuretic peptide A (Nppa) promoter, both TBX5a and TBX5b can interact with GATA4 (Georges et al., 2008, DeBenedittis and Jiao, 2011). Additionally, TBX5a and TBX5b have differential cellular localization, with TBX5a being strictly nuclear localized while TBX5b is localized within the cytoplasm and nucleus (Georges et al., 2008). These studies indicate that relative levels, along with transcriptional targets and protein-protein interactions of each isoform must be examined in order to understand the resultant functions of alternatively spliced transcripts.

The TBX3 isoform ratios were found to be tissue and species specific (Stennard et al., 1999, Fan et al., 2004). Differing levels of TBX3 isoforms have also been reported in several breast cancer cell lines (Bamshad et al., 1999, Fan et al., 2004). Additionally, the ratio of TBX3iso2 to TBX3iso1 increased during osteogenic differentiation in human adipose stromal cells (Lee et al., 2007), thereby suggesting that isoform ratios are important in differentiation. Based on preliminary studies assessing functional differences between TBX3 isoforms, along

with details regarding differential properties of alternatively spliced T-box transcription factors, DeBenedittis et al. proposed that assessment of TBX3 isoform expression levels is of importance for future studies (DeBenedittis and Jiao, 2011).

Residues Ser224 and Met225 within the DNA binding domain of human TBX3iso1 have been shown to interact with target DNA sequences with the TBE through polar and hydrophobic interactions, respectively (see **Figure 1.3.1**) (Coll et al., 2002). The transcribed 2a exon within TBX3iso2 is located at residues 220-240; this alternative splicing event shifts the residues that interact with target DNA, while the effect on transcriptional regulation remains unclear.

Conflicting results have been published regarding functionality of the TBX3 isoforms. Fan et al. reported that TBX3iso2 did not bind to a sequence containing a previously-identified TBE in their *in vitro* oligonucleotide binding assays (Fan et al., 2004), proposing that the 20-amino acid addition in the DNA binding domain of TBX3iso2 alters the protein's binding to target sequences (Fan et al., 2004). Other studies have assessed TBX3iso1 and TBX3iso2 in various assays and found both isoforms to have similar functions *in vitro*, reporting that both TBX3 isoforms were able to bind to the TBE in the Nppa and $p21^{CIP1}$ promoters (Hoogaars et al., 2008). Hoogaars et al. proposed that since the 20-amino acid insertion does not make contact with DNA, it may not alter binding (Hoogaars et al., 2008).

The function of T-box proteins is regulated by protein-protein interactions with other transcription factors (Lu et al., 2010), several of which are mediated through the T-box domain. Some groups have therefore speculated that there may be differential protein-protein interactions between TBX3 isoforms. Through glutathione S-transferase (GST) pull down assays to examine TBX3iso1 and TBX3iso2 interacting proteins, it was revealed that both TBX3 isoforms physically interact with a known T-box interacting protein, NK2 homeobox 5 (Nkx2-5), via the T-box binding domain (Hoogaars et al., 2008). Additionally, while both TBX3 isoforms were able to inhibit transcription of Nanog in luciferase assays, only TBX3iso2 was able to directly bind to Nanog in co-immunoprecipitation experiments (Zhao et al., 2014). More work is therefore needed in order to evaluate which proteins TBX3 physically interacts with, and whether differences exist between isoforms.

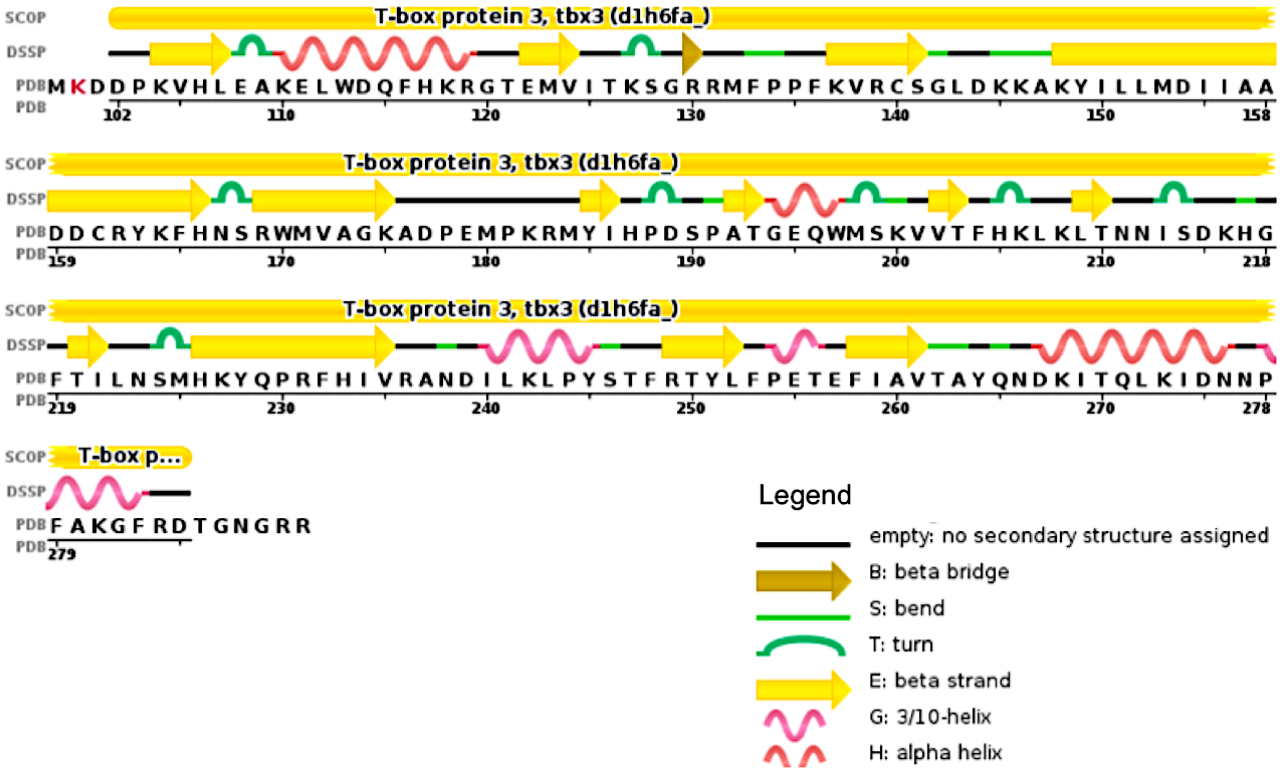

Figure 1.3.1 – TBX3 Protein Sequence Secondary Structure.

Protein structure of TBX3iso1 (with absence of 2a exon at residue 220-240) is shown above. Image was obtained from Protein Data Bank (PDB), available at https://www.rcsb.org.

1.4 **Epithelial-Mesenchymal Transition (EMT)**

Over 90% of cancer-related deaths are due to the process of metastasis (Luzzi et al., 1998, Kumar et al., 2013). Incredible phenotypic plasticity is required for malignant cells of epithelial origin to leave the primary tumor, intravasate into the blood or lymphatic vessels, and then extravasate at a distant secondary site and establish growth (Oltean and Bates, 2014). The acquisition of an epithelial-mesenchymal transition (EMT) phenotype plays an important role in systemic dissemination of cancer cells through the process of metastasis (Chaffer and Weinberg, 2011). In breast cancer specifically, the phenomenon of EMT has been associated with highly aggressive tumors and therapeutic resistance (Blick et al., 2008, Sarrió et al., 2008, Creighton et al., 2009, Polyak and Weinberg, 2009).

EMT is the process whereby epithelial cells lose apical-basal polarity, tight cell-to-cell contacts, and undergo remodelling of the actin cytoskeleton, with the acquisition of a more migratory mesenchymal phenotype. The process of EMT is critical in normal processes such as embryogenesis and wound healing, and is reactivated in invasive and metastatic tumors (Polyak and Weinberg, 2009, Thiery et al., 2009). The most studied transcription factors in the promotion of EMT include TWIST1, SNAIL (*SNAI1*), and SLUG (*SNAI2*) (Shapiro et al., 2011). SNAIL, SLUG and TWIST1 are frequently overexpressed in IDC and have been associated with histological grade, lymph node metastasis, and reduced survival (Blanco et al., 2002, Elloul et al., 2005, Martin et al., 2005, Mironchik et al., 2005, Côme et al., 2006, Palena et al., 2014, Alix-Panabières et al., 2017).

Several studies have shown that expression of EMT markers is associated with poor clinical outcome in several epithelial cancers, including breast cancer (Abba et al., 2004, Thompson et al., 2005, Sabbah et al., 2008, Shapiro et al., 2011, Sørlie et al., 2001). The induction of EMT is associated with alterations in canonical EMT markers, including up-regulation of the mesenchymal proteins vimentin (*VIM*) and N-cadherin (*CDH2*), as well as down-regulation of the epithelial protein E-cadherin (*CDH1*). Both E-cadherin and N-cadherin are members of the cadherin superfamily of cell adhesion molecules involved in homophilic cell-to-cell interactions. E-cadherin is an integral epithelial membrane protein that mediates cell-to-cell adhesion and is widely regarded as a major suppressor of motility and invasiveness of cancer cells (Le Bras et al., 2012). Several EMT transcription factors (SNAIL,

SLUG, ZEB1, ZEB2, Brachyury) are able to directly down-regulate E-cadherin expression (De Craene and Berx, 2013). Combined repression of other junctional proteins, along with E-cadherin, facilitates the de-differentiation program and induction of EMT (De Craene et al., 2005, Vandewalle et al., 2005, Moreno-Bueno et al., 2006, De Craene and Berx, 2013). The switch from E-cadherin to N-cadherin expression is associated with malignant progression and poor clinical outcome in several cancer types (Gravdal et al., 2007, Polyak and Weinberg, 2009). Up-regulation of N-cadherin enhances interaction between cancer cells and endothelial/stromal cells, thereby providing a mechanism for endothelial transmigration (Tran et al., 1999, Hazan et al., 2000).

EMT is also associated with suppression of apoptosis, cellular senescence, and chemo-resistance (Polyak and Weinberg, 2009, De Craene and Berx, 2013, Nieto et al., 2016). Additionally, several correlations have been documented relating expression of EMT markers and a stem-like phenotype, and response to breast cancer therapy (Mani et al., 2008, Morel et al., 2008, Aktas et al., 2009, Creighton et al., 2009). This is likely due to an enrichment of CSCs after standard breast cancer treatments including letrozole or docetaxel (Mani et al., 2008, Creighton et al., 2009).

Direct *in vivo* evidence for EMT has been challenging due to its dynamic and transient nature, as well as the reverse process, mesenchymal-epithelial transition (MET). The process of MET is believed to play a fundamental role once cells have extravasated from the vasculature into distant organs, allowing for clonal outgrowth (Alix-Panabières et al., 2017). While the process of EMT has been documented in mouse models (Oltean et al., 2008), many invasive tumors and metastatic lesions exhibit epithelial morphology and are positive for epithelial markers (Christiansen and Rajasekaran, 2006). This is likely attributed to partial induction of EMT, a restriction of the occurrence of this process to a small number of cells, and the reverse process of MET (Shapiro et al., 2011). The assessment of EMT markers would therefore only measure levels at one point in time, and has mostly been reported at the invasive front of primary tumors of epithelial origin (Scheel et al., 2007, Brabletz, 2012, Puisieux et al., 2014). Interestingly, studies assessing the importance of MET in metastatic colonization have reported that tumor cells that have undergone partial EMT possess the most malignant features (Nieto et al., 2016, Alix-Panabières et al., 2017).

1.4.1 **TBX3 and EMT**

An EMT phenotype is characterized by a cadherin switch, with reduced expression of the epithelial marker E-cadherin, and increased expression of the mesenchymal marker N-cadherin (Polyak and Weinberg, 2009). Importantly, TBX3 is able to directly repress E-cadherin expression levels, which has been documented in HCC and melanoma cell lines (Rodriguez et al., 2008, Dong et al., 2018).

High throughput analyses have linked elevated TBX3 expression with an EMT phenotype (Humtsoe et al., 2012). In this study, Humtsoe et al. conducted microarray analysis to examine gene expression differences between a panel of squamous cell carcinoma (SCC) cell lines displaying either a non-EMT or an EMT-like phenotype (Humtsoe et al., 2012). They revealed strong up-regulation of TBX3 in EMT-like SCC cells, as well as in a model of Snail-induced EMT (Humtsoe et al., 2012). Additionally, they reported a close association between high TBX3 and N-cadherin expression, and low E-cadherin expression across twelve SCC cell lines (Humtsoe et al., 2012), which has been recapitulated in colorectal cancer samples (Shan et al., 2015), and gastric cancer cell lines (Miao et al., 2016). Elevated TBX3 expression is also associated with increased vimentin expression (Krstic et al., 2016, Miao et al., 2016). Lastly, TBX3 was shown to drive a pro-EMT phenotype in *B-RAF* mutant melanomas (Boyd et al., 2013). These examples show that there is an abundance of preliminary studies showing a link between TBX3 and an EMT profile, although the molecular mechanisms remain elusive.

Other T-box transcription factors, including Brachyury and TBX2, are also able to induce EMT (Fernando et al., 2010, Wang et al., 2012). Brachyury directly represses E-cadherin by binding to a TBE in the transcription start site (De Craene and Berx, 2013, Fernando et al., 2010). This binding site in the E-cadherin transcription start site reported for Brachyury (Fernando et al., 2010) overlaps with the identified binding site for TBX3 (Rodriguez et al., 2008).

1.4.2 **SLUG**

SLUG (encoded by the *SNAI2* gene) is a member of the SNAIL family of zinc-finger transcriptional repressors which mediate sequence-specific interactions with DNA (Phillips and Kuperwasser, 2014). SLUG contains a conserved SNAG domain in the N-terminus region, which is required for protein-protein interactions, transcriptional repression, and nuclear localization (Shirley et al., 2010, Chiang and Ayyanathan, 2013, Phillips and Kuperwasser, 2014). The zinc finger domain is located in the C-terminus of the protein, which facilitates binding to E-box motifs (Nieto, 2002, Phillips and Kuperwasser, 2014).

The role of SLUG is well characterized in both embryonic development and tumorigenesis, with most of the literature focusing on its promotion of EMT (Barrallo-Gimeno and Nieto, 2005, Phillips and Kuperwasser, 2014). Physiologically, SLUG has been described as an important regulator of mammary epithelial cell differentiation, where it maintains cells in a basal-like state and repress luminal lineage differentiation (Proia et al., 2011, Phillips et al., 2014, Phillips and Kuperwasser, 2014). Additionally, SLUG plays a critical role in multiple stages of cancer development (Phillips and Kuperwasser, 2014), and has been described as an important early initiator of EMT (Slabáková et al., 2011).

Within breast cancers, elevated SLUG expression is often associated with basal-like tumors and mutations in the breast cancer associated 1 (*BRCA1*) gene (Foulkes et al., 2004, Arnes et al., 2005, Proia et al., 2011). While ER is able to directly repress transcription of SLUG (Ye et al., 2008, Ye et al., 2010), elevated estrogen levels are also able to induce SLUG expression through ERα; the effects mediated by ER on SLUG expression are therefore context-dependent. Elevated expression of SLUG, however, is associated with poor prognosis in both ER positive (Chimge et al., 2011), and ER negative breast cancers (Storci et al., 2008, Liu et al., 2013), as well as lymph node metastasis and therapy resistance (Côme et al., 2006, Alves et al., 2018). Interestingly, elevated SLUG expression in IDC has been associated with the presence of tubule structures, which is one of three criteria for the Scarff-Bloom-Richardson (SBR) grading system (Côme et al., 2006). This study by Côme et al., along with other experimental studies of partial induction of EMT (Dang et al., 2015), suggest the involvement of SLUG in collective cell migration.

1.5 **Angiogenesis**

Solid cancers must form a blood supply through the process of angiogenesis if they are to grow beyond 1-2 mm in size (Knowles and Selby, 2005). This value represents the distance that oxygen, nutrients, and wastes can diffuse freely between a tumor and adjacent blood vessels (Kumar et al., 2013). Angiogenesis is a hallmark of cancer, and the newly-formed blood vessels allow increased delivery of oxygen and nutrients, further providing a growth advantage for the tumor (Hanahan and Weinberg, 2000). Angiogenesis occurs through the formation of new micro-vessels from pre-existing vessels. This process also allows for systemic spread of cancer cells in the process of metastasis. Early studies assessing tumor angiogenesis in breast cancers showed that higher micro-vessel density corresponded to increased rates of distant metastasis (Weidner et al., 1991).

The process of angiogenesis is triggered by tissue hypoxia and/or injury. Angiogenic factors are then released in the microenvironment, which diffuse in the extracellular millieu and are then able to activate endothelial cells (Nishida et al., 2006). Endothelial cells then migrate to the hypoxic area, proliferate, and form vessel structures (Nishida et al., 2006). The process may continue to be influenced through the balance of pro- and anti-angiogenic signaling molecules present within the microenvironment, which dictate the degree of angiogenesis (Knowles and Selby, 2005).

The use of anti-angiogenic therapies for cancer treatment was first proposed by Folkman in 1971 (Folkman, 1971), and this initial proposal has paved the way to a large body of work investigating the role of angiogenesis in tumor growth, along with the effect of its inhibition (Knowles and Selby, 2005). The emerging conclusion from several studies was that anti-angiogenics would be given as an adjuvant therapy in combination with cytotoxic drugs (Knowles and Selby, 2005). To date, the best characterized pro-angiogenic factor has been VEGF. Other notable pro-angiogenic regulators include FGF, the transforming growth factor (TGF) superfamily, hypoxia inducible factor alpha (HIF1α) and osteopontin (OPN; described in **Section 1.5.1**).

1.5.1 **Osteopontin and Angiogenesis**

OPN is a secreted phosphoprotein that is involved in both cell attachment to the extracellular matrix (ECM) through interaction with integrins and CD44, and induction of cell signaling pathways (Rittling and Chambers, 2004). Following binding and receptor activation, a series of signaling pathways are initiated, ultimately resulting in gene expression changes which modulate tumor cell behaviour. Elevated OPN expression has been associated with all six initially-described hallmarks of cancer in several different cancer subtypes (Cook et al., 2005). For breast cancer specifically, elevated OPN expression is associated with early metastasis and poor outcome (Bellahcène and Castronovo, 1995, Rudland et al., 2002, Bramwell et al., 2006, El-Tanani et al., 2006, Tuck et al., 1998, Singhal et al., 1997).

OPN modulates cell migration, invasion, and survival; this is mainly accomplished through interaction with integrins through its arginine-glycine-aspartate (RGD) integrin binding domain (Denhardt and Chambers, 1994, Tuck et al., 1999, Sodek et al., 2000, Lin and Yang-Yen, 2001, Geissinger et al., 2002). Integrins are transmembrane molecules comprised of a heterodimeric α and ß subunits that function by mediating adhesion between cells and interactions with the ECM (Knowles and Selby, 2005). OPN binds to the integrin heterodimers $\alpha_v\beta_1$, $\alpha_v\beta_3$, $\alpha_v\beta_5$, $\alpha_4\beta_1$, $\alpha_5\beta_1$, $\alpha_8\beta_1$, and $\alpha_9\beta_1$ (Wai and Kuo, 2004, El-Tanani et al., 2006). Several of the aforementioned integrins are associated with metastasis and poor outcome, with much of the literature focusing on $\alpha_v\beta_3$ (El-Tanani et al., 2006). In breast cancers, up-regulation of $\alpha_v\beta_3$ is correlated with extent of disease and presence of bone metastasis (Liapis et al., 1996, Gasparini et al., 1998). OPN binds to the transmembrane protein CD44 in an RGD-independent manner (Sodek et al., 2000), resulting in up-regulation of CD44 and increased migration of breast cancer cell lines (Khan et al., 2005). A schematic of OPN protein structure and interactions is shown in **Figure 1.5.1**.

Several studies have also reported crucial roles for tumor-derived OPN on angiogenesis (Pröls et al., 1998, Shijubo et al., 1999, Takano et al., 2000, Asou et al., 2001, Takahashi et al., 2002, Hirama et al., 2003, Leali et al., 2003, Cook et al., 2005, Chakraborty et al., 2006, Chakraborty et al., 2008). While integrins are minimally expressed on the surface of endothelial cells, their expression is significantly up-regulated during angiogenesis (Knowles and Selby, 2005). Binding of OPN within the tumor microenvironment to integrin

receptors (and/or CD44) on endothelial cells promotes angiogenesis through stimulation of endothelial cell migration, survival and lumen formation (Brooks et al., 1994, Senger et al., 1996, Arap et al., 1998, Scatena et al., 1998, Bayless et al., 2000). OPN-induction of VEGF has also been reported (Chakraborty et al., 2008), as well as the reciprocal instance of VEGF-induced OPN expression (Senger et al., 1996). Moreover, OPN, in cooperation with VEGF, has been shown to mediate α_v integrin endothelial cell migration (Senger et al., 1996).

Microarray analysis of transcripts altered upon constitutive OPN overexpression in breast cancer cells detected up-regulation of several genes, including hyaluronan synthase 2 (HAS2) and increased production of hyaluronan (HA), which also mediates the process of angiogenesis (discussed in the **Section 1.5.2)** (Cook et al., 2005).

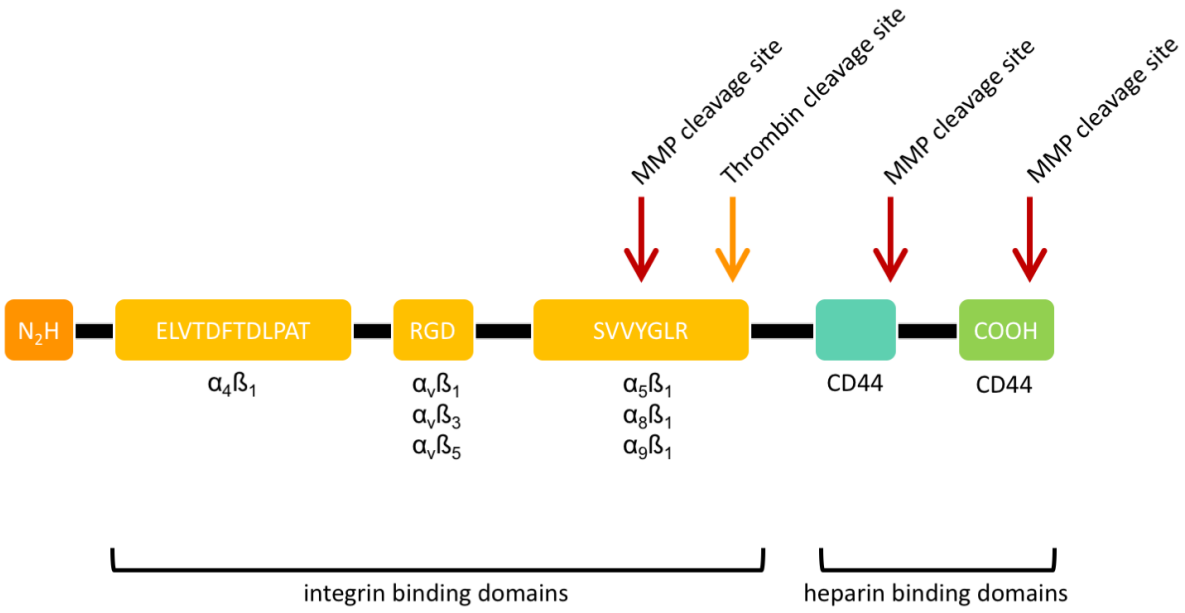

Figure 1.5.1 – OPN protein structure and interactions.

OPN contains many protein domains which facilitate interactions with receptor proteins, including the integrin binding domains (amino acid sequence for the domains is shown), along with the heparin binding domains which facilitates binding to CD44. OPN can be cleaved by two classes of proteases, including thrombin and MMPs, with the cleavage exposing new active domains. Adapted from (Musso et al., 2013).

1.5.2 **Hyaluronan and Angiogenesis**

The ECM plays a critical role in tumor development, providing cells with a scaffold which can be used for attachment, migration, and growth. An important ECM component that is up-regulated by OPN is HA, via up-regulation of HAS2 (Cook et al., 2006). HA is an unbranched polysaccharide consisting of repeating disaccharide subunits and constitutes a major portion of the ECM, particularly in tissues undergoing high rates of proliferation (West and Kumar, 1989). HA regulates the processes of adhesion, migration, proliferation, and differentiation (Itano et al., 1999, Tammi et al., 2002, Toole, 2004, Cook et al., 2006). HA is also able to up-regulate expression of OPN (Kim et al., 2005). Interestingly, both HA and OPN mediate several overlapping functions, and are frequently co-expressed across cancer subtypes (Kim et al., 2005, Lee et al., 2007).

HA is produced at the intracellular face of the plasma membrane by hyaluronan synthase enzymes (HAS1-3) (Weigel and DeAngelis, 2007). The HAS enzymes are distinct in their stability, elongation rate, and size of HA synthesized, along with distinct expression patterns (Itano et al., 1999). Once synthesized by HAS enzymes, HA is then extruded from the cell and either released into the microenvironment, or retained in pericellular coats through interaction with cell surface receptors (Tammi et al., 1998, Evanko et al., 2007, Weigel and DeAngelis, 2007). High levels of synthesis and retention of HA in pericellular coats has an important role in malignant progression (Cook et al., 2006) and is an indicator of poor prognosis in epithelial cancers (Auvinen et al., 2000, Misra et al., 2006, Tammi et al., 2008, Auvinen et al., 2014). HAS2 is the highest expressed among the HAS enzymes in breast cancer tissues and cell lines (Udabage et al., 2005b, Auvinen et al., 2014). Elevated HAS2 expression in breast cancer is associated with invasiveness (Udabage et al., 2005b, Udabage et al., 2005a), induction of EMT (Zoltan-Jones et al., 2003, Porsch et al., 2013), induction of angiogenesis (Koyama et al., 2007), and promotion of metastasis through increased interaction with stromal cells (Cook et al., 2006, Okuda et al., 2012).

The effect of HA on angiogenesis is dependent on its molecular weight, which imparts unique biochemical properties; high molecular weight HA suppresses angiogenesis, while low molecular weight HA (4-20 disaccharides) stimulates endothelial cell migration, proliferation and angiogenesis (West et al., 1985, West and Kumar, 1989). The effect of HA within a tumor is thought to be dynamic; the leading edge of a tumor possesses large

amounts of high molecular weight HA, which aids in invasion via hydration of tissues and expansion of areas through which cancer cells can migrate (Iozzo and Müller-Glauser, 1985, Knudson et al., 1989, Rooney et al., 1995). As the tumor cells invade adjacent tissues, new HA is synthesized, while the remaining HA is degraded by hyaluronidase (HAse) enzymes, creating pro-angiogenic low molecular weight fragments (Rooney et al., 1995).

CD44 is a transmembrane glycoprotein and the principal receptor for HA (Toole, 2009, Auvinen et al., 2013). CD44 is also able to bind several other ligands including OPN, collagens, and MMPs (Goodison et al., 1999, Senbanjo and Chellaiah, 2017). CD44 is ubiquitously expressed in adult and fetal tissues, with elevated expression levels in several cancers (Basakran, 2015). In breast cancer, elevated expression of standard CD44 as well as its splice variants is associated with disease progression and metastasis (McFarlane et al., 2015). Interaction between HA and CD44 results in activation of several signaling pathways (Misra et al., 2006, Toole, 2009). Additionally, HA is able to regulate the activity of several RTKs (most notably HER2) through stabilization of oncogenic CD44/RTK cell surface complexes (Bourguignon et al., 2001, Turley et al., 2002, Ghatak et al., 2005, Misra et al., 2005, Bourguignon et al., 2006, Misra et al., 2006, Slomiany et al., 2009).

The tumor stroma of breast cancer patients is associated with high HA expression near carcinoma cells, which is associated with several clinicopathological features including tumor size, lymph node positivity, and poor differentiation (Auvinen et al., 2013). CD44 is expressed on endothelial cells (Liesveld et al., 1994, Xu et al., 1994), and binding of HA to CD44 on endothelial cells promotes their migration (Trochon et al., 1996, Griffioen et al., 1997, Savani et al., 2001). This provides a mechanism for HA- as well as OPN-induced angiogenesis, as OPN is able to promote elevated HA levels and itself bind CD44 on endothelial cells (Trochon et al., 1996, Griffioen et al., 1997, Savani et al., 2001, Kim et al., 2005, Cook et al., 2006, Lee et al., 2007).

1.6 Summary of Objectives

I hypothesized that the transcriptional regulatory proteins TBX3iso1 and TBX3iso2 have distinct roles in breast cancer progression. This activity is mediated by their downstream transcriptional targets.

To address my hypothesis, I had four main aims which are described over three chapters of my thesis:

Aim 1: Examination of functional and phenotypic changes associated with modulation of TBX3 levels at various stages of breast cancer progression (Chapter 2).

While TBX3 is overexpressed in several cancer types, the full scope of TBX3-associated functional changes in breast cancer was unclear due to the focus on melanoma cell lines within several prominent studies. Initial studies were therefore important in order to characterize the functional and phenotypic changes associated with modulation of TBX3 levels at various stages of breast cancer progression, in an isoform-specific context. The majority of my work has focused on non-invasive DCIS-like 21NT cells and invasive IDC-like 21MT-1 cells, in which increased TBX3 expression was identified in the DCIS to IDC transition (Souter et al., 2010). These findings have been corroborated through functional overexpression studies in 21PT, MCF7, T-47D, SKBR3, and MDA-MB-468 cells. Several prominent TBX3iso1 and TBX3iso2-dependent changes were observed, including alterations in growth, survival, invasiveness, and prominently, the acquisition of an EMT phenotype.

Aims 2 & 3: Elucidation of the molecular mechanism of TBX3-induced EMT, and assessment of identified downstream targets (SLUG, TWIST1) in clinical samples of DCIS and early invasive breast cancer (Chapter 3).

As a follow-up to Aim 1, the molecular mechanism of TBX3-induced EMT was investigated in Aim 2. High throughput studies, including ChIP-array and RNA-Seq, were conducted in order to gain a thorough understanding of both direct and indirect transcriptional changes

mediated by TBX3 isoform overexpression, with a focus on genes similarly altered with both TBX3 isoforms. SLUG was identified as a direct target up-regulated by both TBX3iso1 and TBX3iso2, and an important downstream mediator of TBX3-induced migration and invasion. Another important regulator of EMT indirectly up-regulated by both TBX3 isoforms was TWIST1. For Aim 3, the expression of TBX3 by IHC was assessed in two independent cohorts consisting of early stage breast cancers. Within the second cohort, expression of downstream targets identified in the high-throughput screens (SLUG and TWIST1) was also assessed by IHC. My findings from Aims 2 and 3 are reported together in Chapter 3, with a working schematic on the mechanism whereby TBX3 promotes progression by inducing EMT in low-grade, pre-invasive lesions, which is representative of luminal A breast cancers.

Aim 4: Examination of the effects of TBX3 isoforms *in vivo* in nude mice (Chapter 4).

As overexpression of TBX3 was previously identified in the DCIS to IDC transition, the effect of altered TBX3 expression on *in vivo* tumorigenesis was assessed in nude mice via mammary fat pad xenograft assays. Surprisingly, TBX3iso1 and TBX3iso2 differentially altered tumorigenicity, with overexpression of TBX3iso1 (but not TBX3iso2) in 21NT cells associated with high rates of invasive carcinoma. The mechanism of TBX3iso1-induced tumorigenicity was assessed through further mining and enrichment analysis of RNA-Seq data obtained in Aim 2. Interestingly, TBX3iso1 overexpression was associated with a pro-angiogenic gene signature, with elevated expression of OPN and HAS2, increased hyaluronan retention, and thus increased rates of angiogenesis through *in vitro* assays. These changes likely explain the differential tumorigenicity between TBX3 isoforms *in vivo*.

1.7 **References**

Abba, M. C., Drake, J. A., Hawkins, K. A., Hu, Y., Sun, H., Notcovich, C., Gaddis, S., Sahin, A., Baggerly, K. and Aldaz, C. M. (2004) 'Transcriptomic changes in human breast cancer progression as determined by serial analysis of gene expression', *Breast Cancer Res,* 6(5), pp. R499-513.

Abba, M. C., Gong, T., Lu, Y., Lee, J., Zhong, Y., Lacunza, E., Butti, M., Takata, Y., Gaddis, S., Shen, J., Estecio, M. R., Sahin, A. A. and Aldaz, C. M. (2015) 'A Molecular Portrait of High-Grade Ductal Carcinoma In Situ', *Cancer Res,* 75(18), pp. 3980-90.

Abdel-Fatah, T. M., Powe, D. G., Hodi, Z., Reis-Filho, J. S., Lee, A. H. and Ellis, I. O. (2008) 'Morphologic and molecular evolutionary pathways of low nuclear grade invasive breast cancers and their putative precursor lesions: further evidence to support the concept of low nuclear grade breast neoplasia family', *Am J Surg Pathol,* 32(4), pp. 513-23.

Agulnik, S. I., Garvey, N., Hancock, S., Ruvinsky, I., Chapman, D. L., Agulnik, I., Bollag, R., Papaioannou, V. and Silver, L. M. (1996) 'Evolution of mouse T-box genes by tandem duplication and cluster dispersion', *Genetics,* 144(1), pp. 249-54.

Ahmad, A. (2013) *Breast cancer metastasis and drug resistance : progress and prospects.* New York: Springer.

Aktas, B., Tewes, M., Fehm, T., Hauch, S., Kimmig, R. and Kasimir-Bauer, S. (2009) 'Stem cell and epithelial-mesenchymal transition markers are frequently overexpressed in circulating tumor cells of metastatic breast cancer patients', *Breast Cancer Res,* 11(4), pp. R46.

Alix-Panabières, C., Mader, S. and Pantel, K. (2017) 'Epithelial-mesenchymal plasticity in circulating tumor cells', *J Mol Med (Berl),* 95(2), pp. 133-142.

Allegra, C. J., Aberle, D. R., Ganschow, P., Hahn, S. M., Lee, C. N., Millon-Underwood, S., Pike, M. C., Reed, S. D., Saftlas, A. F., Scarvalone, S. A., Schwartz, A. M., Slomski, C., Yothers, G. and Zon, R. (2010) 'National Institutes of Health State-of-the-Science Conference statement: Diagnosis and Management of Ductal Carcinoma In Situ September 22-24, 2009', *J Natl Cancer Inst,* 102(3), pp. 161-9.

Allred, D. C., Mohsin, S. K. and Fuqua, S. A. (2001) 'Histological and biological evolution of human premalignant breast disease', *Endocr Relat Cancer,* 8(1), pp. 47-61.

Allred, D. C., Wu, Y., Mao, S., Nagtegaal, I. D., Lee, S., Perou, C. M., Mohsin, S. K., O'Connell, P., Tsimelzon, A. and Medina, D. (2008) 'Ductal carcinoma in situ and the emergence of diversity during breast cancer evolution', *Clin Cancer Res,* 14(2), pp. 370-8.

Alves, C. L., Elias, D., Lyng, M. B., Bak, M. and Ditzel, H. J. (2018) 'SNAI2 upregulation is associated with an aggressive phenotype in fulvestrant-resistant breast cancer cells and is an indicator of poor response to endocrine therapy in estrogen receptor-positive metastatic breast cancer', *Breast Cancer Res,* 20(1), pp. 60.

Amari, M., Suzuki, A., Moriya, T., Yoshinaga, K., Amano, G., Sasano, H., Ohuchi, N., Satomi, S. and Horii, A. (1999) 'LOH analyses of premalignant and malignant lesions of human breast: frequent LOH in 8p, 16q, and 17q in atypical ductal hyperplasia', *Oncol Rep,* 6(6), pp. 1277-80.

Amir, S., Simion, C., Umeh-Garcia, M., Krig, S., Moss, T., Carraway, K. L. and Sweeney, C. (2016) 'Regulation of the T-box transcription factor Tbx3 by the tumour suppressor microRNA-206 in breast cancer', *Br J Cancer,* 114(10), pp. 1125-34.

Arap, W., Pasqualini, R. and Ruoslahti, E. (1998) 'Cancer treatment by targeted drug delivery to tumor vasculature in a mouse model', *Science,* 279(5349), pp. 377-80.

Arendt, L. M., St Laurent, J., Wronski, A., Caballero, S., Lyle, S. R., Naber, S. P. and Kuperwasser, C. (2014) 'Human breast progenitor cell numbers are regulated by WNT and TBX3', *PLoS One,* 9(10), pp. e111442.

Arnes, J. B., Brunet, J. S., Stefansson, I., Bégin, L. R., Wong, N., Chappuis, P. O., Akslen, L. A. and Foulkes, W. D. (2005) 'Placental cadherin and the basal epithelial phenotype of BRCA1-related breast cancer', *Clin Cancer Res,* 11(11), pp. 4003-11.

Asou, Y., Rittling, S. R., Yoshitake, H., Tsuji, K., Shinomiya, K., Nifuji, A., Denhardt, D. T. and Noda, M. (2001) 'Osteopontin facilitates angiogenesis, accumulation of osteoclasts, and resorption in ectopic bone', *Endocrinology,* 142(3), pp. 1325-32.

Aswad, L., Yenamandra, S. P., Ow, G. S., Grinchuk, O., Ivshina, A. V. and Kuznetsov, V. A. (2015) 'Genome and transcriptome delineation of two major oncogenic pathways governing invasive ductal breast cancer development', *Oncotarget,* 6(34), pp. 36652-74.

Auvinen, P., Rilla, K., Tumelius, R., Tammi, M., Sironen, R., Soini, Y., Kosma, V. M., Mannermaa, A., Viikari, J. and Tammi, R. (2014) 'Hyaluronan synthases (HAS1-3) in stromal and malignant cells correlate with breast cancer grade and predict patient survival', *Breast Cancer Res Treat,* 143(2), pp. 277-86.

Auvinen, P., Tammi, R., Kosma, V. M., Sironen, R., Soini, Y., Mannermaa, A., Tumelius, R., Uljas, E. and Tammi, M. (2013) 'Increased hyaluronan content and stromal cell CD44 associate with HER2 positivity and poor prognosis in human breast cancer', *Int J Cancer,* 132(3), pp. 531-9.

Auvinen, P., Tammi, R., Parkkinen, J., Tammi, M., Agren, U., Johansson, R., Hirvikoski, P., Eskelinen, M. and Kosma, V. M. (2000) 'Hyaluronan in peritumoral stroma and malignant cells associates with breast cancer spreading and predicts survival', *Am J Pathol,* 156(2), pp. 529-36.

Azzopardi, J. G., Ahmed, A. and Millis, R. R. (1979) 'Problems in breast pathology', *Major Probl Pathol,* 11, pp. i-xvi, 1-466.

Balaguer, F., Link, A., Lozano, J. J., Cuatrecasas, M., Nagasaka, T., Boland, C. R. and Goel, A. (2010) 'Epigenetic silencing of miR-137 is an early event in colorectal carcinogenesis', *Cancer Res,* 70(16), pp. 6609-18.

Bamshad, M., Le, T., Watkins, W. S., Dixon, M. E., Kramer, B. E., Roeder, A. D., Carey, J. C., Root, S., Schinzel, A., Van Maldergem, L., Gardner, R. J., Lin, R. C., Seidman, C. E., Seidman, J. G., Wallerstein, R., Moran, E., Sutphen, R., Campbell, C. E. and Jorde, L. B. (1999) 'The spectrum of mutations in TBX3: Genotype/Phenotype relationship in ulnar-mammary syndrome', *Am J Hum Genet,* 64(6), pp. 1550-62.

Bamshad, M., Lin, R. C., Law, D. J., Watkins, W. C., Krakowiak, P. A., Moore, M. E., Franceschini, P., Lala, R., Holmes, L. B., Gebuhr, T. C., Bruneau, B. G., Schinzel, A., Seidman, J. G., Seidman, C. E. and Jorde, L. B. (1997) 'Mutations in human TBX3 alter limb, apocrine and genital development in ulnar-mammary syndrome', *Nat Genet,* 16(3), pp. 311-5.

Band, V. and Sager, R. (1989) 'Distinctive traits of normal and tumor-derived human mammary epithelial cells expressed in a medium that supports long-term growth of both cell types', *Proc Natl Acad Sci U S A,* 86(4), pp. 1249-53.

Band, V., Zajchowski, D., Stenman, G., Morton, C. C., Kulesa, V., Connolly, J. and Sager, R. (1989) 'A newly established metastatic breast tumor cell line with integrated amplified copies of ERBB2 and double minute chromosomes', *Genes Chromosomes Cancer,* 1(1), pp. 48-58.

Band, V., Zajchowski, D., Swisshelm, K., Trask, D., Kulesa, V., Cohen, C., Connolly, J. and Sager, R. (1990) 'Tumor progression in four mammary epithelial cell lines derived from the same patient', *Cancer Res,* 50(22), pp. 7351-7.

Barrallo-Gimeno, A. and Nieto, M. A. (2005) 'The Snail genes as inducers of cell movement and survival: implications in development and cancer', *Development,* 132(14), pp. 3151-61.

Barsky, S. H. and Karlin, N. J. (2005) 'Myoepithelial cells: autocrine and paracrine suppressors of breast cancer progression', *J Mammary Gland Biol Neoplasia,* 10(3), pp. 249-60.

Bartel, D. P. (2004) 'MicroRNAs: genomics, biogenesis, mechanism, and function', *Cell,* 116(2), pp. 281-97.

Bartlett, J. M., Nofech-Moses, S. and Rakovitch, E. (2014) 'Ductal carcinoma in situ of the breast: can biomarkers improve current management?', *Clin Chem,* 60(1), pp. 60-7.

Basakran, N. S. (2015) 'CD44 as a potential diagnostic tumor marker', *Saudi Med J,* 36(3), pp. 273-9.

Baxter, N. N., Virnig, B. A., Durham, S. B. and Tuttle, T. M. (2004) 'Trends in the treatment of ductal carcinoma in situ of the breast', *J Natl Cancer Inst,* 96(6), pp. 443-8.

Bayless, K. J., Salazar, R. and Davis, G. E. (2000) 'RGD-dependent vacuolation and lumen formation observed during endothelial cell morphogenesis in three-dimensional fibrin matrices involves the alpha(v)beta(3) and alpha(5)beta(1) integrins', *Am J Pathol,* 156(5), pp. 1673-83.

Begum, S. and Papaioannou, V. E. (2011) 'Dynamic expression of Tbx2 and Tbx3 in developing mouse pancreas', *Gene Expr Patterns,* 11(8), pp. 476-83.

Bellahcène, A. and Castronovo, V. (1995) 'Increased expression of osteonectin and osteopontin, two bone matrix proteins, in human breast cancer', *Am J Pathol,* 146(1), pp. 95-100.

Bentley, D. L. (2005) 'Rules of engagement: co-transcriptional recruitment of pre-mRNA processing factors', *Curr Opin Cell Biol,* 17(3), pp. 251-6.

Bijker, N., Meijnen, P., Peterse, J. L., Bogaerts, J., Van Hoorebeeck, I., Julien, J. P., Gennaro, M., Rouanet, P., Avril, A., Fentiman, I. S., Bartelink, H., Rutgers, E. J., Group, E. B. C. C. and Group, E. R. (2006) 'Breast-conserving treatment with or without radiotherapy in ductal carcinoma-in-situ: ten-year results of European Organisation for Research and Treatment of Cancer randomized phase III trial 10853--a study by the EORTC Breast Cancer Cooperative Group and EORTC Radiotherapy Group', *J Clin Oncol,* 24(21), pp. 3381-7.

Bijker, N., Peterse, J. L., Duchateau, L., Julien, J. P., Fentiman, I. S., Duval, C., Di Palma, S., Simony-Lafontaine, J., de Mascarel, I. and van de Vijver, M. J. (2001) 'Risk factors for recurrence and metastasis after breast-conserving therapy for ductal carcinoma-in-situ: analysis of European Organization for Research and Treatment of Cancer Trial 10853', *J Clin Oncol,* 19(8), pp. 2263-71.

Biswas, D. K., Averboukh, L., Sheng, S., Martin, K., Ewaniuk, D. S., Jawde, T. F., Wang, F. and Pardee, A. B. (1998) 'Classification of breast cancer cells on the basis of a functional assay for estrogen receptor', *Mol Med,* 4(7), pp. 454-67.

Biswas, D. K., Cruz, A., Pettit, N., Mutter, G. L. and Pardee, A. B. (2001) 'A therapeutic target for hormone-independent estrogen receptor-positive breast cancers', *Mol Med,* 7(1), pp. 59-67.

Blanco, M. J., Moreno-Bueno, G., Sarrio, D., Locascio, A., Cano, A., Palacios, J. and Nieto, M. A. (2002) 'Correlation of Snail expression with histological grade and lymph node status in breast carcinomas', *Oncogene,* 21(20), pp. 3241-6.

Blencowe, B. J. (2006) 'Alternative splicing: new insights from global analyses', *Cell,* 126(1), pp. 37-47.

Blick, T., Widodo, E., Hugo, H., Waltham, M., Lenburg, M. E., Neve, R. M. and Thompson, E. W. (2008) 'Epithelial mesenchymal transition traits in human breast cancer cell lines', *Clin Exp Metastasis,* 25(6), pp. 629-42.

Bollag, R. J., Siegfried, Z., Cebra-Thomas, J. A., Garvey, N., Davison, E. M. and Silver, L. M. (1994) 'An ancient family of embryonically expressed mouse genes sharing a conserved protein motif with the T locus', *Nat Genet,* 7(3), pp. 383-9.

Bombonati, A. and Sgroi, D. C. (2011) 'The molecular pathology of breast cancer progression', *J Pathol,* 223(2), pp. 307-17.

Boogerd, C. J., Wong, L. Y., van den Boogaard, M., Bakker, M. L., Tessadori, F., Bakkers, J., 't Hoen, P. A., Moorman, A. F., Christoffels, V. M. and Barnett, P. (2011) 'Sox4 mediates Tbx3 transcriptional regulation of the gap junction protein Cx43', *Cell Mol Life Sci,* 68(23), pp. 3949-61.

Bourguignon, L. Y., Gilad, E., Brightman, A., Diedrich, F. and Singleton, P. (2006) 'Hyaluronan-CD44 interaction with leukemia-associated RhoGEF and epidermal growth factor receptor promotes Rho/Ras co-activation, phospholipase C epsilon-Ca2+ signaling, and cytoskeleton modification in head and neck squamous cell carcinoma cells', *J Biol Chem,* 281(20), pp. 14026-40.

Bourguignon, L. Y., Zhu, H., Zhou, B., Diedrich, F., Singleton, P. A. and Hung, M. C. (2001) 'Hyaluronan promotes CD44v3-Vav2 interaction with Grb2-p185(HER2) and induces Rac1 and Ras signaling during ovarian tumor cell migration and growth', *J Biol Chem,* 276(52), pp. 48679-92.

Boyages, J., Delaney, G. and Taylor, R. (1999) 'Predictors of local recurrence after treatment of ductal carcinoma in situ: a meta-analysis', *Cancer,* 85(3), pp. 616-28.

Boyd, S. C., Mijatov, B., Pupo, G. M., Tran, S. L., Gowrishankar, K., Shaw, H. M., Goding, C. R., Scolyer, R. A., Mann, G. J., Kefford, R. F., Rizos, H. and Becker, T. M. (2013) 'Oncogenic B-RAF(V600E) signaling induces the T-Box3 transcriptional repressor to repress E-cadherin and enhance melanoma cell invasion', *J Invest Dermatol,* 133(5), pp. 1269-77.

Brabletz, T. (2012) 'To differentiate or not--routes towards metastasis', *Nat Rev Cancer,* 12(6), pp. 425-36.

Bramwell, V. H., Doig, G. S., Tuck, A. B., Wilson, S. M., Tonkin, K. S., Tomiak, A., Perera, F., Vandenberg, T. A. and Chambers, A. F. (2006) 'Serial plasma osteopontin levels have prognostic value in metastatic breast cancer', *Clin Cancer Res,* 12(11 Pt 1), pp. 3337-43.

Bratthauer, G. L. and Tavassoli, F. A. (2004) 'Assessment of lesions coexisting with various grades of ductal intraepithelial neoplasia of the breast', *Virchows Arch,* 444(4), pp. 340-4.

Bray, F., McCarron, P. and Parkin, D. M. (2004) 'The changing global patterns of female breast cancer incidence and mortality', *Breast Cancer Res,* 6(6), pp. 229-39.

Brooks, P. C., Montgomery, A. M., Rosenfeld, M., Reisfeld, R. A., Hu, T., Klier, G. and Cheresh, D. A. (1994) 'Integrin alpha v beta 3 antagonists promote tumor regression by inducing apoptosis of angiogenic blood vessels', *Cell,* 79(7), pp. 1157-64.

Brummelkamp, T. R., Kortlever, R. M., Lingbeek, M., Trettel, F., MacDonald, M. E., van Lohuizen, M. and Bernards, R. (2002) 'TBX-3, the gene mutated in Ulnar-Mammary Syndrome, is a negative regulator of p19ARF and inhibits senescence', *J Biol Chem,* 277(8), pp. 6567-72.

Brunner, A. L., Li, J., Guo, X., Sweeney, R. T., Varma, S., Zhu, S. X., Li, R., Tibshirani, R. and West, R. B. (2014) 'A shared transcriptional program in early breast neoplasias despite genetic and clinical distinctions', *Genome Biol,* 15(5), pp. R71.

Buerger, H., Mommers, E. C., Littmann, R., Simon, R., Diallo, R., Poremba, C., Dockhorn-Dworniczak, B., van Diest, P. J. and Boecker, W. (2001) 'Ductal invasive G2 and G3 carcinomas of the breast are the end stages of at least two different lines of genetic evolution', *J Pathol,* 194(2), pp. 165-70.

Buerger, H., Otterbach, F., Simon, R., Poremba, C., Diallo, R., Decker, T., Riethdorf, L., Brinkschmidt, C., Dockhorn-Dworniczak, B. and Boecker, W. (1999) 'Comparative genomic hybridization of ductal carcinoma in situ of the breast-evidence of multiple genetic pathways', *J Pathol,* 187(4), pp. 396-402.

Bürger, H., de Boer, M., van Diest, P. J. and Korsching, E. (2013) 'Chromosome 16q loss--a genetic key to the understanding of breast carcinogenesis', *Histol Histopathol,* 28(3), pp. 311-20.

Burgucu, D., Guney, K., Sahinturk, D., Ozbudak, I. H., Ozel, D., Ozbilim, G. and Yavuzer, U. (2012) 'Tbx3 represses PTEN and is over-expressed in head and neck squamous cell carcinoma', *BMC Cancer,* 12, pp. 481.

Burstein, H. J., Polyak, K., Wong, J. S., Lester, S. C. and Kaelin, C. M. (2004) 'Ductal carcinoma in situ of the breast', *N Engl J Med,* 350(14), pp. 1430-41.

Calhoun, B. C., Sobel, A., White, R. L., Gromet, M., Flippo, T., Sarantou, T. and Livasy, C. A. (2015) 'Management of flat epithelial atypia on breast core biopsy may be individualized based on correlation with imaging studies', *Mod Pathol,* 28(5), pp. 670-6.

Canadian Cancer Society, N. C. I. o. C., Advisory Committee on Records and Registries 2017. Canadian cancer statistics. Toronto: Canadian Cancer Society.

Cantley, L. C. and Neel, B. G. (1999) 'New insights into tumor suppression: PTEN suppresses tumor formation by restraining the phosphoinositide 3-kinase/AKT pathway', *Proc Natl Acad Sci U S A,* 96(8), pp. 4240-5.

Cardiff, R. D., Moghanaki, D. and Jensen, R. A. (2000) 'Genetically engineered mouse models of mammary intraepithelial neoplasia', *J Mammary Gland Biol Neoplasia,* 5(4), pp. 421-37.

Carlson, H., Ota, S., Campbell, C. E. and Hurlin, P. J. (2001) 'A dominant repression domain in Tbx3 mediates transcriptional repression and cell immortalization: relevance to mutations in Tbx3 that cause ulnar-mammary syndrome', *Hum Mol Genet,* 10(21), pp. 2403-13.

Carlson, H., Ota, S., Song, Y., Chen, Y. and Hurlin, P. J. (2002) 'Tbx3 impinges on the p53 pathway to suppress apoptosis, facilitate cell transformation and block myogenic differentiation', *Oncogene,* 21(24), pp. 3827-35.

Casey, E. S., O'Reilly, M. A., Conlon, F. L. and Smith, J. C. (1998) 'The T-box transcription factor Brachyury regulates expression of eFGF through binding to a non-palindromic response element', *Development,* 125(19), pp. 3887-94.

Cavard, C., Audebourg, A., Letourneur, F., Audard, V., Beuvon, F., Cagnard, N., Radenen, B., Varlet, P., Vacher-Lavenu, M. C., Perret, C. and Terris, B. (2009) 'Gene expression profiling provides insights into the pathways involved in solid pseudopapillary neoplasm of the pancreas', *J Pathol,* 218(2), pp. 201-9.

Chaffer, C. L. and Weinberg, R. A. (2011) 'A perspective on cancer cell metastasis', *Science,* 331(6024), pp. 1559-64.

Chakraborty, G., Jain, S., Behera, R., Ahmed, M., Sharma, P., Kumar, V. and Kundu, G. C. (2006) 'The multifaceted roles of osteopontin in cell signaling, tumor progression and angiogenesis', *Curr Mol Med,* 6(8), pp. 819-30.

Chakraborty, G., Jain, S. and Kundu, G. C. (2008) 'Osteopontin promotes vascular endothelial growth factor-dependent breast tumor growth and angiogenesis via autocrine and paracrine mechanisms', *Cancer Res,* 68(1), pp. 152-61.

Chen, H., Shalom-Feuerstein, R., Riley, J., Zhang, S. D., Tucci, P., Agostini, M., Aberdam, D., Knight, R. A., Genchi, G., Nicotera, P., Melino, G. and Vasa-Nicotera, M. (2010) 'miR-7 and miR-214 are specifically expressed during neuroblastoma differentiation, cortical development and embryonic stem cells differentiation, and control neurite outgrowth in vitro', *Biochem Biophys Res Commun,* 394(4), pp. 921-7.

Chiang, C. and Ayyanathan, K. (2013) 'Snail/Gfi-1 (SNAG) family zinc finger proteins in transcription regulation, chromatin dynamics, cell signaling, development, and disease', *Cytokine Growth Factor Rev,* 24(2), pp. 123-31.

Chimge, N. O., Baniwal, S. K., Little, G. H., Chen, Y. B., Kahn, M., Tripathy, D., Borok, Z. and Frenkel, B. (2011) 'Regulation of breast cancer metastasis by Runx2 and estrogen signaling: the role of SNAI2', *Breast Cancer Res,* 13(6), pp. R127.

Cho, K. W., Kwon, H. J., Shin, J. O., Lee, J. M., Cho, S. W., Tickle, C. and Jung, H. S. (2012) 'Retinoic acid signaling and the initiation of mammary gland development', *Dev Biol,* 365(1), pp. 259-66.

Christiansen, J. J. and Rajasekaran, A. K. (2006) 'Reassessing epithelial to mesenchymal transition as a prerequisite for carcinoma invasion and metastasis', *Cancer Res,* 66(17), pp. 8319-26.

Cioffi, M., Vallespinos-Serrano, M., Trabulo, S. M., Fernandez-Marcos, P. J., Firment, A. N., Vazquez, B. N., Vieira, C. R., Mulero, F., Camara, J. A., Cronin, U. P., Perez, M., Soriano, J., G Galvez, B., Castells-Garcia, A., Haage, V., Raj, D., Megias, D., Hahn, S., Serrano, L., Moon, A., Aicher, A. and Heeschen, C. (2015) 'MiR-93 Controls Adiposity via Inhibition of Sirt7 and Tbx3', *Cell Rep,* 12(10), pp. 1594-605.

Cleton-Jansen, A. M., Buerger, H., Haar, N., Philippo, K., van de Vijver, M. J., Boecker, W., Smit, V. T. and Cornelisse, C. J. (2004) 'Different mechanisms of chromosome 16 loss of heterozygosity in well- versus poorly differentiated ductal breast cancer', *Genes Chromosomes Cancer,* 41(2), pp. 109-16.

Coll, M., Seidman, J. G. and Müller, C. W. (2002) 'Structure of the DNA-bound T-box domain of human TBX3, a transcription factor responsible for ulnar-mammary syndrome', *Structure,* 10(3), pp. 343-56.

Côme, C., Magnino, F., Bibeau, F., De Santa Barbara, P., Becker, K. F., Theillet, C. and Savagner, P. (2006) 'Snail and slug play distinct roles during breast carcinoma progression', *Clin Cancer Res,* 12(18), pp. 5395-402.

Cook, A. C., Chambers, A. F., Turley, E. A. and Tuck, A. B. (2006) 'Osteopontin induction of hyaluronan synthase 2 expression promotes breast cancer malignancy', *J Biol Chem,* 281(34), pp. 24381-9.

Cook, A. C., Tuck, A. B., McCarthy, S., Turner, J. G., Irby, R. B., Bloom, G. C., Yeatman, T. J. and Chambers, A. F. (2005) 'Osteopontin induces multiple changes in gene expression that reflect the six "hallmarks of cancer" in a model of breast cancer progression', *Mol Carcinog,* 43(4), pp. 225-36.

Correa, C., McGale, P., Taylor, C., Wang, Y., Clarke, M., Davies, C., Peto, R., Bijker, N., Solin, L., Darby, S. and (EBCTCG), E. B. C. T. C. G. (2010) 'Overview of the randomized trials of radiotherapy in ductal carcinoma in situ of the breast', *J Natl Cancer Inst Monogr,* 2010(41), pp. 162-77.

Creighton, C. J., Li, X., Landis, M., Dixon, J. M., Neumeister, V. M., Sjolund, A., Rimm, D. L., Wong, H., Rodriguez, A., Herschkowitz, J. I., Fan, C., Zhang, X., He, X., Pavlick, A., Gutierrez, M. C., Renshaw, L., Larionov, A. A., Faratian, D., Hilsenbeck, S. G., Perou, C. M., Lewis, M. T., Rosen, J. M. and Chang, J. C. (2009) 'Residual breast cancers after conventional therapy display mesenchymal as well as tumor-initiating features', *Proc Natl Acad Sci U S A,* 106(33), pp. 13820-5.

Cress, W. D. and Seto, E. (2000) 'Histone deacetylases, transcriptional control, and cancer', *J Cell Physiol,* 184(1), pp. 1-16.

Crissman, J. D., Visscher, D. W. and Kubus, J. (1990) 'Image cytophotometric DNA analysis of atypical hyperplasias and intraductal carcinomas of the breast', *Arch Pathol Lab Med,* 114(12), pp. 1249-53.

Cuzick, J., Sestak, I., Pinder, S. E., Ellis, I. O., Forsyth, S., Bundred, N. J., Forbes, J. F., Bishop, H., Fentiman, I. S. and George, W. D. (2011) 'Effect of tamoxifen and radiotherapy in women with locally excised ductal carcinoma in situ: long-term results from the UK/ANZ DCIS trial', *Lancet Oncol,* 12(1), pp. 21-9.

Dabbs, D. J., Carter, G., Fudge, M., Peng, Y., Swalsky, P. and Finkelstein, S. (2006) 'Molecular alterations in columnar cell lesions of the breast', *Mod Pathol,* 19(3), pp. 344-9.

Dan, J., Li, M., Yang, J., Li, J., Okuka, M., Ye, X. and Liu, L. (2013) 'Roles for Tbx3 in regulation of two-cell state and telomere elongation in mouse ES cells', *Sci Rep,* 3, pp. 3492.

Dang, T. T., Esparza, M. A., Maine, E. A., Westcott, J. M. and Pearson, G. W. (2015) 'ΔNp63α Promotes Breast Cancer Cell Motility through the Selective Activation of Components of the Epithelial-to-Mesenchymal Transition Program', *Cancer Res,* 75(18), pp. 3925-35.

Davenport, T. G., Jerome-Majewska, L. A. and Papaioannou, V. E. (2003) 'Mammary gland, limb and yolk sac defects in mice lacking Tbx3, the gene mutated in human ulnar mammary syndrome', *Development,* 130(10), pp. 2263-73.

De Craene, B. and Berx, G. (2013) 'Regulatory networks defining EMT during cancer initiation and progression', *Nat Rev Cancer,* 13(2), pp. 97-110.

De Craene, B., Gilbert, B., Stove, C., Bruyneel, E., van Roy, F. and Berx, G. (2005) 'The transcription factor snail induces tumor cell invasion through modulation of the epithelial cell differentiation program', *Cancer Res,* 65(14), pp. 6237-44.

DeBenedittis, P. and Jiao, K. (2011) 'Alternative splicing of T-box transcription factor genes', *Biochem Biophys Res Commun,* 412(4), pp. 513-7.

Demay, F., Bilican, B., Rodriguez, M., Carreira, S., Pontecorvi, M., Ling, Y. and Goding, C. R. (2007) 'T-box factors: targeting to chromatin and interaction with the histone H3 N-terminal tail', *Pigment Cell Res,* 20(4), pp. 279-87.

Deng, G., Lu, Y., Zlotnikov, G., Thor, A. D. and Smith, H. S. (1996) 'Loss of heterozygosity in normal tissue adjacent to breast carcinomas', *Science,* 274(5295), pp. 2057-9.

Denhardt, D. T. and Chambers, A. F. (1994) 'Overcoming obstacles to metastasis--defenses against host defenses: osteopontin (OPN) as a shield against attack by cytotoxic host cells', *J Cell Biochem,* 56(1), pp. 48-51.

Dokmanovic, M. and Marks, P. A. (2005) 'Prospects: histone deacetylase inhibitors', *J Cell Biochem,* 96(2), pp. 293-304.

Dong, L., Dong, Q., Chen, Y., Li, Y., Zhang, B., Zhou, F., Lyu, X., Chen, G. G., Lai, P., Kung, H. F. and He, M. L. (2018) 'Novel HDAC5-interacting motifs of Tbx3 are essential for the suppression of E-cadherin expression and for the promotion of metastasis in hepatocellular carcinoma', *Signal Transduct Target Ther,* 3, pp. 22.

Douglas, N. C. and Papaioannou, V. E. (2013) 'The T-box transcription factors TBX2 and TBX3 in mammary gland development and breast cancer', *J Mammary Gland Biol Neoplasia,* 18(2), pp. 143-7.

Eblaghie, M. C., Song, S. J., Kim, J. Y., Akita, K., Tickle, C. and Jung, H. S. (2004) 'Interactions between FGF and Wnt signals and Tbx3 gene expression in mammary gland initiation in mouse embryos', *J Anat,* 205(1), pp. 1-13.

El-Tanani, M. K., Campbell, F. C., Kurisetty, V., Jin, D., McCann, M. and Rudland, P. S. (2006) 'The regulation and role of osteopontin in malignant transformation and cancer', *Cytokine Growth Factor Rev,* 17(6), pp. 463-74.

Elloul, S., Elstrand, M. B., Nesland, J. M., Tropé, C. G., Kvalheim, G., Goldberg, I., Reich, R. and Davidson, B. (2005) 'Snail, Slug, and Smad-interacting protein 1 as novel parameters of disease aggressiveness in metastatic ovarian and breast carcinoma', *Cancer,* 103(8), pp. 1631-43.

Eriksson, E., Schimmelpenning, H., Silfverswärd, C. and Auer, G. (1992) 'Immunoreactivity with monoclonal antibody A-80 and nuclear DNA content in benign and malignant human breast disease', *Hum Pathol,* 23(12), pp. 1366-72.

Ernster, V. L., Barclay, J., Kerlikowske, K., Grady, D. and Henderson, C. (1996) 'Incidence of and treatment for ductal carcinoma in situ of the breast', *JAMA,* 275(12), pp. 913-8.

Esteva, F. J. and Hortobagyi, G. N. (2004) 'Prognostic molecular markers in early breast cancer', *Breast Cancer Res,* 6(3), pp. 109-18.

Evanko, S. P., Tammi, M. I., Tammi, R. H. and Wight, T. N. (2007) 'Hyaluronan-dependent pericellular matrix', *Adv Drug Deliv Rev,* 59(13), pp. 1351-65.

Fan, W., Huang, X., Chen, C., Gray, J. and Huang, T. (2004) 'TBX3 and its isoform TBX3+2a are functionally distinctive in inhibition of senescence and are overexpressed in a subset of breast cancer cell lines', *Cancer Res,* 64(15), pp. 5132-9.

Faverly, D. R., Burgers, L., Bult, P. and Holland, R. (1994) 'Three dimensional imaging of mammary ductal carcinoma in situ: clinical implications', *Semin Diagn Pathol,* 11(3), pp. 193-8.

Fernando, R. I., Litzinger, M., Trono, P., Hamilton, D. H., Schlom, J. and Palena, C. (2010) 'The T-box transcription factor Brachyury promotes epithelial-mesenchymal transition in human tumor cells', *J Clin Invest,* 120(2), pp. 533-44.

Fillmore, C. M., Gupta, P. B., Rudnick, J. A., Caballero, S., Keller, P. J., Lander, E. S. and Kuperwasser, C. (2010) 'Estrogen expands breast cancer stem-like cells through paracrine FGF/Tbx3 signaling', *Proc Natl Acad Sci U S A,* 107(50), pp. 21737-42.

Fisher, B., Anderson, S., Bryant, J., Margolese, R. G., Deutsch, M., Fisher, E. R., Jeong, J. H. and Wolmark, N. (2002) 'Twenty-year follow-up of a randomized trial comparing total mastectomy, lumpectomy, and lumpectomy plus irradiation for the treatment of invasive breast cancer', *N Engl J Med,* 347(16), pp. 1233-41.

Fisher, B., Costantino, J., Redmond, C., Fisher, E., Margolese, R., Dimitrov, N., Wolmark, N., Wickerham, D. L., Deutsch, M. and Ore, L. (1993) 'Lumpectomy compared with lumpectomy and radiation therapy for the treatment of intraductal breast cancer', *N Engl J Med,* 328(22), pp. 1581-6.

Fisher, B., Dignam, J., Wolmark, N., Mamounas, E., Costantino, J., Poller, W., Fisher, E. R., Wickerham, D. L., Deutsch, M., Margolese, R., Dimitrov, N. and Kavanah, M. (1998) 'Lumpectomy and radiation therapy for the treatment of intraductal breast cancer: findings from National Surgical Adjuvant Breast and Bowel Project B-17', *J Clin Oncol,* 16(2), pp. 441-52.

Fisher, B., Land, S., Mamounas, E., Dignam, J., Fisher, E. R. and Wolmark, N. (2001) 'Prevention of invasive breast cancer in women with ductal carcinoma in situ: an update of the National Surgical Adjuvant Breast and Bowel Project experience', *Semin Oncol,* 28(4), pp. 400-18.

Fitzgibbons, P. L., Henson, D. E. and Hutter, R. V. (1998) 'Benign breast changes and the risk for subsequent breast cancer: an update of the 1985 consensus statement. Cancer Committee of the College of American Pathologists', *Arch Pathol Lab Med,* 122(12), pp. 1053-5.

Folkman, J. (1971) 'Tumor angiogenesis: therapeutic implications', *N Engl J Med,* 285(21), pp. 1182-6.

Formenti, S. C., Arslan, A. A. and Pike, M. C. (2011) 'Re: Long-term outcomes of invasive ipsilateral breast tumor recurrences after lumpectomy in NSABP B-17 and B-24 randomized clinical trials for DCIS', *J Natl Cancer Inst,* 103(22), pp. 1723.

Foulkes, W. D., Brunet, J. S., Stefansson, I. M., Straume, O., Chappuis, P. O., Bégin, L. R., Hamel, N., Goffin, J. R., Wong, N., Trudel, M., Kapusta, L., Porter, P. and Akslen, L. A. (2004) 'The prognostic implication of the basal-like (cyclin E high/p27 low/p53+/glomeruloid-microvascular-proliferation+) phenotype of BRCA1-related breast cancer', *Cancer Res,* 64(3), pp. 830-5.

Fowble, B., Hanlon, A. L., Fein, D. A., Hoffman, J. P., Sigurdson, E. R., Patchefsky, A. and Kessler, H. (1997) 'Results of conservative surgery and radiation for mammographically detected ductal carcinoma in situ (DCIS)', *Int J Radiat Oncol Biol Phys,* 38(5), pp. 949-57.

Gao, Y., Niu, Y., Wang, X., Wei, L. and Lu, S. (2009) 'Genetic changes at specific stages of breast cancer progression detected by comparative genomic hybridization', *J Mol Med (Berl),* 87(2), pp. 145-52.

Gasparini, G., Brooks, P. C., Biganzoli, E., Vermeulen, P. B., Bonoldi, E., Dirix, L. Y., Ranieri, G., Miceli, R. and Cheresh, D. A. (1998) 'Vascular integrin alpha(v)beta3: a new prognostic indicator in breast cancer', *Clin Cancer Res,* 4(11), pp. 2625-34.

Gauthier, M. L., Berman, H. K., Miller, C., Kozakeiwicz, K., Chew, K., Moore, D., Rabban, J., Chen, Y. Y., Kerlikowske, K. and Tlsty, T. D. (2007) 'Abrogated response to cellular stress identifies DCIS associated with subsequent tumor events and defines basal-like breast tumors', *Cancer Cell,* 12(5), pp. 479-91.

Geissinger, E., Weisser, C., Fischer, P., Schartl, M. and Wellbrock, C. (2002) 'Autocrine stimulation by osteopontin contributes to antiapoptotic signalling of melanocytes in dermal collagen', *Cancer Res,* 62(16), pp. 4820-8.

Georges, R., Nemer, G., Morin, M., Lefebvre, C. and Nemer, M. (2008) 'Distinct expression and function of alternatively spliced Tbx5 isoforms in cell growth and differentiation', *Mol Cell Biol,* 28(12), pp. 4052-67.

Ghatak, S., Misra, S. and Toole, B. P. (2005) 'Hyaluronan constitutively regulates ErbB2 phosphorylation and signaling complex formation in carcinoma cells', *J Biol Chem,* 280(10), pp. 8875-83.

Giles, R. H., van Es, J. H. and Clevers, H. (2003) 'Caught up in a Wnt storm: Wnt signaling in cancer', *Biochim Biophys Acta,* 1653(1), pp. 1-24.

Glozak, M. A., Sengupta, N., Zhang, X. and Seto, E. (2005) 'Acetylation and deacetylation of non-histone proteins', *Gene,* 363, pp. 15-23.

Glozak, M. A. and Seto, E. (2007) 'Histone deacetylases and cancer', *Oncogene,* 26(37), pp. 5420-32.

Gluecksohn-Schoenheimer, S. (1938) 'The Development of Two Tailless Mutants in the House Mouse', *Genetics,* 23(6), pp. 573-84.

Go, E. M., Tsang, J. Y., Ni, Y. B., Yu, A. M., Mendoza, P., Chan, S. K., Lam, C. C., Lui, P. C., Tan, P. H. and Tse, G. M. (2012) 'Relationship between columnar cell changes and low-grade carcinoma in situ of the breast--a cytogenetic study', *Hum Pathol,* 43(11), pp. 1924-31.

Goodison, S., Urquidi, V. and Tarin, D. (1999) 'CD44 cell adhesion molecules', *Mol Pathol,* 52(4), pp. 189-96.

Gravdal, K., Halvorsen, O. J., Haukaas, S. A. and Akslen, L. A. (2007) 'A switch from E-cadherin to N-cadherin expression indicates epithelial to mesenchymal transition and is of strong and independent importance for the progress of prostate cancer', *Clin Cancer Res,* 13(23), pp. 7003-11.

Griffioen, A. W., Coenen, M. J., Damen, C. A., Hellwig, S. M., van Weering, D. H., Vooys, W., Blijham, G. H. and Groenewegen, G. (1997) 'CD44 is involved in tumor angiogenesis; an activation antigen on human endothelial cells', *Blood,* 90(3), pp. 1150-9.

Gruneberg, H. (1958) 'Genetical studies on the skeleton of the mouse. XXIII. The development of brachyury and anury', *J Embryol Exp Morphol,* 6(3), pp. 424-43.

Gudmundsson, J., Besenbacher, S., Sulem, P., Gudbjartsson, D. F., Olafsson, I., Arinbjarnarson, S., Agnarsson, B. A., Benediktsdottir, K. R., Isaksson, H. J., Kostic, J. P., Gudjonsson, S. A., Stacey, S. N., Gylfason, A., Sigurdsson, A., Holm, H., Bjornsdottir, U. S., Eyjolfsson, G. I., Navarrete, S., Fuertes, F., Garcia-Prats, M. D., Polo, E., Checherita, I. A., Jinga, M., Badea, P., Aben, K. K., Schalken, J. A., van Oort, I. M., Sweep, F. C., Helfand, B. T., Davis, M., Donovan, J. L., Hamdy, F. C., Kristjansson, K., Gulcher, J. R., Masson, G., Kong, A., Catalona, W. J., Mayordomo, J. I., Geirsson, G., Einarsson, G. V., Barkardottir, R. B., Jonsson, E., Jinga, V., Mates, D., Kiemeney, L. A., Neal, D. E., Thorsteinsdottir, U., Rafnar, T. and Stefansson, K. (2010) 'Genetic correction of PSA values using sequence variants associated with PSA levels', *Sci Transl Med,* 2(62), pp. 62ra92.

Guerra-Wallace, M. M., Christensen, W. N. and White, R. L. (2004) 'A retrospective study of columnar alteration with prominent apical snouts and secretions and the association with cancer', *Am J Surg,* 188(4), pp. 395-8.

Habel, L. A., Daling, J. R., Newcomb, P. A., Self, S. G., Porter, P. L., Stanford, J. L., Seidel, K. and Weiss, N. S. (1998) 'Risk of recurrence after ductal carcinoma in situ of the breast', *Cancer Epidemiol Biomarkers Prev,* 7(8), pp. 689-96.

Han, J., Yuan, P., Yang, H., Zhang, J., Soh, B. S., Li, P., Lim, S. L., Cao, S., Tay, J., Orlov, Y. L., Lufkin, T., Ng, H. H., Tam, W. L. and Lim, B. (2010) 'Tbx3 improves the germ-line competency of induced pluripotent stem cells', *Nature,* 463(7284), pp. 1096-100.

Han, K., Nofech-Mozes, S., Narod, S., Hanna, W., Vesprini, D., Saskin, R., Taylor, C., Kong, I., Paszat, L. and Rakovitch, E. (2012) 'Expression of HER2neu in ductal carcinoma in situ is associated with local recurrence', *Clin Oncol (R Coll Radiol),* 24(3), pp. 183-9.

Hanahan, D. and Weinberg, R. A. (2000) 'The hallmarks of cancer', *Cell,* 100(1), pp. 57-70.

Hansel, D. E., Rahman, A., House, M., Ashfaq, R., Berg, K., Yeo, C. J. and Maitra, A. (2004) 'Met proto-oncogene and insulin-like growth factor binding protein 3 overexpression correlates with metastatic ability in well-differentiated pancreatic endocrine neoplasms', *Clin Cancer Res,* 10(18 Pt 1), pp. 6152-8.

Hartmann, L. C., Degnim, A. C., Santen, R. J., Dupont, W. D. and Ghosh, K. (2015) 'Atypical hyperplasia of the breast--risk assessment and management options', *N Engl J Med,* 372(1), pp. 78-89.

Hazan, R. B., Phillips, G. R., Qiao, R. F., Norton, L. and Aaronson, S. A. (2000) 'Exogenous expression of N-cadherin in breast cancer cells induces cell migration, invasion, and metastasis', *J Cell Biol,* 148(4), pp. 779-90.

Hetelekidis, S., Collins, L., Silver, B., Manola, J., Gelman, R., Cooper, A., Lester, S., Lyons, J. A., Harris, J. R. and Schnitt, S. J. (1999) 'Predictors of local recurrence following excision alone for ductal carcinoma in situ', *Cancer,* 85(2), pp. 427-31.

Hevir, N., Trošt, N., Debeljak, N. and Rižner, T. L. (2011) 'Expression of estrogen and progesterone receptors and estrogen metabolizing enzymes in different breast cancer cell lines', *Chem Biol Interact,* 191(1-3), pp. 206-16.

Hirama, M., Takahashi, F., Takahashi, K., Akutagawa, S., Shimizu, K., Soma, S., Shimanuki, Y., Nishio, K. and Fukuchi, Y. (2003) 'Osteopontin overproduced by tumor cells acts as a potent angiogenic factor contributing to tumor growth', *Cancer Lett,* 198(1), pp. 107-17.

Holmberg, L., Garmo, H., Granstrand, B., Ringberg, A., Arnesson, L. G., Sandelin, K., Karlsson, P., Anderson, H. and Emdin, S. (2008) 'Absolute risk reductions for local recurrence after postoperative radiotherapy after sector resection for ductal carcinoma in situ of the breast', *J Clin Oncol,* 26(8), pp. 1247-52.

Holmes, P., Lloyd, J., Chervoneva, I., Pequinot, E., Cornfield, D. B., Schwartz, G. F., Allen, K. G. and Palazzo, J. P. (2011) 'Prognostic markers and long-term outcomes in ductal carcinoma in situ of the breast treated with excision alone', *Cancer,* 117(16), pp. 3650-7.

Hoogaars, W. M., Barnett, P., Rodriguez, M., Clout, D. E., Moorman, A. F., Goding, C. R. and Christoffels, V. M. (2008) 'TBX3 and its splice variant TBX3 + exon 2a are functionally similar', *Pigment Cell Melanoma Res,* 21(3), pp. 379-87.

Howard, B. and Ashworth, A. (2006) 'Signalling pathways implicated in early mammary gland morphogenesis and breast cancer', *PLoS Genet,* 2(8), pp. e112.

Hu, M., Yao, J., Carroll, D. K., Weremowicz, S., Chen, H., Carrasco, D., Richardson, A., Violette, S., Nikolskaya, T., Nikolsky, Y., Bauerlein, E. L., Hahn, W. C., Gelman, R. S., Allred, C., Bissell, M. J., Schnitt, S. and Polyak, K. (2008) 'Regulation of in situ to invasive breast carcinoma transition', *Cancer Cell,* 13(5), pp. 394-406.

Hughes, L. L., Wang, M., Page, D. L., Gray, R., Solin, L. J., Davidson, N. E., Lowen, M. A., Ingle, J. N., Recht, A. and Wood, W. C. (2009) 'Local excision alone without irradiation for ductal carcinoma in situ of the breast: a trial of the Eastern Cooperative Oncology Group', *J Clin Oncol,* 27(32), pp. 5319-24.

Humtsoe, J. O., Koya, E., Pham, E., Aramoto, T., Zuo, J., Ishikawa, T. and Kramer, R. H. (2012) 'Transcriptional profiling identifies upregulated genes following induction of epithelial-mesenchymal transition in squamous carcinoma cells', *Exp Cell Res,* 318(4), pp. 379-90.

Iozzo, R. V. and Müller-Glauser, W. (1985) 'Neoplastic modulation of extracellular matrix: proteoglycan changes in the rabbit mesentery induced by V2 carcinoma cells', *Cancer Res,* 45(11 Pt 2), pp. 5677-87.

Isaacs, H. V., Pownall, M. E. and Slack, J. M. (1994) 'eFGF regulates Xbra expression during Xenopus gastrulation', *EMBO J,* 13(19), pp. 4469-81.

Itano, N., Sawai, T., Yoshida, M., Lenas, P., Yamada, Y., Imagawa, M., Shinomura, T., Hamaguchi, M., Yoshida, Y., Ohnuki, Y., Miyauchi, S., Spicer, A. P., McDonald, J. A. and Kimata, K. (1999) 'Three isoforms of mammalian hyaluronan synthases have distinct enzymatic properties', *J Biol Chem,* 274(35), pp. 25085-92.

Jackson, L. C., Camacho, F., Levine, E. A., Anderson, R. T. and Stewart, J. H. (2008) 'Patterns of care analysis among women with ductal carcinoma in situ in North Carolina', *Am J Surg,* 195(2), pp. 164-9.

Jiang, K., Ren, C. and Nair, V. D. (2013) 'MicroRNA-137 represses Klf4 and Tbx3 during differentiation of mouse embryonic stem cells', *Stem Cell Res,* 11(3), pp. 1299-313.

Kader, T., Hill, P., Rakha, E. A., Campbell, I. G. and Gorringe, K. L. (2018) 'Atypical ductal hyperplasia: update on diagnosis, management, and molecular landscape', *Breast Cancer Res,* 20(1), pp. 39.

Kang, Y., Chen, C. R. and Massagué, J. (2003) 'A self-enabling TGFbeta response coupled to stress signaling: Smad engages stress response factor ATF3 for Id1 repression in epithelial cells', *Mol Cell,* 11(4), pp. 915-26.

Kenny, P. A., Lee, G. Y., Myers, C. A., Neve, R. M., Semeiks, J. R., Spellman, P. T., Lorenz, K., Lee, E. H., Barcellos-Hoff, M. H., Petersen, O. W., Gray, J. W. and Bissell, M. J. (2007) 'The morphologies of breast cancer cell lines in three-dimensional assays correlate with their profiles of gene expression', *Mol Oncol,* 1(1), pp. 84-96.

Kepple, J., Henry-Tillman, R. S., Klimberg, V. S., Layeeque, R., Siegel, E., Westbrook, K. and Korourian, S. (2006) 'The receptor expression pattern in ductal carcinoma in situ predicts recurrence', *Am J Surg,* 192(1), pp. 68-71.

Kerlikowske, K. (2010) 'Epidemiology of ductal carcinoma in situ', *J Natl Cancer Inst Monogr,* 2010(41), pp. 139-41.

Kerlikowske, K., Molinaro, A. M., Gauthier, M. L., Berman, H. K., Waldman, F., Bennington, J., Sanchez, H., Jimenez, C., Stewart, K., Chew, K., Ljung, B. M. and Tlsty, T. D. (2010) 'Biomarker expression and risk of subsequent tumors after initial ductal carcinoma in situ diagnosis', *J Natl Cancer Inst,* 102(9), pp. 627-37.

Khan, S. A., Cook, A. C., Kappil, M., Günthert, U., Chambers, A. F., Tuck, A. B. and Denhardt, D. T. (2005) 'Enhanced cell surface CD44 variant (v6, v9) expression by osteopontin in breast cancer epithelial cells facilitates tumor cell migration: novel post-transcriptional, post-translational regulation', *Clin Exp Metastasis,* 22(8), pp. 663-73.

Kim, M. S., Park, M. J., Moon, E. J., Kim, S. J., Lee, C. H., Yoo, H., Shin, S. H., Song, E. S. and Lee, S. H. (2005) 'Hyaluronic acid induces osteopontin via the phosphatidylinositol 3-kinase/Akt pathway to enhance the motility of human glioma cells', *Cancer Res,* 65(3), pp. 686-91.

Klinck, R., Bramard, A., Inkel, L., Dufresne-Martin, G., Gervais-Bird, J., Madden, R., Paquet, E. R., Koh, C., Venables, J. P., Prinos, P., Jilaveanu-Pelmus, M., Wellinger, R., Rancourt, C., Chabot, B. and Abou Elela, S. (2008) 'Multiple alternative splicing markers for ovarian cancer', *Cancer Res,* 68(3), pp. 657-63.

Knowles, M. A. and Selby, P. (2005) *Introduction to the cellular and molecular biology of cancer.* New York: Oxford University Press.

Knudson, W., Biswas, C., Li, X. Q., Nemec, R. E. and Toole, B. P. (1989) 'The role and regulation of tumour-associated hyaluronan', *Ciba Found Symp,* 143, pp. 150-9; discussion 159-69, 281-5.

Konecny, G. E., Meng, Y. G., Untch, M., Wang, H. J., Bauerfeind, I., Epstein, M., Stieber, P., Vernes, J. M., Gutierrez, J., Hong, K., Beryt, M., Hepp, H., Slamon, D. J. and Pegram, M. D. (2004) 'Association between HER-2/neu and vascular endothelial growth factor expression predicts clinical outcome in primary breast cancer patients', *Clin Cancer Res,* 10(5), pp. 1706-16.

Kornblihtt, A. R., Schor, I. E., Alló, M., Dujardin, G., Petrillo, E. and Muñoz, M. J. (2013) 'Alternative splicing: a pivotal step between eukaryotic transcription and translation', *Nat Rev Mol Cell Biol,* 14(3), pp. 153-65.

Koyama, H., Hibi, T., Isogai, Z., Yoneda, M., Fujimori, M., Amano, J., Kawakubo, M., Kannagi, R., Kimata, K., Taniguchi, S. and Itano, N. (2007) 'Hyperproduction of hyaluronan in neu-induced mammary tumor accelerates angiogenesis through stromal cell recruitment: possible involvement of versican/PG-M', *Am J Pathol,* 170(3), pp. 1086-99.

Krstic, M., Macmillan, C. D., Leong, H. S., Clifford, A. G., Souter, L. H., Dales, D. W., Postenka, C. O., Chambers, A. F. and Tuck, A. B. (2016) 'The transcriptional regulator TBX3 promotes progression from non-invasive to invasive breast cancer', *BMC Cancer,* 16(1), pp. 671.

Kumar P, P., Emechebe, U., Smith, R., Franklin, S., Moore, B., Yandell, M., Lessnick, S. L. and Moon, A. M. (2014a) 'Coordinated control of senescence by lncRNA and a novel T-box3 co-repressor complex', *Elife,* 3.

Kumar P, P., Franklin, S., Emechebe, U., Hu, H., Moore, B., Lehman, C., Yandell, M. and Moon, A. M. (2014b) 'TBX3 regulates splicing in vivo: a novel molecular mechanism for Ulnar-mammary syndrome', *PLoS Genet,* 10(3), pp. e1004247.

Kumar, V., Abbas, A. K., Aster, J. C. and Robbins, S. L. (2013) *Robbins basic pathology.* 9th edn. Philadelphia, PA: Elsevier/Saunders.

Kunju, L. P. and Kleer, C. G. (2007) 'Significance of flat epithelial atypia on mammotome core needle biopsy: Should it be excised?', *Hum Pathol,* 38(1), pp. 35-41.

Ladomery, M. R., Harper, S. J. and Bates, D. O. (2007) 'Alternative splicing in angiogenesis: the vascular endothelial growth factor paradigm', *Cancer Lett,* 249(2), pp. 133-42.

Lagios, M. D. (1990) 'Duct carcinoma in situ. Pathology and treatment', *Surg Clin North Am,* 70(4), pp. 853-71.

Lagios, M. D., Margolin, F. R., Westdahl, P. R. and Rose, M. R. (1989) 'Mammographically detected duct carcinoma in situ. Frequency of local recurrence following tylectomy and prognostic effect of nuclear grade on local recurrence', *Cancer,* 63(4), pp. 618-24.

Lakhani, S. R., Collins, N., Stratton, M. R. and Sloane, J. P. (1995) 'Atypical ductal hyperplasia of the breast: clonal proliferation with loss of heterozygosity on chromosomes 16q and 17p', *J Clin Pathol,* 48(7), pp. 611-5.

Larson, P. S., de las Morenas, A., Cerda, S. R., Bennett, S. R., Cupples, L. A. and Rosenberg, C. L. (2006) 'Quantitative analysis of allele imbalance supports atypical ductal hyperplasia lesions as direct breast cancer precursors', *J Pathol,* 209(3), pp. 307-16.

Le Bras, G. F., Taubenslag, K. J. and Andl, C. D. (2012) 'The regulation of cell-cell adhesion during epithelial-mesenchymal transition, motility and tumor progression', *Cell Adh Migr,* 6(4), pp. 365-73.

Leali, D., Dell'Era, P., Stabile, H., Sennino, B., Chambers, A. F., Naldini, A., Sozzani, S., Nico, B., Ribatti, D. and Presta, M. (2003) 'Osteopontin (Eta-1) and fibroblast growth factor-2 cross-talk in angiogenesis', *J Immunol,* 171(2), pp. 1085-93.

Lee, H. S., Cho, H. H., Kim, H. K., Bae, Y. C., Baik, H. S. and Jung, J. S. (2007) 'Tbx3, a transcriptional factor, involves in proliferation and osteogenic differentiation of human adipose stromal cells', *Mol Cell Biochem,* 296(1-2), pp. 129-36.

Lerwill, M. F. (2008) 'Flat epithelial atypia of the breast', *Arch Pathol Lab Med,* 132(4), pp. 615-21.

Lester, S. C., Bose, S., Chen, Y. Y., Connolly, J. L., de Baca, M. E., Fitzgibbons, P. L., Hayes, D. F., Kleer, C., O'Malley, F. P., Page, D. L., Smith, B. L., Weaver, D. L., Winer, E. and Members of the Cancer Committee, C. l. o. A. P. (2009) 'Protocol for the examination of specimens from patients with ductal carcinoma in situ of the breast', *Arch Pathol Lab Med,* 133(1), pp. 15-25.

Lewin, B., Krebs, J. E., Kilpatrick, S. T. and Goldstein, E. S. (2011) *Lewin's genes X.* 10th edn. Sudbury, Mass.: Jones and Bartlett.

Li, J., Ballim, D., Rodriguez, M., Cui, R., Goding, C. R., Teng, H. and Prince, S. (2014) 'The anti-proliferative function of the TGF-β1 signaling pathway involves the repression of the oncogenic TBX2 by its homologue TBX3', *J Biol Chem,* 289(51), pp. 35633-43.

Li, J., Weinberg, M. S., Zerbini, L. and Prince, S. (2013) 'The oncogenic TBX3 is a downstream target and mediator of the TGF-β1 signaling pathway', *Mol Biol Cell,* 24(22), pp. 3569-76.

Liapis, H., Flath, A. and Kitazawa, S. (1996) 'Integrin alpha V beta 3 expression by bone-residing breast cancer metastases', *Diagn Mol Pathol,* 5(2), pp. 127-35.

Liesveld, J. L., Frediani, K. E., Harbol, A. W., DiPersio, J. F. and Abboud, C. N. (1994) 'Characterization of the adherence of normal and leukemic CD34+ cells to endothelial monolayers', *Leukemia,* 8(12), pp. 2111-7.

Lin, Y. H. and Yang-Yen, H. F. (2001) 'The osteopontin-CD44 survival signal involves activation of the phosphatidylinositol 3-kinase/Akt signaling pathway', *J Biol Chem,* 276(49), pp. 46024-30.

Lingbeek, M. E., Jacobs, J. J. and van Lohuizen, M. (2002) 'The T-box repressors TBX2 and TBX3 specifically regulate the tumor suppressor gene p14ARF via a variant T-site in the initiator', *J Biol Chem,* 277(29), pp. 26120-7.

Liu, J., Esmailpour, T., Shang, X., Gulsen, G., Liu, A. and Huang, T. (2011) 'TBX3 over-expression causes mammary gland hyperplasia and increases mammary stem-like cells in an inducible transgenic mouse model', *BMC Dev Biol,* 11, pp. 65.

Liu, T., Zhang, X., Shang, M., Zhang, Y., Xia, B., Niu, M., Liu, Y. and Pang, D. (2013) 'Dysregulated expression of Slug, vimentin, and E-cadherin correlates with poor clinical outcome in patients with basal-like breast cancer', *J Surg Oncol,* 107(2), pp. 188-94.

Liu, X. L., Band, H., Gao, Q., Wazer, D. E., Chu, Q. and Band, V. (1994) 'Tumor cell-specific loss of p53 protein in a unique in vitro model of human breast tumor progression', *Carcinogenesis,* 15(9), pp. 1969-73.

Lomnytska, M., Dubrovska, A., Hellman, U., Volodko, N. and Souchelnytskyi, S. (2006) 'Increased expression of cSHMT, Tbx3 and utrophin in plasma of ovarian and breast cancer patients', *Int J Cancer,* 118(2), pp. 412-21.

Lu, J., Li, X. P., Dong, Q., Kung, H. F. and He, M. L. (2010) 'TBX2 and TBX3: the special value for anticancer drug targets', *Biochim Biophys Acta,* 1806(2), pp. 268-74.

Lu, R., Yang, A. and Jin, Y. (2011) 'Dual functions of T-box 3 (Tbx3) in the control of self-renewal and extraembryonic endoderm differentiation in mouse embryonic stem cells', *J Biol Chem,* 286(10), pp. 8425-36.

Luzzi, K. J., MacDonald, I. C., Schmidt, E. E., Kerkvliet, N., Morris, V. L., Chambers, A. F. and Groom, A. C. (1998) 'Multistep nature of metastatic inefficiency: dormancy of solitary cells after successful extravasation and limited survival of early micrometastases', *Am J Pathol,* 153(3), pp. 865-73.

Lyng, H., Brovig, R. S., Svendsrud, D. H., Holm, R., Kaalhus, O., Knutstad, K., Oksefjell, H., Sundfor, K., Kristensen, G. B. and Stokke, T. (2006) 'Gene expressions and copy numbers associated with metastatic phenotypes of uterine cervical cancer', *BMC Genomics,* 7, pp. 268.

Ma, X. J., Salunga, R., Tuggle, J. T., Gaudet, J., Enright, E., McQuary, P., Payette, T., Pistone, M., Stecker, K., Zhang, B. M., Zhou, Y. X., Varnholt, H., Smith, B., Gadd, M., Chatfield, E., Kessler, J., Baer, T. M., Erlander, M. G. and Sgroi, D. C. (2003) 'Gene expression profiles of human breast cancer progression', *Proc Natl Acad Sci U S A,* 100(10), pp. 5974-9.

Madsen, M. W., Lykkesfeldt, A. E., Laursen, I., Nielsen, K. V. and Briand, P. (1992) 'Altered gene expression of c-myc, epidermal growth factor receptor, transforming growth factor-alpha, and c-erb-B2 in an immortalized human breast epithelial cell line, HMT-3522, is associated with decreased growth factor requirements', *Cancer Res,* 52(5), pp. 1210-7.

Mani, S. A., Guo, W., Liao, M. J., Eaton, E. N., Ayyanan, A., Zhou, A. Y., Brooks, M., Reinhard, F., Zhang, C. C., Shipitsin, M., Campbell, L. L., Polyak, K., Brisken, C., Yang, J. and Weinberg, R. A. (2008) 'The epithelial-mesenchymal transition generates cells with properties of stem cells', *Cell,* 133(4), pp. 704-15.

Martel, M., Barron-Rodriguez, P., Tolgay Ocal, I., Dotto, J. and Tavassoli, F. A. (2007) 'Flat DIN 1 (flat epithelial atypia) on core needle biopsy: 63 cases identified retrospectively among 1,751 core biopsies performed over an 8-year period (1992-1999)', *Virchows Arch,* 451(5), pp. 883-91.

Martin, T. A., Goyal, A., Watkins, G. and Jiang, W. G. (2005) 'Expression of the transcription factors snail, slug, and twist and their clinical significance in human breast cancer', *Ann Surg Oncol,* 12(6), pp. 488-96.

Massagué, J. (2012) 'TGFβ signalling in context', *Nat Rev Mol Cell Biol,* 13(10), pp. 616-30.

Matlin, A. J., Clark, F. and Smith, C. W. (2005) 'Understanding alternative splicing: towards a cellular code', *Nat Rev Mol Cell Biol,* 6(5), pp. 386-98.

McFarlane, S., Coulter, J. A., Tibbits, P., O'Grady, A., McFarlane, C., Montgomery, N., Hill, A., McCarthy, H. O., Young, L. S., Kay, E. W., Isacke, C. M. and Waugh, D. J. (2015) 'CD44 increases the efficiency of distant metastasis of breast cancer', *Oncotarget,* 6(13), pp. 11465-76.

Mersfelder, E. L. and Parthun, M. R. (2006) 'The tale beyond the tail: histone core domain modifications and the regulation of chromatin structure', *Nucleic Acids Res,* 34(9), pp. 2653-62.

Miao, Z. F., Liu, X. Y., Xu, H. M., Wang, Z. N., Zhao, T. T., Song, Y. X., Xing, Y. N., Huang, J. Y., Zhang, J. Y., Xu, H. and Xu, Y. Y. (2016) 'Tbx3 overexpression in human gastric cancer is correlated with advanced tumor stage and nodal status and promotes cancer cell growth and invasion', *Virchows Arch,* 469(5), pp. 505-513.

Miller, A. B., Wall, C., Baines, C. J., Sun, P., To, T. and Narod, S. A. (2014) 'Twenty five year follow-up for breast cancer incidence and mortality of the Canadian National Breast Screening Study: randomised screening trial', *BMJ,* 348, pp. g366.

Miller, F. R. (2000) 'Xenograft models of premalignant breast disease', *J Mammary Gland Biol Neoplasia,* 5(4), pp. 379-91.

Miller, F. R., Santner, S. J., Tait, L. and Dawson, P. J. (2000) 'MCF10DCIS.com xenograft model of human comedo ductal carcinoma in situ', *J Natl Cancer Inst,* 92(14), pp. 1185-6.

Mills, S. E. (2007) *Histology for pathologists.* 3rd edn. Philadelphia: Lippincott Williams & Wilkins.

Mironchik, Y., Winnard, P. T., Vesuna, F., Kato, Y., Wildes, F., Pathak, A. P., Kominsky, S., Artemov, D., Bhujwalla, Z., Van Diest, P., Burger, H., Glackin, C. and Raman, V. (2005) 'Twist overexpression induces in vivo angiogenesis and correlates with chromosomal instability in breast cancer', *Cancer Res,* 65(23), pp. 10801-9.

Misra, S., Ghatak, S. and Toole, B. P. (2005) 'Regulation of MDR1 expression and drug resistance by a positive feedback loop involving hyaluronan, phosphoinositide 3-kinase, and ErbB2', *J Biol Chem,* 280(21), pp. 20310-5.

Misra, S., Toole, B. P. and Ghatak, S. (2006) 'Hyaluronan constitutively regulates activation of multiple receptor tyrosine kinases in epithelial and carcinoma cells', *J Biol Chem,* 281(46), pp. 34936-41.

Moinfar, F., Man, Y. G., Bratthauer, G. L., Ratschek, M. and Tavassoli, F. A. (2000) 'Genetic abnormalities in mammary ductal intraepithelial neoplasia-flat type ("clinging ductal carcinoma in situ"): a simulator of normal mammary epithelium', *Cancer,* 88(9), pp. 2072-81.

Mokbel, K. and Cutuli, B. (2006) 'Heterogeneity of ductal carcinoma in situ and its effects on management', *Lancet Oncol,* 7(9), pp. 756-65.

Morel, A. P., Lièvre, M., Thomas, C., Hinkal, G., Ansieau, S. and Puisieux, A. (2008) 'Generation of breast cancer stem cells through epithelial-mesenchymal transition', *PLoS One,* 3(8), pp. e2888.

Moreno-Bueno, G., Cubillo, E., Sarrió, D., Peinado, H., Rodríguez-Pinilla, S. M., Villa, S., Bolós, V., Jordá, M., Fabra, A., Portillo, F., Palacios, J. and Cano, A. (2006) 'Genetic profiling of epithelial cells expressing E-cadherin repressors reveals a distinct role for Snail, Slug, and E47 factors in epithelial-mesenchymal transition', *Cancer Res,* 66(19), pp. 9543-56.

Morrow, M., Schnitt, S. J. and Norton, L. (2015) 'Current management of lesions associated with an increased risk of breast cancer', *Nat Rev Clin Oncol,* 12(4), pp. 227-38.

Moses, H. and Barcellos-Hoff, M. H. (2011) 'TGF-beta biology in mammary development and breast cancer', *Cold Spring Harb Perspect Biol,* 3(1), pp. a003277.

Muggerud, A. A., Hallett, M., Johnsen, H., Kleivi, K., Zhou, W., Tahmasebpoor, S., Amini, R. M., Botling, J., Borresen-Dale, A. L., Sorlie, T. and Warnberg, F. (2010) 'Molecular diversity in ductal carcinoma in situ (DCIS) and early invasive breast cancer', *Mol Oncol,* 4(4), pp. 357-68.

Müller, C. W. and Herrmann, B. G. (1997) 'Crystallographic structure of the T domain-DNA complex of the Brachyury transcription factor', *Nature,* 389(6653), pp. 884-8.

Musso, G., Paschetta, E., Gambino, R., Cassader, M. and Molinaro, F. (2013) 'Interactions among bone, liver, and adipose tissue predisposing to diabesity and fatty liver', *Trends Mol Med,* 19(9), pp. 522-35.

Nieto, M. A. (2002) 'The snail superfamily of zinc-finger transcription factors', *Nat Rev Mol Cell Biol,* 3(3), pp. 155-66.

Nieto, M. A., Huang, R. Y., Jackson, R. A. and Thiery, J. P. (2016) 'EMT: 2016', *Cell,* 166(1), pp. 21-45.

Nishida, N., Yano, H., Nishida, T., Kamura, T. and Kojiro, M. (2006) 'Angiogenesis in cancer', *Vasc Health Risk Manag,* 2(3), pp. 213-9.

Niu, Y., Wang, S., Liu, T., Zhang, T., Wei, X., Wang, Y. and Jiang, L. (2013) 'Expression of centrosomal tubulins associated with DNA ploidy in breast premalignant lesions and carcinoma', *Pathol Res Pract,* 209(4), pp. 221-7.

Niwa, H., Ogawa, K., Shimosato, D. and Adachi, K. (2009) 'A parallel circuit of LIF signalling pathways maintains pluripotency of mouse ES cells', *Nature,* 460(7251), pp. 118-22.

Nofech-Mozes, S., Spayne, J., Rakovitch, E., Kahn, H. J., Seth, A., Pignol, J. P., Lickley, L., Paszat, L. and Hanna, W. (2008) 'Biological Markers Predictive of Invasive Recurrence in DCIS', *Clin Med Oncol,* 2, pp. 7-18.

O'Connell, P., Pekkel, V., Fuqua, S. A., Osborne, C. K., Clark, G. M. and Allred, D. C. (1998) 'Analysis of loss of heterozygosity in 399 premalignant breast lesions at 15 genetic loci', *J Natl Cancer Inst,* 90(9), pp. 697-703.

Okuda, H., Kobayashi, A., Xia, B., Watabe, M., Pai, S. K., Hirota, S., Xing, F., Liu, W., Pandey, P. R., Fukuda, K., Modur, V., Ghosh, A., Wilber, A. and Watabe, K. (2012) 'Hyaluronan synthase HAS2 promotes tumor progression in bone by stimulating the interaction of breast cancer stem-like cells with macrophages and stromal cells', *Cancer Res,* 72(2), pp. 537-47.

Oltean, S. and Bates, D. O. (2014) 'Hallmarks of alternative splicing in cancer', *Oncogene,* 33(46), pp. 5311-8.

Oltean, S., Febbo, P. G. and Garcia-Blanco, M. A. (2008) 'Dunning rat prostate adenocarcinomas and alternative splicing reporters: powerful tools to study epithelial plasticity in prostate tumors in vivo', *Clin Exp Metastasis,* 25(6), pp. 611-9.

Ornitz, D. M. and Itoh, N. (2015) 'The Fibroblast Growth Factor signaling pathway', *Wiley Interdiscip Rev Dev Biol,* 4(3), pp. 215-66.

Page, D. L. and Dupont, W. D. (1992) 'Indicators of increased breast cancer risk in humans', *J Cell Biochem Suppl,* 16G, pp. 175-82.

Page, D. L. and Dupont, W. D. (1993) 'Anatomic indicators (histologic and cytologic) of increased breast cancer risk', *Breast Cancer Res Treat,* 28(2), pp. 157-66.

Page, D. L., Dupont, W. D., Rogers, L. W. and Rados, M. S. (1985) 'Atypical hyperplastic lesions of the female breast. A long-term follow-up study', *Cancer,* 55(11), pp. 2698-708.

Page, D. L. and Rogers, L. W. (1992) 'Combined histologic and cytologic criteria for the diagnosis of mammary atypical ductal hyperplasia', *Hum Pathol,* 23(10), pp. 1095-7.

Paik, S., Shak, S., Tang, G., Kim, C., Baker, J., Cronin, M., Baehner, F. L., Walker, M. G., Watson, D., Park, T., Hiller, W., Fisher, E. R., Wickerham, D. L., Bryant, J. and Wolmark, N. (2004) 'A multigene assay to predict recurrence of tamoxifen-treated, node-negative breast cancer', *N Engl J Med,* 351(27), pp. 2817-26.

Pajares, M. J., Ezponda, T., Catena, R., Calvo, A., Pio, R. and Montuenga, L. M. (2007) 'Alternative splicing: an emerging topic in molecular and clinical oncology', *Lancet Oncol,* 8(4), pp. 349-57.

Palena, C., Roselli, M., Litzinger, M. T., Ferroni, P., Costarelli, L., Spila, A., Cavaliere, F., Huang, B., Fernando, R. I., Hamilton, D. H., Jochems, C., Tsang, K. Y., Cheng, Q., Lyerly, H. K., Schlom, J. and Guadagni, F. (2014) 'Overexpression of the EMT driver brachyury in breast carcinomas: association with poor prognosis', *J Natl Cancer Inst,* 106(5).

Papaioannou, V. E. (2001) 'T-box genes in development: from hydra to humans', *Int Rev Cytol,* 207, pp. 1-70.

Peres, J., Davis, E., Mowla, S., Bennett, D. C., Li, J. A., Wansleben, S. and Prince, S. (2010) 'The Highly Homologous T-Box Transcription Factors, TBX2 and TBX3, Have Distinct Roles in the Oncogenic Process', *Genes Cancer,* 1(3), pp. 272-82.

Peres, J., Kwesi-Maliepaard, E. M., Rambow, F., Larue, L. and Prince, S. (2017) 'The tumour suppressor, miR-137, inhibits malignant melanoma migration by targetting the TBX3 transcription factor', *Cancer Lett,* 405, pp. 111-119.

Peres, J., Mowla, S. and Prince, S. (2015) 'The T-box transcription factor, TBX3, is a key substrate of AKT3 in melanomagenesis', *Oncotarget,* 6(3), pp. 1821-33.

Peres, J. and Prince, S. (2013) 'The T-box transcription factor, TBX3, is sufficient to promote melanoma formation and invasion', *Mol Cancer,* 12(1), pp. 117.

Perkhofer, L., Walter, K., Costa, I. G., Carrasco, M. C., Eiseler, T., Hafner, S., Genze, F., Zenke, M., Bergmann, W., Illing, A., Hohwieler, M., Köhntop, R., Lin, Q., Holzmann, K. H., Seufferlein, T.,

Wagner, M., Liebau, S., Hermann, P. C., Kleger, A. and Müller, M. (2016) 'Tbx3 fosters pancreatic cancer growth by increased angiogenesis and activin/nodal-dependent induction of stemness', *Stem Cell Res,* 17(2), pp. 367-378.

Perou, C. M., Sørlie, T., Eisen, M. B., van de Rijn, M., Jeffrey, S. S., Rees, C. A., Pollack, J. R., Ross, D. T., Johnsen, H., Akslen, L. A., Fluge, O., Pergamenschikov, A., Williams, C., Zhu, S. X., Lønning, P. E., Børresen-Dale, A. L., Brown, P. O. and Botstein, D. (2000) 'Molecular portraits of human breast tumours', *Nature,* 406(6797), pp. 747-52.

Phillips, S. and Kuperwasser, C. (2014) 'SLUG: Critical regulator of epithelial cell identity in breast development and cancer', *Cell Adh Migr,* 8(6), pp. 578-87.

Phillips, S., Prat, A., Sedic, M., Proia, T., Wronski, A., Mazumdar, S., Skibinski, A., Shirley, S. H., Perou, C. M., Gill, G., Gupta, P. B. and Kuperwasser, C. (2014) 'Cell-state transitions regulated by SLUG are critical for tissue regeneration and tumor initiation', *Stem Cell Reports,* 2(5), pp. 633-47.

Pinder, S. E. and Ellis, I. O. (2003) 'The diagnosis and management of pre-invasive breast disease: ductal carcinoma in situ (DCIS) and atypical ductal hyperplasia (ADH)--current definitions and classification', *Breast Cancer Res,* 5(5), pp. 254-7.

Pino, I., Pío, R., Toledo, G., Zabalegui, N., Vicent, S., Rey, N., Lozano, M. D., Torre, W., García-Foncillas, J. and Montuenga, L. M. (2003) 'Altered patterns of expression of members of the heterogeneous nuclear ribonucleoprotein (hnRNP) family in lung cancer', *Lung Cancer,* 41(2), pp. 131-43.

Polyak, K. and Hu, M. (2005) 'Do myoepithelial cells hold the key for breast tumor progression?', *J Mammary Gland Biol Neoplasia,* 10(3), pp. 231-47.

Polyak, K. and Weinberg, R. A. (2009) 'Transitions between epithelial and mesenchymal states: acquisition of malignant and stem cell traits', *Nat Rev Cancer,* 9(4), pp. 265-73.

Porsch, H., Bernert, B., Mehić, M., Theocharis, A. D., Heldin, C. H. and Heldin, P. (2013) 'Efficient TGFβ-induced epithelial-mesenchymal transition depends on hyaluronan synthase HAS2', *Oncogene,* 32(37), pp. 4355-65.

Porter, D., Lahti-Domenici, J., Keshaviah, A., Bae, Y. K., Argani, P., Marks, J., Richardson, A., Cooper, A., Strausberg, R., Riggins, G. J., Schnitt, S., Gabrielson, E., Gelman, R. and Polyak, K. (2003) 'Molecular markers in ductal carcinoma in situ of the breast', *Mol Cancer Res,* 1(5), pp. 362-75.

Proia, T. A., Keller, P. J., Gupta, P. B., Klebba, I., Jones, A. D., Sedic, M., Gilmore, H., Tung, N., Naber, S. P., Schnitt, S., Lander, E. S. and Kuperwasser, C. (2011) 'Genetic predisposition directs breast cancer phenotype by dictating progenitor cell fate', *Cell Stem Cell,* 8(2), pp. 149-63.

Pröls, F., Loser, B. and Marx, M. (1998) 'Differential expression of osteopontin, PC4, and CEC5, a novel mRNA species, during in vitro angiogenesis', *Exp Cell Res,* 239(1), pp. 1-10.

Provenzano, E., Hopper, J. L., Giles, G. G., Marr, G., Venter, D. J. and Armes, J. E. (2003) 'Biological markers that predict clinical recurrence in ductal carcinoma in situ of the breast', *Eur J Cancer,* 39(5), pp. 622-30.

Puisieux, A., Brabletz, T. and Caramel, J. (2014) 'Oncogenic roles of EMT-inducing transcription factors', *Nat Cell Biol,* 16(6), pp. 488-94.

Puri, P. L., Iezzi, S., Stiegler, P., Chen, T. T., Schiltz, R. L., Muscat, G. E., Giordano, A., Kedes, L., Wang, J. Y. and Sartorelli, V. (2001) 'Class I histone deacetylases sequentially interact with MyoD and pRb during skeletal myogenesis', *Mol Cell,* 8(4), pp. 885-97.

Rageth, C. J., O'Flynn, E. A., Comstock, C., Kurtz, C., Kubik, R., Madjar, H., Lepori, D., Kampmann, G., Mundinger, A., Baege, A., Decker, T., Hosch, S., Tausch, C., Delaloye, J. F., Morris, E. and Varga, Z. (2016) 'First International Consensus Conference on lesions of uncertain malignant potential in the breast (B3 lesions)', *Breast Cancer Res Treat,* 159(2), pp. 203-13.

Rakovitch, E., Nofech-Mozes, S., Hanna, W., Baehner, F. L., Saskin, R., Butler, S. M., Tuck, A., Sengupta, S., Elavathil, L., Jani, P. A., Bonin, M., Chang, M. C., Robertson, S. J., Slodkowska, E., Fong, C., Anderson, J. M., Jamshidian, F., Miller, D. P., Cherbavaz, D. B., Shak, S. and Paszat, L. (2015) 'A population-based validation study of the DCIS Score predicting recurrence risk in individuals treated by breast-conserving surgery alone', *Breast Cancer Res Treat,* 152(2), pp. 389-98.

Rakovitch, E., Nofech-Mozes, S., Hanna, W., Narod, S., Thiruchelvam, D., Saskin, R., Spayne, J., Taylor, C. and Paszat, L. (2012) 'HER2/neu and Ki-67 expression predict non-invasive recurrence following breast-conserving therapy for ductal carcinoma in situ', *Br J Cancer,* 106(6), pp. 1160-5.

Rayess, H., Wang, M. B. and Srivatsan, E. S. (2012) 'Cellular senescence and tumor suppressor gene p16', *Int J Cancer,* 130(8), pp. 1715-25.

Renard, C. A., Labalette, C., Armengol, C., Cougot, D., Wei, Y., Cairo, S., Pineau, P., Neuveut, C., de Reynies, A., Dejean, A., Perret, C. and Buendia, M. A. (2007) 'Tbx3 is a downstream target of the Wnt/beta-catenin pathway and a critical mediator of beta-catenin survival functions in liver cancer', *Cancer Res,* 67(3), pp. 901-10.

Ringberg, A., Anagnostaki, L., Anderson, H., Idvall, I., Fernö, M. and Group, S. S. B. C. (2001) 'Cell biological factors in ductal carcinoma in situ (DCIS) of the breast-relationship to ipsilateral local recurrence and histopathological characteristics', *Eur J Cancer,* 37(12), pp. 1514-22.

Rittling, S. R. and Chambers, A. F. (2004) 'Role of osteopontin in tumour progression', *Br J Cancer,* 90(10), pp. 1877-81.

Rizki, A., Weaver, V. M., Lee, S. Y., Rozenberg, G. I., Chin, K., Myers, C. A., Bascom, J. L., Mott, J. D., Semeiks, J. R., Grate, L. R., Mian, I. S., Borowsky, A. D., Jensen, R. A., Idowu, M. O., Chen, F., Chen, D. J., Petersen, O. W., Gray, J. W. and Bissell, M. J. (2008) 'A human breast cell model of preinvasive to invasive transition', *Cancer Res,* 68(5), pp. 1378-87.

Rodriguez, M., Aladowicz, E., Lanfrancone, L. and Goding, C. R. (2008) 'Tbx3 represses E-cadherin expression and enhances melanoma invasiveness', *Cancer Res,* 68(19), pp. 7872-81.

Rooney, P., Kumar, S., Ponting, J. and Wang, M. (1995) 'The role of hyaluronan in tumour neovascularization (review)', *Int J Cancer,* 60(5), pp. 632-6.

Rowley, M., Grothey, E. and Couch, F. J. (2004) 'The role of Tbx2 and Tbx3 in mammary development and tumorigenesis', *J Mammary Gland Biol Neoplasia,* 9(2), pp. 109-18.

Roylance, R., Gorman, P., Harris, W., Liebmann, R., Barnes, D., Hanby, A. and Sheer, D. (1999) 'Comparative genomic hybridization of breast tumors stratified by histological grade reveals new insights into the biological progression of breast cancer', *Cancer Res,* 59(7), pp. 1433-6.

Ruas, M. and Peters, G. (1998) 'The p16INK4a/CDKN2A tumor suppressor and its relatives', *Biochim Biophys Acta,* 1378(2), pp. F115-77.

Rudland, P. S., Platt-Higgins, A., El-Tanani, M., De Silva Rudland, S., Barraclough, R., Winstanley, J. H., Howitt, R. and West, C. R. (2002) 'Prognostic significance of the metastasis-associated protein osteopontin in human breast cancer', *Cancer Res,* 62(12), pp. 3417-27.

Ruiz, A., Almenar, S., Callaghan, R. C. and Llombart-Bosch, A. (1999) 'Benign, preinvasive and invasive ductal breast lesions. A comparative study with quantitative techniques: morphometry, image- and flow cytometry', *Pathol Res Pract,* 195(11), pp. 741-6.

Sabbah, M., Emami, S., Redeuilh, G., Julien, S., Prévost, G., Zimber, A., Ouelaa, R., Bracke, M., De Wever, O. and Gespach, C. (2008) 'Molecular signature and therapeutic perspective of the epithelial-to-mesenchymal transitions in epithelial cancers', *Drug Resist Updat,* 11(4-5), pp. 123-51.

Sagara, Y., Mallory, M. A., Wong, S., Aydogan, F., DeSantis, S., Barry, W. T. and Golshan, M. (2015) 'Survival Benefit of Breast Surgery for Low-Grade Ductal Carcinoma In Situ: A Population-Based Cohort Study', *JAMA Surg,* 150(8), pp. 739-45.

Sanders, M. E., Schuyler, P. A., Dupont, W. D. and Page, D. L. (2005) 'The natural history of low-grade ductal carcinoma in situ of the breast in women treated by biopsy only revealed over 30 years of long-term follow-up', *Cancer,* 103(12), pp. 2481-4.

Santner, S. J., Dawson, P. J., Tait, L., Soule, H. D., Eliason, J., Mohamed, A. N., Wolman, S. R., Heppner, G. H. and Miller, F. R. (2001) 'Malignant MCF10CA1 cell lines derived from premalignant human breast epithelial MCF10AT cells', *Breast Cancer Res Treat,* 65(2), pp. 101-10.

Sarrió, D., Rodriguez-Pinilla, S. M., Hardisson, D., Cano, A., Moreno-Bueno, G. and Palacios, J. (2008) 'Epithelial-mesenchymal transition in breast cancer relates to the basal-like phenotype', *Cancer Res,* 68(4), pp. 989-97.

Savani, R. C., Cao, G., Pooler, P. M., Zaman, A., Zhou, Z. and DeLisser, H. M. (2001) 'Differential involvement of the hyaluronan (HA) receptors CD44 and receptor for HA-mediated motility in endothelial cell function and angiogenesis', *J Biol Chem,* 276(39), pp. 36770-8.

Scatena, M., Almeida, M., Chaisson, M. L., Fausto, N., Nicosia, R. F. and Giachelli, C. M. (1998) 'NF-kappaB mediates alphavbeta3 integrin-induced endothelial cell survival', *J Cell Biol,* 141(4), pp. 1083-93.

Scheel, C., Onder, T., Karnoub, A. and Weinberg, R. A. (2007) 'Adaptation versus selection: the origins of metastatic behavior', *Cancer Res,* 67(24), pp. 11476-9; discussion 11479-80.

Schnitt, S. J. (2003) 'The diagnosis and management of pre-invasive breast disease: flat epithelial atypia--classification, pathologic features and clinical significance', *Breast Cancer Res,* 5(5), pp. 263-8.

Schuetz, C. S., Bonin, M., Clare, S. E., Nieselt, K., Sotlar, K., Walter, M., Fehm, T., Solomayer, E., Riess, O., Wallwiener, D., Kurek, R. and Neubauer, H. J. (2006) 'Progression-specific genes identified by expression profiling of matched ductal carcinomas in situ and invasive breast tumors, combining laser capture microdissection and oligonucleotide microarray analysis', *Cancer Res,* 66(10), pp. 5278-86.

Schulte-Merker, S. and Smith, J. C. (1995) 'Mesoderm formation in response to Brachyury requires FGF signalling', *Curr Biol,* 5(1), pp. 62-7.

Schwartz, G. F., Finkel, G. C., Garcia, J. C. and Patchefsky, A. S. (1992) 'Subclinical ductal carcinoma in situ of the breast. Treatment by local excision and surveillance alone', *Cancer,* 70(10), pp. 2468-74.

Senbanjo, L. T. and Chellaiah, M. A. (2017) 'CD44: A Multifunctional Cell Surface Adhesion Receptor Is a Regulator of Progression and Metastasis of Cancer Cells', *Front Cell Dev Biol,* 5, pp. 18.

Senger, D. R., Ledbetter, S. R., Claffey, K. P., Papadopoulos-Sergiou, A., Peruzzi, C. A. and Detmar, M. (1996) 'Stimulation of endothelial cell migration by vascular permeability factor/vascular endothelial growth factor through cooperative mechanisms involving the alphavbeta3 integrin, osteopontin, and thrombin', *Am J Pathol,* 149(1), pp. 293-305.

Shan, Z. Z., Yan, X. B., Yan, L. L., Tian, Y., Meng, Q. C., Qiu, W. W., Zhang, Z. and Jin, Z. M. (2015) 'Overexpression of Tbx3 is correlated with Epithelial-Mesenchymal Transition phenotype and predicts poor prognosis of colorectal cancer', *Am J Cancer Res,* 5(1), pp. 344-53.

Shapiro, I. M., Cheng, A. W., Flytzanis, N. C., Balsamo, M., Condeelis, J. S., Oktay, M. H., Burge, C. B. and Gertler, F. B. (2011) 'An EMT-driven alternative splicing program occurs in human breast cancer and modulates cellular phenotype', *PLoS Genet,* 7(8), pp. e1002218.

Shekhar, P. V., Chen, M. L., Werdell, J., Heppner, G. H., Miller, F. R. and Christman, J. K. (1998) 'Transcriptional activation of functional endogenous estrogen receptor gene expression in MCF10AT cells: a model for early breast cancer', *Int J Oncol,* 13(5), pp. 907-15.

Shen, S., Wang, Y., Wang, C., Wu, Y. N. and Xing, Y. (2016) 'SURVIV for survival analysis of mRNA isoform variation', *Nat Commun,* 7, pp. 11548.

Shijubo, N., Uede, T., Kon, S., Maeda, M., Segawa, T., Imada, A., Hirasawa, M. and Abe, S. (1999) 'Vascular endothelial growth factor and osteopontin in stage I lung adenocarcinoma', *Am J Respir Crit Care Med,* 160(4), pp. 1269-73.

Shimbo, T., Dunnick, J. K., Brix, A., Mav, D., Shah, R., Roberts, J. D. and Wade, P. A. (2017) 'DNA Methylation Changes in Tbx3 in a Mouse Model Exposed to Polybrominated Diphenyl Ethers', *Int J Toxicol,* 36(3), pp. 229-238.

Shirley, S. H., Hudson, L. G., He, J. and Kusewitt, D. F. (2010) 'The skinny on Slug', *Mol Carcinog,* 49(10), pp. 851-61.

Silber, J., Lim, D. A., Petritsch, C., Persson, A. I., Maunakea, A. K., Yu, M., Vandenberg, S. R., Ginzinger, D. G., James, C. D., Costello, J. F., Bergers, G., Weiss, W. A., Alvarez-Buylla, A. and Hodgson, J. G. (2008) 'miR-124 and miR-137 inhibit proliferation of glioblastoma multiforme cells and induce differentiation of brain tumor stem cells', *BMC Med,* 6, pp. 14.

Silverstein, M. J., Barth, A., Poller, D. N., Gierson, E. D., Colburn, W. J., Waisman, J. R. and Gamagami, P. (1995a) 'Ten-year results comparing mastectomy to excision and radiation therapy for ductal carcinoma in situ of the breast', *Eur J Cancer,* 31A(9), pp. 1425-7.

Silverstein, M. J., Lagios, M. D., Craig, P. H., Waisman, J. R., Lewinsky, B. S., Colburn, W. J. and Poller, D. N. (1996) 'A prognostic index for ductal carcinoma in situ of the breast', *Cancer,* 77(11), pp. 2267-74.

Silverstein, M. J., Poller, D. N., Waisman, J. R., Colburn, W. J., Barth, A., Gierson, E. D., Lewinsky, B., Gamagami, P. and Slamon, D. J. (1995b) 'Prognostic classification of breast ductal carcinoma-in-situ', *Lancet,* 345(8958), pp. 1154-7.

Simpson, P. T., Gale, T., Reis-Filho, J. S., Jones, C., Parry, S., Sloane, J. P., Hanby, A., Pinder, S. E., Lee, A. H., Humphreys, S., Ellis, I. O. and Lakhani, S. R. (2005) 'Columnar cell lesions of the breast: the missing link in breast cancer progression? A morphological and molecular analysis', *Am J Surg Pathol,* 29(6), pp. 734-46.

Singhal, H., Bautista, D. S., Tonkin, K. S., O'Malley, F. P., Tuck, A. B., Chambers, A. F. and Harris, J. F. (1997) 'Elevated plasma osteopontin in metastatic breast cancer associated with increased tumor burden and decreased survival', *Clin Cancer Res,* 3(4), pp. 605-11.

Slabáková, E., Pernicová, Z., Slavíčková, E., Staršíchová, A., Kozubík, A. and Souček, K. (2011) 'TGF-β1-induced EMT of non-transformed prostate hyperplasia cells is characterized by early induction of SNAI2/Slug', *Prostate,* 71(12), pp. 1332-43.

Slomiany, M. G., Dai, L., Tolliver, L. B., Grass, G. D., Zeng, Y. and Toole, B. P. (2009) 'Inhibition of Functional Hyaluronan-CD44 Interactions in CD133-positive Primary Human Ovarian Carcinoma Cells by Small Hyaluronan Oligosaccharides', *Clin Cancer Res,* 15(24), pp. 7593-7601.

Smith, J. (1999) 'T-box genes: what they do and how they do it', *Trends Genet,* 15(4), pp. 154-8.

Sodek, J., Ganss, B. and McKee, M. D. (2000) 'Osteopontin', *Crit Rev Oral Biol Med,* 11(3), pp. 279-303.

Solin, L. J., Gray, R., Baehner, F. L., Butler, S. M., Hughes, L. L., Yoshizawa, C., Cherbavaz, D. B., Shak, S., Page, D. L., Sledge, G. W., Jr., Davidson, N. E., Ingle, J. N., Perez, E. A., Wood, W. C., Sparano, J. A. and Badve, S. (2013) 'A multigene expression assay to predict local recurrence risk for ductal carcinoma in situ of the breast', *J Natl Cancer Inst,* 105(10), pp. 701-10.

Sørlie, T., Perou, C. M., Tibshirani, R., Aas, T., Geisler, S., Johnsen, H., Hastie, T., Eisen, M. B., van de Rijn, M., Jeffrey, S. S., Thorsen, T., Quist, H., Matese, J. C., Brown, P. O., Botstein, D., Lønning, P. E. and Børresen-Dale, A. L. (2001) 'Gene expression patterns of breast carcinomas distinguish tumor subclasses with clinical implications', *Proc Natl Acad Sci U S A,* 98(19), pp. 10869-74.

Souter, L. H., Andrews, J. D., Zhang, G., Cook, A. C., Postenka, C. O., Al-Katib, W., Leong, H. S., Rodenhiser, D. I., Chambers, A. F. and Tuck, A. B. (2010) 'Human 21T breast epithelial cell lines mimic breast cancer progression in vivo and in vitro and show stage-specific gene expression patterns', *Lab Invest,* 90(8), pp. 1247-58.

Stennard, F., Zorn, A. M., Ryan, K., Garrett, N. and Gurdon, J. B. (1999) 'Differential expression of VegT and Antipodean protein isoforms in Xenopus', *Mech Dev,* 86(1-2), pp. 87-98.

Stomper, P. C., Stewart, C. C., Penetrante, R. B., Nava, M. E. and Tsangaris, T. N. (1992) 'Flow cytometric DNA analysis of excised breast lesions: use of fresh tissue needle aspirates obtained under guidance with mammography of the specimen', *Radiology,* 185(2), pp. 415-22.

Storci, G., Sansone, P., Trere, D., Tavolari, S., Taffurelli, M., Ceccarelli, C., Guarnieri, T., Paterini, P., Pariali, M., Montanaro, L., Santini, D., Chieco, P. and Bonafé, M. (2008) 'The basal-like breast carcinoma phenotype is regulated by SLUG gene expression', *J Pathol,* 214(1), pp. 25-37.

Stott, D., Kispert, A. and Herrmann, B. G. (1993) 'Rescue of the tail defect of Brachyury mice', *Genes Dev,* 7(2), pp. 197-203.

Strickland, L. B., Dawson, P. J., Santner, S. J. and Miller, F. R. (2000) 'Progression of premalignant MCF10AT generates heterogeneous malignant variants with characteristic histologic types and immunohistochemical markers', *Breast Cancer Res Treat,* 64(3), pp. 235-40.

Sun, S. G., Zheng, B., Han, M., Fang, X. M., Li, H. X., Miao, S. B., Su, M., Han, Y., Shi, H. J. and Wen, J. K. (2011) 'miR-146a and Krüppel-like factor 4 form a feedback loop to participate in vascular smooth muscle cell proliferation', *EMBO Rep,* 12(1), pp. 56-62.

Szulwach, K. E., Li, X., Smrt, R. D., Li, Y., Luo, Y., Lin, L., Santistevan, N. J., Li, W., Zhao, X. and Jin, P. (2010) 'Cross talk between microRNA and epigenetic regulation in adult neurogenesis', *J Cell Biol,* 189(1), pp. 127-41.

Tait, L., Dawson, P., Wolman, S., Galea, K. and Miller, F. (1996) 'Multipotent human breast stem cell line MCF1OAT', *Int J Oncol,* 9(2), pp. 263-7.

Takahashi, F., Akutagawa, S., Fukumoto, H., Tsukiyama, S., Ohe, Y., Takahashi, K., Fukuchi, Y., Saijo, N. and Nishio, K. (2002) 'Osteopontin induces angiogenesis of murine neuroblastoma cells in mice', *Int J Cancer,* 98(5), pp. 707-12.

Takano, S., Tsuboi, K., Tomono, Y., Mitsui, Y. and Nose, T. (2000) 'Tissue factor, osteopontin, alphavbeta3 integrin expression in microvasculature of gliomas associated with vascular endothelial growth factor expression', *Br J Cancer,* 82(12), pp. 1967-73.

Tammi, M. I., Day, A. J. and Turley, E. A. (2002) 'Hyaluronan and homeostasis: a balancing act', *J Biol Chem,* 277(7), pp. 4581-4.

Tammi, R., MacCallum, D., Hascall, V. C., Pienimäki, J. P., Hyttinen, M. and Tammi, M. (1998) 'Hyaluronan bound to CD44 on keratinocytes is displaced by hyaluronan decasaccharides and not hexasaccharides', *J Biol Chem,* 273(44), pp. 28878-88.

Tammi, R. H., Kultti, A., Kosma, V. M., Pirinen, R., Auvinen, P. and Tammi, M. I. (2008) 'Hyaluronan in human tumors: pathobiological and prognostic messages from cell-associated and stromal hyaluronan', *Semin Cancer Biol,* 18(4), pp. 288-95.

Tao, W. and Levine, A. J. (1999) 'P19(ARF) stabilizes p53 by blocking nucleo-cytoplasmic shuttling of Mdm2', *Proc Natl Acad Sci U S A,* 96(12), pp. 6937-41.

Tavassoli, F. A. and Norris, H. J. (1990) 'A comparison of the results of long-term follow-up for atypical intraductal hyperplasia and intraductal hyperplasia of the breast', *Cancer,* 65(3), pp. 518-29.

Thiery, J. P., Acloque, H., Huang, R. Y. and Nieto, M. A. (2009) 'Epithelial-mesenchymal transitions in development and disease', *Cell,* 139(5), pp. 871-90.

Thompson, E. W., Newgreen, D. F. and Tarin, D. (2005) 'Carcinoma invasion and metastasis: a role for epithelial-mesenchymal transition?', *Cancer Res,* 65(14), pp. 5991-5; discussion 5995.

Thorat, M. A., Parmar, V., Nadkarni, M. S. and Badwe, R. A. (2007) 'Radiation therapy for ductal carcinoma in situ: is it really worth it?', *J Clin Oncol,* 25(4), pp. 461-2; author reply 462.

Tian, F., DaCosta Byfield, S., Parks, W. T., Yoo, S., Felici, A., Tang, B., Piek, E., Wakefield, L. M. and Roberts, A. B. (2003) 'Reduction in Smad2/3 signaling enhances tumorigenesis but suppresses metastasis of breast cancer cell lines', *Cancer Res,* 63(23), pp. 8284-92.

Toole, B. P. (2004) 'Hyaluronan: from extracellular glue to pericellular cue', *Nat Rev Cancer,* 4(7), pp. 528-39.

Toole, B. P. (2009) 'Hyaluronan-CD44 Interactions in Cancer: Paradoxes and Possibilities', *Clin Cancer Res,* 15(24), pp. 7462-7468.

Tran, N. L., Nagle, R. B., Cress, A. E. and Heimark, R. L. (1999) 'N-Cadherin expression in human prostate carcinoma cell lines. An epithelial-mesenchymal transformation mediating adhesion withStromal cells', *Am J Pathol,* 155(3), pp. 787-98.

Trochon, V., Mabilat, C., Bertrand, P., Legrand, Y., Smadja-Joffe, F., Soria, C., Delpech, B. and Lu, H. (1996) 'Evidence of involvement of CD44 in endothelial cell proliferation, migration and angiogenesis in vitro', *Int J Cancer,* 66(5), pp. 664-8.

Troxell, M. L., Brunner, A. L., Neff, T., Warrick, A., Beadling, C., Montgomery, K., Zhu, S., Corless, C. L. and West, R. B. (2012) 'Phosphatidylinositol-3-kinase pathway mutations are common in breast columnar cell lesions', *Mod Pathol,* 25(7), pp. 930-7.

Tuck, A. B., Arsenault, D. M., O'Malley, F. P., Hota, C., Ling, M. C., Wilson, S. M. and Chambers, A. F. (1999) 'Osteopontin induces increased invasiveness and plasminogen activator expression of human mammary epithelial cells', *Oncogene,* 18(29), pp. 4237-46.

Tuck, A. B., O'Malley, F. P., Singhal, H., Harris, J. F., Tonkin, K. S., Kerkvliet, N., Saad, Z., Doig, G. S. and Chambers, A. F. (1998) 'Osteopontin expression in a group of lymph node negative breast cancer patients', *Int J Cancer,* 79(5), pp. 502-8.

Turashvili, G., Hayes, M., Gilks, B., Watson, P. and Aparicio, S. (2008) 'Are columnar cell lesions the earliest histologically detectable non-obligate precursor of breast cancer?', *Virchows Arch,* 452(6), pp. 589-98.

Turley, E. A., Noble, P. W. and Bourguignon, L. Y. (2002) 'Signaling properties of hyaluronan receptors', *J Biol Chem,* 277(7), pp. 4589-92.

Udabage, L., Brownlee, G. R., Nilsson, S. K. and Brown, T. J. (2005a) 'The over-expression of HAS2, Hyal-2 and CD44 is implicated in the invasiveness of breast cancer', *Exp Cell Res,* 310(1), pp. 205-17.

Udabage, L., Brownlee, G. R., Waltham, M., Blick, T., Walker, E. C., Heldin, P., Nilsson, S. K., Thompson, E. W. and Brown, T. J. (2005b) 'Antisense-mediated suppression of hyaluronan synthase 2 inhibits the tumorigenesis and progression of breast cancer', *Cancer Res,* 65(14), pp. 6139-50.

van 't Veer, L. J., Dai, H., van de Vijver, M. J., He, Y. D., Hart, A. A., Mao, M., Peterse, H. L., van der Kooy, K., Marton, M. J., Witteveen, A. T., Schreiber, G. J., Kerkhoven, R. M., Roberts, C., Linsley, P. S., Bernards, R. and Friend, S. H. (2002) 'Gene expression profiling predicts clinical outcome of breast cancer', *Nature,* 415(6871), pp. 530-6.

van de Vijver, M. J., He, Y. D., van't Veer, L. J., Dai, H., Hart, A. A., Voskuil, D. W., Schreiber, G. J., Peterse, J. L., Roberts, C., Marton, M. J., Parrish, M., Atsma, D., Witteveen, A., Glas, A., Delahaye, L., van der Velde, T., Bartelink, H., Rodenhuis, S., Rutgers, E. T., Friend, S. H. and Bernards, R. (2002) 'A gene-expression signature as a predictor of survival in breast cancer', *N Engl J Med,* 347(25), pp. 1999-2009.

van Dongen, J. A., Fentiman, I. S., Harris, J. R., Holland, R., Peterse, J. L., Salvadori, B. and Stewart, H. J. (1989) 'In-situ breast cancer: the EORTC consensus meeting', *Lancet,* 2(8653), pp. 25-7.

Vandewalle, C., Comijn, J., De Craene, B., Vermassen, P., Bruyneel, E., Andersen, H., Tulchinsky, E., Van Roy, F. and Berx, G. (2005) 'SIP1/ZEB2 induces EMT by repressing genes of different epithelial cell-cell junctions', *Nucleic Acids Res,* 33(20), pp. 6566-78.

Venables, J. P. (2004) 'Aberrant and alternative splicing in cancer', *Cancer Res,* 64(21), pp. 7647-54.

Venables, J. P., Klinck, R., Bramard, A., Inkel, L., Dufresne-Martin, G., Koh, C., Gervais-Bird, J., Lapointe, E., Froehlich, U., Durand, M., Gendron, D., Brosseau, J. P., Thibault, P., Lucier, J. F., Tremblay, K., Prinos, P., Wellinger, R. J., Chabot, B., Rancourt, C. and Elela, S. A. (2008) 'Identification of alternative splicing markers for breast cancer', *Cancer Res,* 68(22), pp. 9525-31.

Wai, P. Y. and Kuo, P. C. (2004) 'The role of Osteopontin in tumor metastasis', *J Surg Res,* 121(2), pp. 228-41.

Waldman, F. M., DeVries, S., Chew, K. L., Moore, D. H., Kerlikowske, K. and Ljung, B. M. (2000) 'Chromosomal alterations in ductal carcinomas in situ and their in situ recurrences', *J Natl Cancer Inst,* 92(4), pp. 313-20.

Waldman, T., Kinzler, K. W. and Vogelstein, B. (1995) 'p21 is necessary for the p53-mediated G1 arrest in human cancer cells', *Cancer Res,* 55(22), pp. 5187-90.

Wang, B., Lindley, L. E., Fernandez-Vega, V., Rieger, M. E., Sims, A. H. and Briegel, K. J. (2012) 'The T box transcription factor TBX2 promotes epithelial-mesenchymal transition and invasion of normal and malignant breast epithelial cells', *PLoS One,* 7(7), pp. e41355.

Wang, H. C., Meng, Q. C., Shan, Z. Z., Yuan, Z. and Huang, X. Y. (2015) 'Overexpression of Tbx3 predicts poor prognosis of patients with resectable pancreatic carcinoma', *Asian Pac J Cancer Prev,* 16(4), pp. 1397-401.

Wapnir, I. L., Dignam, J. J., Fisher, B., Mamounas, E. P., Anderson, S. J., Julian, T. B., Land, S. R., Margolese, R. G., Swain, S. M., Costantino, J. P. and Wolmark, N. (2011) 'Long-term outcomes of invasive ipsilateral breast tumor recurrences after lumpectomy in NSABP B-17 and B-24 randomized clinical trials for DCIS', *J Natl Cancer Inst,* 103(6), pp. 478-88.

Warneke, J., Grossklaus, D., Davis, J., Stea, B., Bebb, G., Taylor, C., Hastings, R. and Villar, H. (1995) 'Influence of local treatment on the recurrence rate of ductal carcinoma in situ', *J Am Coll Surg,* 180(6), pp. 683-8.

Weidner, N., Semple, J. P., Welch, W. R. and Folkman, J. (1991) 'Tumor angiogenesis and metastasis--correlation in invasive breast carcinoma', *N Engl J Med,* 324(1), pp. 1-8.

Weigel, P. H. and DeAngelis, P. L. (2007) 'Hyaluronan synthases: a decade-plus of novel glycosyltransferases', *J Biol Chem,* 282(51), pp. 36777-81.

Wellings, S. R. and Jensen, H. M. (1973) 'On the origin and progression of ductal carcinoma in the human breast', *J Natl Cancer Inst,* 50(5), pp. 1111-8.

Wellings, S. R., Jensen, H. M. and Marcum, R. G. (1975) 'An atlas of subgross pathology of the human breast with special reference to possible precancerous lesions', *J Natl Cancer Inst,* 55(2), pp. 231-73.

West, D. C., Hampson, I. N., Arnold, F. and Kumar, S. (1985) 'Angiogenesis induced by degradation products of hyaluronic acid', *Science,* 228(4705), pp. 1324-6.

West, D. C. and Kumar, S. (1989) 'Hyaluronan and angiogenesis', *Ciba Found Symp,* 143, pp. 187-201; discussion 201-7, 281-5.

Willmer, T., Cooper, A., Peres, J., Omar, R. and Prince, S. (2017) 'The T-Box transcription factor 3 in development and cancer', *Biosci Trends,* 11(3), pp. 254-266.

Willmer, T., Cooper, A., Sims, D., Govender, D. and Prince, S. (2016a) 'The T-box transcription factor 3 is a promising biomarker and a key regulator of the oncogenic phenotype of a diverse range of sarcoma subtypes', *Oncogenesis,* 5, pp. e199.

Willmer, T., Hare, S., Peres, J. and Prince, S. (2016b) 'The T-box transcription factor TBX3 drives proliferation by direct repression of the p21(WAF1) cyclin-dependent kinase inhibitor', *Cell Div,* 11, pp. 6.

Wilson, V. and Conlon, F. L. (2002) 'The T-box family', *Genome Biol,* 3(6), pp. REVIEWS3008.

Witte, J. S. (2010) 'Personalized prostate cancer screening: improving PSA tests with genomic information', *Sci Transl Med,* 2(62), pp. 62ps55.

Wong, J. S., Chen, Y. H., Gadd, M. A., Gelman, R., Lester, S. C., Schnitt, S. J., Sgroi, D. C., Silver, B. J., Smith, B. L., Troyan, S. L. and Harris, J. R. (2014) 'Eight-year update of a prospective study of wide excision alone for small low- or intermediate-grade ductal carcinoma in situ (DCIS)', *Breast Cancer Res Treat,* 143(2), pp. 343-50.

Wu, Y., Feng, J., Hu, W. and Zhang, Y. (2017) 'T-box 3 overexpression is associated with poor prognosis of non-small cell lung cancer', *Oncol Lett,* 13(5), pp. 3335-3341.

Xu, J., Souter, L. H., Chambers, A. F., Rodenhiser, D. I. and Tuck, A. B. (2008) 'Distinct karyotypes in three breast cancer cell lines --21PTCi, 21NTCi, and 21MT-1 --derived from the same patient and representing different stages of tumor progression', *Cancer Genet Cytogenet,* 186(1), pp. 33-40.

Xu, Y., Swerlick, R. A., Sepp, N., Bosse, D., Ades, E. W. and Lawley, T. J. (1994) 'Characterization of expression and modulation of cell adhesion molecules on an immortalized human dermal microvascular endothelial cell line (HMEC-1)', *J Invest Dermatol,* 102(6), pp. 833-7.

Yamaguchi, A., Goi, T., Taguchi, S., Ohtaki, N., Seki, K., Hirose, K., Nakagawara, G., Urano, T. and Furukawa, K. (1998) 'Clinical significance of serum levels of CD44 variant exons 8-10 protein in colorectal cancer', *J Gastroenterol,* 33(3), pp. 349-53.

Yanagisawa, K. O., Fujimoto, H. and Urushihara, H. (1981) 'Effects of the brachyury (T) mutation on morphogenetic movement in the mouse embryo', *Dev Biol,* 87(2), pp. 242-8.

Yarosh, W., Barrientos, T., Esmailpour, T., Lin, L., Carpenter, P. M., Osann, K., Anton-Culver, H. and Huang, T. (2008) 'TBX3 is overexpressed in breast cancer and represses p14 ARF by interacting with histone deacetylases', *Cancer Res,* 68(3), pp. 693-9.

Ye, Y., Xiao, Y., Wang, W., Yearsley, K., Gao, J. X. and Barsky, S. H. (2008) 'ERalpha suppresses slug expression directly by transcriptional repression', *Biochem J,* 416(2), pp. 179-87.

Ye, Y., Xiao, Y., Wang, W., Yearsley, K., Gao, J. X., Shetuni, B. and Barsky, S. H. (2010) 'ERalpha signaling through slug regulates E-cadherin and EMT', *Oncogene,* 29(10), pp. 1451-62.

Zafrani, B., Leroyer, A., Fourquet, A., Laurent, M., Trophilme, D., Validire, P. and Sastre-Garau, X. (1994) 'Mammographically-detected ductal in situ carcinoma of the breast analyzed with a new classification. A study of 127 cases: correlation with estrogen and progesterone receptors, p53 and c-erbB-2 proteins, and proliferative activity', *Semin Diagn Pathol,* 11(3), pp. 208-14.

Zhang, J. F., He, M. L., Qi Dong, Xie, W. D., Chen, Y. C., Lin, M. C., Leung, P. C., Zhang, Y. O. and Kung, H. F. (2011a) 'Aqueous extracts of Fructus Ligustri Lucidi enhance the sensitivity of human colorectal carcinoma DLD-1 cells to doxorubicin-induced apoptosis via Tbx3 suppression', *Integr Cancer Ther,* 10(1), pp. 85-91.

Zhang, Z., O'Rourke, J. R., McManus, M. T., Lewandoski, M., Harfe, B. D. and Sun, X. (2011b) 'The microRNA-processing enzyme Dicer is dispensable for somite segmentation but essential for limb bud positioning', *Dev Biol,* 351(2), pp. 254-65.

Zhang, Z., Yamashita, H., Toyama, T., Sugiura, H., Ando, Y., Mita, K., Hamaguchi, M., Hara, Y., Kobayashi, S. and Iwase, H. (2005) 'Quantitation of HDAC1 mRNA expression in invasive carcinoma of the breast*', *Breast Cancer Res Treat,* 94(1), pp. 11-6.

Zhao, D., Wu, Y. and Chen, K. (2014) 'Tbx3 isoforms are involved in pluripotency maintaining through distinct regulation of Nanog transcriptional activity', *Biochem Biophys Res Commun,* 444(3), pp. 411-4.

Zhu, B., Zhang, M., Williams, E. M., Keller, C., Mansoor, A. and Davie, J. K. (2016) 'TBX2 represses PTEN in rhabdomyosarcoma and skeletal muscle', *Oncogene,* 35(32), pp. 4212-24.

Zhuang, Z., Merino, M. J., Chuaqui, R., Liotta, L. A. and Emmert-Buck, M. R. (1995) 'Identical allelic loss on chromosome 11q13 in microdissected in situ and invasive human breast cancer', *Cancer Res,* 55(3), pp. 467-71.

Zoltan-Jones, A., Huang, L., Ghatak, S. and Toole, B. P. (2003) 'Elevated hyaluronan production induces mesenchymal and transformed properties in epithelial cells', *J Biol Chem,* 278(46), pp. 45801-10.

Chapter 2

Examination of functional and phenotypic changes associated with modulation of TBX3 levels at various stages of breast cancer progression

2 Examination of functional and phenotypic changes associated with modulation of TBX3 levels at various stages of breast cancer progression

SUMMARY OF FINDINGS

TBX3 is abundant in the invasive 21MT-1 cell line, while being minimally expressed in the non-invasive 21NT and 21PT cell lines. Overexpression of either TBX3iso1 or TBX3iso2 in 21NT cells resulted in increased cell survival/colony forming ability, growth vs. apoptosis and invasion in Matrigel. In contrast, short hairpin RNA-mediated knockdown of TBX3 in the 21MT-1 cells resulted in smaller colonies, with a more regular, less dispersed (less infiltrative) morphology. Array profiling of the 21NT TBX3iso1 and TBX3iso2 transfectants showed that there are common alterations in expression of several genes involved in signal transduction, cell cycle control/cell survival, epithelial-mesenchymal transition (EMT) and invasiveness. Overall, these results indicate that TBX3 expression can promote progression in a model of early breast cancer by altering cell properties involved in cell survival/colony formation and invasiveness, as well as key regulatory and EMT/invasiveness-related gene expressions.

Chapter 2 in this dissertation has been published (Krstic et al. 2016, BMC Cancer).

2.1 Introduction

Arguably the most critical stage of early breast cancer progression is the transition from DCIS to invasive mammary carcinoma (IMC). Although a number of molecular changes have been identified that accompany invasive breast cancer (Page et al., 1985, Page and Dupont, 1993, Lakhani et al., 1995, Allred et al., 2001, Arpino et al., 2005, Allred et al., 2008), those which may directly control the transition from DCIS to IMC remain elusive.

Using microarray analysis, we previously identified TBX3 as a potential regulator of progression from DCIS to IMC, using the 21T cell lines which represent distinct stages of breast cancer progression (Souter et al., 2010). Specifically, we found that invasive and metastatic 21MT-1 cells expressed higher levels of TBX3 than non-invasive DCIS-like 21NT cells and non-invasive ADH-like 21PT cells (Souter et al., 2010). TBX3 is a member of the T-box family of transcription factors that play an important role in development of many animal species. In mouse embryo development, a model has emerged in which TBX3 expression is both induced and maintained in early mammary gland initiation by Wnt and fibroblast growth factor (FGF) (Eblaghie et al., 2004). In humans, Ulnar-mammary syndrome, a congenital autosomal dominant disorder, is caused by mutations that result in haploinsufficiency of TBX3 and is characterized by upper-limb anomalies and mammary gland hypoplasia (Bamshad et al., 1999).

TBX3 has been linked to tumorigenesis and is involved in cell cycle control and inhibition of cell senescence, through both p53-dependent and independent pathways (Brummelkamp et al., 2002, Carlson et al., 2002). The p53-dependent pathway signals through $p14^{ARF}$, a tumor suppressor and cell cycle control protein that is a product of the cyclin-dependent kinase inhibitor 2A (CDKN2A) gene, along with $p16^{INK4A}$. TBX3 directly represses transcription of $p14^{ARF}$ (Brummelkamp et al., 2002, Rowley et al., 2004). Down-regulation or inhibition of $p14^{ARF}$ leads to increased proliferation and immortalization, as well as failure of apoptosis (Rowley et al., 2004). Aside from its role in the cell cycle, TBX3 is a known repressor of E-cadherin expression in melanoma, leading to enhanced invasiveness (Rodriguez et al., 2008, Boyd et al., 2013). TBX3 expression has also been found to be associated with cell survival in hepatocellular carcinoma, where it is induced by Wnt/β-catenin signalling (Renard et al., 2007).

Two different isoforms of TBX3 have been identified, TBX3iso1 and TBX3iso2. The TBX3iso2 variant has an extra 20 amino acids, encoded by exon 2a, inserted into the T-box domain (Bamshad et al., 1999). As the 2a insertion is within the T-box domain, which is required for DNA-binding and protein-protein interactions, it was initially proposed that this variant may have altered DNA-binding properties, and that it may in fact interfere with the senescence-inhibiting properties (Fan et al., 2004). However, it has been found that TBX3iso2 can indeed bind to TBEs and act as an anti-senescence factor (Hoogaars et al., 2008).

Here we examined whether either or both isoforms of TBX3 can influence breast cancer progression, in particular the transition from non-invasive to invasive disease. We show that both isoforms of TBX3 have a similar functional effect in promoting breast cancer progression to a more malignant phenotype, and identify TBX3-induced changes in expression of genes involved in signal transduction, cell cycle control, cell survival and epithelial-mesenchymal transition (EMT)/invasiveness that may play a role in this progression.

2.2 Methods

Cell lines and culture conditions

The 21T parental cell lines (21PT, 21NT, and 21MT-1) were a kind gift from Dr. Vimla Band (Dana Farber Cancer Institute, Boston, MA) (Band et al., 1990) and were cultured in alpha modification of Eagle's medium supplemented with 2.8μM hydrocortisone, 12.5ng/ml epidermal growth factor, 2mM L-glutamine, 1μg/ml insulin, 10mM HEPES, 1mM sodium pyruvate, 0.1mM non-essential amino acids and 50μg/ml gentamycin reagent (called αHE – all supplements from Wisent Bioproducts). For regular culture conditions, the αHE media was further supplemented with 10% fetal bovine serum (FBS) (Sigma-Aldrich) and named αHE10F. Stably transfected cells were cultured in αHE10F containing either 500μg/ml G418 (Wisent Bioproducts) or 0.8μg/ml puromycin (Sigma-Aldrich).

Generation of TBX3 expression vectors

Expression vectors were constructed for each TBX3 isoform (TBX3iso1and TBX3iso2). To obtain TBX3iso2, PCR amplification of the whole transcript was performed from a pOTB7 expression vector containing TBX3iso2 [Genbank:BC025258] (Open Biosystems Thermo Scientific) as the cDNA template using Phusion High-Fidelity DNA Taq polymerase (New England BioLabs). Primers used to amplify TBX3iso2 were: forward: 5'-GCC ACC ATG AGC CTC TCC ATG AGA-3' and reverse: 5'-TTC GGG ACC GCC TGC GGG ACC TGT CCG GC-3'. To produce TBX3iso1, two PCR product fragments, representing the transcript before (fragment 1) and after (fragment 2) the 60bp TBX3iso2 addition, were PCR amplified. Primers used for fragment 1 of TBX3iso1 were: forward: 5'-GCC ACC ATG AGC CTC TCC ATG AGA-3' and reverse: 5'-CAT GGA GTT CAA TAT AGT AAA TCC ATG TTT GAC-3'. Primers used for fragment 2 of TBX3iso1 were: forward: 5'-TGG ATT TAC TAT ATT GAA CTC CAT GCA CAA AT-3' and reverse: 5'-TTC GGG ACC GCC TGC GGG ACC TGT CCG GC-3'. All primers used for generation of the TBX3 expression vectors were purchased from Sigma-Aldrich. Products were separated on 1% agarose gel and bands representing TBX3iso2 at ~2000kb were extracted and pooled. For TBX3iso1, a band at ~660kb for fragment 1 and a band at ~1380kb for fragment 2 were gel extracted and pooled. When designing the PCR primers for the two fragments of TBX3iso1, the reverse primer of the upstream amplicon (fragment 1) and the forward primer for the downstream amplicon (fragment 2) had a 20bp

overlap to ensure that the ends of these amplicons would anneal in a subsequent PCR reaction to melt the fragments together. This annealed TBX3iso1 PCR product was purified and amplified again. After running this PCR product on a 1% agarose gel and extracting at ~2000bp, both TBX3iso1 and TBX3iso2 PCR products were incubated with T4 polynucleotide kinase (New England BioLabs), and purified. Both products were inserted separately into pZsGreen1-N1 plasmids (Clonetech Laboratories), such that the ZsGreen was fused to the C-terminus of TBX3. To prepare the pZsGreen1-N1 plasmid, it was digested with Afe1 (New England BioLabs) and incubated with calf intestinal alkaline phosphatase (New England BioLabs) to dephosphorylate the cut ends. The digested plasmid was electrophoresed and gel extracted. The plasmid and TBX3 PCR products were incubated overnight with ATP and T4 DNA Ligase (New England BioLabs) at 16°C to complete ligation. Competent bacteria (DH5α) were transformed with the ligated plasmid and kanamycin resistant clones were expanded to isolate DNA. Clones were digested with the following enzyme pairs to check for proper size and orientation: AgeI/KpnI, MfeI/XhoI, and NheI/HndIII. Suitable clones were sequenced (DNA Sequencing Facility at Robarts Research Institute, London, ON).

The use of untagged TBX3 was required so the TBX3 expression vectors underwent site directed mutagenesis in order to introduce a stop codon at the end of full length TBX3iso1 and TBX3iso2 using QuikChange Site-Directed Mutagenesis Kit (Agilent Technologies) according to the manufacturer's protocol. Clones were sent to the DNA Sequencing Facility at Robarts Research Institute for sequencing. Clones with the proper sequence were used for stable transfections.

Transfections

Purified TBX3iso1 and TBX3iso2 plasmid DNA was transfected using PolyJet DNA In Vitro Transfection Reagent (SignaGen Laboratories) following the manufacturer's protocol. Empty vector (EV) plasmids were transfected as a control. Stable transfectants were selected in αHE10F containing 500μg/ml G418 (Wisent Bioproducts). Approximately two weeks post-transfection, resistant clones were pooled, expanded, and frozen for later use.

Generation of lentiviral particles and transduction

Generation of short hairpin (sh) RNA containing lentivirus particles and knockdown of target genes were described previously (Moffat et al., 2006, MacMillan et al., 2014). The shRNA target sequence for TBX3 was GCA TAC CAG AAT GAT AAG ATA which targeted the coding sequence of both TBX3iso1 and TBX3iso2. The shRNA target sequence for Luciferase (off-target knockdown control) was ACG CTG AGT ACT TCG AAA TGT. The TBX3 shRNA lentivirus particles generated were used to knockdown TBX3 in the 21MT-1 cell line and Luciferase shRNA was used a negative control. One week post-transduction, stable clones were selected in αHE10F containing 0.8μg/ml puromycin (Sigma-Aldrich) and resistant clones were pooled, expanded, and frozen for later use.

Isolation of RNA and quantitative real-time polymerase chain reaction (qRT-PCR)

Cells were harvested with trypsin and RNA was isolated using the RNeasy Mini Kit (Qiagen). Samples were treated with 30U DNase I (Qiagen), and 500ng of RNA was converted into cDNA with the Superscript III First-Strand Synthesis System (Invitrogen) using Oligo(dT) 12-18 primers (Invitrogen). qRT-PCR was performed using RT2 SYBR Green ROX qPCR Mastermix (Qiagen) on an Mx3000P QPCR system. Primers used for total TBX3 were: forward: 5'-CGC TGT GAC TGC ATA CCA GA-3' and reverse: 5'-GTG TCC CGG AAA CCT TTT GC-3'. Primers used for TBX3iso1 were: forward: 5'-AGT GGA TGT CCA AAG TCG TCA C-3' and reverse: 5'-CAT GGA GTT CAA TAT AGT AAA TCC ATG TTT GTC TG-3'. Primers used for TBX3iso2 were: forward: 5'-AGT GGA TGT CCA AAG TCG TCA C-3' and reverse: 5'-CAC TTG GGA AGG CCA AAG TAA ATC CAT G-3'. Primers used for GAPDH were: forward: 5'-AGG CTG GGG CTC ATT TGC AG-3' and reverse: 5-'CCA TCC ACA GTC TTC TGG GTG-3'. All primers were purchased from Sigma-Aldrich. Output values were reported relative to GAPDH as fold expression normalized to control cell lines.

Preparation of 21T cell lysates

Radioimmunoprecipitation (RIPA) buffer (10nM Tris-HCl pH 7.5, 1mM EDTA, 0.5mM EGTA, 150nM NaCl, 1% Triton-X 100, 0.5% DOC, and 1% SDS) containing one protease inhibitor tablet per 10mL (Complete, Mini, EDTA-free Protease Inhibitor Cocktail, Roche) was used to lyse cells grown as subconfluent monolayers in 10cm dishes. The cells were removed with a cell scraper, collected in a clean microcentrifuge tube, and placed on a rotator for 20 minutes

at 4°C. Tubes were spun at 13,000 RPM for 10 minutes at 4°C and the resulting supernatant was collected.

Electrophoresis and Western blotting

Proteins were electrophoresed on 10% polyacrylamide gels and subsequently analyzed after transfer by Western blot with anti-TBX3 antibody (Abcam, ab58264; 1:2,000), anti-Vimentin (Dako, clone 3B4; 1/1,000), anti-Twist (Abcam, ab50887; 1:1,000), anti-Src (Cell Signaling, 2108; 1:1,000), and anti-β-actin antibody (Abcam, ab49900; 1:150,000). After incubation with the appropriate horseradish peroxidase-conjugated secondary antibody (anti-mouse, Amersham GE Healthcare; anti-rabbit, Sigma) diluted 1:10,000, protein bands were detected using ECL Plus Western Blotting Detection Reagents (Amersham GE Healthcare) and then exposed to film in a dark room. Densitometric quantification was performed using ImageJ (Open source software, National Institutes of Health, USA).

Immunohistochemistry of 21T cell pellets

Trypsinized cells were washed twice in phosphate buffered saline (PBS), and pelleted in 15mL conical tubes. Pellets were re-suspended in 10% neutral buffered formalin (NBF) and stored at 4°C overnight. Formalin was removed, and pellets re-suspended in 1mL of 1% agarose cooled to 35°C. The hardened pellets were wrapped in lens paper, cassetted, and processed to paraffin. For histology, 4µm sections were deparaffinized, pre-treated with 10mM citrate buffer pH 6 and blocked for endogenous peroxidises in 3% H_2O_2/methanol. Sections were immunostained with rabbit anti-TBX3 antibody (Abcam, ab99302) diluted 1:300 at 4°C overnight. Signal detection was accomplished using ThermoScientific UltraVision LP Detection System (TL-060-HD).

Three-dimensional Matrigel culture and immunofluorescence

Three-dimensional Matrigel culture was described previously (Debnath et al., 2003, Lee et al., 2007a, MacMillan et al., 2014). Following a 9 day growth period, images were taken at both 4X and 10X objective using an inverted microscope. ImageJ (Open source software) was used to determine colony formation rates by quantifying the percentage of the population that formed colonies greater than 50µm in diameter. ImageJ was also used to determine the

proportion of circular colonies; a binary quantification method was utilized, with a circular colony having a circularity index above 0.75.

For immunofluorescence of Matrigel cultures, after 9 days of growth, the Matrigel plugs were fixed (10% NBF) and permeabilized (0.5% Triton X-100 in PBS). After blocking with normal goat serum (Invitrogen), rabbit anti-Ki67 (Abcam, ab833) and anti-cleaved caspase 3 (Cell Signaling, 9661) antibodies were incubated at 1:150 dilution in 10% normal goat serum overnight at 4ºC. Cells were incubated with Alexa Fluor 488 Goat Anti-Rabbit secondary antibody (Invitrogen, A11034) and counterstained with Hoechst 33342 (Invitrogen, H1399) and Alexa Fluor 546 Phalloidin (Invitrogen, A22238). Coverslips were mounted over the stained Matrigel plugs with ProLong Gold Antifade Reagent (Invitrogen). Imaging was done using an Olympus Confocal Imaging System (FluoView FV1000 coupled to the IX81 Motorized Inverted System Microscope). Nuclei per colony were manually counted after acquiring 3D colony images.

Transwell migration and invasion assays

To assess the migratory potential of 21NT cells overexpressing TBX3 isoforms, transwell inserts with 8.0µm pores (Corning, 3422; 24-well plate) were coated with a thin layer of gelatin (6µg) to serve as a substrate for migration without obstructing movement through the pores. A 100µL cell suspension ($5x10^5$ cells/mL in αHE with 0.1% bovine serum albumin (BSA)) was added to the upper chambers and 0.75mL αHE10F media was added to the bottom wells. After incubation at 37°C and 5% CO_2 for 22 hours, migrated cells were fixed with 1% glutaraldehyde for 20 minutes and stained with full-strength Hematoxylin for 15 minutes. Cells that remained on top of the membrane were removed using a cotton swab. Images of 5 non-overlapping fields of view were acquired using Image-Pro Analysis Software (Media Cybernetics) coupled to an inverted microscope at 10X objective. Cells were counted from the acquired images using ImageJ (Open source software). Similarly, to assess the invasive potential, transwell inserts with 8.0µm pores precoated with Matrigel (Corning, 354480) were used and incubation lasted 22 hours. Means derived from 4 replicates were used during analysis.

RT^2 PCR arrays

RNA was isolated from TBX3iso1 and TBX3iso2 transfectants, as well as vector controls, using the RNeasy Mini Kit (Qiagen). 1µg RNA was converted into cDNA using the RT2 First Strand Kit (Qiagen). RT2 SYBR Green Mastermix was combined with the cDNA and dH_2O as per the manufacturer's protocol. Expression of 84 key genes commonly dysregulated in breast cancer were assessed using Human Breast Cancer RT^2 PCR arrays (Qiagen, PAHS-131ZA-2). Data analysis was conducted by SA Biosciences PCR Array Data Analysis Web portal using the ΔΔCt method normalized to acidic ribosomal phosphoprotein P0 (RPLP0) expression. Heat map showing absolute expression of mRNA was generated using the SA Biosciences RT2 profiler PCR Array Data Analysis Web Portal.

Statistical analysis

Statistical analyses were done using GraphPad Prism 5.0 software (La Jolla, CA). Colony morphology experiments, stain quantification, migration and invasion assays, and mRNA and protein levels were analyzed using one-way ANOVAs followed by Tukey's post hoc test (for comparison between more than two groups) or Student's *t*-test (for comparison between two groups). Proportions were analyzed via Fisher's exact test. For all analyses, $p<0.05$ was considered statistically significant.

2.3 Results

2.3.1 TBX3iso1 and TBX3iso2 are differentially expressed in the 21T cell lines.

We have previously reported that TBX3 is expressed in the 21T cell lines, with low levels in the ADH-like 21PT and DCIS-like 21NT cells, and increased expression in the IMC-like 21MT-1 cells (Souter et al., 2010). This finding is consistent with previous reports that TBX3 is up-regulated in invasive stages of cancer. Expression of TBX3 was examined in the parental 21T cell lines at the mRNA and protein level. Total TBX3 expression was higher in invasive 21MT-1 cells relative to the non-invasive (21PT and 21NT) cell lines (Figure 2.3.1 A,D,E). Similarly, both TBX3iso1 and TBX3iso2 were up-regulated in 21MT-1 relative to 21PT and 21NT cells (Figure 2.3.1 B,C). In contrast, no difference in either total TBX3 expression, or expression of either isoform, was observed between the ADH-like 21PT cells and DCIS-like 21NT cells (Figure 2.3.1 A-E).

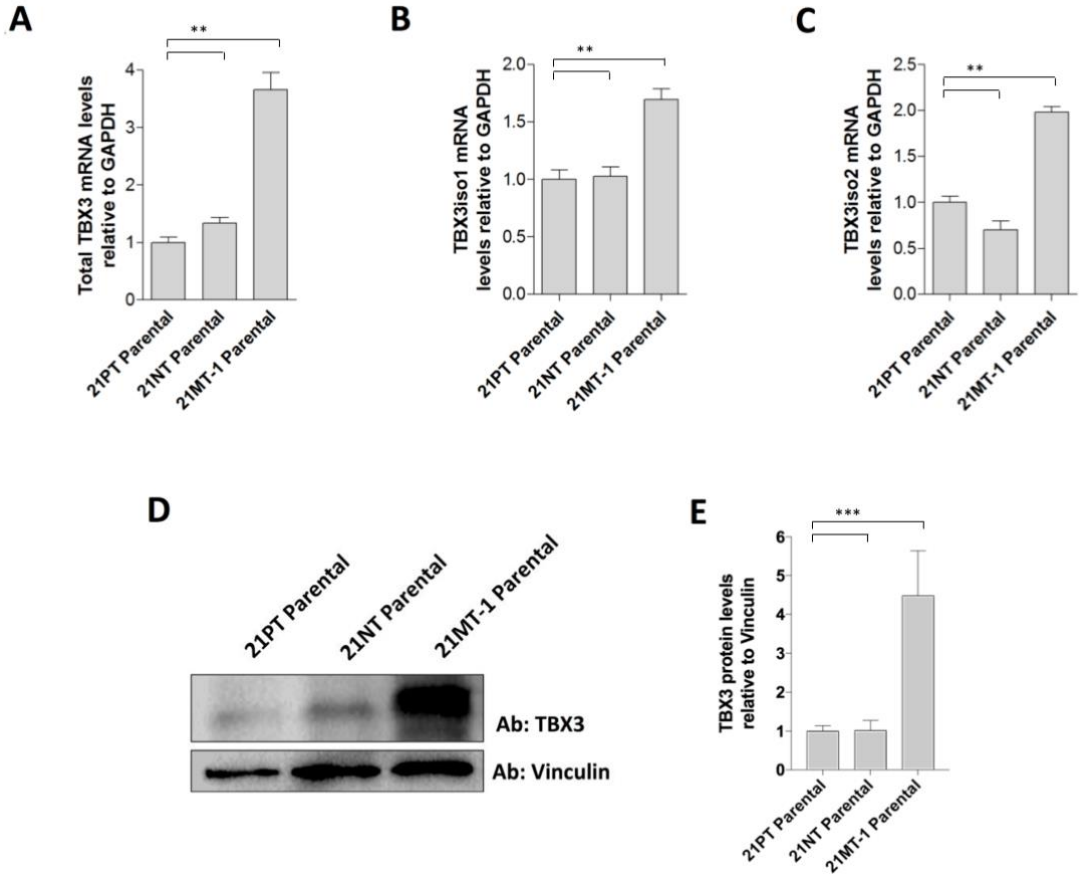

Figure 2.3.1 – TBX3iso1 and TBX3iso2 are differentially expressed in the 21T cell lines.

(A-C) Primers specific for either total TBX3, TBX3iso1, or TBX3iso2 were used to assess relative abundance of each transcript in 21T parental cell lines by qRT-PCR. **(D-E)** Total TBX3 protein is differentially expressed in the parental 21T cell lines. An antibody recognizing both isoforms of TBX3 was used to assess the relative abundance of TBX3 within the 21T cell lines. Means were analyzed using one-way ANOVA followed by Tukey's post hoc test and $p<0.05$ was considered statistically significant; ** $p<0.01$. Error bars indicate standard deviation. Results are representative of at least 3 independent experiments.

2.3.2 TBX3 expression is increased in DCIS-like 21NT cells after stable transfection.

In order to assess the effect of TBX3 on breast cancer progression, TBX3iso1 or TBX3iso2 were overexpressed in the DCIS-like 21NT cell line and results were compared to an empty vector (EV) control containing the same antibiotic resistant gene (neomycin). The relative mRNA expression level of total TBX3, TBX3iso1 and TBX3iso2 was assessed by qRT-PCR in the stably transfected cells. Total TBX3 mRNA was significantly up-regulated in both TBX3iso1 and TBX3iso2 transfectants (Figure 2.3.2 A), and the overexpression of TBX3 was isoform specific (Figure 2.3.2 B,C). Likewise, western blot analysis shows an increase in total TBX3 protein levels in the TBX3 transfectant cells compared to the empty vector control (Figure 2.3.2 D,E). Cell pellets of TBX3 transfectants were assessed by immunohistochemistry (Figure 2.3.2 F,G). TBX3 protein was localized to the nucleus, and nuclear expression was significantly higher in TBX3 transfectants. Nuclear localization, as observed by immunohistochemistry, is consistent with the known function of TBX3 as a transcriptional regulator.

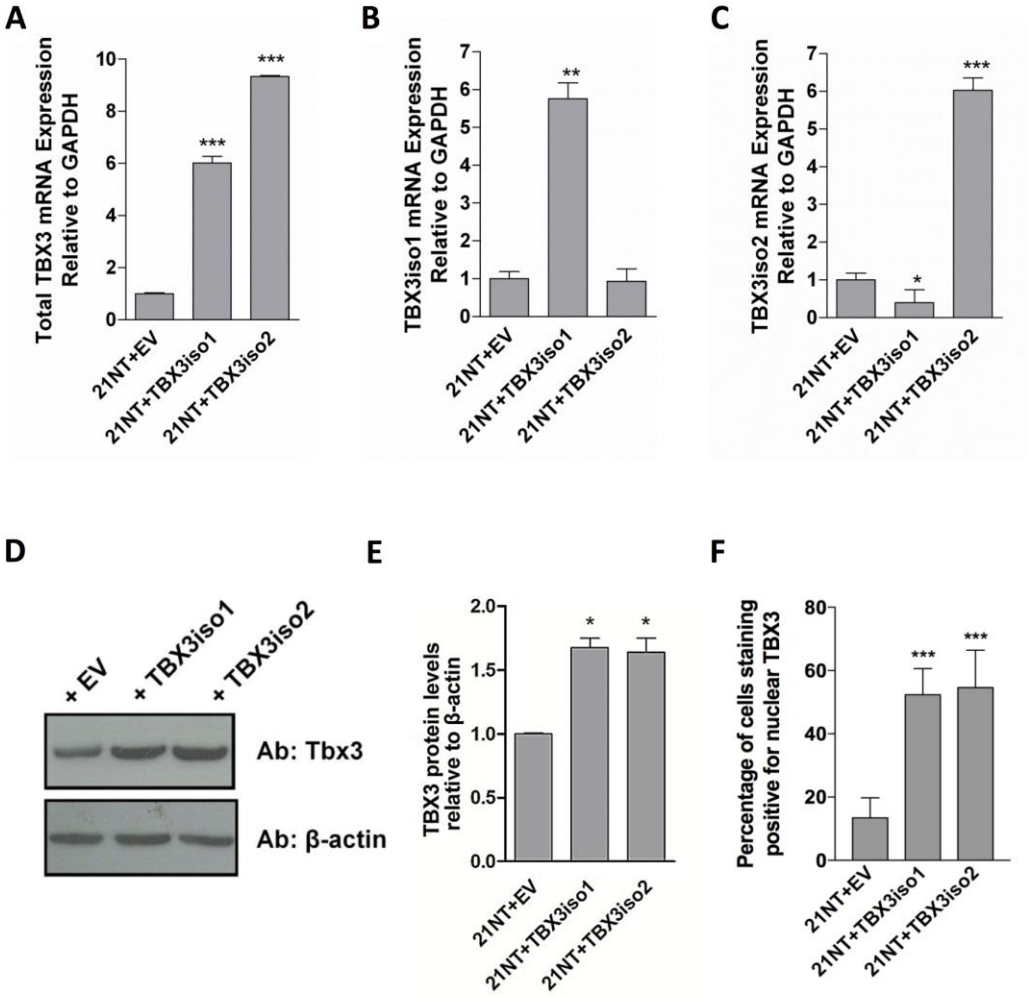
A
Total TBX3 mRNA Expression Relative to GAPDH
10
8
6
4
2
0
***
***
21NT+EV
21NT+TBX3iso1
21NT+TBX3iso2
B
TBX3iso1 mRNA Expression Relative to GAPDH
7
6
5
4
3
2
1
0
**
21NT+EV
21NT+TBX3iso1
21NT+TBX3iso2
C
TBX3iso2 mRNA Expression Relative to GAPDH
7
6
5
4
3
2
1
0
*
***
21NT+EV
21NT+TBX3iso1
21NT+TBX3iso2
D
+ EV
+ TBX3iso1
+ TBX3iso2
Ab: Tbx3
Ab: β-actin
E
TBX3 protein levels relative to β-actin
2.0
1.5
1.0
0.5
0.0
*
*
21NT+EV
21NT+TBX3iso1
21NT+TBX3iso2
F
Percentage of cells staining positive for nuclear TBX3
80
60
40
20
0
***
***
21NT+EV
21NT+TBX3iso1
21NT+TBX3iso2
G
21NT+EV
21NT+TBX3iso1
21NT+TBX3iso2
Ab: α-TBX3
Counterstain: Hx
Ab: α-TBX3
Counterstain: Hx
Ab: α-TBX3
Counterstain: Hx

Figure 2.3.2 – TBX3 expression is increased in 21NT cell transfectants.

21NT cell lines were stably transfected with either a TBX3iso1 or TBX3iso2 containing plasmid, or an empty vector control. **(A-C)** Assessment of relative transcript levels of total TBX3, TBX3iso1, and TBX3iso2 by qRT-PCR in stably transfected 21NT cells. **(D-E)** Assessment of total TBX3 protein levels by western blot in stably transfected 21NT cells. **(F-G)** Assessment of percentage of nuclei staining positive for TBX3 by IHC in stably transfected 21NT cell pellets. Cell pellets were stained using an anti-human TBX3 antibody and counter stained with Harris's Hematoxylin (Hx). Means were analyzed using one-way ANOVA followed by Tukey's post hoc test and $p<0.05$ was considered statistically significant; * $p<0.05$, ** $p<0.01$, *** $p<0.001$. Error bars indicate standard deviation. Results are representative of at least 3 independent experiments.

2.3.3 **TBX3 overexpression promotes progression of 21NT (DCIS) cells.**

To assess the role of TBX3 in the progression of DCIS to a more malignant phenotype, the 3D morphology of the 21NT transfectants was assessed using a 3D Matrigel assay (Figure 2.3.3 A-B). TBX3 isoform overexpression resulted in an increase in colony formation rates (Figure 2.3.3 C). As an index of the infiltrative vs. non-infiltrative nature of the colonies forming, we used a circularity index to determine the proportion of colonies that were circular (non-infiltrative) vs. non-circular (infiltrative). TBX3 isoform overexpression resulted in significantly less rounded, more infiltrative colonies (Figure 2.3.3 D). Immunofluorescence staining of colonies after 9 days of growth in Matrigel revealed significantly more nuclei per colony with TBX3 isoform overexpression (Figure 2.3.3 E). Additionally, immunofluorescence assessment of Ki67 and cleaved caspase 3 showed a significant increase in Ki67 (Figure 2.3.3 F) and decrease in cleaved caspase 3 (Figure 2.3.3 G) expression in TBX3 isoform transfectants. This resulted in an increase in the proliferation to apoptosis (Ki67 / cleaved caspase 3) ratio for both TBX3 isoform transfectants (Figure 2.3.3 H).

To further assess the migratory and invasive ability of TBX3-transfected 21NT cells, transwell assays were used. Cells were placed in the upper chamber of transwells (8.0μm pores coated with either a thin layer of gelatin for migration assays, or Matrigel for invasion assays) and allowed to migrate/invade through the pores towards a chemoattractant in the lower chamber. TBX3 isoform overexpression increased the ability of the cells to both migrate over gelatin (Figure 2.3.4 A-B) and invade through Matrigel (Figure 2.3.4 4C-D).

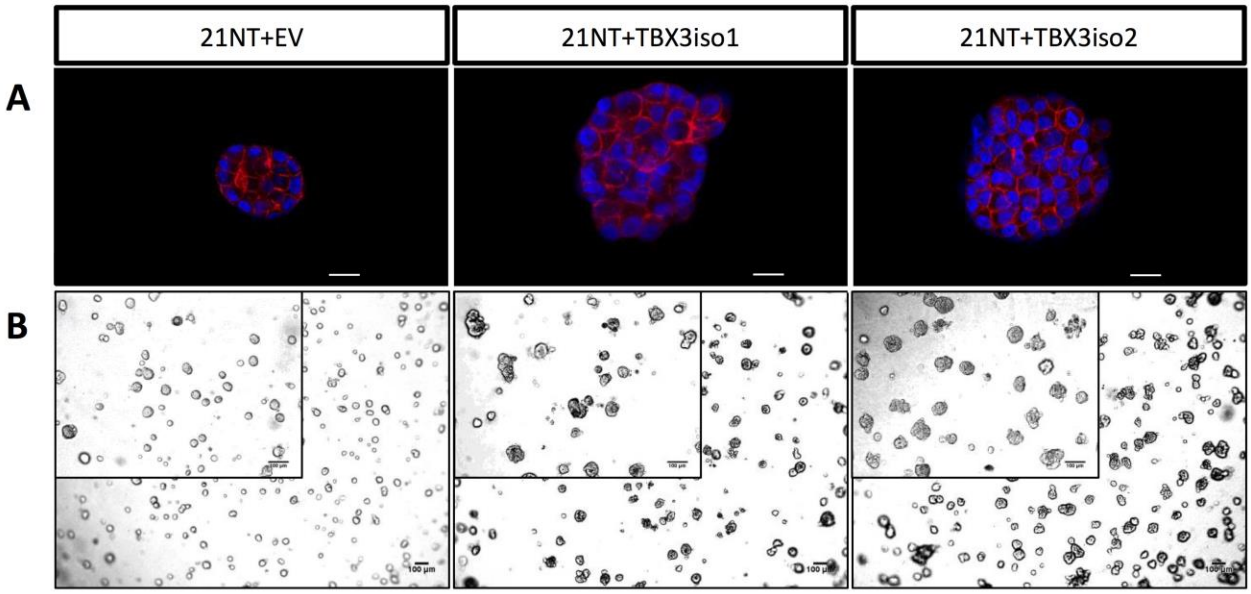
21NT+EV
21NT+TBX3iso1
21NT+TBX3iso2
A
B

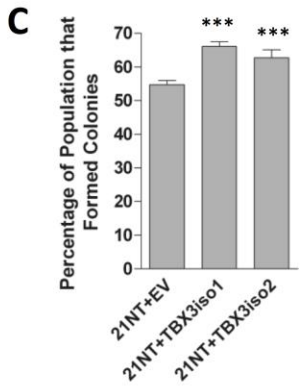
C
Percentage of Population that Formed Colonies
***
***
21NT+EV
21NT+TBX3iso1
21NT+TBX3iso2

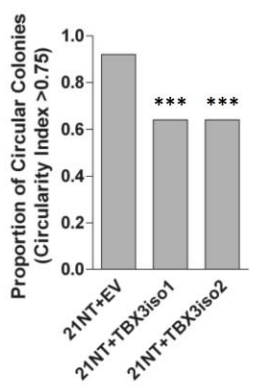
D
Proportion of Circular Colonies (Circularity Index >0.75)
***
***
21NT+EV
21NT+TBX3iso1
21NT+TBX3iso2

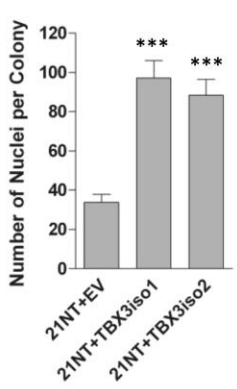
E
Number of Nuclei per Colony
***
***
21NT+EV
21NT+TBX3iso1
21NT+TBX3iso2

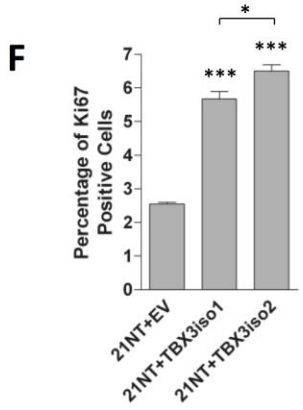
F
Percentage of Ki67 Positive Cells
*
***
***
21NT+EV
21NT+TBX3iso1
21NT+TBX3iso2

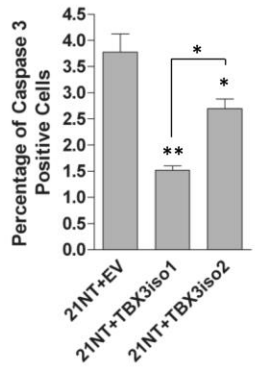
G
Percentage of Caspase 3 Positive Cells
*
**
*
21NT+EV
21NT+TBX3iso1
21NT+TBX3iso2

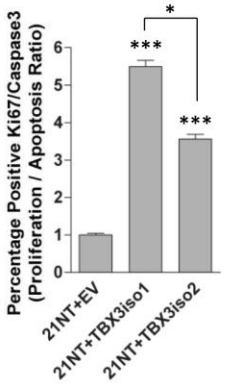
H
Percentage Positive Ki67/Caspase3 (Proliferation / Apoptosis Ratio)
*
***
***
21NT+EV
21NT+TBX3iso1
21NT+TBX3iso2

Figure 2.3.3 – TBX3 overexpression in DCIS-like 21NT cells results in a more aggressive phenotype in 3D Matrigel.

TBX3 transfectants were seeded in 3D Matrigel at 3,000 cells per well and incubated at 37ºC and 5% CO_2 for 9 days. **(A)** Immunofluorescence images depicting colony size of 21NT transfectants. Cells were grown in Matrigel for 9 days, then stained with Hoechst and Phalloidin and imaged using 60X objective. Scale bars represent 20µm. **(B)** Brightfield and phase contrast images showing growth of colonies after 9 days in 3D Matrigel. Brightfield images were taken using 4X objective, with the scale bar representing 100µm. Phase contrast images (inset) were taken using 40X objective, with the scale bar representing 20µm. **(C)** TBX3 overexpression increases colony formation rates. A colony was considered to be successfully formed when larger than 50µm in diameter. Analysis was conducted using ImageJ. **(D)** TBX3 overexpression decreased the proportion of round colonies. Analysis was conducted using ImageJ. A binary quantification method was utilized; a circularity index above 0.75 was considered circular. **(E)** TBX3 overexpression increases the number of nuclei per cell colony. **(F)** TBX3 overexpression resulted in an increase in the percentage of Ki-67 positive cells within colonies. **(G)** TBX3 overexpression resulted in a decrease in the percentage of cleaved caspase 3 positive cells within colonies. **(H)** The proliferation/apoptosis ratio, defined as the percentage of positive Ki67 cells divided by the percentage of positive cleaved caspase 3 cells, increased with overexpression of both TBX3 isoforms. Means were analyzed using one-way ANOVA followed by Tukey's post hoc test. The proportion of circular colonies was analyzed using Fisher's exact test. A value of $p<0.05$ was considered statistically significant; $*p<0.05$, $**p<0.01$, $***p<0.001$. Error bars indicate Standard Deviation. Results are representative of at least 3 independent experiments.

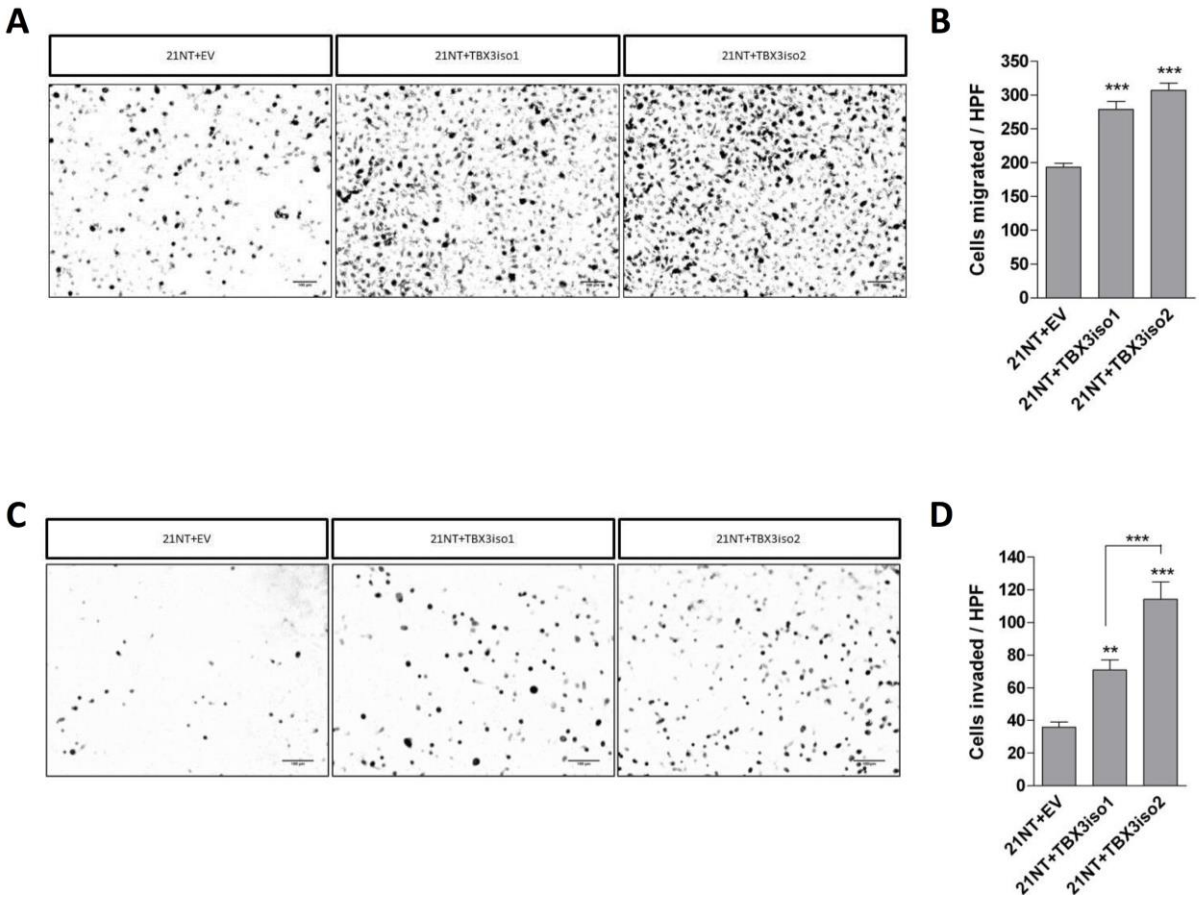

Figure 2.3.4 – TBX3 overexpression increases migration and invasion of 21NT cells.

(A-B) TBX3 overexpression increases migration using a transwell migration assay. 21NT cell transfectants were placed in the upper chamber of a transwell migration system with media containing 1% BSA and allowed to migrate towards αHE10F chemoattractant in the bottom chamber for 22 hours at 37ºC. Stable transfectants of both TBX3 isoforms showed an increase in migration using the transwell system. Scale bars represent 100μm. Results are quantified in panel b. **(C-D)** TBX3 overexpression increases invasion using a transwell invasion system. 21NT cell transfectants were placed in the upper chamber of a transwell invasion system with media containing 1% BSA and allowed to invade towards αHE10F chemoattractant in the bottom chamber for 22 hours at 37ºC. Stable transfectants of both TBX3 isoforms showed an increase in invasion using the transwell system. Scale bars represent 100μm. Results are quantified in panel D. Means were analyzed using one-way ANOVA followed by Tukey's post hoc test. A value of $p<0.05$ was considered statistically significant; *$p<0.05$, **$p<0.01$, ***$p<0.001$. Error bars indicate Standard Deviation. Results are representative of 4 independent experiments.

2.3.4 TBX3 knockdown reduces some characteristics of an aggressive phenotype in 21MT-1 (IMC) cells.

To examine whether reduction of TBX3 expression has an effect at a later stage of progression, TBX3 was knocked down in the invasive 21MT-1 cell line, using shRNA targeting both isoforms. TBX3 expression in the knockdown with the greatest reduction in both TBX3iso1 and TBX3iso2 mRNA expression is shown, with shLUC representing the off-target luciferase control (Figure 2.3.5 A-C). Quantitative RT-PCR analysis showed a five-fold reduction in total TBX3, TBX3iso1, and TBX3iso2 mRNA expression (Figure 2.3.5 A-C). There was also a corresponding reduction in total TBX3 at the protein level (Figure 2.3.5 D,E). While the TBX3 knockdown cells were still able to form colonies at a rate comparable with the shLUC control cells in the 9-day Matrigel assay (Figure 2.3.5 F,G), TBX3 knockdown resulted in an increased proportion of round/circular colonies (i.e. less dispersed/infiltrative; Figure 2.3.5 H) and fewer nuclei per colony (Figure 2.3.5 I), suggesting a reduction in invasiveness and impaired growth in 3D.

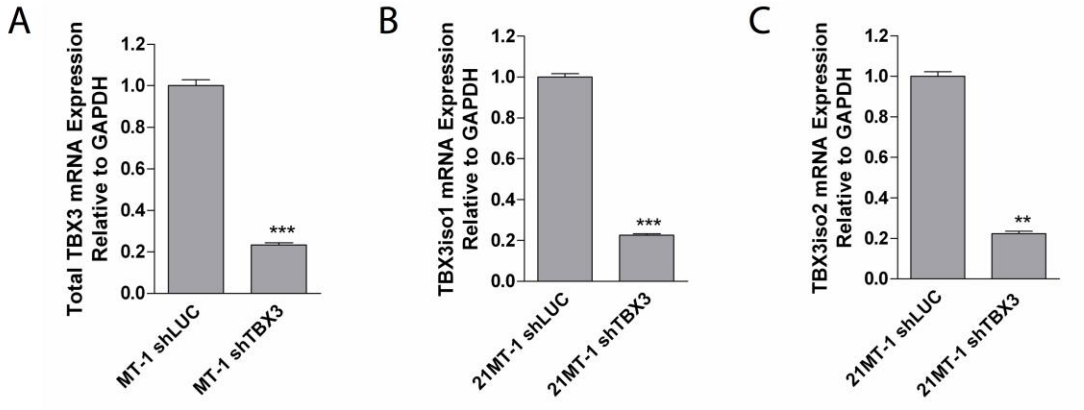
A
Total TBX3 mRNA Expression Relative to GAPDH
1.2
1.0
0.8
0.6
0.4
0.2
0.0
***
MT-1 shLUC
MT-1 shTBX3
B
TBX3iso1 mRNA Expression Relative to GAPDH
1.2
1.0
0.8
0.6
0.4
0.2
0.0
***
21MT-1 shLUC
21MT-1 shTBX3
C
TBX3iso2 mRNA Expression Relative to GAPDH
1.2
1.0
0.8
0.6
0.4
0.2
0.0
**
21MT-1 shLUC
21MT-1 shTBX3

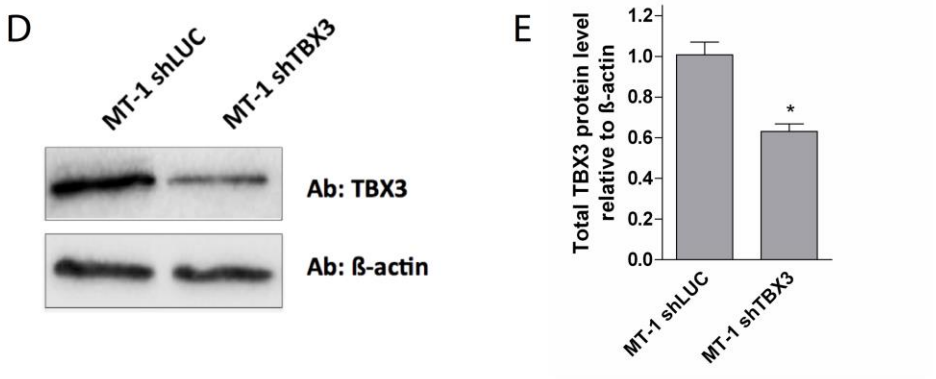
D
MT-1 shLUC
MT-1 shTBX3
Ab: TBX3
Ab: ß-actin
E
Total TBX3 protein level relative to ß-actin
1.2
1.0
0.8
0.6
0.4
0.2
0.0
*
MT-1 shLUC
MT-1 shTBX3

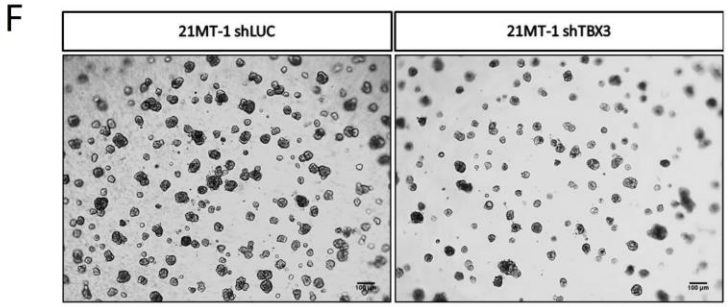
F
21MT-1 shLUC
21MT-1 shTBX3

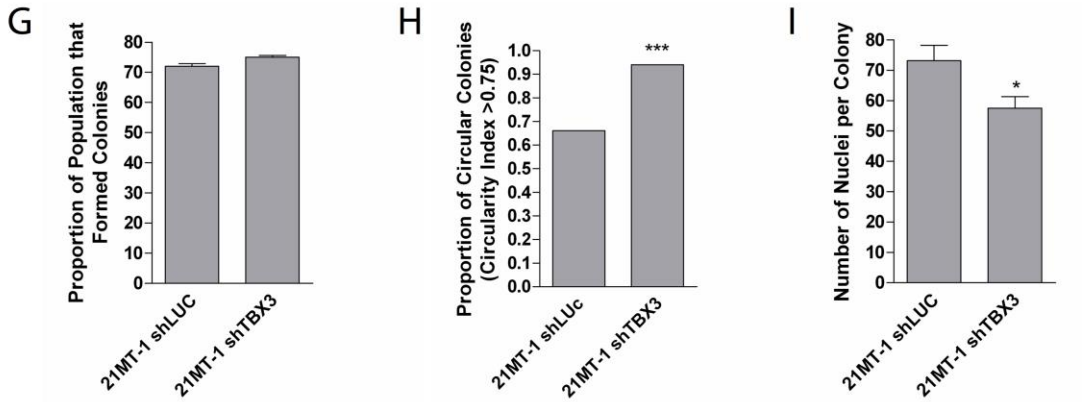
G
Proportion of Population that Formed Colonies
80
70
60
50
40
30
20
10
0
21MT-1 shLUC
21MT-1 shTBX3
H
Proportion of Circular Colonies (Circularity Index >0.75)
1.0
0.9
0.8
0.7
0.6
0.5
0.4
0.3
0.2
0.1
0.0
***
21MT-1 shLUc
21MT-1 shTBX3
I
Number of Nuclei per Colony
80
70
60
50
40
30
20
10
0
*
21MT-1 shLUC
21MT-1 shTBX3

Figure 2.3.5 – TBX3 knockdown results in a less aggressive phenotype of IMC-like 21MT-1 cells in 3D Matrigel.

(A) Total TBX3 mRNA is decreased in 21MT-1 shTBX3 cells after TBX3 knockdown. **(B)** TBX3iso1 mRNA is decreased in 21MT-1 shTBX3 after TBX3 knockdown. **(C)** TBX3iso2 mRNA is decreased in 21MT-1 after TBX3 knockdown. **(D)** Western blot showing total TBX3 protein is decreased in 21MT-1 shTBX3 cells after TBX3 knockdown. **(E)** Densitometry quantification of western blot shows a significant decrease in total TBX3 protein expression in the 21MT-1 shTBX3 cells. **(F)** Brightfield images showing colonies after 9 days in 3D Matrigel. Images were taken at 4X objective. Scale bars represent 100μm. **(G-I)** Cells were seeded in Matrigel and grown for 9 days. All of the cell lines were able to form colonies (G), but shTBX3 colonies were rounder (i.e. less dispersed, less invasive) (H) and smaller (I). Means were analyzed using one-way ANOVA followed by Tukey's post hoc test. The proportion of circular colonies was analyzed using Fisher's exact test. A value of $p<0.05$ was considered statistically significant; $*p<0.05$, $**p<0.01$, $***p<0.001$. Error bars indicate Standard Deviation. Results are representative of at least 3 independent experiments.

2.3.5 Up-regulation of TBX3 in 21NT (DCIS) cells results in alterations in expression of key regulatory and EMT/invasion associated genes.

We assessed the mRNA expression patterns of TBX3iso1 and TBX3iso2 transfected 21NT cells by RT^2 PCR arrays, and found a number of alterations in expression of key regulatory and EMT/invasion-associated genes. As 21NT cells transfected with either TBX3iso1 or TBX3iso2 had shown a similar more aggressive phenotype, we focused our interest on genes whose expression changed in common in both TBX3iso1 and TBX3iso2 transfected cells. We identified altered expression of a number of genes involved in signal transduction, cell cycle control, cell survival and EMT/invasiveness (Figure 2.3.6). In reference to pathways potentially involved in control of cell cycle, proliferation, apoptosis and cell survival, we observed significant down-regulation of CDKN2A (previously shown to be a key gene directly regulated by TBX3 in blocking cell senescence (Rowley et al., 2004, Yarosh et al., 2008)) with up-regulation of marker of proliferation Ki67 (MKI67); Jun proto-oncogene (JUN); nuclear receptor subfamily 3, group C, member 1 glucocorticoid receptor (NR3C1); epidermal growth factor receptor (EGFR); androgen receptor (AR); interleukin-6 (IL6); SRC proto-oncogene (SRC); and V-Akt murine thymoma viral oncogene homolog 1 (AKT1). Although the observed increase in retinoblastoma 1 (RB1), stratifin (SFN), breast cancer 1, early onset (BRCA1) and breast cancer 2, early onset (BRCA2) may seem counter-intuitive when the TBX3 up-regulated cells are found to be actively cycling and faster-growing, it is likely that these are attempted adaptation responses to the more direct effect of CDKN2A down-regulation by TBX3, the expected result of which would be release of cell-cycle checkpoint control, inhibition of senescence and apoptosis and promotion of progression through the cell cycle and cell proliferation.

Several genes potentially associated with EMT and cellular invasiveness were also altered in TBX3 isoform transfectants. Transcriptional regulators twist family BHLH transcription factor 1 (TWIST1) and snail family zinc finger 2 (SNAI2) were both up-regulated, as was SRC, and there was also altered expression of several proteases and protease inhibitors (including up-regulation of plasminogen activator, urokinase (PLAU), serpin peptidase inhibitor, clade E, member 1 (SERPINE1), and matrix metallopeptidase 9 (MMP9); and down-regulation of cystatin E/M (CST6)). Up-regulation of mesenchymal marker vimentin, as well as EMT-markers Twist and Src were confirmed at the protein level as well

(Figure 2.3.6 E). Whether directly or indirectly, up-regulation of either isoform of TBX3 in 21NT cells thus induced alterations in gene expression in pathways potentially involving cell cycle, cell survival, cell growth control and EMT/invasiveness, with the resulting *in vitro* phenotypes of more efficient and larger colony formation, increased proliferation/apoptosis ratio and increased motility and invasiveness through Matrigel.

A

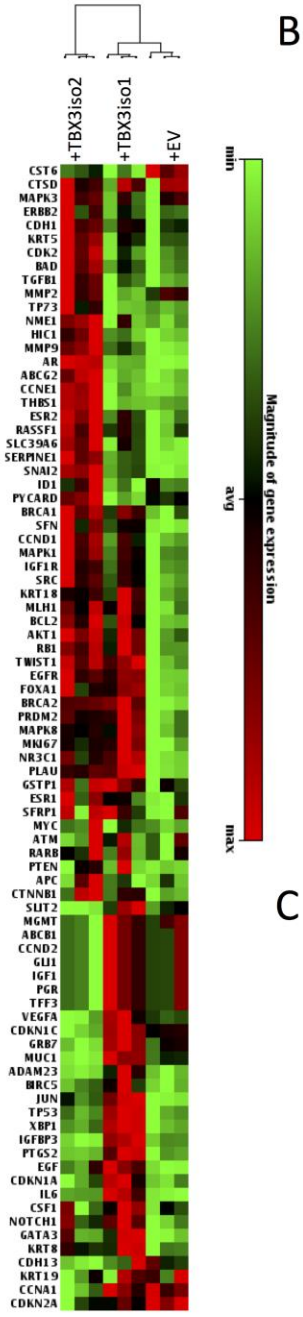

B

	+TBX3iso1 fold change	+TBX3iso2 fold change
CST6	-1.93 *	-1.46 **
CDKN2A	-1.18 *	-1.39 *
MLH1	1.51 *	1.52 *
MMP9	1.57 **	2.68 ***
RB1	1.69 *	1.77 **
AKT1	1.73 *	1.99 **
BRCA1	1.73 *	2.17 **
SRC	1.75 *	2.28 **
SNAI2	1.76 *	3.6 ***
MAPK8	1.88 *	1.59 **
MKI67	1.94 **	1.58 **
KRT8	1.95 *	1.52 *
NR3C1	1.95 **	1.6 *
FOXA1	2.17 **	1.97 *
SFN	2.24 **	2.97 *
TWIST1	2.25 **	2.3 **
PRDM2	2.31 **	1.95 **
BRCA2	2.66 ***	2.39 ***
SERPINE1	2.87 *	7.28 ***
EGFR	3.02 **	3.09 **
AR	3.54 **	22.26 ***
PLAU	4.1 **	3.19 ***
JUN	5.13 ***	2.43 *
IL6	6.36 **	2.09 ***

C

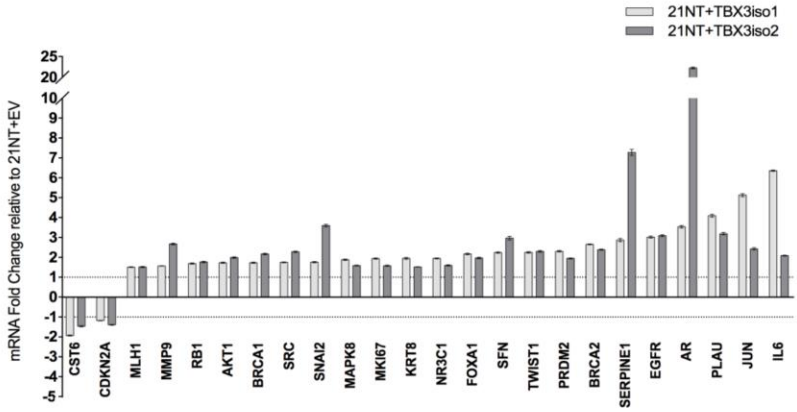

D

Signal Transduction	AKT1, AR, BRCA1, MAPK8, NR3C1, RB1, SNAI2
Apoptosis	AKT1, CDKN2A, IL6, JUN, SFN, TWIST1
Transcription Factors	AR, FOXA1, JUN, NR3C1, PRDM2, RB1
Cell Cycle	CDKN2A, JUN, MK167, RB1, SFN
Angiogenesis	IL6, JUN, PLAU, SERPINE1
DNA Damage	BRCA1, BRCA2, MLH1, SFN
Tumour Classification Marker	EGFR, FOXA1, KRT8
Proteolysis	CST6, MMP9, PLAU
Epithelial to Mesenchymal Transition (EMT)	SRC, TWIST1

E

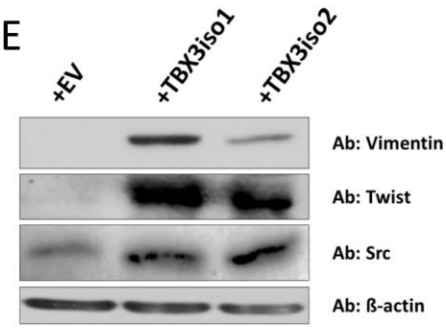

Figure 2.3.6 – TBX3 overexpression in DCIS-like 21NT cells alters expression of key regulatory and EMT/invasion-associated genes.

(A) Heat map (84 genes commonly dysregulated in breast cancer) showing absolute mRNA expression of 84 breast-cancer related genes within the 21NT transfectant cells. **(B)** Fold changes (mRNA) of genes significantly altered in expression in a similar fashion with overexpression of both TBX3iso1 and TBX3iso2 in 21NT cells. Data analysis was conducted by SA Biosciences PCR Array Data Analysis Web portal using the ΔΔCt method normalized to acidic ribosomal phosphoprotein P0 (RPLP0) expression. Fold changes are compared to 21NT+EV control and are organized based on increasing fold change of TBX3iso1. The 24 genes shown had similar alterations in gene expression with statistically significant fold changes for both isoforms (* $p<0.05$, ** $p<0.01$, ***$p<0.001$). Genes in green had reduced expression, and genes in red had increased expression at the mRNA level with TBX3 isoform overexpression. Results are representative of 3 RT^2 PCR arrays per cell line. **(C)** Graphical representation of fold changes in panel (A). Dotted line represents normalized expression of transcript levels of empty vector control cells (fold change = 1). **(D)** Gene expression changes with TBX3 isoform overexpression organized based on gene function groupings. Genes in green had reduced expression, and genes in red had increased expression at the mRNA level with TBX3 isoform overexpression. **(e)** Western blot showing increased expression of Vimentin, Twist and Src protein levels with TBX3 overexpression.

2.4 **Discussion**

By using the 21T cell line series to model the effects of putative drivers of the transition from pre-invasive to invasive breast cancer progression, we are able to demonstrate that overexpression of TBX3 can promote the transition of DCIS to IMC as assessed by *in vitro* 3D Matrigel growth assays. In particular, 21NT (DCIS-like) cells overexpressing TBX3iso1 or TBX3iso2 showed increased colony-forming ability, with increased numbers of cells per colony and a more dispersed (less “rounded”) colony morphology. Increased cell invasiveness was also observed, both in terms of more dispersed colonies in 3D Matrigel and increased invasion through Matrigel. In parallel, down-regulation of TBX3 in 21MT-1 cells resulted in a less aggressive phenotype in 3D Matrigel, with smaller and less dispersed (less invasive) colony morphology.

No significant difference in functional activity in any of these *in vitro* measures of malignancy was observed between the TBX3 isoforms. Interestingly, RT^2 PCR array analysis did show several differences in gene expression profiles induced by TBX3iso1 and TBX3iso2, as well as a number of commonalities (Figure 2.3.6 A). As we saw no difference in functional effect, our analysis was focused on gene expression alterations occurring in common between the two isoforms, which could potentially explain characteristics of the more aggressive phenotype observed in both TBX3iso1 and TBX3iso2 transfectants.

Firstly, the increased colony-forming ability in 3D Matrigel, with larger colony size and increased proliferation vs. apoptosis ratio observed with both TBX3iso1 and TBX3iso2 21NT transfectants indicated an increased cell survival and predisposition for proliferation vs. apoptosis (or senescence), effects that have been previously ascribed to TBX3 in other systems (Brummelkamp et al., 2002, Carlson et al., 2002, Rowley et al., 2004, Yarosh et al., 2008). Gene expression profiling of the TBX3 transfectants in our study showed altered expression of several genes potentially involved in these processes in both TBX3iso1 and TBX3iso2 transfected cells (i.e. down-regulation of CDKN2A ($p14^{ARF}$, $p16^{INK4A}$), with up-regulation of MKI67, JUN, NR3C1, EGFR, AR, IL6, SRC and AKT1). Perhaps most interesting of these is the down regulation of CDKN2A ($p14^{ARF}$, $p16^{INK4A}$) by both TBX3 isoforms, as previous studies have indicated $p14^{ARF}$ in particular to be a direct transcriptional target of TBX3 in other systems (Yarosh et al., 2008), and that isolated down-regulation of

$p14^{ARF}$ can accomplish the same effect of increasing cell proliferation, decreasing cell senescence and apoptosis (Rowley et al., 2004). Further work is required to determine whether $p14^{ARF}$ or others of the candidate genes identified are responsible for the cell survival/proliferation vs. apoptosis/senescence aspects of the TBX3 phenotype in these cells.

Another prominent aspect of the altered phenotype observed with both TBX3iso1 and TBX3iso2 21NT transfectants was a more irregular/dispersed colony morphology in 3D Matrigel, with increased cellular invasiveness in transwell assays, suggestive of an EMT effect. In keeping with this, both TBX3iso1 and TBX3iso2 transfectants showed alteration in expression of a number of EMT and invasion-related genes that are consistent with an EMT phenomenon, including up-regulation of TWIST1, SRC, SNAI2, PLAU, SERPINE1, and MMP9, with down-regulation of CST6. Western blot analysis showed up-regulation of Twist and Src, along with mesenchymal marker Vimentin at the protein level as well.

Our work is in agreement with that of previous studies with other mammary epithelial cells (MCF7, MDA-MB-435, HC11) (Platonova et al., 2007, Peres et al., 2010) in which TBX3 was shown to have functional effects including inhibition of senescence and promotion of cell survival, proliferation and migration. We present the added novel finding, using a progression series of mammary epithelial cells, that overexpression of TBX3 can trigger non-invasive (DCIS-like, 21NT) cells to become invasive, possibly through an EMT-like process. In addition, knockdown of TBX3 in invasive (21MT-1) cells can revert them to a less aggressive phenotype, with less potential for 3D growth and a less infiltrative phenotype. Furthermore, we have shown that these effects are not isoform specific, as both TBX3iso1 and TBX3iso2 were able to induce the same phenotypes in transfected 21NT cells. Finally, examination of TBX3-induced changes in gene expression of 21NT cells has revealed specific cell survival/anti-senescence/proliferation and EMT/invasiveness category alterations, which may be involved in the functional changes observed. Future work will be necessary to establish which of these changes may be key players in the TBX3-induced phenotypes.

We have demonstrated a role for both TBX3iso1 and TBX3iso2 in promoting the transition from non-invasive to invasive breast cancer. We have shown that overexpression of TBX3 can alter cell properties involved in cell survival/colony formation and invasiveness, as well as regulate EMT/invasiveness-related genes. The identification of TBX3 as a potential

regulator of early breast cancer progression from DCIS to IMC is of potential clinical utility not only in identifying which DCIS lesions may be more likely to progress to invasion, but along with a better understanding of the role of specific TBX3-induced gene expression changes, in providing other potential molecular targets to block breast cancer progression at this early, pre-invasive stage. The recent finding that TBX3 alterations may be key driver mutations in breast cancer, and the suggestion that altered (probably increased) TBX3 function may be associated with at least some cases of familial breast cancer (Stephens et al., 2012a), adds particular significance to the potential of TBX3 as an important regulator of breast cancer progression, and added urgency to a better understanding of its role in the malignancy of breast cancer.

2.5 References

Allred, D. C., Mohsin, S. K. and Fuqua, S. A. (2001) 'Histological and biological evolution of human premalignant breast disease', *Endocr Relat Cancer,* 8(1), pp. 47-61.

Allred, D. C., Wu, Y., Mao, S., Nagtegaal, I. D., Lee, S., Perou, C. M., Mohsin, S. K., O'Connell, P., Tsimelzon, A. and Medina, D. (2008) 'Ductal carcinoma in situ and the emergence of diversity during breast cancer evolution', *Clin Cancer Res,* 14(2), pp. 370-8.

Arpino, G., Laucirica, R. and Elledge, R. M. (2005) 'Premalignant and in situ breast disease: biology and clinical implications', *Ann Intern Med,* 143(6), pp. 446-57.

Bamshad, M., Le, T., Watkins, W. S., Dixon, M. E., Kramer, B. E., Roeder, A. D., Carey, J. C., Root, S., Schinzel, A., Van Maldergem, L., Gardner, R. J., Lin, R. C., Seidman, C. E., Seidman, J. G., Wallerstein, R., Moran, E., Sutphen, R., Campbell, C. E. and Jorde, L. B. (1999) 'The spectrum of mutations in TBX3: Genotype/Phenotype relationship in ulnar-mammary syndrome', *Am J Hum Genet,* 64(6), pp. 1550-62.

Band, V., Zajchowski, D., Swisshelm, K., Trask, D., Kulesa, V., Cohen, C., Connolly, J. and Sager, R. (1990) 'Tumor progression in four mammary epithelial cell lines derived from the same patient', *Cancer Res,* 50(22), pp. 7351-7.

Boyd, S. C., Mijatov, B., Pupo, G. M., Tran, S. L., Gowrishankar, K., Shaw, H. M., Goding, C. R., Scolyer, R. A., Mann, G. J., Kefford, R. F., Rizos, H. and Becker, T. M. (2013) 'Oncogenic B-RAF(V600E) signaling induces the T-Box3 transcriptional repressor to repress E-cadherin and enhance melanoma cell invasion', *J Invest Dermatol,* 133(5), pp. 1269-77.

Brummelkamp, T. R., Kortlever, R. M., Lingbeek, M., Trettel, F., MacDonald, M. E., van Lohuizen, M. and Bernards, R. (2002) 'TBX-3, the gene mutated in Ulnar-Mammary Syndrome, is a negative regulator of p19ARF and inhibits senescence', *J Biol Chem,* 277(8), pp. 6567-72.

Carlson, H., Ota, S., Song, Y., Chen, Y. and Hurlin, P. J. (2002) 'Tbx3 impinges on the p53 pathway to suppress apoptosis, facilitate cell transformation and block myogenic differentiation', *Oncogene,* 21(24), pp. 3827-35.

Debnath, J., Muthuswamy, S. K. and Brugge, J. S. (2003) 'Morphogenesis and oncogenesis of MCF-10A mammary epithelial acini grown in three-dimensional basement membrane cultures', *Methods,* 30(3), pp. 256-68.

Eblaghie, M. C., Song, S. J., Kim, J. Y., Akita, K., Tickle, C. and Jung, H. S. (2004) 'Interactions between FGF and Wnt signals and Tbx3 gene expression in mammary gland initiation in mouse embryos', *J Anat,* 205(1), pp. 1-13.

Fan, W., Huang, X., Chen, C., Gray, J. and Huang, T. (2004) 'TBX3 and its isoform TBX3+2a are functionally distinctive in inhibition of senescence and are overexpressed in a subset of breast cancer cell lines', *Cancer Res,* 64(15), pp. 5132-9.

Hoogaars, W. M., Barnett, P., Rodriguez, M., Clout, D. E., Moorman, A. F., Goding, C. R. and Christoffels, V. M. (2008) 'TBX3 and its splice variant TBX3 + exon 2a are functionally similar', *Pigment Cell Melanoma Res,* 21(3), pp. 379-87.

Lakhani, S. R., Collins, N., Stratton, M. R. and Sloane, J. P. (1995) 'Atypical ductal hyperplasia of the breast: clonal proliferation with loss of heterozygosity on chromosomes 16q and 17p', *J Clin Pathol,* 48(7), pp. 611-5.

Lee, G. Y., Kenny, P. A., Lee, E. H. and Bissell, M. J. (2007) 'Three-dimensional culture models of normal and malignant breast epithelial cells', *Nat Methods,* 4(4), pp. 359-65.

MacMillan, C. D., Leong, H. S., Dales, D. W., Robertson, A. E., Lewis, J. D., Chambers, A. F. and Tuck, A. B. (2014) 'Stage of breast cancer progression influences cellular response to activation of the WNT/planar cell polarity pathway', *Sci Rep,* 4, pp. 6315.

Moffat, J., Grueneberg, D. A., Yang, X., Kim, S. Y., Kloepfer, A. M., Hinkle, G., Piqani, B., Eisenhaure, T. M., Luo, B., Grenier, J. K., Carpenter, A. E., Foo, S. Y., Stewart, S. A., Stockwell, B. R., Hacohen, N., Hahn, W. C., Lander, E. S., Sabatini, D. M. and Root, D. E. (2006) 'A lentiviral RNAi library for human and mouse genes applied to an arrayed viral high-content screen', *Cell,* 124(6), pp. 1283-98.

Page, D. L. and Dupont, W. D. (1993) 'Anatomic indicators (histologic and cytologic) of increased breast cancer risk', *Breast Cancer Res Treat,* 28(2), pp. 157-66.

Page, D. L., Dupont, W. D., Rogers, L. W. and Rados, M. S. (1985) 'Atypical hyperplastic lesions of the female breast. A long-term follow-up study', *Cancer,* 55(11), pp. 2698-708.

Peres, J., Davis, E., Mowla, S., Bennett, D. C., Li, J. A., Wansleben, S. and Prince, S. (2010) 'The Highly Homologous T-Box Transcription Factors, TBX2 and TBX3, Have Distinct Roles in the Oncogenic Process', *Genes Cancer,* 1(3), pp. 272-82.

Platonova, N., Scotti, M., Babich, P., Bertoli, G., Mento, E., Meneghini, V., Egeo, A., Zucchi, I. and Merlo, G. R. (2007) 'TBX3, the gene mutated in ulnar-mammary syndrome, promotes growth of mammary epithelial cells via repression of p19ARF, independently of p53', *Cell Tissue Res,* 328(2), pp. 301-16.

Renard, C. A., Labalette, C., Armengol, C., Cougot, D., Wei, Y., Cairo, S., Pineau, P., Neuveut, C., de Reynies, A., Dejean, A., Perret, C. and Buendia, M. A. (2007) 'Tbx3 is a downstream target of the Wnt/beta-catenin pathway and a critical mediator of beta-catenin survival functions in liver cancer', *Cancer Res,* 67(3), pp. 901-10.

Rodriguez, M., Aladowicz, E., Lanfrancone, L. and Goding, C. R. (2008) 'Tbx3 represses E-cadherin expression and enhances melanoma invasiveness', *Cancer Res,* 68(19), pp. 7872-81.

Rowley, M., Grothey, E. and Couch, F. J. (2004) 'The role of Tbx2 and Tbx3 in mammary development and tumorigenesis', *J Mammary Gland Biol Neoplasia,* 9(2), pp. 109-18.

Souter, L. H., Andrews, J. D., Zhang, G., Cook, A. C., Postenka, C. O., Al-Katib, W., Leong, H. S., Rodenhiser, D. I., Chambers, A. F. and Tuck, A. B. (2010) 'Human 21T breast epithelial cell lines mimic breast cancer progression in vivo and in vitro and show stage-specific gene expression patterns', *Lab Invest,* 90(8), pp. 1247-58.

Stephens, P. J., Tarpey, P. S., Davies, H., Van Loo, P., Greenman, C., Wedge, D. C., Nik-Zainal, S., Martin, S., Varela, I., Bignell, G. R., Yates, L. R., Papaemmanuil, E., Beare, D., Butler, A., Cheverton, A., Gamble, J., Hinton, J., Jia, M., Jayakumar, A., Jones, D., Latimer, C., Lau, K. W., McLaren, S., McBride, D. J., Menzies, A., Mudie, L., Raine, K., Rad, R., Chapman, M. S., Teague, J., Easton, D., Langerod, A., Lee, M. T., Shen, C. Y., Tee, B. T., Huimin, B. W., Broeks, A., Vargas, A. C., Turashvili, G., Martens, J., Fatima, A., Miron, P., Chin, S. F., Thomas, G., Boyault, S., Mariani, O., Lakhani, S. R., van de Vijver, M., van 't Veer, L., Foekens, J., Desmedt, C., Sotiriou, C., Tutt, A., Caldas, C., Reis-Filho, J. S., Aparicio, S. A., Salomon, A. V., Borresen-Dale, A. L., Richardson, A. L., Campbell, P. J., Futreal, P. A. and Stratton, M. R. (2012) 'The landscape of cancer genes and mutational processes in breast cancer', *Nature,* 486(7403), pp. 400-4.

Yarosh, W., Barrientos, T., Esmailpour, T., Lin, L., Carpenter, P. M., Osann, K., Anton-Culver, H. and Huang, T. (2008) 'TBX3 is overexpressed in breast cancer and represses p14 ARF by interacting with histone deacetylases', *Cancer Res,* 68(3), pp. 693-9.

Chapter 3

TBX3 promotes progression of pre-invasive breast cancer cells by inducing EMT and directly up-regulating SLUG

3 TBX3 promotes progression of pre-invasive breast cancer cells by inducing EMT and directly up-regulating SLUG

SUMMARY OF FINDINGS

The acquisition of cellular invasiveness by breast epithelial cells and subsequent transition from ductal carcinoma in situ (DCIS) to invasive breast cancer is a critical step in breast cancer progression. Little is known about the molecular dynamics governing this transition. We have previously shown that overexpression of the transcriptional regulator TBX3 in DCIS-like cells increases survival, growth, and invasiveness. To explore this mechanism further and assess direct transcriptional targets of TBX3 in a high-resolution, isoform-specific context, we conducted genome-wide ChIP-arrays coupled with transcriptomic analysis. We show that TBX3 regulates expression of several epithelial-mesenchymal transition (EMT) related genes, including SLUG and TWIST1. Importantly, we demonstrate that TBX3 is a direct regulator of SLUG, and SLUG expression is required for TBX3-induced migration and invasion. Assessing TBX3 expression by immunohistochemistry in early stage (Stage 0 and Stage I) breast cancers revealed high expression in low-grade lesions. Within a second independent, early stage (Stage 0 and Stage I), non-high-grade cohort, we observed an association between TBX3 expression in the DCIS and size of the invasive focus. Additionally, there was a positive correlation between TBX3 and SLUG expression, and TBX3 and TWIST1 expression in the invasive carcinoma. Pathway analysis revealed altered expression of several proteases and their inhibitors, consistent with the ability to degrade basement membrane in vivo. These findings strongly suggest the involvement of TBX3 in the promotion of invasiveness and progression of early stage pre-invasive breast cancer to invasive carcinoma through the low-grade molecular pathway.

Chapter 3 in this dissertation has been submitted, and is currently under peer-review.

3.1 **Introduction**

Tumorigenesis within the breast is thought to involve advancement through distinct stages, from benign ductal epithelial hyperplasia, to atypical ductal hyperplasia (ADH), ductal carcinoma in situ (DCIS), and ultimately invasive and metastatic carcinoma (Burstein et al., 2004). A very critical stage of this progression pathway is the acquisition of cellular invasiveness. It is estimated that approximately 25-50% of DCIS will progress to invasive carcinoma during the lifetime of the patient, a process generating potentially life-threatening disease (Sagara et al., 2015). Clinical management of patients with DCIS usually consists of surgical resection with additional radiation therapy for most patients (Fisher et al., 1999, Mokbel and Cutuli, 2006). Several recent studies, however, have suggested that a subset of patients with early-stage (non-high-grade) DCIS do not benefit from either surgery alone or combined surgery and radiation, raising concern regarding over-treatment of this subpopulation (Thorat et al., 2007, Formenti et al., 2011, Sagara et al., 2015). Paradoxically, we are currently limited in our ability to identify patients with DCIS that have an intrinsically higher risk of local and invasive recurrence, such that there is also a risk of under-treatment if excision is incomplete or radiation therapy is omitted.

The 21T series cell lines have been proposed as a unique experimental model of breast cancer progression (Band et al., 1990). Three cell lines were isolated from a single patient and stably represent distinct stages of progression: 21PT cells mimic ADH (non-tumorigenic), 21NT cells mimic DCIS (tumorigenic and non-metastatic), and 21MT-1 cells depict characteristics of invasive mammary carcinoma (tumorigenic and metastatic) when injected orthotopically into nude mice (Band et al., 1990, Souter et al., 2010). We have previously conducted extensive characterization of these cell lines, including examination of global gene-expression levels coupled with assessment of clinical literature on progression (Souter et al., 2010). Importantly, we found that during the transition from the clonally-related DCIS-like 21NT cells to invasive 21MT-1 cells, TBX3 was within the list of clinically-relevant up-regulated transcripts (Souter et al., 2010).

TBX3 is a member of T-box family of transcription factors implicated in skeletal, cardiac and mammary gland development (Willmer et al., 2017). TBX3 levels are up-regulated in several cancers, with most of the literature focusing on breast cancer (Fan et al.,

2004, Lomnytska et al., 2006, Yarosh et al., 2008, Souter et al., 2010) and melanoma (Rodriguez et al., 2008, Peres and Prince, 2013). Due to alternative splicing, two TBX3 isoforms exist: TBX3iso1 and TBX3iso2. TBX3iso2 contains an additional 20-amino acid sequence in the DNA binding domain attributed to the 2a exon, which TBX3iso1 lacks. Differing expression levels of these isoforms has been reported in several breast cancer cell lines (Fan et al., 2004). While the role of TBX3 in tumorigenesis is currently unclear, accumulating evidence suggests that the TBX3-mediated transcriptional repression of $p14^{ARF}$ (Lingbeek et al., 2002, Yarosh et al., 2008) and/or $p21^{CIP1}$ (Hoogaars et al., 2008) plays a role in bypassing cellular senescence and driving cancer progression. Recent work has begun to identify a link between TBX3 expression levels and epithelial-mesenchymal transition (EMT), with direct down-regulation of E-cadherin (Rodriguez et al., 2008). These findings are important, as the switch from an epithelial to a mesenchymal phenotype has been implicated in the acquisition of migratory and invasive properties, suppression of senescence and apoptosis, as well as therapeutic resistance (De Craene and Berx, 2013). SLUG (encoded by the *SNAI2* gene) is a member of the SNAIL family of transcription factors and a key mediator in the promotion of EMT (De Craene and Berx, 2013, Phillips and Kuperwasser, 2014). Specifically, SLUG has been shown to trigger the initial phases of the EMT process (Savagner et al., 1997).

In this study we explore the role of TBX3 in breast cancer progression pathways, focusing specifically on its involvement in the induction of EMT and the transition from DCIS to invasive mammary carcinoma. Immunohistochemical analysis has revealed that TBX3 levels are elevated in low-grade, pre-invasive DCIS lesions with an associated invasive component, and significantly correlated with the size of the invasive focus. Using genome-wide bioinformatic approaches in conjunction with more conventional *in vitro* studies, we have identified SLUG and TWIST1 as downstream targets of TBX3 and have assessed their expression by immunohistochemistry in two different patient cohorts. Our findings suggest that TBX3 facilitates the process of early invasion in DCIS, by promoting the induction of EMT and tumor progression through the low-grade pathway, as described by Bombonati and Sgroi (Bombonati and Sgroi, 2011). Finally, we propose a progression model in which SLUG is an important and necessary effector downstream of TBX3, leading to increased motility, invasiveness, and induction of key invasiveness-associated genes.

3.2 Methods

Cell lines and culture conditions

The 21T series cell lines (21NT and 21MT-1) were obtained as a gift from Dr. Vimla Band (Dana Farber Cancer Institute) (Band et al., 1990). 21T series cell lines underwent authentication testing by Idexx Radil (Case No. 20250-2013). Cells were maintained in αMEM media supplemented with 2mM L-glutamine, 1μg/mL insulin, 12.5ng/mL EGF, 2.8μM hydrocortisone, 10mM HEPES, 1mM sodium pyruvate, 0.1mM non-essential amino acids, and 50μg/mL gentamycin sulfate and further supplemented with 10% FBS (αHE10F). All reagents were obtained from Wisent Inc. Stable 21NT transfectants previously generated (Krstic et al., 2016) were maintained in αHE10F medium supplemented with 500μg/mL G418 as a selection marker. Stable lentiviral transductants were maintained in αHE10F medium supplemented with either 0.8μg/mL puromycin (TBX3 knockdown lines) or 500μM hygromycin (SLUG knockdown lines) as a selection marker.

Cell lines representing other molecular breast cancer subtypes were purchased from ATCC. Cell lines were maintained in their respective media: T47D (RPMI), SKBR3 (McCoy's 5A), and MDA-MB-468 (αMEM) supplemented with 10% FBS. All cell lines were regularly tested and negative for Mycoplasma contamination using the Mycoplasma PCR Primer Set (Agilent Technologies, 302008).

Stable Transfection

21NT parental cell lines were seeded into 6-well plates at 350,000 cells per well, and transfected the following day at 3μg of DNA plasmid per well using the Lipofectamine 3000 Transfection Kit (Invitrogen, L3000). Plasmid DNA constructs were previously described (Krstic et al., 2016) and consist of an empty vector (EV), TBX3iso1, and TBX3iso2 construct within a pcDNA3.1 (Invitrogen, V79020) vector. Selection was performed using αHE medium supplemented with 500μg/mL G418. Resistant clones were pooled, expanded, and frozen for later use.

Transient Transfection

For assessment of E-cadherin expression and localization, 21NT parental cell lines were seeded into 6-well plates at 350,000 cells per well, and transfected the following day with

3μg of DNA plasmid per well using the Lipofectamine 3000 Transfection Kit (Invitrogen, L3000). Plasmid DNA constructs consisted of an empty vector (EV), TBX3iso1, and TBX3iso2 construct within pZsGreen1-N1 vector containing the ZsGreen reporter gene. For immunofluorescence studies, transfected cells were grown under normal conditions for 72 hours and then underwent immunofluorescent staining.

For invasion assay studies, cells (T-47D, SKBR3, MDA-MB-468) were incubated with transfection reagent and the appropriate plasmid for 24 hours, then harvested and assays were performed. Plasmid DNA constructs consist of an empty vector (EV), TBX3iso1, and TBX3iso2 construct within pZsGreen1-N1 vector containing the ZsGreen reporter gene.

Lentiviral Transduction

The generation of shRNA-encoding lentivirus particles for TBX3 knockdown was conducted as previously described (Krstic et al., 2016). The shRNA target sequence for TBX3 was GCATACCAGAATGATAAGATA, which targeted the coding sequence of both TBX3iso1 and TBX3iso2. The shRNA target sequence for Luciferase (representing an off-target control) was ACGCTGAGTACTTCGAAATGT. The lentivirus particles were used to generate 21MT-1 shLUC and 21MT-1 shTBX3 cell lines. Selection was performed using αHE medium supplemented with 0.8μg/mL puromycin. Resistant clones were pooled, expanded, and frozen for later use.

Down-regulation of SLUG (*SNAI2*) was performed using lentivirus-mediated shRNA transduction. 293T packaging cells were seeded at 80% confluence in 6-well plates with low-antibiotic growth media (DMEM with 10% FBS and 0.1x Penicillin/Streptomycin). The following day the packaging cells were transfected with the packaging plasmid (Addgene, pCMV-dR8.91, 900ng), envelope plasmid (Addgene, VSV-G/pDM2.G, 100ng), and psi-LVRU6H vector encoding one of 4 shRNAs specific to *SNAI2* (Genecopoeia, HSH017502-LVRU6H, 1μg) or an empty vector control (Genecopoeia, CSHCTR001-LVRU6H, 1μg) (quantities reported per well). The FuGENE transfection reagent (Promega, E2311) was mixed with the 3-plasmid mix as per the manufacturer's protocol. The transfection mix was incubated for 30 minutes at room temperature, and 200μL was added to the packaging cells. Viral harvesting was done three times, spaced out by 12-24 hours by replacing media with 6mL of high-BSA growth media (20g BSA per 100mL DMEM). The three viral harvests were pooled and the viral supernatant was frozen.

21NT transfectants (21NT+EV, 21NT+TBX3iso1, 21NT+TBX3iso2) were seeded at 200,000 cells per well in 6-well plates. The following day 300μL of the shRNA-encoding lentiviral particles were added to the cells along with 2μg polybrene (Sigma, TR-1003-G) per 2mL media. The cells were incubated at 37ºC overnight and transduced cells were selected for by including 500μM hygromycin (Invitrogen, 10687-010) in the media (aHE10F with 500μM hygromycin, 500ug/mL G418). Media was replaced again the following day, and cells were trypsinized and expanded into T25 flasks on the third day.

Preparation of 21T protein lysates

Protein lysates were prepared by adding 1mL of RIPA buffer (150mM NaCl, 1% Triton-X, 0.5% deoxycholic acid, 0.1% SDS, 50mM Tris-base; pH 8.0) with Halt Protease Inhibitor Cocktail (Thermo Scientific, 78429) to confluent 10cm plates. Cells were scraped, collected in a microcentrifuge tube, and incubated on ice for 10 minutes. Lysates were then centrifuged at 13,000 RPM for 10 minutes at 4ºC. The supernatant was collected and protein concentrations were determined using a Bradford Protein Assay kit (BioRad, 5000002) by comparing to BSA standards.

Preparation of Conditioned Media and Western Blotting

For assessment of secreted protein expression (MMP9), conditioned media was prepared by seeding $1.0x10^6$ cells into T75 flasks, and cells were maintained in low serum media (αMEM with 0.1% FBS) for 48 hours. Media was collected and concentrated 25X using centrifugal filters (Amicon Ultra-4, UFC803024). Protein was resolved (40μg) on a 10% SDS-PAGE gel. Immediately after transferring proteins to a PVDF membrane, total protein was visualized by Ponceau Stain using the BioRad ChemiDoc imaging system, and an image of the membrane was acquired for subsequent normalization. The membrane was then de-stained and MMP9 protein levels were assessed by western blot (specifications can be found in ‘Electrophoresis and Western Blotting’ section).

Electrophoresis and Western Blotting

Protein (10-50μg) was resolved on a 10% SDS-PAGE gel. The membrane was blocked with 5% milk for one hour (or 5% BSA where specified), then incubated with primary antibody overnight at 4ºC; anti-TBX3 (Invitrogen, 424800; 1:1,000), anti-SLUG (Abcam, ab27568;

1:1,000 in BSA), anti-Vimentin (Abcam, ab92547; 1:1,000), anti-Fibronectin (Abcam, ab2413; 1:1,000), anti-uPa (Abcam, ab133563; 1:250), anti-MMP9 (Abcam, ab38898, 1:1,000), anti-MMP14 (Abcam, ab51074; 1:500), anti-Src (Cell Signaling, 2110; 1:1,000), anti-pSrc (Y416) (Cell Signaling, 2101; 1:1,000 in BSA), anti-pSrc (Y527) (Cell Signaling, 2105; 1:1,000 in BSA), anti-TWIST1 (Abcam, ab50887; 1:100 in BSA), anti-CST6 (Sigma, WH0001474M1; 1:1,000), anti-N-Cadherin (Abcam, 18203, 1:1,000), anti-Vinculin (Sigma, V9264; 1:20,000). The membrane was incubated with secondary antibody conjugated to HRP, either anti-rabbit (Sigma, A0545; 1:1,000) or anti-mouse (GE Healthcare, NXA931; 1:1,000) as appropriate, for 1 hour at room temperature. The western blots were visualized using Luminata Crescendo (EDM Millipore, WBLUR0500) and images were taken using the BioRad ChemiDoc imaging system. Densitometric quantification was performed using ImageLab (BioRad), and quantities were normalized to vinculin expression. Where quantifications of western blots is shown, data was acquired through densitometric quantifications across three biological replicates.

Immunofluorescence

ZsGreen vector transiently transfected cells (described above) were fixed with 10% neutral buffered formalin for 10 minutes, and permeabilized with 0.5% Triton X-100 in PBS for 10 minutes. Blocking was conducted with normal goat serum (Invitrogen, 50-0627) at room temperature for 1 hour. Rabbit anti-E-cadherin antibody (BD Biosciences, 610181) was added at a dilution of 1:150 in 10% normal goat serum and was incubated overnight at 4ºC. The following day, cells were washed three times with PBS, and secondary antibody Alexa647 Goat Anti-Rabbit IgG (Invitrogen, A21245) was added at a dilution of 1:1,000 in 10% normal goat serum and incubated for 1 hour at room temperature. Cells were washed 5 times with PBS. Hoechst 33342 (Invitrogen, H1399) diluted to 1:5,000 in PBS was incubated for 30 minutes at room temperature. Cells were washed once with PBS. Coverslips were mounted with ProLong Gold Antifade Reagent (Invitrogen, P36930). Images were captured at 40X magnification using an Olympus Confocal Imaging System (FluoView FV1000 coupled to the IX81 Motorized Inverted System Microscope). Images were converted to 8-bit images by separating channels. Mean grey area was quantified within the red channel across ZsGreen positive (transfected) cells. E-cadherin expression across the cell lines was normalized to the empty vector control.

Scratch Wound (Migration) Assay

Cells were cultured to near confluence in 6-well plates and starved in low serum media (αMEM with 0.1% FBS) for 16 hours. A 2 mm wide scratch was then made in the confluent monolayer. The cells were rinsed with PBS and fresh media (αMEM media with 10% FBS) was added. Cell migration was visualized and phase contrast images were taken at 10X using the Olympus IX70 inverted microscope after 6h, 12h and 24h. Cell migration was calculated by comparing the wound area at the specified time points using ImageJ (Open source, https://imagej.nih.gov/ij/). Means derived from four biological replicates were used during analysis.

Transwell Invasion Assay

Transwell invasion assays were conducted to examine the invasive potential of the transfected cell lines. Stably transfected 21NT cells (representing luminal B subtype) were used for initial studies. For stable 21NT transfectant cells, 50,000 cells per 100μL of media were added to the upper chamber of a 8.0μm pore transwell insert (Corning, 3422; 24-well plate) coated with 10μg of Matrigel (Corning, 354480). After incubation at 37ºC and 5% CO_2 for 18 hours, the membranes were fixed with 1% glutaraldehyde for 20 min and stained with full-strength Hematoxylin for 15 minutes. Cells which did not migrate and remained on the upper surface of the membrane were removed using a cotton swab. Images of 5 non-overlapping fields of view were acquired using an Olympus IX70 inverted microscope at 10X objective. Cells were counted from the acquired images using ImageJ. Means derived from 4 replicates were used during analysis.

Invasiveness of transiently transfected cells was also assessed, including T-47D (luminal A), SKBR3 (HER2-enriched), and MDA-MB-468 (basal-like) cells transfected with either an empty vector (EV), TBX3iso1, or TBX3iso2 construct within the pZsGreen1-N1 vector containing a ZsGreen reporter gene. Twenty-four hours post-transfection, cells were trypsinized, harvested, and suspended in their respective media in the absence of FBS and addition of 0.1% BSA. Cells were then added to the upper layer of a 8.0μM transwell insert coated with 10μg of Matrigel at 50,000 cells per 100μL of media. After incubation at 37ºC and 5% CO_2 for 18 hours, the membranes were fixed with 1% glutaraldehyde for 20 min. Cells which did not migrate and remained on the upper surface of the membrane were

removed using a cotton swab. Green fluorescent images and brightfield images of 3 non-overlapping fields of view were acquired and superimposed using an EVOS FL Auto microscope at 10X objective. The number of green cells was determined using ImageJ software. Means derived from four biological replicates were used during analysis.

Cell-Cell Adhesion Assay

The cell-cell adhesion assay was done as described (Rodriguez et al., 2008). Briefly, T75 plates were rinsed twice with PBS and cells were dissociated using 3mM EDTA. Cells were resuspended in αHE10F media and passed through a cell strainer to dissociate cell clusters. Cells (200,000) were added to the appropriate media (αHE10F with 3mM EDTA, or αHE10F with 1mM $CaCl_2$) in a 6 cm petri dish. Plates were incubated at 37ºC on a shaking platform for 30 minutes. After this incubation period, 10 non-overlapping fields of view per dish were captured using the Olympus IX70 inverted microscope at 10X objective. Clusters containing more than 4 cells were counted, and counts from 10 fields of view were added together for each plate. Means derived from four biological replicates were used during analysis.

Gelatin Zymography

Cells ($1.5x10^6$) were seeded onto 10cm plates. The following day, media was replaced by 10mL of serum-free αHE media with 500µg/mL G418, and cells were serum-starved for 24 hours. Media was collected and concentrated 25X using centrifugal filters (Amicon Ultra-4, UFC803024). Equal volumes (normalized to $1.5x10^6$ cells) of the conditioned media was loaded into a 10% Criterion Zymogram gel (BioRad, 3450080) without boiling/reducing and resolved at 4ºC. To remove SDS from the gel, the gel was washed with renaturation buffer (2.5% Triton X-100) twice for 30 minutes each, followed by two 20 minute washes with distilled water. The gel was then incubated in development buffer (50mM Tris, 200mM NaCl, 5mM $CaCl_2$ (anhydrous), 0.02% Brij-35, pH 7.5) at 37ºC for 16 hours. The gel was then stained (40% methanol, 10% acetic acid, 0.5% Coomassie Blue R-250) for 1 hour at room temperature with gentle agitation, followed by de-staining (40% methanol, 10% acetic acid) until clear bands appeared. Images were taken using the BioRad ChemiDoc imaging system. Reverse images were used for quantification. Means derived from three biological replicates were used during analysis.

Chick Chorioallantoic Membrane (CAM) Extravasation Assays

Cells were pre-labeled with 1µM CellTracker conjugated to Green CMFDA Dye (Thermo Fischer Scientific, C7025) and washed once with PBS. Using the chorioallantoic membrane (CAM) of the chicken embryo, embryonic day 12 embryos were intravenously (IV) injected with 50,000 cells (50µL of 1×10^6 cells/mL cell suspension).

For the extravasation assays, rhodamine-labelled lectin (75µL of 0.1mg/mL, Vector Laboratories Inc, RLK-2200) was intravenously injected 10 minutes after injection of fluorescently-labelled cells in order to visualize the luminal surface of endothelial cells in the CAM. Immediately following IV injection of lectin-rhodamine, a 1cm×1cm field of the CAM marked by foil markers at the corners was made for each animal and the number of cells that were intravascular, in the process of extravasation and extravasated into the CAM stroma were counted at T=10 min and T=24 hours. A resonance scanner confocal microscope (Olympus FluoView FV1000 coupled to the IX81 Motorized Inverted System Microscope) was used to determine each cell's location within the CAM with respect to lectin-rhodamine signal in real time. All quantifications were conducted blinded. Values reported represent the percentage of cells that successfully extravasated in the 1cm×1cm field across 30 biological replicates. All quantifications were conducted blinded.

For *in vivo* invadopodia assays, the chick embryos were returned to their incubators after injection of labelled cells, and at the 6-hour time-point were intravenously injected with rhodamine-labelled lectin (75µL of 0.1 mg/mL, Vector Laboratories Inc.) in order to visualize the luminal surface of the endothelial cells in the CAM. A resonance scanner confocal microscope was used to determine each cell's location within the CAM with respect to lectin-rhodamine signal in real time. By scanning across the Z-axis, green fluorescently labeled cells were assessed for the presence of functional invadopodia protruding between the intravascular/extravascular boundary. Values reported represent the percentage of cells displaying functional invadopodia *in vivo* across 6 biological replicates consisting of approximately 30 scanned cells each. All quantifications were conducted blinded.

Invadopodia Formation Assay

The *in vitro* invadopodia formation assay was conducted as described (Artym et al., 2009). Briefly, cover slips were coated with 1mL of cold poly-L–lysine (Sigma, P7405; 50µg/mL in PBS) and aspirated after 20 minutes, followed by a 15 minute incubation with 0.5%

glutaraldehyde. Coverslips were then inverted on an 80µl drop of 0.2% gelatin in PBS labelled with Alexa594 (Thermo Fischer Scientific, G13187), and incubated for 10 minutes. Coverslips were lifted, then incubated with 5mg/mL sodium borohydride for 15 minutes to quench reactive groups in the gelatin matrix, followed by extensive washing with PBS. Cells were trypsinized and plated on coverslips for 12-24 hours (as optimized) followed by fixation with 4% paraformaldehyde and permeabilization with 0.1% Triton X-100 in PBS. Samples were blocked with 5% skim milk powder, followed by staining with Alexa488-labelled phalloidin (Thermo Fischer Scientific, A12379) to label F-actin. Cells were imaged using the Nikon Fast A1R Upright Microscope. Cells with actin cores overlaying spots of degradation were counted as invadopodia forming cells. Percentage of cells forming invadopodia was quantified from 4 biological replicates, assessing invadopodia formation in 10-20 random, non-overlapping fields.

RNA Isolation and Quantitative Real-Time PCR (qRT-PCR)

RNA was isolated using the RNeasy Mini Kit (Qiagen, 74104). RNA (500ng) was transcribed into cDNA using the qScript cDNA SuperMix (Quanta Biosciences, 84034). The RT^2 SYBR Green ROX qPCR Mastermix (Qiagen, 330521) was utilized for quantitative PCR with the primer sequences as listed in Table 3.1. The output Ct values were normalized to GAPDH and RPLP0 expression for 21NT transfected and transduced cells, respectively, using the $\Delta\Delta$Ct method. Means derived from a minimum of three biological replicates were used during analysis.

Table 3.1 – Primer sequences utilized for qRT-PCR in mRNA studies.

mRNA Probe	(F) Forward and (R) Reverse Primer Sequences, 5' to 3'
Total TBX3	F: CGCTGTGACTGCATACCAGA R: GTGTCCCGGAAACCTTTTGC
TBX3iso1	F: AGTGGATGTCCAAAGTCGTCAC R: CATGGAGTTCAATATAGTAAATCCATGTTTGTCTG
TBX3iso2	F: AGTGGATGTCCAAAGTCGTCAC R: CACTTGGGAAGGCCAAAGTAAATCCATG
CDH2 (N-cadherin)	F: GACGATCCCAATGCCCTCAA R: ACATGTTGGGTGAAGGGGTG
CST6	F: TGAGGTCCTTGTGGTTCCCT R: CCCTCGGGGACTTATCACATC
FN1 (Fibronectin)	F: AGGAGAATGGACCTGCAAGC R: GAAGTGCAAGTGATGCGTCC
GAPDH	F: AGGCTGGGGCTCATTTGAAG R: CCATCCACAGTCTTCTGGGTG
MMP14	F: CCAGCAACTTTATGGGGGTG R: GGCCCATAGGTGGGGTTTTT
MMP9	F: CTTTGAGTCCGGTGGACGAT R: TCGCCAGTACTTCCCATCCT
TWIST1	F: GCAAGAAGTCGAGCGAAGAT R: GCTCTGCAGCTCCTCGAA
RPLP0	F: CCTCATATCCGGGGGAATGTG R: GCAGCAGCTGGCACCTTATTG
SLUG	F: GCCAAACTACAGCGAACTGG R: GATGGGGCTGTATGCTCCTG
SRC	F: GCACAGGACAGACAGGCTAC R: TCTGACTCCCGTCTGGTGAT
uPa	F: TCCAAAGGCAGCAATGAACT R: GTGCTGCCCTCCGAATTTCT
VIM (Vimentin)	F: GGACCAGCTAACCAACGA R: AAGGTCAAGACGTGCCAGAG

Chromatin Immunoprecipitation

Twenty million cells (per replicate) were grown to confluence for each cell line. The cells were washed twice with cold PBS, and then cross-linked with 10mL of PBS with 1% formaldehyde solution for 15 minutes at room temperature on a rocking platform. The reaction was quenched with 1mL of 2.625M glycine. The cells were then scraped into the supernatant and washed twice with cold PBS.

Pellets were resuspended in 1mL nuclei isolation buffer (50mM Tris pH 8.0, 60mM KCl, 0.5% NP-40) with protease inhibitors (Thermo Scientific, 78429) and incubated on ice

for 10 minutes, then spun at 3,000 RPM for 3 minutes at 4ºC for nuclei isolation. Nuclei were resuspended in 1mL of Lysis Buffer (0.5% SDS, 10mM EDTA, 0.5mM EGTA, 50mM Tris HCl, pH 8.0) with protease inhibitors. Chromatin was sonicated for 40 minutes at 2ºC (using Diagenode Bioruptor Pico; 30 seconds on, 30 seconds off). The sonicated samples were centrifuged at 13,000 RPM for 10 minutes at 4ºC to remove cell debris. Sonicated chromatin was then pre-cleared with 200μL Protein-A Dynabeads (Life Technologies, 10002D) for 1 hour at 4ºC on a rocking platform. Simultaneously, 50μL of Protein-A Dynabeads were washed with 0.5% BSA-PBS and incubated with 5μg of normal rabbit IgG antibody (Invitrogen, 10500C) or 5μg of rabbit anti-TBX3 antibody (Invitrogen, 424800) in 100μL of dilution buffer (PBS with 0.2% Tween20 and 1% BSA) for 2 hours at room temperature on a rocking platform (quantities listed per biological replicate). The bead-antibody complex was then washed twice with 0.5% BSA-PBS, resuspended in dilution buffer and then added to the sample. Immunoprecipitation was conducted overnight (16 hours) at 4ºC on a rocking platform.

Bound chromatin was eluted the following day. Each wash step was performed at 4ºC for 5 minutes on a rocking platform. Chromatin was washed with Wash Buffer I (20mM Tris HCl, 150mM NaCl, 2mM EDTA, 1% Triton X-100, 0.1% SDS) twice, Wash Buffer II (20mM Tris HCl, 500mM NaCl, 2mM EDTA, 1% Triton X-100, 0.1% SDS) once, and TE buffer (10mM Tris HCl, 1mM EDTA, pH 8.0) twice. Bound chromatin was eluted using 200μL of Elution Buffer (100mM $NaHCO_3$, 1% SDS) at 65ºC for 20 minutes. NaCl was added to a final concentration of 200mM and incubated with the chromatin overnight at 65ºC for de-crosslinking. Proteinase K (Thermo Scientific, AM2546) was added and incubated for 2 hours at 50ºC, followed by RNase A (Thermo Scientific, 12091039) treatment for 60 minutes at 37ºC for protein and RNA degradation, respectively. The DNA was purified using the QIAquick PCR Purification Kit (Qiagen, 28106) and eluted with 20μL elution buffer.

For ChIP array purposes, the eluted DNA was amplified using the Whole Genome Amplification Kit (Sigma, WGA2) as per the manufacturer's protocol, with the omission of the fragmentation step. In order to obtain sufficient DNA for ChIP-array hybridization, the amplified DNA was re-amplified using the GenomePlex Complete Whole Genome Reamplification kit (Sigma, WGA3) with the incorporation of dUTP (Jena Bioscience, NU-1021S) at a final concentration of 2mM, and dTTP was reduced to 8mM. The DNA was once again purified using the QIAquick PCR Purification Kit.

For validation of select ChIP targets, 5uL of the eluate was used for qPCR. The % input method was utilized for quantification of enrichment. An input of 5% was saved prior to immunoprecipitation and was de-crosslinked and purified as described above. The Ct values for the input was subtracted from the Ct values of the immunoprecipitated samples. A fold change was then calculated consisting of TBX3 IP over IgG control (signal over noise) to allow for easy comparison between primer sets. The primers used for ChIP-qPCR experiments are listed in Table 3.2. The CDH1 transcription start site (TSS) and coding region served as the positive and negative control, respectively. The CDH1 control primer sequences were obtained from a previously published study reporting the TBX3 binding site within E-cadherin in melanoma cell lines (Rodriguez et al., 2008).

Table 3.2 – Primer sequences utilized for ChIP-qPCR validation studies.

DNA Probe	(F) Forward and (R) Reverse Primer Sequences, 5' to 3'
CDH1 TSS	F: TCACAGGTGCTTTGCAGTTC R: GTGAACCCTCAGCCAATCAG
CDH1 coding region	F: AACAGCTGCTTGGTGACGTT R: CAAGCCTGGGAGTTAGGTG
SNAI2	F: AATGGGGCTTTCTGAGCCAC R: TCCACGCCCAGCTACCCAA

RNA-Seq

Cells were grown to 80% confluence and RNA was isolated using the RNeasy Mini Kit (Qiagen, 74104) incorporating DNase I digestion (Qiagen, 79254). Samples were sent to the Donnelly Sequencing Centre (Toronto, Canada) and assessed for RNA integrity using an Agilent bioanalyzer. For each sample, stranded mRNA libraries were prepared and sequenced on an Illumina HiSeq 2500 sequencer using V4 chemistry. Paired-end read length was 51 base pairs. Raw reads were then uploaded to Basespace (https://basespace.illumina.com/) and imported into Galaxy software (https://usegalaxy.org). The FastqGroomer tool within Galaxy was used to prepare the files for alignment, and the TopHat tool within Galaxy was used to align the FASTQ files to the reference genome (Hg19) using the default parameters, except that the maximum number of alignments was capped at 10. Aligned sequences were imported as .bam files into Partek Genomics Suite (PGS; http://www.partek.com/pgs) software and analyzed using the RNA-Seq analysis workflow. Gene reads were normalized for transcript length using the RPKM normalization

algorithm, and differentially expressed genes between TBX3iso1 or TBX3iso2 compared to empty vector were determined using ANOVA statistical tests. For each comparison, final gene lists were created using a minimum fold change cut-off of 1.5-fold, and a maximum False Discovery Rate (FDR) of 0.05 (step-up FDR algorithm of Benjamini and Hochberg).

ChIP Promoter Arrays

Chromatin was immunoprecipitated as described above. The amplified product (7.5μg) was fragmented, labeled, and hybridized to the GeneChip Human Promoter 1.0R Array (Affymetrix, 900776), and the hybridized array was scanned as per manufacturer's instructions. All microarray work was done at the London Regional Genomics Centre (Robarts Research Institute, London, Canada). Resultant .cel files were then imported into Partek Genomic Suites (PGS) and analyzed using the Chromatin Immunoprecipitation workflow. Differential probe intensities between TBX3iso1 or TBX3iso2 vs. empty vector were determined by ANOVA and enriched regions of significance were determined using the MAT algorithm. To be further considered, an enriched region had to have a minimum MAT score of 5 at $p<0.05$.

Bioinformatics Analysis

To compare RNA-Seq and ChIP-array datasets, gene lists were constructed using Venny 2.1 (Spanish National Biotechnology Centre; http://bioinfogp.cnb.csic.es/tools/venny/). Genes of interest include those significantly altered with overexpression of both TBX3 isoforms by RNA-Seq (fold change >1.5 relative to the empty vector, $p<0.05$), and genes which both TBX3 isoforms directly bound in ChIP-array datasets (MAT score >5, $p<0.05$). Altered biological functions with TBX3 isoform overexpression were examined using Ingenuity Pathway Analysis (IPA) (Qiagen) by examining RNA-Seq data. Gene reads and ChIP binding locations were visualized using Interactive Gene Viewer (IGV) software (Broad Institute). Consensus binding motifs of highly conserved T-box proteins (TBX1, TBX2, TBX4, TBX5, TBX15, TBX20, TBX21) within the JASPAR database (University of Copenhagen Centre for Molecular Medicine and Therapeutics; http://jaspar.genereg.net) were assessed, and coordinates that had overlap for all aforementioned related T-box transcription factors were imported into IGV. DNase I hypersensitivity and RNA polymerase II ChIP tracks were also imported into IGV. A cutoff threshold of >40 for each coordinate occurring in the RNA pol II

(POLR2A) ChIA-PET combined dataset in various cell lines was introduced to assess consistent binding sites. The aforementioned ENCODE tracks are listed in Table 3.3.

The TCGA BRCA, Farmer Breast and Desmedt Breast datasets were interrogated and data was exported using XenaBrowser (University of California, Santa Cruz; https://xenabrowser.net/datapages/). The aforementioned datasets are listed in Table 3.3.

The PANTHER database (University of Southern California; http://pantherdb.org) was used to conduct over-representation analysis using Fischer's exact test with FDR multiple test correction and focusing on protein class and Gene Ontology (GO) biological pathways.

Enrichr pathway analysis (Icahn School of Medicine, Mount Sinai; http://amp.pharm.mssm.edu/Enrichr/) was conducted with the input list consisting of 194 genes significantly altered (fold change >1.5, $p<0.05$) for cells overexpressing either TBX3iso1 or TBX3iso2 relative to the empty vector control from the normalized RNA-Seq data. Results assessing Jensen TISSUES expression data are reported.

Table 3.3 – Publicly-available datasets utilized for analysis.

FILE	SOURCE	REFERENCE (or *LINK)*
POLR2A ChIA-PET	ENCODE: **ENCSR000CAA**	*http://hgdownload.cse.ucsc.edu/goldenPath/hg19/encodeDCC/wgEncodeGisChiaPet/*
DNase I hypersensitivity (master list)	ENCODE: **wgEncodeAwgDnaseMasterSites**	*http://hgdownload.cse.ucsc.edu/goldenpath/hg19/encodeDCC/wgEncodeAwgDnaseMasterSites/*
TCGA Breast Cancer (BRCA)	GDC Project ID: **TCGA-BRCA**	*https://portal.gdc.cancer.gov/projects/TCGA-BRCA*
Farmer Breast	GEO: **GSE1561**	Farmer P, Bonnefoi H, Becette V, Tubiana-Hulin M et al. Identification of molecular apocrine breast tumours by microarray analysis. *Oncogene* 2005 Jul 7;24(29):4660-71. PMID: 15897907
Desmedt Breast	GEO: **GSE7390**	Desmedt C, Piette F, Loi S, Want Y et al. Strong time dependence of the 76-gene prognostic signature for node-negative breast cancer patients in the TRANSBIG multicenter independent validation series. *Clin Cancer Res* 2007 Jun 1;13(11)3207-14. PMID: 17545524

Patient Characteristics in Immunohistochemistry Study

Patients with early-stage breast cancer were identified from the London Breast Cancer Database on the basis of having either DCIS only (Stage 0), or DCIS with an associated invasive component (Stage I; ≤2cm, and either pN0 or pN0mi). Cohort 1 consisted of 186 patients with low, intermediate, or high grade DCIS with the aforementioned characteristics of no invasion or early invasion (Stage 0 or Stage I). Cohort 2 consisted of 118 patients with non-high grade DCIS with the aforementioned characteristics, with either no invasion or early invasion (Stage 0 or Stage I). Clinicopathological variables for cohort 1 and cohort 2 patients entered into this study are listed in Table 3.4, left and right panel, respectively. There was no overlap between patients in cohort 1 and cohort 2. The study was conducted under a protocol approved by the Western University Health Sciences Research Ethics Board and the Clinical Research Impact Committee of Lawson Health Research Institute.

Immunohistochemistry

Formalin-fixed, paraffin embedded tissues were sectioned at 4.0μm and added to a charged glass slide. Sections were de-paraffinized, rehydrated, and incubated in TBS-Tween or TBS-Triton (Tris buffered saline (TBS) + 0.5% Tween-20 for TBX3 and SLUG stains, and TBS + 0.1% Triton-X for TWIST1 stain) for 20 minutes for membrane permeabilization. Heat induced antigen retrieval was conducted with citrate buffer (pH 6.0) for 20 minutes. The UltraVision LP Detection System (Thermo Fischer Scientific, TL-015-HD) was used with optimization of incubation length. Endogenous peroxidase activity was blocked for 10 minutes for all samples. For the TBX3 stain, slides were blocked for 5 minutes, incubated in TBX3 primary antibody (Abcam, ab99302) at 1/200 dilution for 15 minutes at room temperature, and 11 minutes in the HRP polymer. For the SLUG stain, slides were blocked for 6 minutes using the UltraVision protein block and an additional 30 minutes using the Dako protein block (Dako, CD310081) in order to reduce non-specific background staining. Slides were incubated in SLUG primary antibody (Abcam, ab27568) at 1/750 dilution for 70 minutes at room temperature, and 15 minutes in the HRP polymer. For the TWIST1 stain, slides were blocked for 6 minutes, incubated in TWIST1 primary antibody (Abcam, ab50887) at 1/200 dilution for 1 hour at room temperature, 10 minutes in primary antibody enhancer, and 15 minutes in the HRP polymer. Signal for all markers was developed using DAB and slides were counter-stained in Harris's Hematoxylin.

Quantification of Immunohistochemistry

Slides were stained and scanned using an Aperio AT2 slide scanner (Leica Biosystems). Full scanned digital slides were analyzed by an anatomical pathologist (blinded as to the diagnosis) and representative images were captured at 20x magnification using the Aperio ImageScope slide viewing software. Each image represented one of four tissue compartments including benign non-columnar cells, benign columnar cell lesions (CCLs; includes columnar cell change, columnar cell hyperplasia or flat epithelial atypia), ductal carcinoma in situ (DCIS), and invasive cancer. The expression of each molecular marker was assessed using the ImmunoRatio plugin (University of Tampere, Finland) for ImageJ to assess percentage of positive cells. For each image, the cell type of interest was solely analyzed and the remaining cells (i.e. stromal cells) were cropped out. A control slide representing serial sections was run for each batch of slides (with quantification and statistical analysis) to ensure identical and reproducible staining for each run.

Statistical Analysis

Statistical analyses were conducted using GraphPad Prism 5. One-way ANOVAs were used for experiments containing three or more groups, with either a Tukey or Dunnett's post-hoc test. T-tests were used for experiments containing two groups. Error bars represent standard deviation. P-values less than 0.05 were considered statistically significant.

3.3 **Results**

3.3.1 TBX3 overexpression is associated with an invasive and EMT phenotype.

To examine the role of TBX3 in breast cancer, non-invasive 21NT cells (which endogenously express low levels of TBX3) were stably transfected with either an empty vector, TBX3iso1 or TBX3iso2. Isoform specific up-regulation was confirmed at the mRNA level using isoform specific primers, in addition to up-regulation of total TBX3 protein levels (Figures 3.3.1 A-B and Appendix 1A). Functionally, up-regulation of either TBX3 isoform in DCIS-like 21NT cells led to an increase in migration using the wound scratch assay (Appendix 2A). TBX3 overexpressing 21NT cells also exhibited reduced cell-to-cell adhesion *in vitro* (Appendix 2B). In the presence of calcium ions (+$CaCl_2$), or after adding increasing doses of EDTA to chelate free calcium, there were reduced levels of cell-to-cell adhesion, implying that several cell-adhesion molecules may be involved (not solely Ca^{2+} dependent cadherins). As TBX3 has previously been shown to directly down-regulate E-cadherin (CDH1) in melanoma lines (Rodriguez et al., 2008), and as loss of E-cadherin has been associated with the switch to an EMT phenotype, we assessed E-cadherin expression by immunofluorescence. We confirmed a down-regulation of E-cadherin protein levels as well as decreased membrane localization with TBX3 overexpression (Appendix 2C).

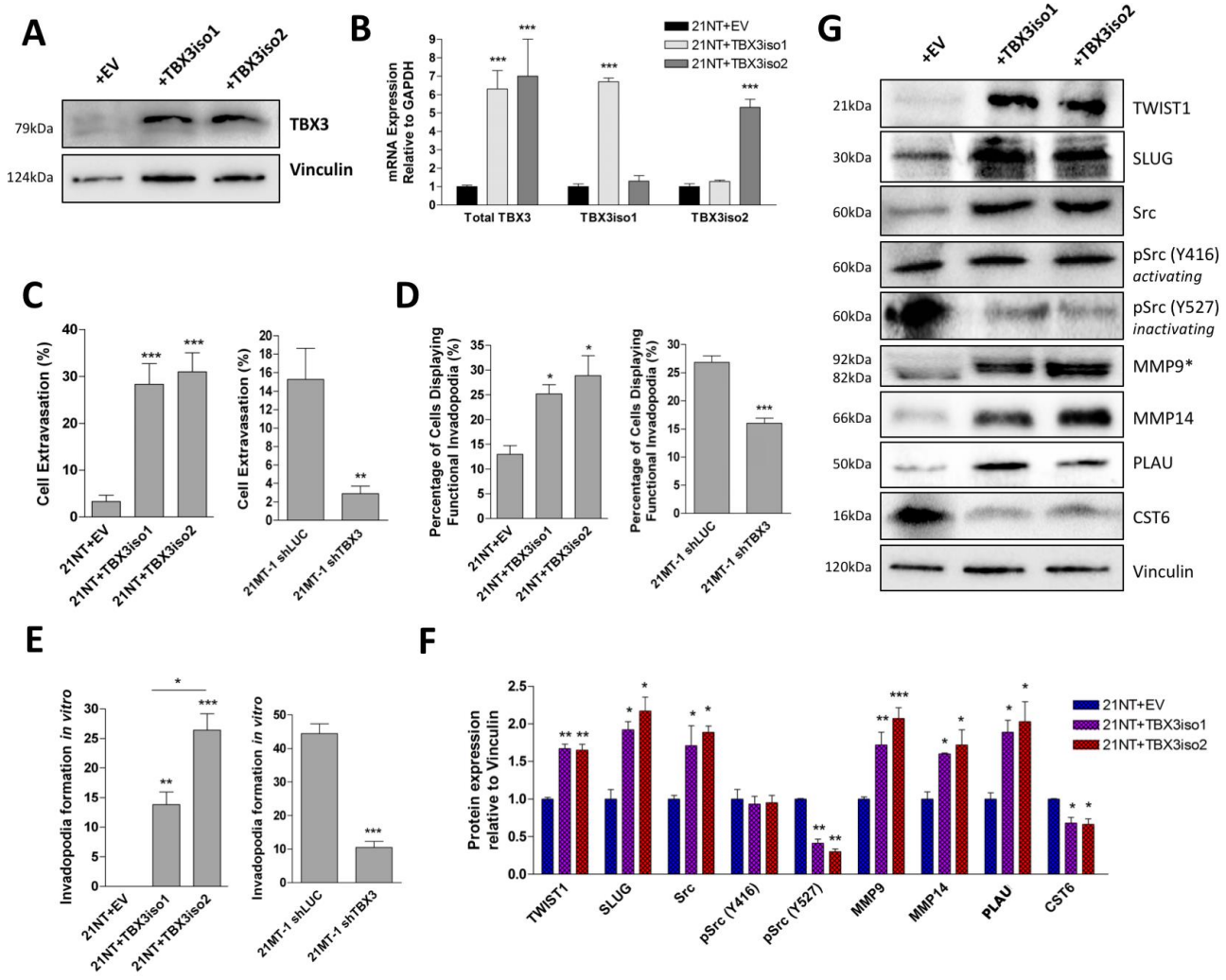
A
+EV
+TBX3iso1
+TBX3iso2
79kDa
TBX3
124kDa
Vinculin
B
21NT+EV
21NT+TBX3iso1
21NT+TBX3iso2
mRNA Expression Relative to GAPDH
Total TBX3
TBX3iso1
TBX3iso2
C
Cell Extravasation (%)
21NT+EV
21NT+TBX3iso1
21NT+TBX3iso2
21MT-1 shLUC
21MT-1 shTBX3
D
Percentage of Cells Displaying Functional Invadopodia (%)
E
Invadopodia formation in vitro
F
Protein expression relative to Vinculin
TWIST1
SLUG
Src
pSrc (Y416)
pSrc (Y527)
MMP9
MMP14
PLAU
CST6
G
21kDa
30kDa
60kDa
60kDa
60kDa
92kDa
82kDa
66kDa
50kDa
16kDa
120kDa
pSrc (Y416) activating
pSrc (Y527) inactivating
MMP9*

Figure 3.3.1 – TBX3 overexpression is associated with an invasive and EMT phenotype.

(A) Total TBX3 protein levels were assessed by western blot in 21NT transfectant cells. **(B)** Total TBX3, TBX3iso1, and TBX3iso2 transcript levels were assessed by qRT-PCR in 21NT transfectant cells, normalized to GAPDH expression levels, and depicted as fold change relative to the empty vector control. Means derived from three biological replicates were used during analysis. **(C-D)** Assessment of cell extravasation and functional invadopodia formation *in vivo* in the chick chorioallantoic membrane (CAM) model. Green (CMFDA) fluorescently labeled cells were injected into the vasculature of the CAM (50,000 cells each), and the vasculature was labeled red with lectin-rhodamine at T=0. For cell extravasation, cells were counted 24 hours post injection in a $1cm^2$ area across 30 biological replicates. For functional invadopodia formation, a binary quantification of *in vivo* invadopodia formation was conducted 6 hours post cell injection. Cells were deemed positive for invadopodia formation when they possessed protrusions from the vasculature into the stroma. Values reported represent the percentage of cells displaying functional invadopodia *in vivo* across 6 biological replicates consisting of approximately 30 scanned cells each. **(E)** *In vitro* invadopodia formation assay for assessment of local cell invasion. Cells were added to red fluorescently labeled gelatin and incubated for 12-24 hours (as optimized) to allow for substrate degradation. Cells were visualized using labelled phalloidin for identification of cellular F-actin cores at sites of local matrix degradation, signifying the presence of invadopodia. Percentage of cells forming invadopodia was quantified from 4 biological replicates, assessing invadopodia formation in 10-20 random, non-overlapping fields. **(F-G)** Protein expression of EMT markers was assessed by western blot. Protein samples were separated by 10% SDS-PAGE and quantified by densitometry. Protein levels were normalized to Vinculin, which served as the loading control for all proteins aside from MMP9 (* secreted protein); in the latter case, MMP9 levels in the conditioned media samples were normalized to total protein per lane based on Ponceau staining of the membrane. Where quantification of western blots are shown, data was acquired through densitometric quantifications across three biological replicates.

**p<0.05, **p<0.01, ***p<0.001 by one-way ANOVA with Tukey post-hoc for comparison between three groups, and Student's t-test for comparison between two groups. Error bars represent standard deviation.*

In order to assess the aggressiveness of the cell lines in an *in vivo* system, we made use of the chick embryo chorioallantoic membrane (CAM) model. Fluorescently labeled cells were injected into the vasculature of chicks at embryonic day 12 and cell extravasation was assessed as previously described (Kim et al., 2016) (Figure 3.3.1 C). Stable overexpression of either isoform in 21NT cells resulted in an increase in extravasation within the CAM model. Extravasation levels were reduced drastically with shRNA-mediated knockdown of TBX3 in invasive 21MT-1 cells, which natively express TBX3 at high levels (protein levels shown in Appendix 1B-C). In order to confirm that the cells are indeed better able to exit the vasculature (and are not simply better able to survive at T=24h), we performed live functional invadopodia assays within the CAM using confocal microscopy. Six hours after the injection of fluorescently labeled cells into the vasculature of chick embryos, rhodamine-labelled lectin was injected to visualize the vessel lumen and a binary quantification of invadopodia formation was conducted (Figure 3.3.1 D). An increase in functional invadopodia was observed with overexpression of either TBX3 isoform in 21NT cells. Furthermore, the presence of functional invadopodia was reduced with TBX3 knockdown in 21MT-1 cells. Changes to rates of invadopodia formation were also verified using a standard *in vitro* invadopodia formation assay (Figure 1E), which mirrored the *in vivo* CAM data obtained.

More invasive phenotypes were also observed using transient transfections of TBX3iso1 or TBX3iso2 into T47D (luminal A; ER+/PR+/HER2-), SKBR3 (HER2-enriched; ER-/PR-/HER2+), and MDA-MB-468 (basal-like; ER-/PR-/HER2-) breast cancer cell lines, representing different molecular subtypes (Appendix 3A-C). Collectively, this suggests that these findings have broad applicability and are not cell-type specific.

The functional alterations associated with TBX3 isoform overexpression here suggest a more invasive, epithelial-mesenchymal transition (EMT) phenotype. We examined the expression of several EMT markers and observed alterations in multiple proteolytic enzymes and their inhibitors (MMP9, MMP14, uPA up-regulated; CST6, down-regulated), as well as EMT-associated transcription factors (TWIST1, SLUG up-regulated) with stable overexpression of either TBX3 isoform. These were confirmed at both the mRNA and protein levels (Figure 3.3.1 F-G and Appendix 4A). We observed an increase in levels of active MMP2, as assayed by gelatin zymography (Appendix 4B), indicating functional activation of pathways involved in substrate degradation and invasiveness

3.3.2 TBX3 overexpression leads to an alteration of mesenchymal transcript levels and direct up-regulation of SLUG.

To examine transcriptional changes associated with TBX3 isoform overexpression and elucidate mechanisms involved, RNA-Seq was conducted for TBX3iso1 and TBX3iso2 overexpressing cell lines. Ingenuity Pathway Analysis (IPA) indicated that the top predicted functional changes associated with the unique transcriptional profiles obtained for the TBX3 transfectants include alterations in cellular movement, cellular growth and proliferation, cell death, cell survival and cancer-associated processes (Figure 3.3.2 A). Enrichment analysis (Enrichr) was conducted, with the input list consisting of genes significantly altered (>1.5 fold up or down, FDR<0.05) for cells overexpressing either TBX3iso1 or TBX3iso2 relative to the empty vector control. Comparison to the Jensen TISSUES expression database of large-scale tissue expression profiles revealed mesenchymal genes as most enriched (Figure 3.3.2 B). The dbEMT database (Zhao et al., 2015) was used to compile a list of 377 EMT-related genes for analysis of RNA-Seq data. Relative to the empty vector, alterations in abundance of a large proportion of EMT-related genes were detected with TBX3 isoform overexpression (Figure 3.3.2 C).

To determine whether the TBX3-dependent changes in gene expression are direct, chromatin immunoprecipitation (ChIP) experiments were conducted using either an anti-TBX3 antibody or rabbit IgG antibody as a non-specific control for background, and immunoprecipitated DNA was hybridized to Affymetrix Promoter 1.0R arrays. Using this approach we identified 5652 and 5512 specific binding sites for TBX3iso1 and TBX3iso2, respectively. Further comparison of TBX3 binding sites with our expression analysis identified 194 genes that were directly regulated by both TBX3 isoforms (>1.5 fold up or down, FDR<0.05) (Figure 3.3.2 D). These 194 genes were analyzed using the PANTHER database by conducting over-representation analysis and focusing on protein class (Appendix 5). The lowest p-value and corrected FDR statistic corresponded to the protease inhibitor protein class. Several other protein classes related to EMT were also altered, including extracellular matrix proteins, metalloproteases, and serine protease inhibitors. Importantly, within this list of 194 genes directly induced by TBX3 was SLUG (encoded by the *SNAI2* gene), a transcriptional regulator and potent inducer of EMT, that may provide a

mechanism for the previously described EMT and invasion-associated functional changes in the TBX3-transfected cells.

Both TBX3 isoforms were shown to bind near an intron/exon junction of the *SNAI2* (SLUG) gene based on the ChIP-array data (Figure 3.3.2 E). TBX3 has previously been shown to bind to the consensus T-box binding element (TBE) in several different contexts (Coll et al., 2002b). Consensus TBEs were investigated using the JASPAR database of transcription factor binding sites by assessing predicted binding coordinates of highly conserved T-box proteins (Figure 3.3.2 E). A highly conserved TBE was found within the *SNAI2* (SLUG) gene region that coincides with binding of both TBX3 isoforms in the ChIP-array dataset. We conducted ChIP qRT-PCR validation, using ChIP primers spanning this identified TBE. Published primer sequences were used for the transcription start site (CDH1 TSS) and coding region (CDH1 coding) of E-cadherin (Rodriguez et al., 2008), representing positive and negative controls, respectively (Figure 3.3.2 F). With TBX3 overexpression, there was a 3-4-fold enrichment of TBX3 protein bound to the conserved TBE of the *SNAI2* (SLUG) gene. Interestingly, this binding region overlaps with a DNase I hypersensitive region and RNA polymerase II binding region, which is suggestive of open and transcriptionally active chromatin (Figure 3.3.2 E).

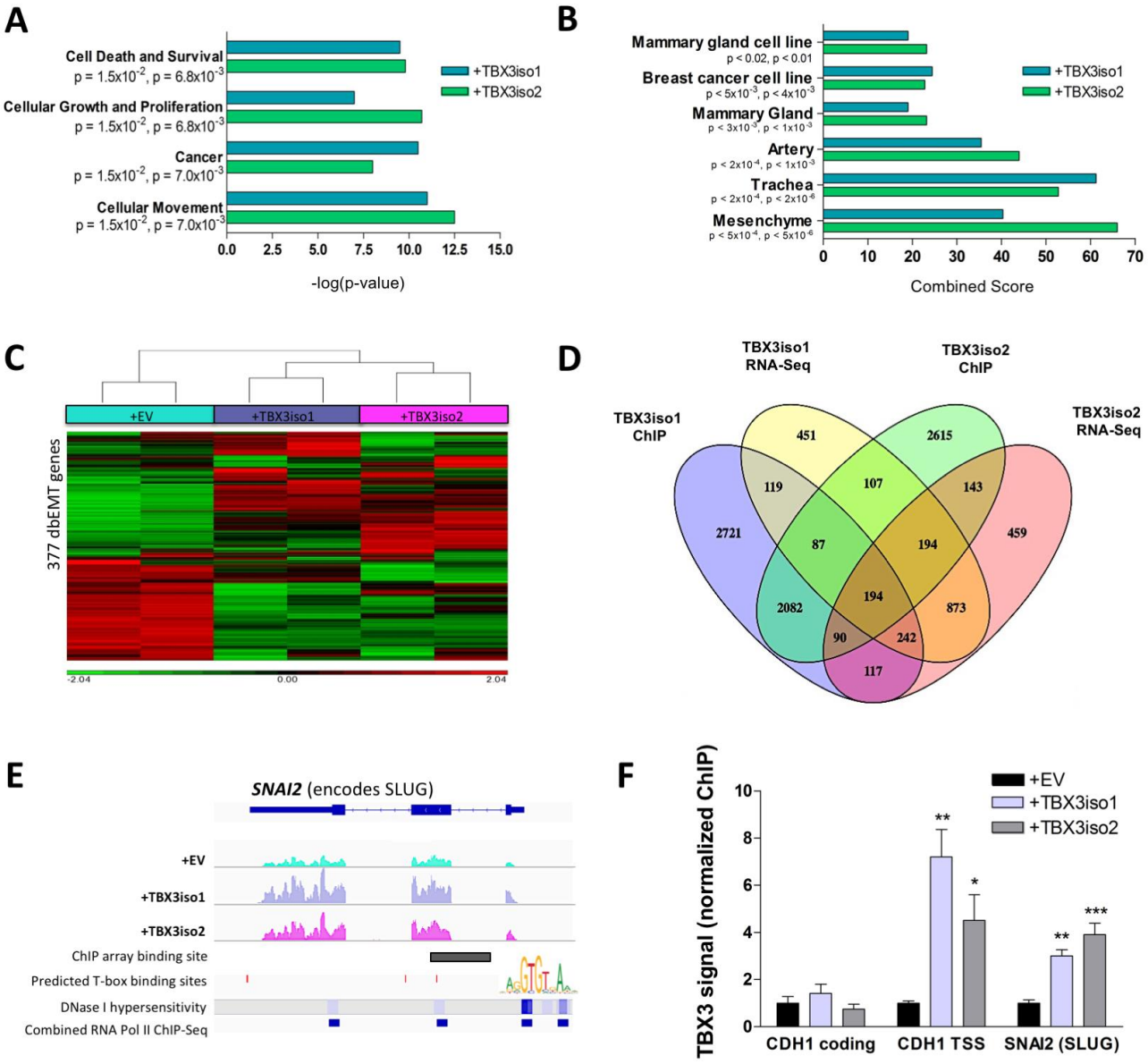
A
Cell Death and Survival
p = 1.5x10-2, p = 6.8x10-3
Cellular Growth and Proliferation
p = 1.5x10-2, p = 6.8x10-3
Cancer
p = 1.5x10-2, p = 7.0x10-3
Cellular Movement
p = 1.5x10-2, p = 7.0x10-3
+TBX3iso1
+TBX3iso2
0.0 2.5 5.0 7.5 10.0 12.5 15.0
-log(p-value)
B
Mammary gland cell line
p < 0.02, p < 0.01
Breast cancer cell line
p < 5x10-3, p < 4x10-3
Mammary Gland
p < 3x10-3, p < 1x10-3
Artery
p < 2x10-4, p < 1x10-3
Trachea
p < 2x10-4, p < 2x10-6
Mesenchyme
p < 5x10-4, p < 5x10-6
+TBX3iso1
+TBX3iso2
0 10 20 30 40 50 60 70
Combined Score
C
+EV
+TBX3iso1
+TBX3iso2
377 dbEMT genes
-2.04
0.00
2.04
D
TBX3iso1 RNA-Seq
TBX3iso2 ChIP
TBX3iso1 ChIP
TBX3iso2 RNA-Seq
451
2615
119
107
143
2721
87
194
459
194
2082
873
90
242
117
E
SNAI2 (encodes SLUG)
+EV
+TBX3iso1
+TBX3iso2
ChIP array binding site
Predicted T-box binding sites
DNase I hypersensitivity
Combined RNA Pol II ChIP-Seq
F
TBX3 signal (normalized ChIP)
+EV
+TBX3iso1
+TBX3iso2
0 2 4 6 8 10
**
*
**
***
CDH1 coding
CDH1 TSS
SNAI2 (SLUG)

Figure 3.3.2 – TBX3 overexpression leads to an alteration of mesenchymal transcript levels and direct up-regulation of SLUG.

Total mRNA was isolated from 21NT+EV, 21NT+TBX3iso1 and 21NT+TBX3iso2 cells in duplicate and examined by RNA-Seq. **(A)** Pathway Analysis was conducted using all output RNA-Seq data for TBX3iso1 and TBX3iso2 overexpressing cells and compared to the empty vector control. **(B)** Enrichment analysis was conducted with the input list consisting of genes significantly altered (fold change >1.5, FDR<0.05) for cells overexpressing either TBX3iso1 or TBX3iso2 relative to the empty vector control. Results comparing resultant RNA-Seq profiles with the Jensen tissue dataset and lowest p-value tissue sites are shown. **(C)** Heat map of EMT genes. The dbEMT database was used to compile a list of 377 EMT genes and hierarchial clustering was conducted of RNA-Seq data. Duplicate samples are shown for each cell line. **(D)** Chromatin Immunoprecipitation (ChIP) experiments were conducted with either specific anti-TBX3 antibody or a nonspecific rabbit IgG control antibody. Immunoprecipitated DNA was hybridized to an Affymetrix Promoter Array. Datasets from RNA-Seq and ChIP-array experiments were integrated in order to examine the effects of TBX3 isoform binding on gene transcript levels (all fold change >1.5, FDR<0.05). **(E)** RNA-Seq reads across the *SNAI2* (SLUG) gene for 21NT+EV, 21NT+TBX3iso1 and 21NT+TBX3iso2 cell lines are shown in the top three lines, followed by the identified TBX3 ChIP array binding site. Binding sites for highly conserved T-box proteins within the *SNAI2* (SLUG) gene were assessed using the Jaspar database of transcription factor binding sites. Highly conserved T-box binding elements (TBEs) are shown. DNAse I hypersensitivity and RNA polymerase II binding sites are shown in the bottom two lines. **(F)** TBX3 binds directly to the *SNAI2* (SLUG) gene. ChIP experiments were conducted with either a specific anti-TBX3 antibody or a nonspecific rabbit IgG control antibody. Relative amounts of immunoprecipitated DNA were assessed by qRT-PCR, using published sequences of the E-cadherin (CDH1) coding region and transcription start site (TSS) as negative and positive controls, respectively. The SLUG primers used spanned both the predicted overlapping TBE site identified *in silico* and the identified binding site from ChIP-array experiments. Values shown represent input-adjusted, IgG control subtracted values for the specific TBX3 IP normalized to the empty vector control. Means derived from four biological replicates were used during analysis. **p<0.05, **p<0.01, ***p<0.001 by one-way ANOVA with Tukey post-hoc for comparison between three groups. Error bars represent standard deviation.*

3.3.3 SLUG up-regulation by TBX3 is essential for increased migration and invasion.

We have shown that TBX3iso1 and TBX3iso2 directly bind to a consensus TBE within the *SNAI2* (SLUG) gene and leads to its transcriptional up-regulation. Given the strong evidence within existing literature of SLUG involvement in the induction of EMT (De Craene and Berx, 2013, Phillips and Kuperwasser, 2014), we proceeded to investigate whether SLUG was essential for the phenotypes observed with TBX3 overexpression. SLUG levels were efficiently knocked down in 21NT control and TBX3 transfectant cell lines using stable shRNA-mediated lentiviral transduction (Figure 3.3.3 A-B). In the scramble control (SCR), cells overexpressing either TBX3iso1 or TBX3iso2 had higher rates of migration and invasion relative to the empty vector control, similar to levels we previously reported in these cell lines (Krstic et al., 2016). With SLUG knockdown, the rates of migration and invasion of TBX3 isoform transfectants were reduced to baseline levels, despite expressing high levels of TBX3 (Figure 3.3.3 C-D).

A large proportion (7/10) of our previous list of EMT and invasion-associated genes were still significantly altered with high TBX3 isoform expression in cells with SLUG knockdown (Figure 3.3.3 E-F). However, the induction of several key invasiveness-associated genes up-regulated by TBX3 was significantly impaired in the absence of SLUG, including MMP14, vimentin and fibronectin (Figure 3.3.3 E-F). Importantly, these findings suggest that there are TBX3-induced changes in expression of EMT-related genes that are both SLUG-dependent and SLUG-independent, and that the SLUG-dependent changes are required (although not necessarily sufficient) for TBX3-induced migration and invasion.

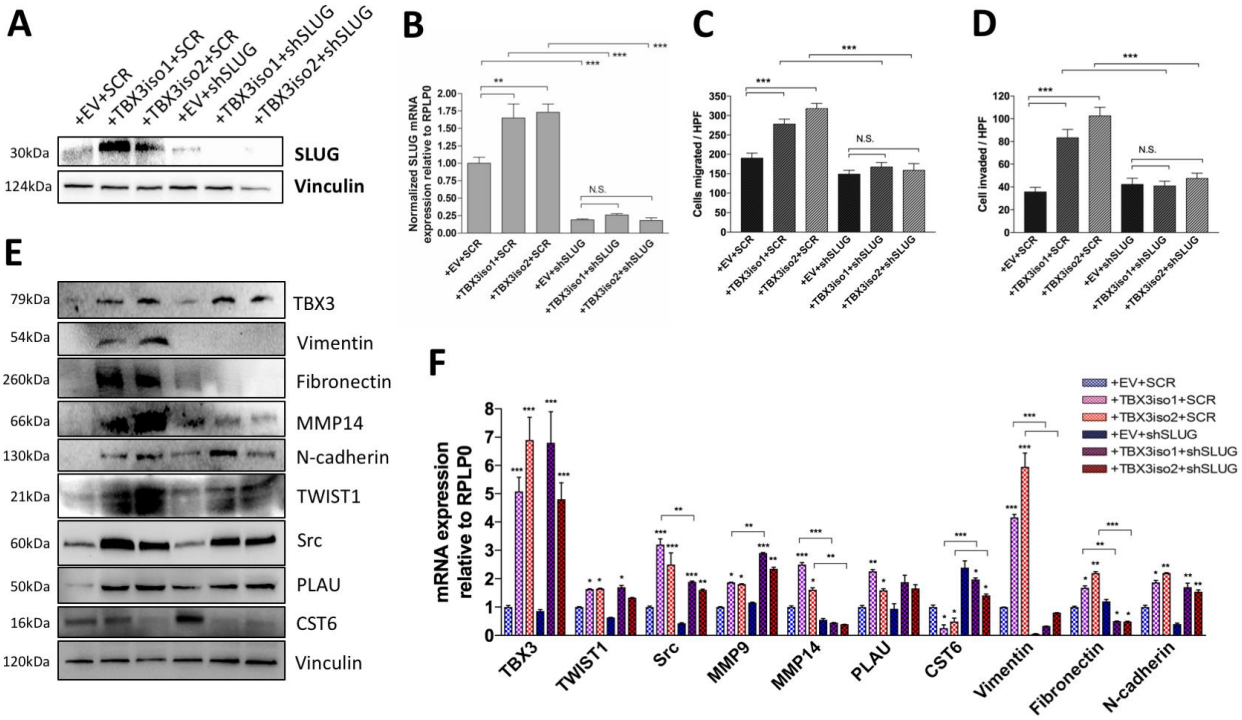

Figure 3.3.3 – SLUG up-regulation by TBX3 is essential for increased migration and invasion.

(A) Western blot analysis showing knockdown of SLUG protein expression in shRNA transductants. Protein levels were normalized to Vinculin, which served as the loading control. **(B)** SLUG transcript levels were assessed by qRT-PCR, normalized to RPLP0 expression levels, and depicted as fold change relative to the empty vector control. **(C-D)** Migration and invasion assays were conducted using 8.0µm pore transwells coated with either gelatin (migration) or Matrigel (invasion). Cells were allowed to migrate or invade for 22 hours. The number of cells that migrated or invaded per high power field are shown. Means derived from four biological replicates were used during analysis. **(E)** Protein expression levels of EMT and invasion-associated genes were assessed by western blot. Protein samples were separated by 10% SDS-PAGE and normalized to Vinculin, which served as the loading control for all proteins. **(F)** The mRNA expression of several EMT and invasion-associated genes was evaluated by qRT-PCR. Expression was normalized to RPLP0 transcript levels and is depicted as fold change relative to the empty vector shScramble control (+EV+SCR). Means derived from three biological replicates were used during analysis. **p<0.05, **p<0.01, ***p<0.001 by either one-way ANOVA with Tukey post-hoc or two-way ANOVA with Tukey post-hoc for comparison within and between sub-groups, respectively. Error bars represent standard deviation.*

3.3.4 TBX3 expression is elevated in low-grade, hormone-receptor positive invasive breast cancers and associated precursor lesions.

Based on the association between TBX3 and an invasive and EMT phenotype *in vitro* and *in vivo* in chick embryo assays, along with a direct link to SLUG signaling, we extended our studies to human patient samples. To first assess the expression levels of TBX3, we focused on nuclear TBX3 expression by immunohistochemistry in 186 pre-invasive (Stage 0, DCIS only) and early invasive breast cancer (Stage I, invasion ≤2.0 cm) patient samples from the London Breast Cancer Database. Clinicopathologic variables for cohort 1 patients entered into this study are listed in Table 3.4 (left panel). We examined 4 sub-populations of cells including 1) benign non-columnar, 2) benign columnar, 3) DCIS, and 4) invasive cancer, after observing high expression of TBX3 in benign columnar cells (Figure 3.3.4 A). Earlier studies, based on genome sequencing data and mutational association, suggest that columnar cell lesions (CCL; includes columnar cell change, columnar cell hyperplasia, flat epithelial atypia (FEA)) may be an early morphologic indicator of propensity for, or non-obligate precursor to the development of breast cancer (Dabbs et al., 2006, Turashvili et al., 2008). We did not see a significant association between level of TBX3 in the DCIS and the presence vs. absence of invasion in cohort 1. We confirmed an association between TBX3 and estrogen receptor (ER) and progesterone receptor (PR) expression in invasive breast cancers (Figure 3.3.4 B-C), which has been suggested by previous studies (Fillmore et al., 2010). TBX3 positivity was highest in low and intermediate grade DCIS and significantly lower in high-grade DCIS (Figure 3.3.4 D). We then examined a second independent patient cohort of 118 patients with non-high-grade (low and intermediate grade) DCIS, with or without associated early invasive cancer (Stage 0 and Stage I) for increased power in evaluation of TBX3 association with invasiveness of low-grade breast cancers. Clinicopathologic variables for cohort 2 patients entered into this study are listed in Table 3.4 (right panel). Based on results from our second cohort assessing patient samples with early invasion, we found that nuclear TBX3 expression by immunohistochemistry in the DCIS was associated with the size of the invasive focus ($p<0.001$) (Figure 3.3.4 E).

Possible downstream effectors of TBX3 were identified in our ChIP-array and RNA-Seq studies. We conducted immunohistochemical staining for EMT transcription factors SLUG and TWIST1 (which were shown to be directly and indirectly up-regulated by TBX3,

respectively) in our second patient cohort (staining patterns shown in Figure 3.3.4 A). Expression of each marker was assessed in all four cell populations in the same manner as for TBX3. We identified a positive correlation between TBX3 expression and both SLUG ($p<0.05$) and TWIST1 ($p<0.001$) expression in the invasive component (Figure 3.3.4 F-G). Additionally, both SLUG and TWIST1 protein levels were up-regulated in CCLs, and SLUG levels were significantly higher in low grade (Grade 1) DCIS lesions relative to both Grade 1+2 (mixed) and Grade 2 DCIS lesions (Figure 3.3.4 H), exhibiting staining patterns similar to TBX3. Collectively, these results suggest that TBX3 may be facilitating the process of early invasion even at the earliest stages of progression (i.e. CCLs, DCIS), and offer potential roles for downstream EMT-related proteins such as SLUG and TWIST1 in invasiveness of early stage breast cancer.

Table 3.4 – Clinicopathologic variables for patients entered into this study.

	COHORT 1	COHORT 2
Characteristic	**No. of patients (%)**	**No. of patients (%)**
Total	186 (100)	118 (100)
Age (yr)		
≤50	17 (9.1)	14 (11.9)
>50	169 (90.9)	104 (88.1)
Associated invasion		
No invasion	100 (53.8)	84 (71.2)
Micro-invasion	12 (6.5)	2 (1.7)
Invasion	74 (39.8)	32 (27.1)
Histological type of invasive cancer		
Total cases with invasion	74 (100)	34 (100)
NST	55 (74.3)	26 (76.5)
NST with lobular features	9 (12.2)	3 (8.8)
NST with tubular features	3 (4.1)	3 (8.8)
NST with mucinous features	3 (4.1)	0 (0.0)
NST with micropapillary features	1 (1.4)	0 (0.0)
Invasive lobular carcinoma	1 (1.4)	0 (0.0)
Invasive tubular carcinoma	1 (1.4)	1 (2.9)
Invasive mucinous carcinoma	1 (1.4)	1 (2.9)
IMC histologic grade		
Total cases with invasion	74 (100)	34 (100)
Low	26 (35.1)	16 (47.1)
Intermediate	36 (48.6)	18 (52.9)
High	12 (16.2)	0 (0.0)
DCIS nuclear grade		
Total cases with DCIS	100 (100)	118 (100)
Low	10 (10.0)	16 (13.6)
Low + Intermediate	0 (0.0)	44 (37.3)
Intermediate	41 (41.0)	58 (49.2)
High	49 (49.0)	0 (0.0)
Hormone receptor status *		
ER positive	66/82 (80.5)	33/34 (97.1)
PR positive	52/71 (73.2)	29/34 (85.3)
HER2 positive	16/57 (28.1)	3/34 (8.8)
Recurrence		
No recurrence	162 (87.1)	0 (0.0)
Yes recurrence	13 (7.0)	
Invasive recurrence	10 (76.9)	
Non-invasive recurrence	3 (23.1)	
Unknown	11 (5.9)	
Micro-metastasis	8 (4.3)	0 (0.0)

Table 3.4. Clinicopathologic variables for patients entered into Cohort 1 and 2.

NST, no special type; IMC, invasive mammary carcinoma; DCIS, ductal carcinoma *in situ*; ER, estrogen receptor; PR, progesterone receptor; HER2, human epidermal growth factor receptor 2; *only available for patients with IMC

COHORT 1 (TBX3)
N = 186 patients with early-stage disease
DCIS only (Stage 0) or
DCIS with IMC (Stage 1)

COHORT 2 (TBX3, SLUG, TWIST1)
N = 118 patients with non high-grade DCIS and/or IMC
Non-high grade DCIS (Stage 0) or
Non-high grade DCIS with IMC (Stage 1)

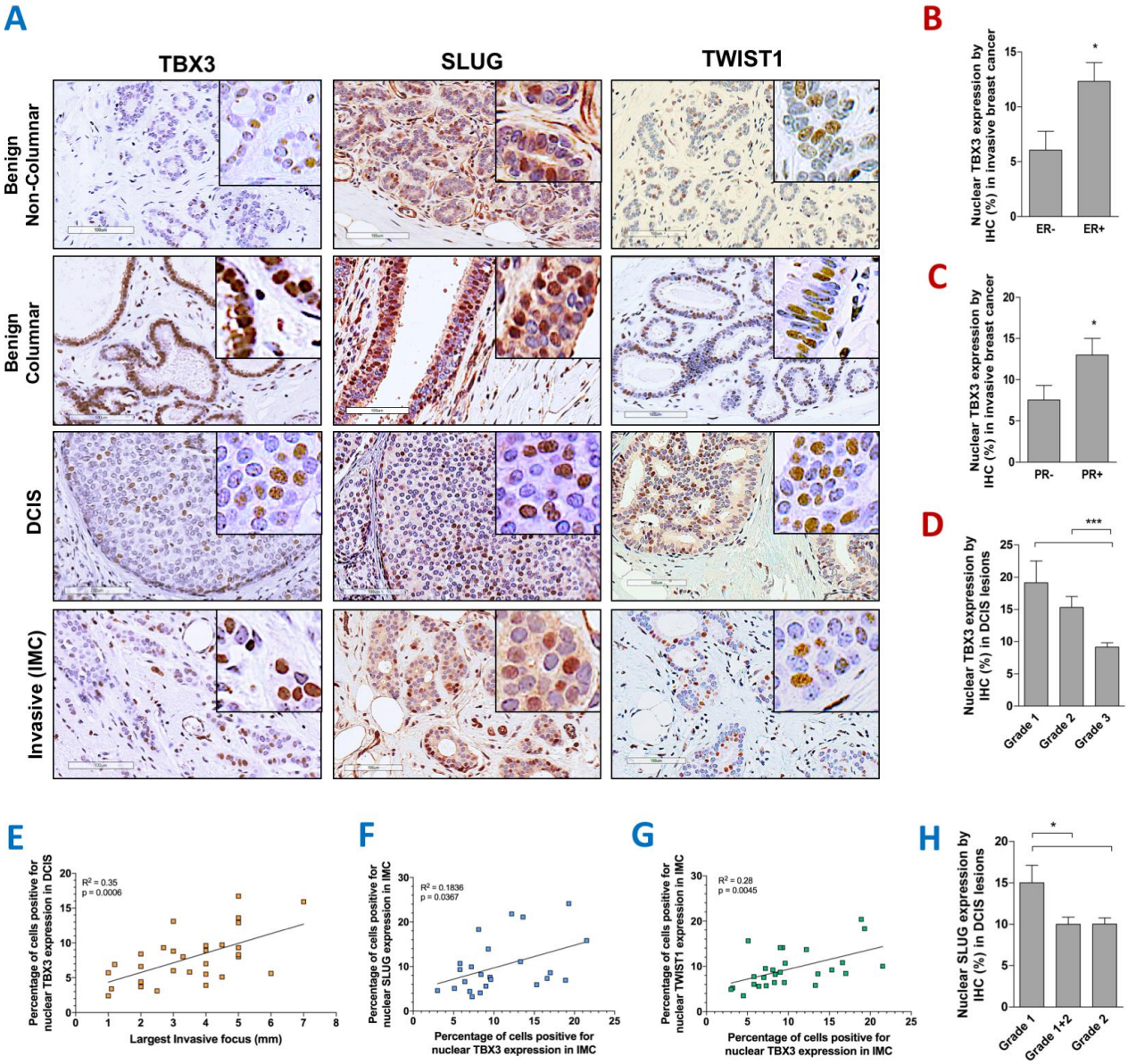

Figure 3.3.4 – TBX3 expression is elevated in low-grade, hormone-receptor positive invasive breast cancers and associated precursor lesions.

Patient samples representing Cohort 1 were immunohistochemically stained and assessed for nuclear TBX3 expression, and Cohort 2 samples were stained and assessed for nuclear TBX3, SLUG and TWIST1 expression. **(A)** Representative expression and staining patterns of Cohort 2 samples (TBX3 expression and staining patterns were similar in Cohort 1; not shown). **(B-D)** Nuclear TBX3 expression was assessed by immunohistochemistry in Cohort 1, consisting of 186 patients with early-stage breast cancer (all nuclear grades) identified from the London Breast Cancer Database on the basis of having either DCIS only (Stage 0), or DCIS with an associated early invasive component (Stage I; ≤2cm, and either pN0 or pN0mi). Nuclear TBX3 expression was compared across ductal epithelial cell types (benign non-columnar, benign columnar, DCIS and invasive mammary carcinoma). The association between TBX3 expression and (B) estrogen receptor (ER), (C) progesterone receptor (PR), and (D) DCIS nuclear grade is shown. **(E-H)** Nuclear TBX3, SLUG and TWIST1 expression was assessed by immunohistochemistry in Cohort 2, consisting of 118 patients with non-high-grade (nuclear grade 1 or 2) DCIS lesions, with or without associated early invasive cancer (Stage 0 or Stage I). Expression levels were compared across ductal epithelial cell types and clinical data. (E) Correlation analysis for nuclear TBX3 expression and size of the invasive focus in patients with Stage I breast cancer. (F-G) Correlation analysis of TBX3/SLUG expression and TBX3/TWIST1 expression in the invasive carcinoma. (H) Association between nuclear SLUG expression and DCIS nuclear grade.

**p<0.05, **p<0.01, ***p<0.001 by one-way ANOVA with Tukey post-hoc for comparison between three groups, and Student's t-test for comparison between two groups. Correlation and p-values were calculated using the Pearson correlation statistic. Error bars represent standard deviation.*

3.3.5 Elevated TBX3 levels are associated with poor prognosis of breast cancer and are highly correlated with SLUG expression.

To assess the applicability of our findings in a broader breast cancer and pan-cancer context we compared our findings with that of available transcriptomic datasets. Using the ICGC US donor cohort, we found that TBX3 mRNA levels are elevated in tumor cells of several cancer subtypes, including breast cancer (data not shown). By further profiling transcriptomic data from the TCGA BRCA and the Farmer Breast study (Farmer et al., 2005), we identified an association of higher TBX3 levels in luminal subtypes of breast cancer, and estrogen receptor (ER) and progesterone receptor (PR) positive cancers (Figure 3.3.5 A-B). Survival analysis of luminal A patients in the TCGA BRCA dataset showed a statistically significant difference in survival ($p<0.001$) between patients with high and low TBX3 expression relative to the median (Figure 3.3.5 C).

Our immunohistochemical biomarker analysis revealed a significant positive correlation between TBX3, SLUG and TWIST1 expression within invasive breast cancer lesions. To further examine the association between TBX3 and our identified downstream targets SLUG and TWIST1 and relate it to histopathological grade, we interrogated transcriptomics datasets with relevant grade information: TCGA BRCA (n=680 with grade information) and Desmedt (n=196, node-negative breast cancers, all with grade information (Desmedt et al., 2007)). TBX3 and SLUG mRNA levels were significantly lower in high-grade breast cancers relative to low and intermediate-grade breast cancers (Figure 3.3.5 D) ($p<0.001$), consistent with our immunohistochemical data. The Desmedt dataset also showed reduced TWIST1 levels in high-grade breast cancers. There was a high degree of overlap between TBX3 and SLUG in terms of patient characteristics and lesion types identified in our immunohistochemical staining and within the transcriptomics datasets. Additionally, upon examination of the TCGA TARGET GTEx dataset, we observed high co-expression of SLUG and TBX3 in 19,120 normal and tumor samples represented, and tight association with MMP14 with high expression of both transcription factors (Figure 3.3.5 E). Collectively, analysis of publicly available data further supports the association and likely involvement of TBX3, along with downstream EMT transcription factors SLUG and TWIST1 in aggressiveness of low-grade breast cancers.

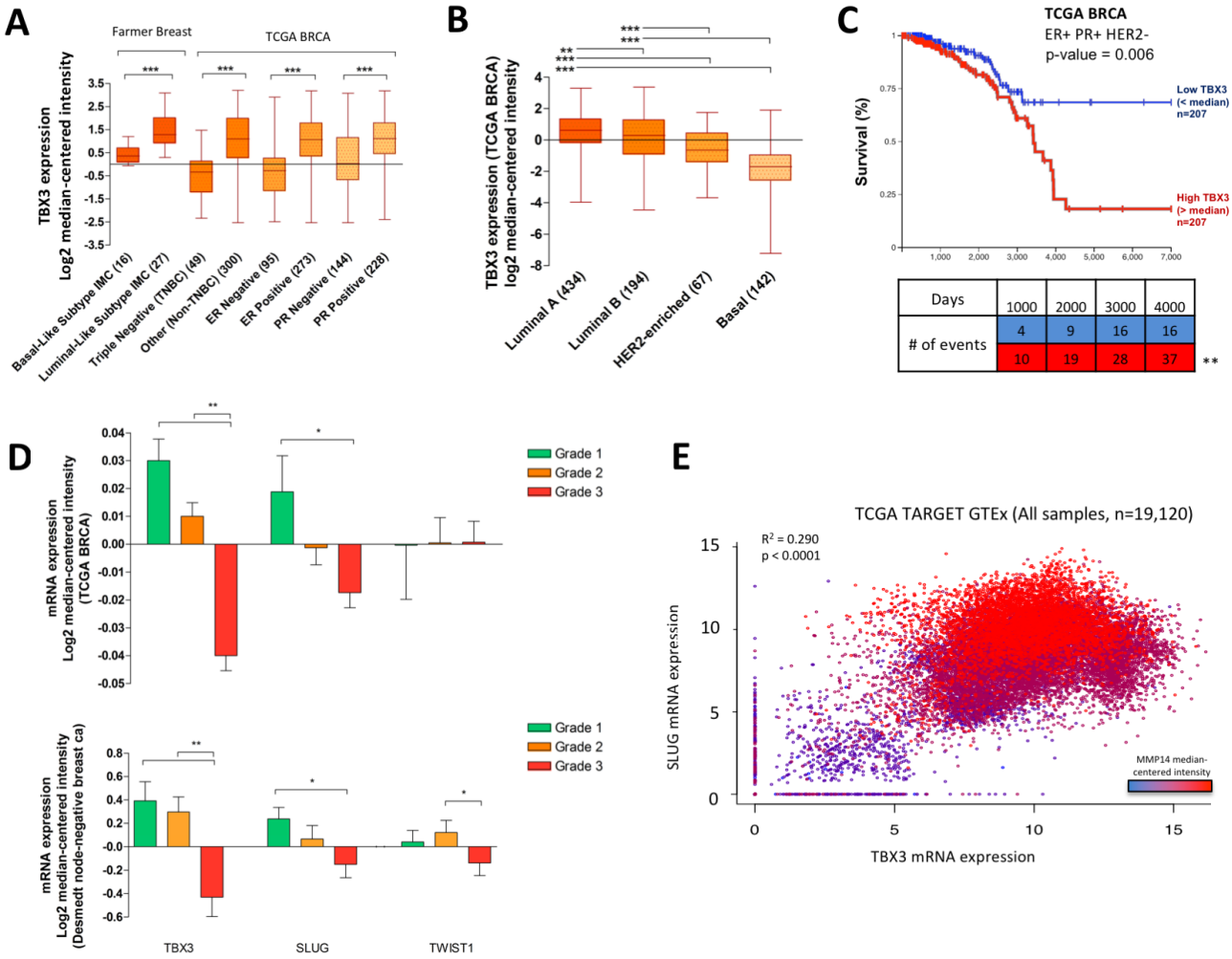
A
Farmer Breast
TCGA BRCA
TBX3 expression
Log2 median-centered intensity
Basal-Like Subtype IMC (16)
Luminal-Like Subtype IMC (27)
Triple Negative (TNBC) (49)
Other (Non-TNBC) (300)
ER Negative (95)
ER Positive (273)
PR Negative (144)
PR Positive (228)
B
TBX3 expression (TCGA BRCA)
log2 median-centered intensity
Luminal A (434)
Luminal B (194)
HER2-enriched (67)
Basal (142)
C
TCGA BRCA
ER+ PR+ HER2-
p-value = 0.006
Survival (%)
Low TBX3
(< median)
n=207
High TBX3
(> median)
n=207
Days
1000
2000
3000
4000
# of events
4
9
16
16
10
19
28
37
D
mRNA expression
Log2 median-centered intensity
(TCGA BRCA)
Grade 1
Grade 2
Grade 3
mRNA expression
Log2 median-centered intensity
(Desmedt node-negative breast ca)
TBX3
SLUG
TWIST1
E
TCGA TARGET GTEx (All samples, n=19,120)
R² = 0.290
p < 0.0001
SLUG mRNA expression
TBX3 mRNA expression
MMP14 median-centered intensity

Figure 3.3.5 – Elevated TBX3 levels are associated with poor prognosis of breast cancer, and are highly correlated with SLUG expression.

(A-B) TBX3 expression was assessed across tumor characteristics in deposited transcriptomics data consisting of the Farmer Breast and TCGA BRCA cohorts. TBX3 mRNA expression by molecular subtype was further investigated in the TCGA BRCA dataset. **(C)** Kaplan Meier survival curves for luminal A patients (ER+ PR+ HER2-) from the TCGA BRCA dataset, separated into high (above median) vs. low (below median) TBX3 expression. Number of events (breast cancer related deaths) are shown in the associated table. **(D)** Expression of TBX3, SLUG and TWIST1 was assessed in the TCGA BRCA and Desmedt datasets to compare expression levels across grades. Data shown represent median-centered, z-score normalized values. **(E)** Correlation of SLUG, TBX3 and MMP14 expression was assessed in the TCGA Target GTEx dataset, consisting of 19,120 normal and tumor patient samples.

**p<0.05, **p<0.01, ***p<0.001 by one-way ANOVA with Tukey post-hoc for comparison between three groups. Survival analysis for Kaplan-Meier curve was calculated using the log-rank test statistic. Correlation and p-values were calculated using the Pearson correlation statistic. Error bars represent standard deviation.*

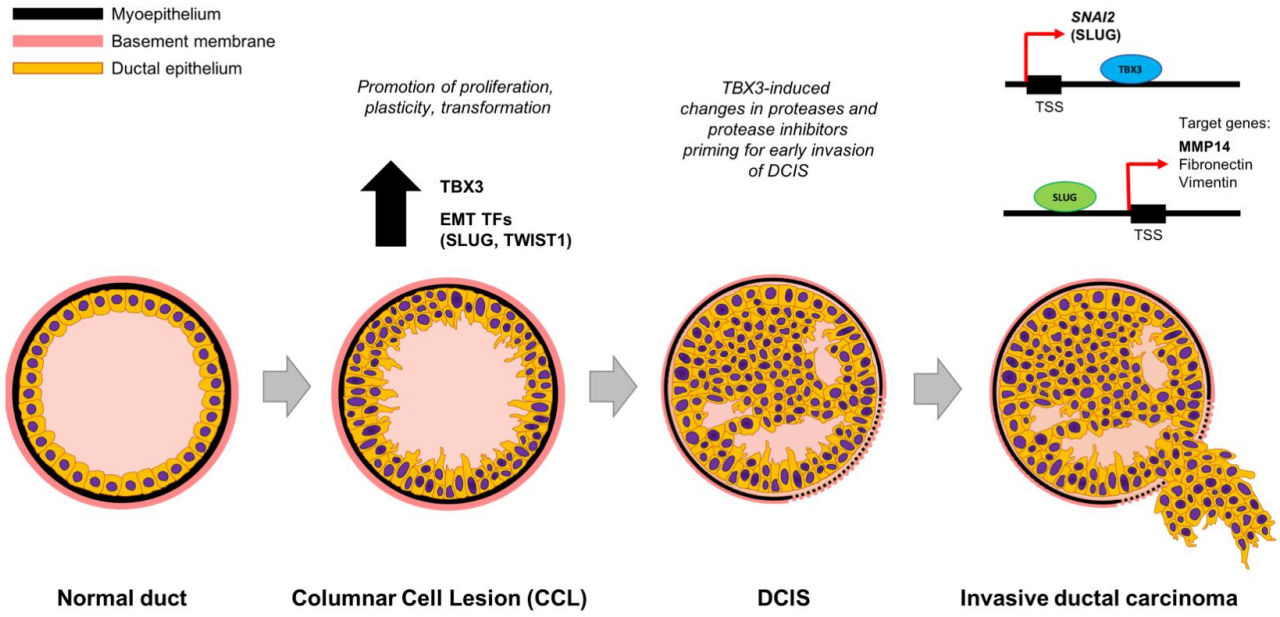

Figure 3.3.6 – TBX3 promotes progression of pre-invasive breast cancer cells by inducing EMT and directly up-regulating SLUG.

Proposed model through which TBX3 promotes progression of pre-invasive ductal carcinoma in situ (DCIS) lesions. TBX3 levels are low in benign non-columnar ductal breast epithelial cells. In columnar cell lesions (CCLs), expression of TBX3 levels are up-regulated, with a concomitant increase in SLUG and TWIST1 expression levels. This is predicted to promote proliferation and plasticity of early, pre-invasive lesions. In a subset of low-grade DCIS, TBX3 expression is particularly high. Overexpression of TBX3 induces altered expression of several proteases and protease inhibitors, leading to degradation of the basement membrane and priming for early invasion of DCIS into adjacent stroma. These events are facilitated by TBX3-induced and SLUG-dependent expression of pro-migratory molecules such as MMP14 (membrane-bound), fibronectin (extracellular matrix), and vimentin (intracellular).

3.4 Discussion

The use of screening mammography over the past four decades has drastically increased our ability to detect DCIS (Kerlikowske, 2010), but has been criticized as causing an over-diagnosis of breast cancer (Miller et al., 2014). Gene expression profiling has allowed for the successful stratification of node-negative invasive breast cancer patients into low-risk and high-risk groups, providing information useful in clinical decision-making for this population (van 't Veer et al., 2002). These techniques have been extended to DCIS with some success (Solin et al., 2013, Bartlett et al., 2014, Rakovitch et al., 2015). Additionally, panels of selected markers, including p16, COX2 and Ki67 have shown some utility in their ability to predict behaviour of DCIS in specific subsets of patients (Kerlikowske et al., 2010). Despite these efforts, there are few validated diagnostic tests or biomarkers to aid in optimization of treatment strategies for women with DCIS, and none that reliably predict risk for invasion, leading to the possibility of both over-treatment and under-treatment of this subpopulation.

We have previously established a role for the transcriptional regulatory protein TBX3 in invasiveness of breast cancer (Krstic et al., 2016). In this current study we further explored the mechanism of this activity, particularly as associated with the phenomenon of EMT. We sought to take a high-resolution approach to identifying downstream targets of TBX3, beginning with identification of transcriptomic changes with TBX3 overexpression and assessment of direct TBX3 binding sites. From these initial genomic studies, we identified SLUG and TWIST1 as potential downstream effectors up-regulated with TBX3 overexpression, and SLUG as a direct downstream mediator of TBX3-induced migration and invasion. Importantly, we have discerned expression differences in these proteins between benign non-columnar ductal epithelial cells, columnar cell lesions (CCLs), DCIS, and within the invasive carcinoma. Our examination of TBX3 expression by immunohistochemistry in two independent patient cohorts revealed that expression is highest in hormone receptor positive, low-grade DCIS (and co-existing columnar cell lesions) and is associated with the extent of invasion in early-stage breast cancers. These findings, coupled with our *in vitro* data of an EMT-link, are consistent with a role for the TBX3 transcription factor in early invasion events, likely working in conjunction with other EMT-related factors such as SLUG and TWIST1, to facilitate a phenotype conducive to invasion.

The prevailing breast cancer progression model supported by numerous genomic and transcriptomic studies includes two divergent molecular pathways of progression – the low-grade (ER+/PR+) and high-grade (ER-/PR-) pathway (Bombonati and Sgroi, 2011). Only a subset of DCIS within each pathway will progress to invasive cancer. Interestingly, sequencing and hierarchical clustering of DCIS and invasive samples has shown that samples do not cluster by diagnosis, but rather by intrinsic molecular subtype (Muggerud et al., 2010). This suggests that factors associated with invasiveness are distinct from histologic grade and stage, and may indeed be present within the pre-invasive DCIS (Muggerud et al., 2010).

Our proposed model of the stage-specific role of TBX3 in early breast cancer progression is depicted in Figure 3.3.6. As observed in our immunohistochemical studies, expression of EMT-related transcription factors (including TBX3) is low in benign non-columnar breast epithelium. We have identified that TBX3 levels are significantly elevated in CCLs. This is in accordance with existing studies examining patterns of gene expression changes through breast cancer progression showing up-regulation of several malignancy-associated genes at the pre-invasive stage (Ma et al., 2003). This pro-EMT phenotype in CCLs, with concomitant up-regulation of SLUG and TWIST1, is predicted to promote proliferation and plasticity of the breast epithelial cells (De Craene and Berx, 2013). There is accumulating evidence that CCLs, and in particular the CCL variant termed ‘flat epithelial atypia’ (FEA), may be non-obligate precursors to the development of breast cancer (Dabbs et al., 2006, Turashvili et al., 2008). Only some columnar cell lesions progress, even though TBX3 and EMT transcription factors SLUG and TWIST1 are expressed in most (at least when observed in association with DCIS). This suggests that there are likely other changes that act in concert to allow for progression to occur.

In our present study, the significant level of enrichment of proteases, protease inhibitors and enzyme modulators in RNA-Seq and ChIP-array datasets of DCIS-like 21NT cells overexpressing TBX3 is consistent with the propensity to break down basement membrane and invade. Previous studies have suggested that the gradual loss of basement membrane, leading to changes in cell organization and polarity (rather than the acquisition of additional mutations) is the main driver in the transition from an in situ to invasive phenotype (Hu et al., 2008). We have confirmed up-regulation of MMP14 and urokinase-type

plasminogen activator (uPA), and down-regulation of CST6 by qRT-PCR and western blot analysis. Consistent with this, uPA and MMP14 overexpression have been shown to be strong and independent predictors of breast cancer survival (Look et al., 2002, Têtu et al., 2006). Furthermore, CST6 has been shown to be down-regulated in breast cancer progression, with promoter hypermethylation documented at the DCIS stage (Ai et al., 2006). We have shown that induction of MMP14 with TBX3 overexpression is a SLUG-dependent process, and this signaling cascade may be important for TBX3-induced migration and invasion. In keeping with this, it has been previously reported that MMP14 is among the main regulators of the basement membrane transmigration process *in vivo* (Hotary et al., 2006), likely due to MMP14 dependent activation of the main type IV collagenase MMP2 (Duffy et al., 2000). Importantly, we have shown increased activity of MMP2 with TBX3 overexpression. Additionally, increased expression of several proteases has been shown to indirectly enhance the activity of EMT transcription factors, leading to a positive feedback loop (De Craene and Berx, 2013), potentially resulting in high expression levels of EMT transcription factors and proteases as we have observed both *in vitro* and in our two patient cohorts.

In conclusion, we propose a unique pathway in which TBX3 promotes progression through advancement of low-grade DCIS to invasive carcinoma (Figure 3.3.6). Our proposed model is particularly relevant in the non-high grade, ER-positive pathway of progression. Overexpression of TBX3 at early pre-invasive stages (CCL, DCIS) of breast cancer progression, inducing other molecular regulators of EMT (including SLUG and TWIST1), acts as an enabler to set the stage for basement membrane breakdown and invasion into adjacent stroma. Further validation of our findings in an independent cohort of Stage 0 and Stage I breast cancer patients and comparison with follow-up data should be conducted in order to assess whether TBX3 expression may provide reliable risk stratification for patients diagnosed with DCIS, possibly in concert with multiple biomarkers such as Ki67, p16, COX2, and/or multi-parameter gene expression assays (Kerlikowske et al., 2010, Bartlett et al., 2014). As T-box proteins such as TBX3 have been shown to have detrimental effects with respect to cancer progression and survival, a thorough understanding of the underlying mechanisms involved is crucial.

3.5 References

Artym, V. V., Yamada, K. M. and Mueller, S. C. (2009) 'ECM degradation assays for analyzing local cell invasion', *Methods Mol Biol,* 522, pp. 211-9.

Band, V., Zajchowski, D., Swisshelm, K., Trask, D., Kulesa, V., Cohen, C., Connolly, J. and Sager, R. (1990) 'Tumor progression in four mammary epithelial cell lines derived from the same patient', *Cancer Res,* 50(22), pp. 7351-7.

Bartlett, J. M., Nofech-Moses, S. and Rakovitch, E. (2014) 'Ductal carcinoma in situ of the breast: can biomarkers improve current management?', *Clin Chem,* 60(1), pp. 60-7.

Bombonati, A. and Sgroi, D. C. (2011) 'The molecular pathology of breast cancer progression', *J Pathol,* 223(2), pp. 307-17.

Burgucu, D., Guney, K., Sahinturk, D., Ozbudak, I. H., Ozel, D., Ozbilim, G. and Yavuzer, U. (2012) 'Tbx3 represses PTEN and is over-expressed in head and neck squamous cell carcinoma', *BMC Cancer,* 12, pp. 481.

Burstein, H. J., Polyak, K., Wong, J. S., Lester, S. C. and Kaelin, C. M. (2004) 'Ductal carcinoma in situ of the breast', *N Engl J Med,* 350(14), pp. 1430-41.

Coll, M., Seidman, J. G. and Müller, C. W. (2002) 'Structure of the DNA-bound T-box domain of human TBX3, a transcription factor responsible for ulnar-mammary syndrome', *Structure,* 10(3), pp. 343-56.

Dabbs, D. J., Carter, G., Fudge, M., Peng, Y., Swalsky, P. and Finkelstein, S. (2006) 'Molecular alterations in columnar cell lesions of the breast', *Mod Pathol,* 19(3), pp. 344-9.

De Craene, B. and Berx, G. (2013) 'Regulatory networks defining EMT during cancer initiation and progression', *Nat Rev Cancer,* 13(2), pp. 97-110.

Desmedt, C., Piette, F., Loi, S., Wang, Y., Lallemand, F., Haibe-Kains, B., Viale, G., Delorenzi, M., Zhang, Y., d'Assignies, M. S., Bergh, J., Lidereau, R., Ellis, P., Harris, A. L., Klijn, J. G., Foekens, J. A., Cardoso, F., Piccart, M. J., Buyse, M., Sotiriou, C. and Consortium, T. (2007) 'Strong time dependence of the 76-gene prognostic signature for node-negative breast cancer patients in the TRANSBIG multicenter independent validation series', *Clin Cancer Res,* 13(11), pp. 3207-14.

Diaz, L. K. and Sneige, N. (2005) 'Estrogen receptor analysis for breast cancer: current issues and keys to increasing testing accuracy', *Adv Anat Pathol,* 12(1), pp. 10-9.

Duffy, M. J., Maguire, T. M., Hill, A., McDermott, E. and O'Higgins, N. (2000) 'Metalloproteinases: role in breast carcinogenesis, invasion and metastasis', *Breast Cancer Res,* 2(4), pp. 252-7.

Fan, W., Huang, X., Chen, C., Gray, J. and Huang, T. (2004) 'TBX3 and its isoform TBX3+2a are functionally distinctive in inhibition of senescence and are overexpressed in a subset of breast cancer cell lines', *Cancer Res,* 64(15), pp. 5132-9.

Farmer, P., Bonnefoi, H., Becette, V., Tubiana-Hulin, M., Fumoleau, P., Larsimont, D., Macgrogan, G., Bergh, J., Cameron, D., Goldstein, D., Duss, S., Nicoulaz, A. L., Brisken, C., Fiche, M., Delorenzi, M. and Iggo, R. (2005) 'Identification of molecular apocrine breast tumours by microarray analysis', *Oncogene,* 24(29), pp. 4660-71.

Fillmore, C. M., Gupta, P. B., Rudnick, J. A., Caballero, S., Keller, P. J., Lander, E. S. and Kuperwasser, C. (2010) 'Estrogen expands breast cancer stem-like cells through paracrine FGF/Tbx3 signaling', *Proc Natl Acad Sci U S A,* 107(50), pp. 21737-42.

Fisher, E. R., Dignam, J., Tan-Chiu, E., Costantino, J., Fisher, B., Paik, S. and Wolmark, N. (1999) 'Pathologic findings from the National Surgical Adjuvant Breast Project (NSABP) eight-year update of Protocol B-17: intraductal carcinoma', *Cancer,* 86(3), pp. 429-38.

Formenti, S. C., Arslan, A. A. and Pike, M. C. (2011) 'Re: Long-term outcomes of invasive ipsilateral breast tumor recurrences after lumpectomy in NSABP B-17 and B-24 randomized clinical trials for DCIS', *J Natl Cancer Inst,* 103(22), pp. 1723.

Hoogaars, W. M., Barnett, P., Rodriguez, M., Clout, D. E., Moorman, A. F., Goding, C. R. and Christoffels, V. M. (2008) 'TBX3 and its splice variant TBX3 + exon 2a are functionally similar', *Pigment Cell Melanoma Res,* 21(3), pp. 379-87.

Hotary, K., Li, X. Y., Allen, E., Stevens, S. L. and Weiss, S. J. (2006) 'A cancer cell metalloprotease triad regulates the basement membrane transmigration program', *Genes Dev,* 20(19), pp. 2673-86.

Hu, M., Yao, J., Carroll, D. K., Weremowicz, S., Chen, H., Carrasco, D., Richardson, A., Violette, S., Nikolskaya, T., Nikolsky, Y., Bauerlein, E. L., Hahn, W. C., Gelman, R. S., Allred, C., Bissell, M. J., Schnitt, S. and Polyak, K. (2008) 'Regulation of in situ to invasive breast carcinoma transition', *Cancer Cell,* 13(5), pp. 394-406.

Kerlikowske, K. (2010) 'Epidemiology of ductal carcinoma in situ', *J Natl Cancer Inst Monogr,* 2010(41), pp. 139-41.

Kerlikowske, K., Molinaro, A. M., Gauthier, M. L., Berman, H. K., Waldman, F., Bennington, J., Sanchez, H., Jimenez, C., Stewart, K., Chew, K., Ljung, B. M. and Tlsty, T. D. (2010) 'Biomarker expression and risk of subsequent tumors after initial ductal carcinoma in situ diagnosis', *J Natl Cancer Inst,* 102(9), pp. 627-37.

Kim, Y., Williams, K. C., Gavin, C. T., Jardine, E., Chambers, A. F. and Leong, H. S. (2016) 'Quantification of cancer cell extravasation in vivo', *Nat Protoc,* 11(5), pp. 937-48.

Krstic, M., Macmillan, C. D., Leong, H. S., Clifford, A. G., Souter, L. H., Dales, D. W., Postenka, C. O., Chambers, A. F. and Tuck, A. B. (2016) 'The transcriptional regulator TBX3 promotes progression from non-invasive to invasive breast cancer', *BMC Cancer,* 16(1), pp. 671.

Lehr, H. A., Jacobs, T. W., Yaziji, H., Schnitt, S. J. and Gown, A. M. (2001) 'Quantitative evaluation of HER-2/neu status in breast cancer by fluorescence in situ hybridization and by immunohistochemistry with image analysis', *Am J Clin Pathol,* 115(6), pp. 814-22.

Lingbeek, M. E., Jacobs, J. J. and van Lohuizen, M. (2002) 'The T-box repressors TBX2 and TBX3 specifically regulate the tumor suppressor gene p14ARF via a variant T-site in the initiator', *J Biol Chem,* 277(29), pp. 26120-7.

Lomnytska, M., Dubrovska, A., Hellman, U., Volodko, N. and Souchelnytskyi, S. (2006) 'Increased expression of cSHMT, Tbx3 and utrophin in plasma of ovarian and breast cancer patients', *Int J Cancer,* 118(2), pp. 412-21.

Ma, X. J., Salunga, R., Tuggle, J. T., Gaudet, J., Enright, E., McQuary, P., Payette, T., Pistone, M., Stecker, K., Zhang, B. M., Zhou, Y. X., Varnholt, H., Smith, B., Gadd, M., Chatfield, E., Kessler, J., Baer, T. M., Erlander, M. G. and Sgroi, D. C. (2003) 'Gene expression profiles of human breast cancer progression', *Proc Natl Acad Sci U S A,* 100(10), pp. 5974-9.

Miller, A. B., Wall, C., Baines, C. J., Sun, P., To, T. and Narod, S. A. (2014) 'Twenty five year follow-up for breast cancer incidence and mortality of the Canadian National Breast Screening Study: randomised screening trial', *BMJ,* 348, pp. g366.

Mokbel, K. and Cutuli, B. (2006) 'Heterogeneity of ductal carcinoma in situ and its effects on management', *Lancet Oncol,* 7(9), pp. 756-65.

Muggerud, A. A., Hallett, M., Johnsen, H., Kleivi, K., Zhou, W., Tahmasebpoor, S., Amini, R. M., Botling, J., Borresen-Dale, A. L., Sorlie, T. and Warnberg, F. (2010) 'Molecular diversity in ductal carcinoma in situ (DCIS) and early invasive breast cancer', *Mol Oncol,* 4(4), pp. 357-68.

Peres, J. and Prince, S. (2013) 'The T-box transcription factor, TBX3, is sufficient to promote melanoma formation and invasion', *Mol Cancer,* 12(1), pp. 117.

Phillips, S. and Kuperwasser, C. (2014) 'SLUG: Critical regulator of epithelial cell identity in breast development and cancer', *Cell Adh Migr,* 8(6), pp. 578-87.

Rakovitch, E., Nofech-Mozes, S., Hanna, W., Baehner, F. L., Saskin, R., Butler, S. M., Tuck, A., Sengupta, S., Elavathil, L., Jani, P. A., Bonin, M., Chang, M. C., Robertson, S. J., Slodkowska, E., Fong, C., Anderson, J. M., Jamshidian, F., Miller, D. P., Cherbavaz, D. B., Shak, S. and Paszat, L. (2015) 'A population-based validation study of the DCIS Score predicting recurrence risk in individuals treated by breast-conserving surgery alone', *Breast Cancer Res Treat,* 152(2), pp. 389-98.

Rodriguez, M., Aladowicz, E., Lanfrancone, L. and Goding, C. R. (2008) 'Tbx3 represses E-cadherin expression and enhances melanoma invasiveness', *Cancer Res,* 68(19), pp. 7872-81.

Sagara, Y., Mallory, M. A., Wong, S., Aydogan, F., DeSantis, S., Barry, W. T. and Golshan, M. (2015) 'Survival Benefit of Breast Surgery for Low-Grade Ductal Carcinoma In Situ: A Population-Based Cohort Study', *JAMA Surg,* 150(8), pp. 739-45.

Savagner, P., Yamada, K. M. and Thiery, J. P. (1997) 'The zinc-finger protein slug causes desmosome dissociation, an initial and necessary step for growth factor-induced epithelial-mesenchymal transition', *J Cell Biol,* 137(6), pp. 1403-19.

Shan, Z. Z., Yan, X. B., Yan, L. L., Tian, Y., Meng, Q. C., Qiu, W. W., Zhang, Z. and Jin, Z. M. (2015) 'Overexpression of Tbx3 is correlated with Epithelial-Mesenchymal Transition phenotype and predicts poor prognosis of colorectal cancer', *Am J Cancer Res,* 5(1), pp. 344-53.

Solin, L. J., Gray, R., Baehner, F. L., Butler, S. M., Hughes, L. L., Yoshizawa, C., Cherbavaz, D. B., Shak, S., Page, D. L., Sledge, G. W., Jr., Davidson, N. E., Ingle, J. N., Perez, E. A., Wood, W. C., Sparano, J. A. and Badve, S. (2013) 'A multigene expression assay to predict local recurrence risk for ductal carcinoma in situ of the breast', *J Natl Cancer Inst,* 105(10), pp. 701-10.

Souter, L. H., Andrews, J. D., Zhang, G., Cook, A. C., Postenka, C. O., Al-Katib, W., Leong, H. S., Rodenhiser, D. I., Chambers, A. F. and Tuck, A. B. (2010) 'Human 21T breast epithelial cell lines mimic breast cancer progression in vivo and in vitro and show stage-specific gene expression patterns', *Lab Invest,* 90(8), pp. 1247-58.

Thorat, M. A., Parmar, V., Nadkarni, M. S. and Badwe, R. A. (2007) 'Radiation therapy for ductal carcinoma in situ: is it really worth it?', *J Clin Oncol,* 25(4), pp. 461-2; author reply 462.

Turashvili, G., Hayes, M., Gilks, B., Watson, P. and Aparicio, S. (2008) 'Are columnar cell lesions the earliest histologically detectable non-obligate precursor of breast cancer?', *Virchows Arch,* 452(6), pp. 589-98.

van 't Veer, L. J., Dai, H., van de Vijver, M. J., He, Y. D., Hart, A. A., Mao, M., Peterse, H. L., van der Kooy, K., Marton, M. J., Witteveen, A. T., Schreiber, G. J., Kerkhoven, R. M., Roberts, C., Linsley, P. S.,

Bernards, R. and Friend, S. H. (2002) 'Gene expression profiling predicts clinical outcome of breast cancer', *Nature,* 415(6871), pp. 530-6.

Wang, H. C., Meng, Q. C., Shan, Z. Z., Yuan, Z. and Huang, X. Y. (2015) 'Overexpression of Tbx3 predicts poor prognosis of patients with resectable pancreatic carcinoma', *Asian Pac J Cancer Prev,* 16(4), pp. 1397-401.

Willmer, T., Cooper, A., Peres, J., Omar, R. and Prince, S. (2017) 'The T-Box transcription factor 3 in development and cancer', *Biosci Trends,* 11(3), pp. 254-266.

Yarosh, W., Barrientos, T., Esmailpour, T., Lin, L., Carpenter, P. M., Osann, K., Anton-Culver, H. and Huang, T. (2008) 'TBX3 is overexpressed in breast cancer and represses p14 ARF by interacting with histone deacetylases', *Cancer Res,* 68(3), pp. 693-9.

Zhao, M., Kong, L., Liu, Y. and Qu, H. (2015) 'dbEMT: an epithelial-mesenchymal transition associated gene resource', *Sci Rep,* 5, pp. 11459.

Chapter 4

Isoform-specific promotion of breast cancer tumorigenicity by TBX3 involves induction of angiogenesis

4 Isoform-specific promotion of breast cancer tumorigenicity by TBX3 involves induction of angiogenesis

SUMMARY OF FINDINGS

TBX3 is a member of the highly conserved family of T-box transcription factors involved in embryogenesis, organogenesis and tumor progression. While the functional role of TBX3 in tumorigenesis has been widely studied, less is known about the specific functions of the different TBX3 isoforms. Through alternative splicing and exon skipping events, TBX3 encodes two isoforms – TBX3iso1 and TBX3iso2. TBX3iso2 contains an additional 20 amino acid sequence inserted into the DNA binding domain which TBX3iso1 lacks. We report, for the first time, that TBX3 isoforms have differential tumorigenic potential in nude mouse xenograft experiments when transfected into non-tumorigenic DCIS-like 21NT cells, with overexpression of TBX3iso1 more commonly associated with invasive carcinoma. Histologic examination showed high vascularity of tumors that arise from TBX3iso1 overexpressing cells. Through transcriptomic analysis of signaling pathways altered with TBX3iso1 and TBX3iso2 overexpression, we reveal that there are significant differences in angiogenesis-related genes. Importantly, osteopontin (OPN), a cancer-associated secreted phosphoprotein, was shown to be significantly up-regulated with TBX3iso1 overexpression. This pattern was observed across three non/weakly-tumorigenic breast cancer cell lines (21PT, 21NT, MCF7). Up-regulation of OPN in TBX3iso1 overexpressing cells resulted in induction of hyaluronan synthase 2 (HAS2) expression and increased retention of hyaluronan in pericellular matrices. The described changes involving TBX3iso1-dependent promotion of angiogenesis may explain the differences in tumor formation rates between TBX3 isoforms *in vivo*. Within the TCGA breast cancer cohort, there was an 8.1-fold higher TBX3iso1/TBX3iso2 ratio in tumors relative to control, and this ratio was positively associated with tumor grade. This shift of an increased TBX3iso1/TBX3iso2 ratio in tumors relative to control tissue is observed across several TCGA tumor subtypes that overexpress TBX3.

4.1 Introduction

TBX3 is a member of the highly conserved family of T-box transcription factors involved in embryogenesis and organogenesis. Germline mutations or haploinsufficiency of TBX3 results in ulnar-mammary syndrome (UMS, OMIM 181450), characterized by mammary gland hypoplasia, apocrine gland, dental, and genital defects, emphasizing its broad expression profile (Bamshad et al., 1999, Bamshad et al., 1997). TBX3 levels are up-regulated in several cancer types, including breast (Fan et al., 2004, Lomnytska et al., 2006, Yarosh et al., 2008, Souter et al., 2010), melanoma (Rodriguez et al., 2008), colorectal (Shan et al., 2015), pancreatic (Cavard et al., 2009), cervical (Lyng et al., 2006), ovarian (Lomnytska et al., 2006), gastric (Miao et al., 2016), and prostate cancers (Gudmundsson et al., 2010), suggesting its potential role as an oncogenic driver in multiple cancer types.

TBX3 is alternatively spliced, leading to two predominant isoforms: TBX3iso1 and TBX3iso2. TBX3iso2 contains a unique 20 amino acid sequence inserted into the DNA binding domain attributed to the 2a exon. Addition of the 2a exon within TBX3iso2 shifts residues critical for TBX3 interaction with DNA (particularly Ser224 and Met225) (Coll et al., 2002), however, the effect on transcriptional regulation and its functional relevance remains unclear.

TBX3 isoform ratios have been found to be tissue and species specific (Fan et al., 2004), with differing relative levels of TBX3iso1/TBX3iso2 reported in several breast cancer cell lines (Bamshad et al., 1999, Fan et al., 2004). Additionally, the T-box binding domain which differs between the two TBX3 isoforms has been shown to be important for protein-protein interactions, facilitating interactions with core histones and chromatin-interacting proteins such as methyltransferases (Demay et al., 2007, DeBenedittis and Jiao, 2011, Miller et al., 2008).

Conflicting results have been published regarding functionality of the TBX3 isoforms. Fan et al. reported that the 20-amino acid addition in TBX3iso2 hinders its binding to a previously identified T-box element (TBE) through *in vitro* oligonucleotide binding assays, suggesting that the protein's DNA binding is altered (Fan et al., 2004). In a study by Hoogaars et al., both TBX3 isoforms were able to bind to the TBE in the Nppa and $p21^{CIP1}$ promoters, suggesting that they have similar functions *in vitro* (Hoogaars et al., 2008). Due to the growing amount of literature implicating TBX3 in the promotion of tumorigenesis in several cancer

types (Fan et al., 2004, Lomnytska et al., 2006, Yarosh et al., 2008, Souter et al., 2010, Rodriguez et al., 2008, Cavard et al., 2009, Lyng et al., 2006, Gudmundsson et al., 2010, Krstic et al., 2016), it is essential to address the functional relevance of TBX3 isoforms and their altered expression in cancer.

In this study, we provide evidence for differential tumorigenicity of TBX3 isoforms through *in vivo* nude mouse xenograft experiments. Importantly, by conducting high throughput RNA sequencing, we have shown that TBX3iso1-induced tumorigenicity is associated with selective up-regulation of angiogenesis-promoting genes, including osteopontin (OPN), and subsequent induction of hyaluronan synthase 2 (HAS2) expression. This is accompanied by induction of endothelial cell tubule formation by conditioned media from TBX3iso1 overexpressing cells *in vitro*. Increased expression of OPN has been associated with advanced tumor stage and poor prognosis of breast cancer (Rudland et al., 2002, Tuck et al., 1998), and both OPN and hyaluronan promote the process of angiogenesis (Chakraborty et al., 2008, Chakraborty et al., 2006, Takahashi et al., 2002, Cook et al., 2005, Hirama et al., 2003, Takano et al., 2000, Shijubo et al., 1999, Asou et al., 2001, Pröls et al., 1998, Koyama et al., 2007, Rooney et al., 1995). Lastly, we utilized the TCGA breast cancer dataset to determine differential expression of TBX3 isoforms. We found an 8.1-fold higher TBX3iso1/TBX3iso2 ratio in tumor tissues relative to control. This pattern of an increased TBX3iso1/TBX3iso2 ratio for tumor tissues relative to control was observed across several different tumor types which overexpress TBX3. This study is the first of its kind to report significant functional differences between the two TBX3 isoforms, both *in vivo* and *in vitro*.

4.2 **Methods**

Cell lines and culture conditions

The 21T series cell lines (21PT, 21NT) were obtained as a gift from Dr. Vimla Band (Dana Farber Cancer Institute) (Band et al., 1990). The 21PT and 21NT cell lines and transfectants underwent cell line authentication by Idexx Radil (Case No. 20250-2013). The 21PT and 21NT cell lines were maintained in αMEM media supplemented with 2mM L-glutamine, 1µg/mL insulin, 12.5ng/mL EGF, 2.8µM hydrocortisone, 10mM HEPES, 1mM sodium pyruvate, 0.1mM non-essential amino acids, 50µg/mL gentamycin sulfate, and 10% FBS. MCF7 cells were maintained in DMEM media supplemented with 10% FBS. Stable 21PT, 21NT and MCF7 transfectants were maintained in their respective media supplemented with 500µg/mL G418 as a selection marker. All reagents for culture of breast cancer cell lines were obtained from Wisent Inc. Human neonatal dermal microvascular endothelial cells (HDMECs) were obtained from Lonza (CC2516; Walkersville, MD). Cells were expanded in Endothelial Basal Media-2 (EBM-2; Lonza, 00190860) supplemented with 20% FBS and SingleQuots (Lonza, CC-4176) growth factors. The minimum density for sub-culturing was maintained at 2500 cells/cm^2. Only HDMECs under passage 10 were used for experiments.

Generation of stable transfectant cell lines

Stable transfectants were generated using plasmid constructs previously described (Krstic et al., 2016), consisting of either an empty vector (EV), TBX3iso1, or TBX3iso2 construct within a pcDNA3.1 vector (Invitrogen, V79020). Briefly, cells (21PT, 21NT, MCF7) were seeded into 6-well plates at 350,000 cells per well. The following day, cells were transfected using the Lipofectamine 3000 Transfection Kit (Invitrogen, L3000; 3µg of plasmid DNA per well) as per the manufacturer's protocol. Selection was performed using the aforementioned media for each cell line, further supplemented with 500µg/mL G418. Resistant clones were pooled, expanded, and frozen for later use.

RNA isolation and qRT-PCR

RNA was isolated using the RNeasy Mini Kit (Qiagen, 74104) and converted into cDNA using the qScript cDNA SuperMix (Quanta Biosciences, 84034). The RT^2 SYBR Green ROX qPCR Mastermix (Qiagen, 330521) was utilized for quantitative PCR with the primer sequences

listed in Table 4.1. The output values were normalized to GAPDH expression and are shown as fold changes relative to the empty vector control.

Table 4.1 – Primer sequences utilized for qRT-PCR in mRNA studies.

mRNA Probe	Primer Sequences (Forward and Reverse, 5' to 3')
Total TBX3	F: CGCTGTGACTGCATACCAGA R: GTGTCCCGGAAACCTTTTGC
TBX3iso1	F: AGTGGATGTCCAAAGTCGTCAC R: CATGGAGTTCAATATAGTAAATCCATGTTTGTCTG
TBX3iso2	F: AGTGGATGTCCAAAGTCGTCAC R: CACTTGGGAAGGCCAAAGTAAATCCATG
GAPDH	F: AGGCTGGGGCTCATTTGAAG R: CCATCCACAGTCTTCTGGGTG
COX1	F: CGCCAGTGAATCCCTGTTGT R: GTCACACTGGTAGCGGTCAA
HAS2	F: GTTGGGGGAGATGTCCAGATTT R: CGGTTCGTGAGATGCCTGT
IL1RN	F: AGCAAGATGCAAGCCTTCAG R: CCTTGCAAGTATCCAGCAACTA
OPN	F: TTGCAGTGATTTGCTTTTGC R: TCAATGGAGTCCTGGCTGTC
VEGFR2	F: CCCAGATGACAACCAGACGG R: GCCTTCAGATGCCACAGACT

Nude mouse xenografts

Cells were grown to confluence on 150mm tissue culture dishes. Cells were harvested, washed twice with ice cold PBS, and resuspended in serum-free αHE media. The cell suspension (100µL containing $1.0x10^7$ cells) was injected into the second thoracic mammary fat pad of 8 to 9 week old female nude mice at 10 mice per group. Mice were monitored regularly for tumor growth up to 1 year post-injection and euthanized either when tumors reached a volume of 2,500mm^3 or one year post-injection, whichever occurred first. The primary tumor and/or mammary fat pad, brain, liver, spleen, kidneys, lungs, along with left and right axillary, brachial, and inguinal lymph nodes were collected. All tissues were formalin-fixed, paraffin-embedded, sectioned and H&E stained. Tissues were examined by an anatomic pathologist, and where indicated, sections were stained using anti-human mitochondrial antibody to confirm metastasis of xenograft cells. Animal care and surgical

procedures were conducted in accordance with the recommendations of the Canadian Council on Animal Care, under a protocol approved by Western University's Council on Animal Care.

Immunohistochemistry of mouse xenograft tissues

Formalin-fixed, paraffin embedded tissues were sectioned at 4.0µm thickness onto charged glass slides. Sections were de-paraffinized and rehydrated. Antigen retrieval was conducted with 10mM citrate buffer (pH 6.0) for 20 minutes, maintaining sub-boiling conditions. The UltraVision LP Detection System (Thermo Fischer Scientific, TL-015-HD) was used as per the manufacturer's protocol. Suspect tissues and lymph nodes were stained using an anti-human mitochondrial antibody (Thermo Fischer Scientific, MS-1372-P0; 1/100 for 20 minutes at room temperature) to confirm metastases. The degree of angiogenesis was assessed across primary tumors using an anti-mouse CD31 antibody (BD Pharmingen, 550274; 1/50 at 4ºC overnight). OPN expression was assessed across primary tumors using an anti-human OPN antibody (AssayDesigns mAb53, 905-629; 1/750 for 90 minutes at room temperature). Signal for all stains was developed using DAB, and slides were counter-stained in Harris's Hematoxylin. Expression of human mitochondria was classified as either positive or negative. For quantification of CD31 expression by immunohistochemistry, images of 10 non-overlapping areas exhibiting high vessel density were acquired using the Olympus IX70 inverted microscope at 10X objective, and the number of vessels per high power field was assessed using ImageJ. For quantification of OPN expression by immunohistochemistry, images of 10 random, non-overlapping areas were acquired using the Olympus IX70 inverted microscope at 10X objective across. Images were imported to ImageJ, and colour deconvolution using the H DAB setting was conducted. DAB images representing positive OPN signal were kept, thresholded, and the percentage of positive signal within the image area was quantified.

***In vitro* endothelial tubule formation assay**

In vitro endothelial tubule formation assays were conducted as previously described (Arnaoutova and Kleinman, 2010). Briefly, human neonatal dermal microvascular endothelial cells (HDMECs) were grown to 80% confluency. Growth factor reduced Matrigel (Thermo Fischer Scientific, CB356239) was added to 96 well plates (50µL/well). HDMECs were

trypsinized, washed twice with PBS, and re-suspended at 200,000 cells/mL in media (1:1 mixture of conditioned media and basal EBM-2 media with 20% FBS and no SingleQuots growth factors). Conditioned media was prepared by seeding $1.0x10^6$ cells into T75 flasks, and cells were maintained in low serum media (αMEM with 0.1% FBS) for 48 hours. The endothelial cells suspended in conditioned media were added to the 96 well plate on top of the Matrigel (100µL, 20,000 cells per well) and incubated at 37ºC for 16 hours. For all studies, tubule formation was observed after 16 hours and phase contrast images were taken of 3 non-overlapping fields of view per well using the Olympus IX70 inverted microscope at 10X objective. The number of endothelial cell tubules formed per well were counted using ImageJ (represented as branch points per 3 high power fields). All experiments were done with HDMECs under 10 passages.

Analysis of secreted OPN by ELISA

Cells were seeded at a density of $1.0x10^6$ into T75 flasks (with 10mL media) and grown in serum-free αMEM media (with the aforementioned supplements) for 48 hours. Conditioned media (100µL) were subject to ELISA using a Dual Mono ELISA kit (Enzo Life Sciences, ADI-900-142) following the manufacturer's instructions. Human recombinant OPN provided within the kit was used to create a standard curve. OPN levels were normalized to equal amounts of cells.

Particle exclusion assay

Particle exclusion assays were conducted to visualize pericellular matrices, as previously described (Cook et al., 2006). Briefly, $1.5x10^4$ cells were plated in 6-well plates in triplicate and allowed to adhere overnight. The following day, cells were pre-treated in the presence or absence of hyaluronidase (Sigma, H1136) (16 units/mL in αHE media with 0.1% BSA) for 20 minutes at 37ºC. The media was then removed, and fixed sheep erythrocytes (Innovative Research, IC100-0210) were added in PBS with 0.1% BSA and allowed to settle for 10 minutes. Plates were imaged using the phase contrast setting on an Olympus IX70 inverted microscope at 10X objective. Pericellular matrices appeared as halos surrounding cell surfaces from which fixed red blood cells were excluded. In order to quantify matrix production, a ratio of the pericellular matrix area over the cell area was calculated by tracing

around the cell coats (matrices) and cell areas of 30 randomly selected cells using ImageJ. A ratio of 1.0 indicated the absence of a pericellular matrix for a particular cell.

Bioinformatics analyses

RNA-Seq data from 21NT+EV, 21NT+TBX3iso1 and 21NT+TBX3iso2 cell lines was analyzed in order to examine differences in resultant transcriptional profiles with overexpression of TBX3iso1 and TBX3iso2. Enrichment analysis (Enrichr; Icahn School of Medicine, Mount Sinai) was conducted for cells overexpressing either TBX3iso1 or TBX3iso2 relative to the empty vector control, focusing on genes altered >1.5 fold up or down for only one isoform, or >1.5 fold in opposite directions for both isoforms, and all with corrected FDR<0.05 (http://amp.pharm.mssm.edu/Enrichr/). Results from WikiPathways analysis are reported.

An angiogenesis gene signature consisting of 222 genes was compiled by integration of genes with the Ingenuity Pathway Analysis (IPA; Qiagen) gene ontology term ‘angiogenesis of tumor’, along with the angiogenesis gene lists from the databases in Table 2 (top datasets, white).

The ICGC (US donors) data was exported using XenaBrowser (University of California, Santa Cruz; https://xenabrowser.net/datapages/), and TBX3 mRNA expression was assessed across all cancer subtypes. Transcript levels of TBX3 isoforms were acquired from the TCGA portal, and examined in the breast cancer (BRCA) dataset. A ratio of total transcript reads for TBX3iso1 (uc001tvu) over total transcript reads for TBX3iso2 (uc001tvt) was compared against clinical data and tumor characteristics. Grade information for patients within the TCGA BRCA was obtained from Budczies et al. (Budczies et al., 2015). The TCGA and GTEx datasets were compared simultaneously through the use of the ‘transcripts’ function in XenaBrowser. The aforementioned datasets are listed in Table 4.2 (bottom datasets, black).

Table 4.2 – Publicly-available datasets utilized for analysis.

Project	Dataset	REFERENCE (or *LINK)*
	MsigDB (Broad Institute)	*http://software.broadinstitute.org/gsea/index.jsp*
	PubAngioGen (East China Normal University)	http://www.megabionet.org/aspd Li et al, 2015 (Li et al., 2015)
	AngioDB (Pusan National University)	Sohn et al, 2002 (Sohn et al., 2002)
	dbANGIO (Memorial University of Newfoundland)	*http://www.med.mun.ca/angio/* Savas et al, 2012 (Savas, 2012)
	ICGC (US Donors)	*https://xenabrowser.net/datapages/*
	TCGA breast cancer (BRCA)	*https://portal.gdc.cancer.gov/projects/TCGA-BRCA*
	TCGA BRCA grade information	Budczies et al, 2015 (Budczies et al., 2015)
	GTEx (Genotype Tissue Expression)	*https://xenabrowser.net/transcripts/*

Statistical Analysis

Statistical analyses were conducted using GraphPad Prism 5. One-way ANOVA with Tukey post-hoc tests were conducted for the majority of analyses unless otherwise specified. Error bars are representative of standard deviation measurements. P-values less than 0.05 were considered statistically significant.

4.3 **Results**

4.3.1 TBX3iso1 possesses enhanced tumorigenic potential in nude mice.

In order to examine tumorigenicity of TBX3 isoforms, we overexpressed either TBX3iso1 or TBX3iso2 in non-tumorigenic, DCIS-like 21NT breast cancer cell lines (Figure 4.3.1 A). Cells were injected into the mammary fat pad of nude mice. Mice were monitored for up to a year, or until primary tumors reached a volume of 2,500 mm^3, whichever occurred first. A majority (6/10) of mice injected with cells overexpressing TBX3iso1 developed invasive carcinoma and reached the end-point tumor volume, a significantly higher rate than mice injected with cells overexpressing TBX3iso2 (1/9; $p<0.05$ relative to TBX3iso1) or the empty vector control (0/10; $p<0.01$ relative to TBX3iso1) (Figure 4.3.1 B-D). Additionally, the TBX3iso1 tumors exhibited a shorter lag period of *in vivo* growth, all forming before the TBX3iso2 tumor (Figure 4.3.1 C). All primary tumors (or mammary fat pad injection site) were assessed histologically by an anatomical pathologist, and the presence of precursor lesions (atypical ductal hyperplasia, ADH; ductal carcinoma *in situ*, DCIS) was documented (Figure 4.3.1 D). Representative images of histological lesions observed are shown in Figure 1E, representing DCIS, invasive mammary carcinoma (IMC) invading into skeletal muscle, and a metastatic lesion within the brachial lymph node (Figure 4.3.1 E). All collected organs were assessed for metastases, and suspect tissues were stained using anti-human mitochondrial antibody for confirmation (Figure 4.3.1 E, bottom right panel). One of the mice in the TBX3iso2 group developed lymphoma and was removed from the study.

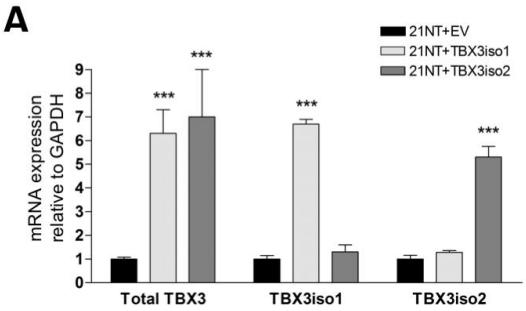

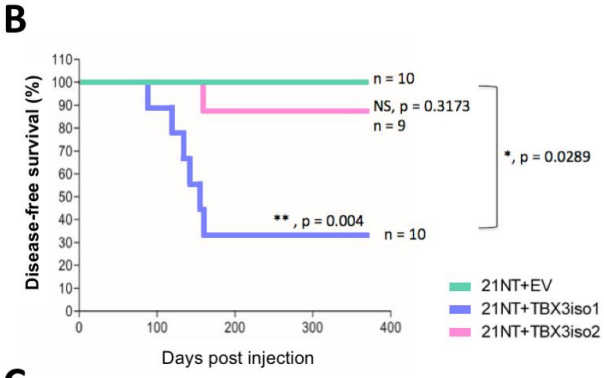

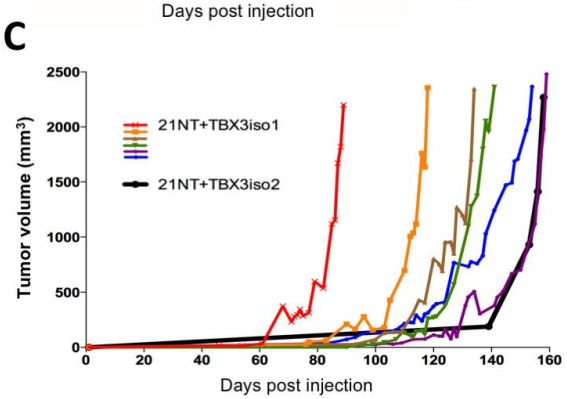

D

	ADH	DCIS	IMC	Metastasis
21NT+EV	1/10	0/10	0/10	0/10
21NT+TBX3iso1	1/10	1/10	6/10	1/10
21NT+TBX3iso2	0/9	1/9	1/9	0/9

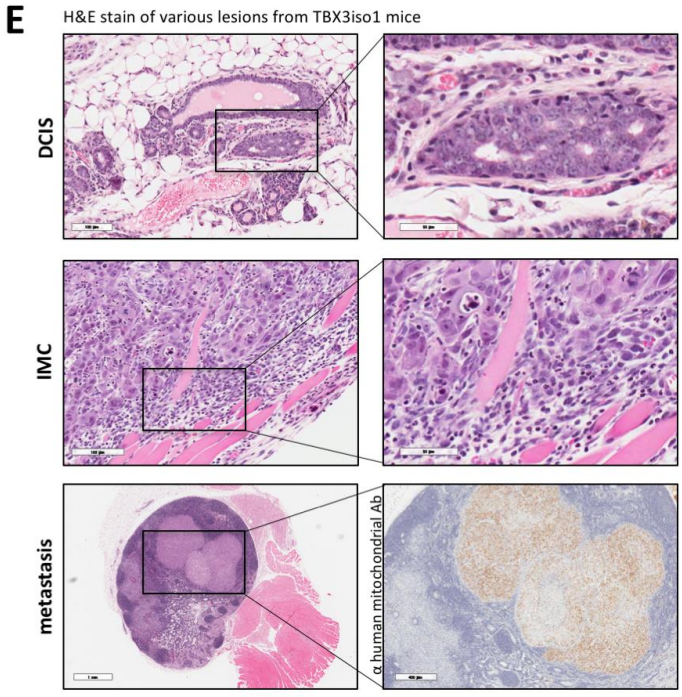

Figure 4.3.1 – TBX3iso1 possess enhanced tumorigenic potential in nude mice.

(A) Total TBX3, TBX3iso1 and TBX3iso2 expression was assessed by qRT-PCR, normalized to GAPDH expression levels, and depicted as fold change relative to the empty vector control. **(B)** Cells ($1x10^7$) were injected into the mammary fat pad of nude mice. Mice were sacrificed when the tumor volume reached 2,500mm^3, or one-year post injection, whichever occurred first. The Kaplan-Meier plot shows disease-free survival over 365 days post-injection. An event was defined as tumor volume reaching the 2,500mm^3 end-point. **(C)** Tumor volume showing growth kinetics over time. TBX3iso1 tumors are shown in different colours, while the TBX3iso2 tumor is shown in black. **(D)** Histological analysis of H&E stained slides was conducted by an anatomical pathologist for all mammary fat pads and primary tumors. Cases with atypical ductal hyperplasia (ADH), ductal carcinoma *in situ* (DCIS), invasive mammary carcinoma (IMC) and metastasis were documented. All tissues and lymph nodes collected were examined for metastases in mice with IMC. Metastases were confirmed through positive immunohistochemical staining for anti-human mitochondria. **(E)** Representative images of cases of DCIS, IMC showing invasion into skeletal muscle, and metastasis into right brachial lymph node. Suspect metastases from H&E slides were confirmed through immunohistochemistry with anti-human mitochondrial antibody.

**p<0.05, **p<0.01, ***p<0.001 by one way ANOVA with Tukey post-hoc for comparison between three groups. Survival analysis for Kaplan-Meier curve was calculated using the log-rank test statistic. Error bars represent standard deviation.*

4.3.2 TBX3iso1 promotes angiogenesis *in vivo* and *in vitro*.

Differential tumorigenicity between TBX3 isoform transfectants was a striking and novel finding. We re-examined our previous RNA-Seq dataset of 21NT transfectant cell lines (21NT+EV, 21NT+TBX3iso1, 21NT+TBX3iso2) to specifically assess for differences in expression profiles between the two TBX3 isoform transfectants. Interestingly, all of the cell lines had distinct expression signatures and clustering patterns (Figure 4.3.2 A), suggesting differential transcriptional function of the TBX3 isoforms. We observed 470 differentially expressed genes between TBX3iso1 and TBX3iso2. Pathway analysis of up-regulated genes with TBX3iso1 overexpression identified its potential role in osteopontin signaling, glycolysis/gluconeogenesis, and angiogenesis (Figure 4.3.2 B). Alternatively, pathway analysis of the up-regulated genes with TBX3iso2 overexpression identified alterations in the cytokines and inflammatory responses (Figure 4.3.2 C). Notably, TBX3iso2 overexpression resulted in down-regulation of genes involved in glycolysis/gluconeogenesis, showing inverse patterns from TBX3iso1 overexpressing cells.

Gross examinations of xenograft tumors revealed high vascularity of tumors formed by TBX3iso1 overexpressing cells. Given this observation, and our finding of an enrichment of angiogenesis-related genes upon TBX3iso1 overexpression, we examined tumor vascularity through CD31 immunohistochemistry and quantification of microvascular density (Figure 4.3.2 D). Microvascular density within the TBX3iso1 tumors was significantly higher than the TBX3iso2 tumor for the majority (4/6) of tumors tested. In order to functionally examine for angiogenic properties, we isolated conditioned media from 21NT transfectant cells and incubated them with human dermal microvascular endothelial cells (HDMECs) on Matrigel for 16 hours to allow for endothelial cell migration and formation of tubule structures, mimicking angiogenesis *in vitro* (Figure 4.3.2 E). We observed marked differences in the promotion of angiogenesis *in vitro* between conditioned media from cells overexpressing TBX3iso1, which resulted in significantly higher rates of tubule formation by endothelial cells, relative to conditioned media from TBX3iso2 overexpressing cells or the empty vector control.

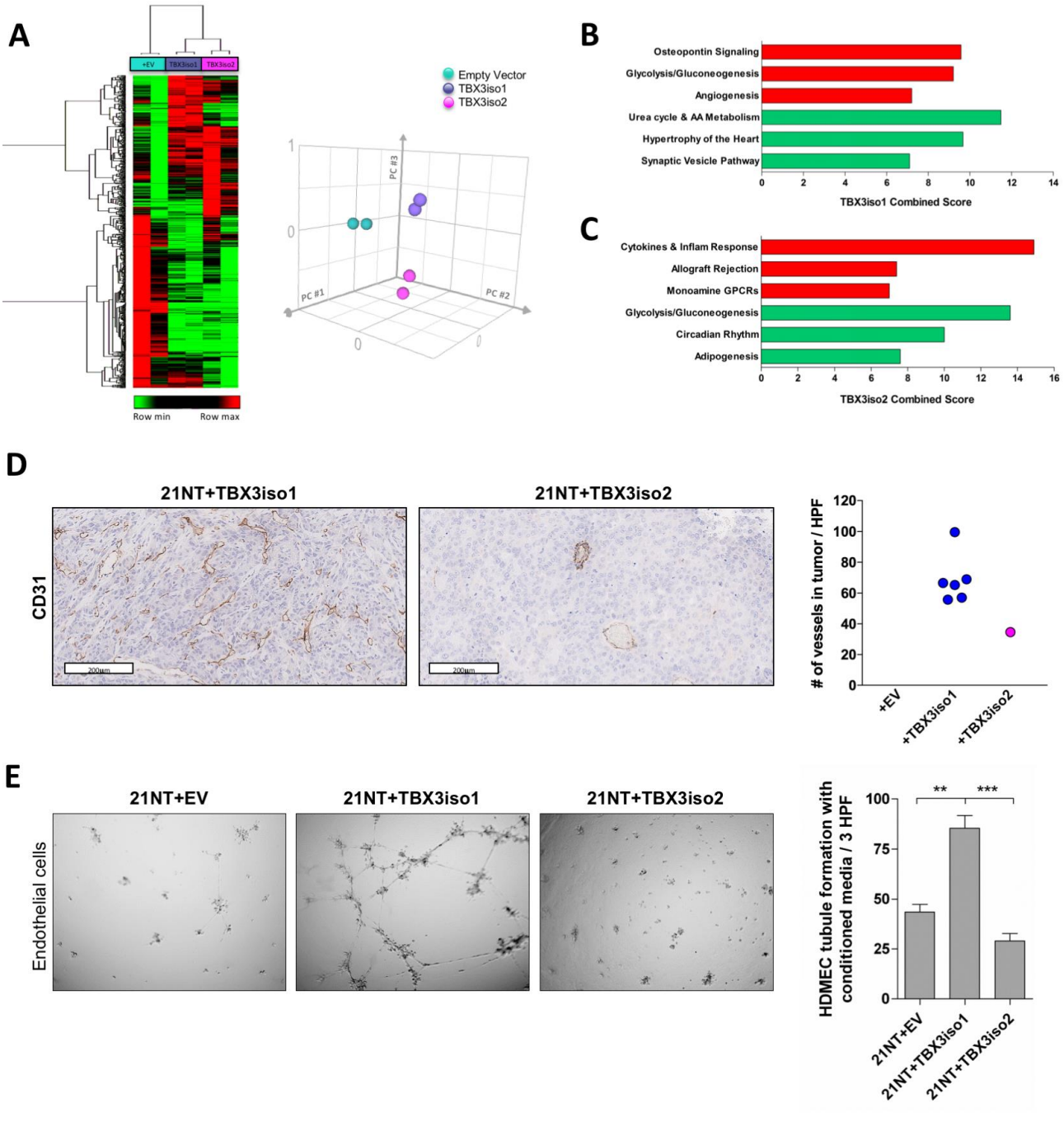
A
+EV
TBX3iso1
TBX3iso2
Row min
Row max
Empty Vector
TBX3iso1
TBX3iso2
PC #1
PC #2
PC #3
B
Osteopontin Signaling
Glycolysis/Gluconeogenesis
Angiogenesis
Urea cycle & AA Metabolism
Hypertrophy of the Heart
Synaptic Vesicle Pathway
TBX3iso1 Combined Score
C
Cytokines & Inflam Response
Allograft Rejection
Monoamine GPCRs
Glycolysis/Gluconeogenesis
Circadian Rhythm
Adipogenesis
TBX3iso2 Combined Score
D
21NT+TBX3iso1
21NT+TBX3iso2
CD31
200µm
# of vessels in tumor / HPF
+EV
+TBX3iso1
+TBX3iso2
E
21NT+EV
21NT+TBX3iso1
21NT+TBX3iso2
Endothelial cells
HDMEC tubule formation with conditioned media / 3 HPF
**
***

Figure 4.3.2 – TBX3iso1 promotes angiogenesis *in vitro* and *in vivo*.

(A) Heat map showing large-scale transcriptional changes by RNA-Seq across 21NT+EV, 21NT+TBX3iso1, and 21NT+TBX3iso2 cell lines. Principle component analysis (PCA) was conducted to assess the similarity in global transcriptional profiles between transfectant cell lines. **(B)** Enrichment analysis highlights pathways associated with transcripts up-regulated (red) and down-regulated (green) with TBX3iso1 overexpression relative to the empty vector control. **(C)** Enrichment analysis highlights pathways associated with transcripts up-regulated (red) and down-regulated (green) with TBX3iso2 overexpression relative to the empty vector control. **(D)** Assessment of blood vessel density within primary tumors by CD31 immunohistochemistry. Primary tumors were stained for CD31 by immunohistochemistry and the number of vessels per non-overlapping high power field were quantified across 10 tumor hotspots. Averages across 10 hotspots for each mouse is shown. **(E)** Tubule formation assay to asses *in vitro* angiogenesis. Conditioned media was collected after 48h incubation with $1x10^6$ cells of each cell type. Conditioned media was incubated with human dermal microvascular endothelial cells (HDMEC) on growth factor reduced Matrigel for 16 hours at 37ºC. Tubule branch points per 3 high power fields (one well) was quantified at the 16h mark.

**p<0.05, **p<0.01, ***p<0.001 by one way ANOVA with Tukey post-hoc for comparison between three groups. Error bars represent standard deviation.*

4.3.3 Osteopontin is specifically up-regulated by TBX3iso1.

In order to explore differences in transcriptional profiles between the two TBX3 isoforms on angiogenesis-related gene expression, we generated an angiogenesis gene signature consisting of 222 genes using publicly-available databases (as described in Bioinformatics Methods, Table 4.2) and conducted hierarchical clustering of RNA-Seq expression data for all cell lines (Figure 4.3.3 A). Investigation of the depicted cluster at a higher resolution revealed up-regulation of a subset of pro-angiogenic transcripts in TBX3iso1 overexpressing cells and down-regulation in TBX3iso2 overexpressing cells relative to the empty vector (Figure 4.3.3 B). Genes showing the most pronounced differences between TBX3iso1 and TBX3iso2 transfectants (OPN, COX1, IL1RN) were validated by qRT-PCR (Figure 4.3.3 C). The VEGF family is commonly referred to as the main pro-angiogenic factors across cancer subtypes (Oltean and Bates, 2014, Ladomery et al., 2007), with VEGFR2 acting as the key receptor responsible for mediating VEGF-induced angiogenic activity (Takahashi et al., 2002). For this reason, expression of VEGFR2 was also validated by qRT-PCR and found to be down-regulated in TBX3iso2 overexpressing cells (as observed in RNA-Seq data) (Appendix 10).

We focused our further studies on OPN since its mRNA levels displayed the greatest difference between TBX3iso1 and TBX3iso2 overexpressing cells, and OPN is known to be pro-angiogenic (Takahashi et al., 2002, Asou et al., 2001, Pröls et al., 1998, Takano et al., 2000, Cook et al., 2005). OPN expression was then assessed in additional stable TBX3 transfectant cell lines (TBX3 expression levels for 21PT and MCF7 transfectant cell lines are shown in Appendix 11 A-B). Overexpression of TBX3iso1 resulted in significant up-regulation of OPN mRNA levels in all three transfectant cell lines (Figure 4.3.3 C-D). Additionally, OPN mRNA levels were significantly down-regulated in all three cell lines overexpressing TBX3iso2. We then proceeded to evaluate the levels of OPN protein released into the conditioned media previously used for *in vitro* tubule formation assays. OPN protein levels were quantified by ELISA by comparing to recombinant human osteopontin standards (Figure 4.3.3 E). Relative to the empty vector control, there was a 49.0-fold and 3.9-fold increase in secreted OPN levels for TBX3iso1 and TBX3iso2 overexpressing cells, respectively. As another mode of confirmation, we conducted immunohistochemical staining for OPN in the xenograft primary tumors and observed a significantly higher proportion of

OPN positive tumor cells in TBX3iso1 tumors relative to the TBX3iso2 tumor (Figure 4.3.3 F).

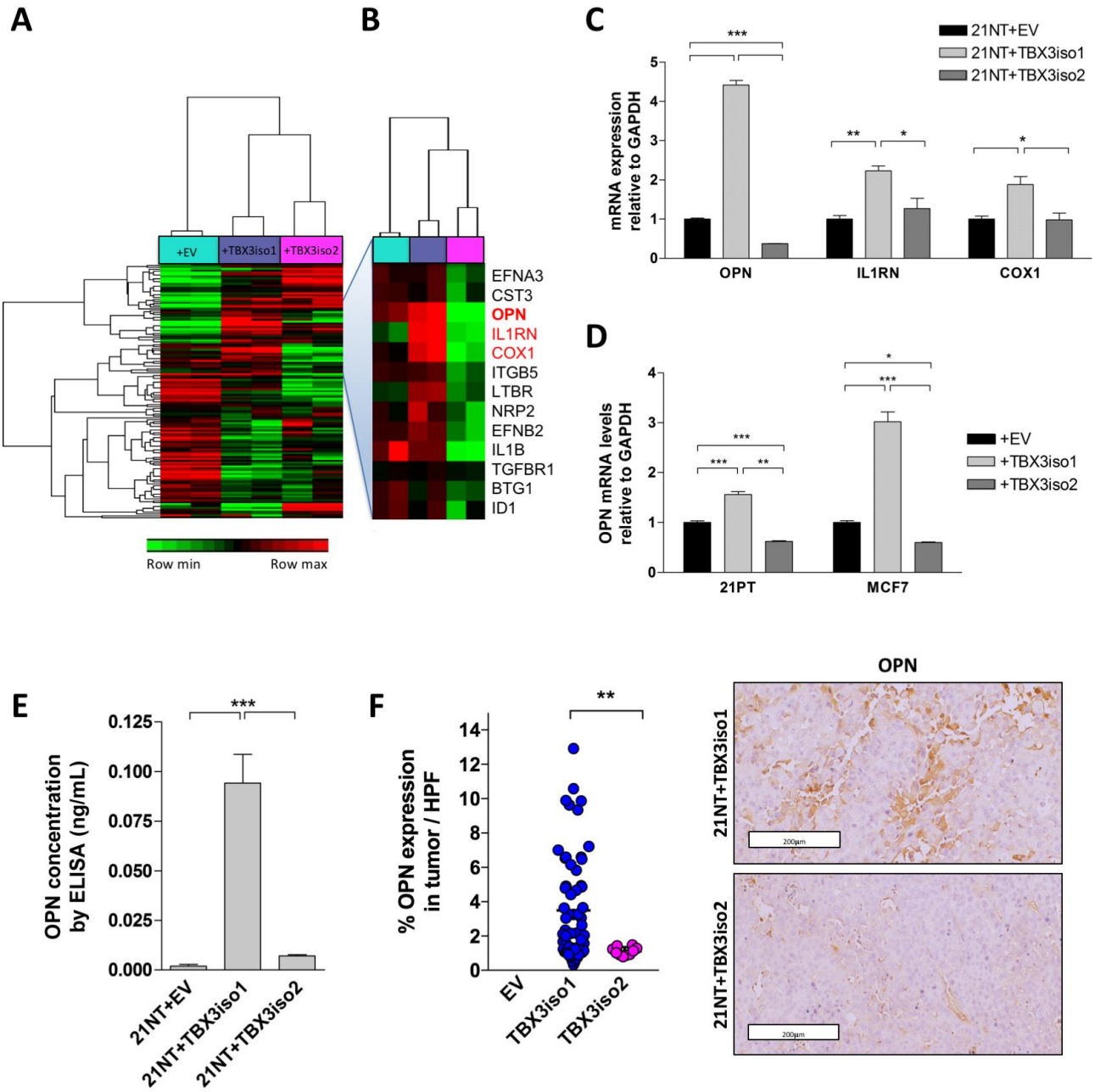

Figure 4.3.3 – Osteopontin is specifically up-regulated by TBX3iso1.

(A) Heat map showing expression of 222 angiogenesis-related genes by RNA-Seq across 21NT+EV, 21NT+TBX3iso1, and 21NT+TBX3iso2 cell lines. **(B)** Cluster showing up-regulation of pro-angiogenic transcript with TBX3iso1 overexpression and down-regulation with TBX3iso2 overexpression. Osteopontin (OPN) mRNA expression is shown in red. **(C)** Expression of OPN mRNA levels in 21PT, 21NT and MCF7 transfectant cell lines was assessed by qRT-PCR, normalized to GAPDH expression levels, and depicted as fold change relative to the empty vector control. **(D)** OPN protein levels from conditioned media was assessed by ELISA and normalized to cell numbers. Human recombinant OPN (hrOPN) was used to generate a standard curve for determination of OPN protein concentration. **(E)** Primary tumors were stained for OPN by immunohistochemistry. Color deconvolution was conducted using ImageJ, followed by thresholding of brown signal to assess percentage of high power field positive for OPN expression across ten non-overlapping areas. Percentage of the high power field (HPF) positive for OPN is shown across 10 fields of view per tumor.

**p<0.05, **p<0.01, ***p<0.001 by one way ANOVA with Tukey post-hoc for comparison between three groups, and Student's t-test for comparison between two groups. Error bars represent standard deviation.*

4.3.4 TBX3iso1 overexpression leads to increased HAS2 levels and pericellular hyaluronan retention.

We have previously shown that OPN induction of hyaluronan synthase 2 (HAS2) and hence hyaluronan (HA) production is associated with aggressiveness of 21NT cells (Cook et al., 2006). Given that all three of the cell lines we tested (21PT, 21NT, MCF7) showed up-regulation of OPN only with TBX3iso1 overexpression, we examined HAS2 mRNA levels. For all three cell line transfectants, overexpression of TBX3iso1 was associated with a significant up-regulation of HAS2 expression (Figure 4.3.4 A). Alternatively, overexpression of TBX3iso2 resulted in down-regulation of HAS2 mRNA expression in 21PT and MCF7 transfectant cell lines, with no change in HAS2 expression in the 21NT transfectant cell line. Hyaluronan (HA) is produced by hyaluronan synthase enzymes (HAS1-3) at the intracellular face of the plasma membrane, and then extruded from the cell and either released into the microenvironment, or retained in pericellular coats (Weigel and DeAngelis, 2007, Tammi et al., 1998, Evanko et al., 2007). High levels of synthesis and retention of HA in pericellular coats has been shown to have an important role in malignant progression (Cook et al., 2006) and is an indicator of poor prognosis in epithelial cancers (Auvinen et al., 2014, Tammi et al., 2008, Auvinen et al., 2000). In order to examine the phenomenon of HA retention, particle exclusion experiments were conducted using fixed sheep erythrocytes in order to visualize matrix production and retention (Figure 4.3.4 B-C). Due to the unique biochemical properties of HA, including its highly polar structure and large size, addition of partially negatively charged erythrocytes allows for visualization of matrices due to erythrocyte exclusion. Cells overexpressing TBX3iso1 had significantly larger pericellular coats relative to TBX3iso2 overexpressing cells and the empty vector control, suggesting higher levels of hyaluronan production. Administration of hyaluronidase (HAse) completely abolished matrix assembly in TBX3iso1 overexpressing cells, confirming the presence of HA in the pericellular coats.

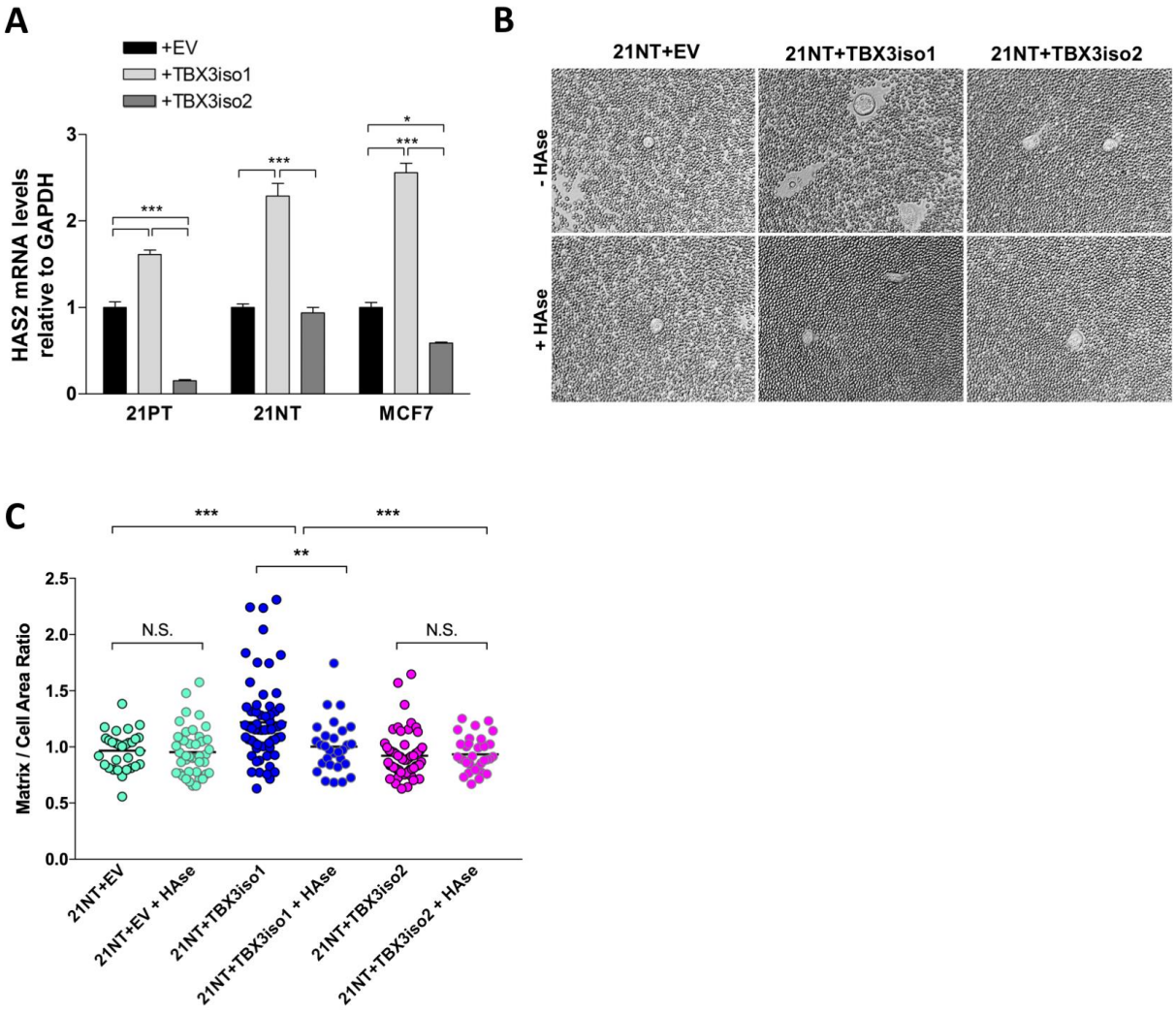

Figure 4.3.4 – TBX3iso1 overexpression leads to increased HAS2 levels and pericellular hyaluronan retention.

(A) Expression of HAS2 mRNA levels in 21PT, 21NT and MCF7 transfectant cell lines was assessed by qRT-PCR, normalized to GAPDH expression levels, and depicted as fold change relative to the empty vector control. **(B-C)** Particle exclusion experiment for visualization of pericellular matrices. Cells were pre-treated in the presence or absence of hyaluronidase for 20 minutes, followed by removal of media and addition of fixed sheep erythrocytes. Pericellular matrix area was calculated by tracing around cell coats (matrices) and cell areas across 30 randomly selected cells. A ratio of 1.0 indicated the absence of a pericellular matrix for a particular cell.

**p<0.05, **p<0.01, ***p<0.001 by one way ANOVA with Tukey post-hoc for comparison between three or more groups. Error bars represent standard deviation.*

4.3.5 Cancer progression involves transcriptional changes resulting in an increase in the TBX3iso1/TBX3iso2 ratio.

TBX3 is overexpressed in several different cancer types (Fan et al., 2004, Lomnytska et al., 2006, Yarosh et al., 2008, Souter et al., 2010, Rodriguez et al., 2008, Cavard et al., 2009, Lyng et al., 2006b, Gudmundsson et al., 2010, Miao et al., 2016). Examination of ICGC data (US Donor-centric) revealed breast cancer as amongst the cancers with the highest expression of all tumor tissue sites (Figure 4.3.5 A). We then interrogated TBX3 isoform expression in the TCGA breast cancer cohort, assessing the ratio of transcript reads for TBX3iso1 over TBX3iso2 for each breast cancer patient and comparing to clinical characteristics (Summarized in Figure 4.3.5 B). The TBX3iso1/TBX3iso2 expression ratio was 8.1-fold higher in tumor samples relative to normal controls (Figure 4.3.5 C). Additionally, this ratio was positively associated with higher tumor grade (Figure 4.3.5 D) along with more aggressive breast cancer subtypes (Figure 4.3.5 E). Upon examination of isoform-specific expression in tumor types where TBX3 overexpression has been documented (breast cancer, melanoma, colon, and pancreatic cancer), we observed an upwards shift in TBX3iso1 expression and downwards shift in TBX3iso2 expression within tumor tissues (TCGA cohorts) relative to an expanded cohort of normal tissue controls (GTEx normal tissue dataset) (Appendix 12).

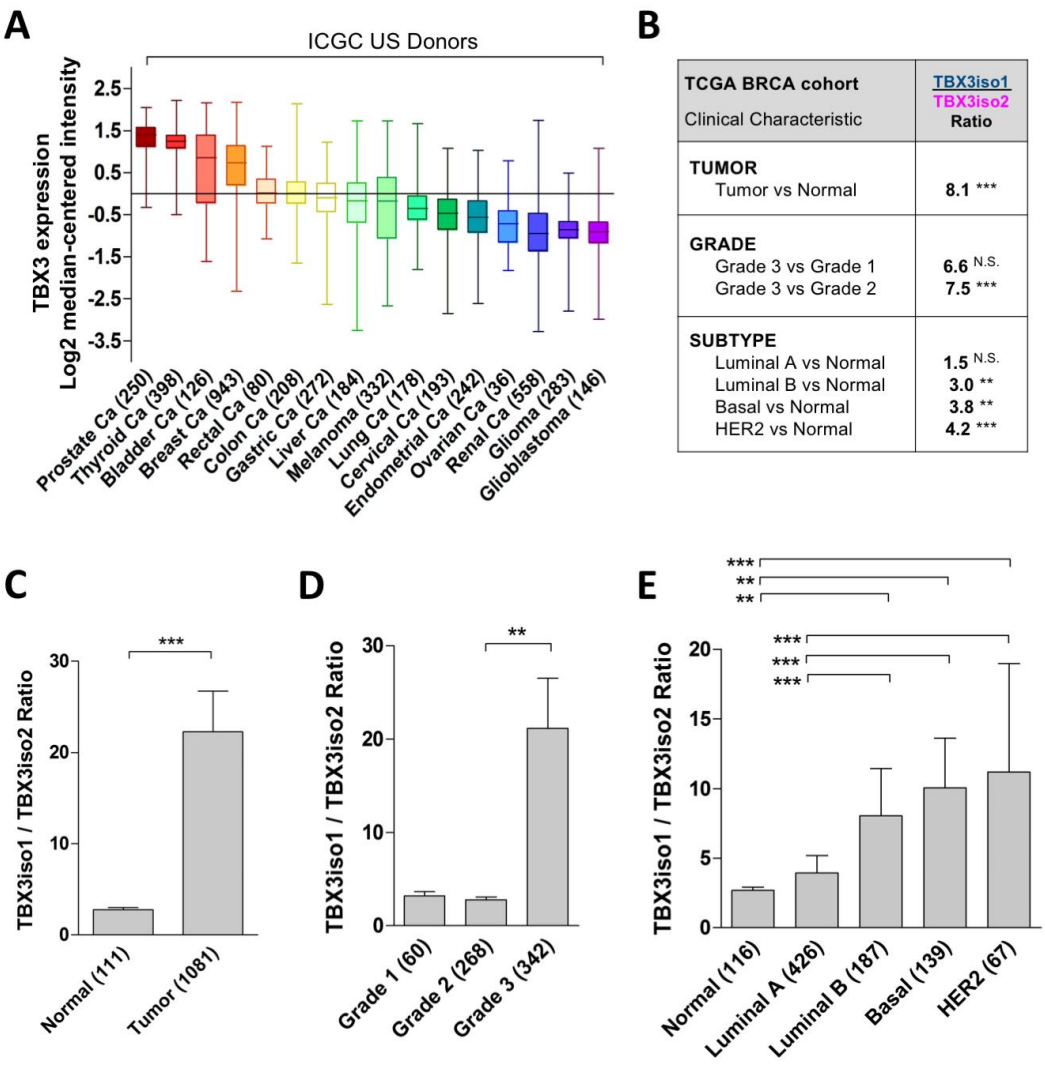

Figure 4.3.5 – Cancer progression involves transcriptional changes resulting in an increase in TBX3iso1 to TBX3iso2 ratio.

(A) Assessment of ICGC data (US Donor-centric) data shows total TBX3 levels across tumor subtypes. Total TBX3 transcript expression in breast cancer is shown in orange. **(B)** TBX3 isoform ratios were interrogated in the TCGA breast cancer cohort by calculating the total transcript reads for TBX3iso1 over the total transcript reads for TBX3iso2 for each patient. Ratios were compared between normal and tumor tissues. **(C)** The TBX3iso1/TBX3iso2 across breast cancer grades.

**p<0.05, **p<0.01, ***p<0.001 by the non-parametric Kruskal-Wallis statistic with Dunn's multiple comparison post-hoc test due to non-Gaussian distribution of ratios. Error bars represent standard deviation.*

4.4 Discussion

Alternative splicing is a post-transcriptional mechanism that adds an enhanced layer of complexity and diversification to genes encoded in the genome. Cancer cells are able to exploit the process of alternative splicing to produce isoform switches, resulting in enhanced survival, proliferation and invasiveness (Oltean and Bates, 2014, Shen et al., 2016). Interestingly, transcriptional analysis of alternative-splicing and assessment of exon inclusion events have been shown to outperform gene expression-based survival predictors across 6 different cancer types, including breast cancer (Shen et al., 2016).

Existing literature examining TBX3-induced tumorigenicity through the use of xenograft models (Rodriguez et al., 2008, Peres and Prince, 2013, Willmer et al., 2016), along with the single published transgenic TBX3-inducible mouse model (Liu et al., 2011), have focused on only one isoform of TBX3 in different parental cell lines which makes comparison of results difficult. Liu et al. showed that inducible overexpression of TBX3iso2 in murine mammary glands results in mild focal hyperplasia and importantly no tumor formation (Liu et al., 2011). For several other studies, which isoform was cloned and overexpressed is not stated (Peres and Prince, 2013, Perkhofer et al., 2016). Additionally, studies which employed knockdown of total TBX3 expression followed by xenotransplantation of cells into mice has revealed that TBX3 is associated with tumor formation, but not whether differences exist between isoforms (Peres et al., 2010).

We therefore sought to investigate the functional consequence of this highly conserved splice event as it relates to TBX3-induced tumorigenesis. We have conducted nude mouse xenograft experiments utilizing non-tumorigenic, DCIS-like 21NT cell lines, and have reported significant differences between TBX3 isoforms in the promotion of tumorigenesis, with TBX3iso1 overexpression more commonly associated with invasive carcinoma *in vivo*. This difference is likely associated with differing ability to induce angiogenesis, and is related to differential expression of a number of angiogenesis-associated genes.

While angiogenesis has a limited role in normal physiology, it is a fundamental requirement in malignant progression (Hanahan and Weinberg, 2000). This requirement of angiogenesis is due to the inability of avascular tumors to access oxygen and nutrients through diffusion alone (Rooney et al., 1995, Hanahan and Weinberg, 2000, Ladomery et al.,

2007). After cytokines are released from cells, they are able to diffuse into the extracellular milieu and act on nearby quiescent endothelial cells to induce proliferation and migration towards the tumor (Ladomery et al., 2007). As observed by *in vitro* tubule formation assays, pro-angiogenic factors are released from cells overexpressing TBX3iso1 that are functional in activating endothelial cells. We report that one key pro-angiogenic factor up-regulated by TBX3iso1 is OPN. OPN has previously been described to act as a cytokine in various contexts (Ashkar et al., 2000, Denhardt et al., 2001, Takahashi et al., 2002), with several studies ascribing it a pro-angiogenic function (Pröls et al., 1998, Takano et al., 2000, Asou et al., 2001, Takahashi et al., 2002). Importantly, elevated OPN expression is associated with several breast cancer-related prognostic factors, including early metastasis and poor outcome (Bellahcène and Castronovo, 1995, Rudland et al., 2002, El-Tanani et al., 2004, Bramwell et al., 2006, El-Tanani et al., 2006). A great deal of overlap has been reported on the cellular functions affected by OPN and HA (Kim et al., 2005). The two markers have both been correlated with cancer survival (Bellahcène and Castronovo, 1995, Auvinen et al., 2000, Rudland et al., 2002, El-Tanani et al., 2004, Bramwell et al., 2006, El-Tanani et al., 2006, Tammi et al., 2008, Veiseh et al., 2014) and are frequently co-expressed (Kim et al., 2005, Lee et al., 2007). We have previously reported OPN-induced up-regulation of HAS2 in 21NT breast cancer cell lines is necessary for both anchorage-independent growth and adhesion of tumor cells to bone marrow endothelial cells (Cook et al., 2006). Moreover, both HA and OPN are ligands for CD44 (in this case on endothelial cells) (Weber et al., 1996), and their binding promotes angiogenesis through stimulation of endothelial cell migration, survival and lumen formation (Brooks et al., 1994, Senger et al., 1996, Trochon et al., 1996, Griffioen et al., 1997, Arap et al., 1998, Scatena et al., 1998, Bayless et al., 2000, Cao et al., 2006).

Our novel *in vivo* findings relating to differential tumorigenicity of TBX3 isoforms and downstream confirmation of associated pathways suggest that the assessment of relative levels of splice variants may be more important than the assessment of total transcript levels per gene (Blencowe, 2006, Li et al., 2006, Zhang et al., 2006). This focus on isoform ratios has been suggested by several studies (Venables, 2004, Blencowe, 2006, Ladomery et al., 2007, Pajares et al., 2007). There are additional examples of alternatively spliced transcripts having diverse and even antagonistic functions (Pajares et al., 2007). A prominent example includes alternative splicing of VEGF; most splice variants are actively pro-angiogenic, while the VEGFb splice variant is only six amino acids different relative to its most similar isoform

but is actively anti-angiogenic (Ladomery et al., 2007). A splicing switch from the anti-angiogenic to pro-angiogenic variant is observed both in cancer progression (Venables, 2004, Pajares et al., 2007, Oltean and Bates, 2014), along with diseases such as proliferative diabetic retinopathy (Blencowe, 2006, Ladomery et al., 2007).

It is unknown whether this increase of TBX3iso1 over TBX3iso2 expression is a cause or effect of the tumorigenic process; a splice shift phenomenon may be due to several factors, including potential epigenetic changes within the TBX3 gene, or due to changes in upstream splicing machinery (Cui et al., 2004, Ladomery et al., 2007). It is becoming quite clear that splice changes and isoform shifts in cancer are non-random and play a key role in cancer progression (Venables, 2004, Ladomery et al., 2007, Pajares et al., 2007). Various strategies are being employed in an attempt to exploit alternative splicing in diagnosis, prognosis and treatment of cancer (Yamaguchi et al., 1998, Venables, 2004, Ladomery et al., 2007). On this note, Venables et al. examined expression of breast cancer-associated genes and their alternatively spliced transcripts through assessment of isoform ratios (Venables et al., 2008). They reported cancer-specific exon loss for several transcripts as well as a significant overlap with previously identified ovarian cancer-specific splice changes (Klinck et al., 2008, Venables et al., 2008). This suggests that a subset of the alternative splicing events identified by high throughput transcriptomic analysis may be common across cancer subtypes.

It is well established that TBX3 is aberrantly overexpressed in several cancer types (Fan et al., 2004, Lomnytska et al., 2006, Lyng et al., 2006, Rodriguez et al., 2008, Yarosh et al., 2008, Cavard et al., 2009, Souter et al., 2010, Shan et al., 2015, Miao et al., 2016, Gudmundsson et al., 2010). We have added to the existing literature and reported that in particular, an increased TBX3iso1/TBX3iso2 ratio is associated with several clinicopathological parameters in the TCGA breast cancer cohort. Additionally, TBX3iso1 promotes a pro-angiogenic gene signature associated with elevated OPN and HAS2 expression, as well as increased pericellular HA retention. These pro-angiogenic changes associated with elevated TBX3iso1 expression promote vascular channel formation by endothelial cells *in vitro,* and likely explain the high tumor formation rates and high vascularity of primary tumors formed in mouse xenograft assays. A thorough understanding of transcriptional control by TBX3, in an isoform-specific context, is therefore vital in order to

understand the effect of TBX3 in promotion of tumorigenicity in breast cancer as well as other cancer types.

4.5 References

Arap, W., Pasqualini, R. and Ruoslahti, E. (1998) 'Cancer treatment by targeted drug delivery to tumor vasculature in a mouse model', *Science,* 279(5349), pp. 377-80.

Arnaoutova, I. and Kleinman, H. K. (2010) 'In vitro angiogenesis: endothelial cell tube formation on gelled basement membrane extract', *Nat Protoc,* 5(4), pp. 628-35.

Ashkar, S., Weber, G. F., Panoutsakopoulou, V., Sanchirico, M. E., Jansson, M., Zawaideh, S., Rittling, S. R., Denhardt, D. T., Glimcher, M. J. and Cantor, H. (2000) 'Eta-1 (osteopontin): an early component of type-1 (cell-mediated) immunity', *Science,* 287(5454), pp. 860-4.

Asou, Y., Rittling, S. R., Yoshitake, H., Tsuji, K., Shinomiya, K., Nifuji, A., Denhardt, D. T. and Noda, M. (2001) 'Osteopontin facilitates angiogenesis, accumulation of osteoclasts, and resorption in ectopic bone', *Endocrinology,* 142(3), pp. 1325-32.

Auvinen, P., Rilla, K., Tumelius, R., Tammi, M., Sironen, R., Soini, Y., Kosma, V. M., Mannermaa, A., Viikari, J. and Tammi, R. (2014) 'Hyaluronan synthases (HAS1-3) in stromal and malignant cells correlate with breast cancer grade and predict patient survival', *Breast Cancer Res Treat,* 143(2), pp. 277-86.

Auvinen, P., Tammi, R., Parkkinen, J., Tammi, M., Agren, U., Johansson, R., Hirvikoski, P., Eskelinen, M. and Kosma, V. M. (2000) 'Hyaluronan in peritumoral stroma and malignant cells associates with breast cancer spreading and predicts survival', *Am J Pathol,* 156(2), pp. 529-36.

Bamshad, M., Le, T., Watkins, W. S., Dixon, M. E., Kramer, B. E., Roeder, A. D., Carey, J. C., Root, S., Schinzel, A., Van Maldergem, L., Gardner, R. J., Lin, R. C., Seidman, C. E., Seidman, J. G., Wallerstein, R., Moran, E., Sutphen, R., Campbell, C. E. and Jorde, L. B. (1999) 'The spectrum of mutations in TBX3: Genotype/Phenotype relationship in ulnar-mammary syndrome', *Am J Hum Genet,* 64(6), pp. 1550-62.

Bamshad, M., Lin, R. C., Law, D. J., Watkins, W. C., Krakowiak, P. A., Moore, M. E., Franceschini, P., Lala, R., Holmes, L. B., Gebuhr, T. C., Bruneau, B. G., Schinzel, A., Seidman, J. G., Seidman, C. E. and Jorde, L. B. (1997) 'Mutations in human TBX3 alter limb, apocrine and genital development in ulnar-mammary syndrome', *Nat Genet,* 16(3), pp. 311-5.

Band, V., Zajchowski, D., Swisshelm, K., Trask, D., Kulesa, V., Cohen, C., Connolly, J. and Sager, R. (1990) 'Tumor progression in four mammary epithelial cell lines derived from the same patient', *Cancer Res,* 50(22), pp. 7351-7.

Bayless, K. J., Salazar, R. and Davis, G. E. (2000) 'RGD-dependent vacuolation and lumen formation observed during endothelial cell morphogenesis in three-dimensional fibrin matrices involves the alpha(v)beta(3) and alpha(5)beta(1) integrins', *Am J Pathol,* 156(5), pp. 1673-83.

Bellahcène, A. and Castronovo, V. (1995) 'Increased expression of osteonectin and osteopontin, two bone matrix proteins, in human breast cancer', *Am J Pathol,* 146(1), pp. 95-100.

Blencowe, B. J. (2006) 'Alternative splicing: new insights from global analyses', *Cell,* 126(1), pp. 37-47.

Bramwell, V. H., Doig, G. S., Tuck, A. B., Wilson, S. M., Tonkin, K. S., Tomiak, A., Perera, F., Vandenberg, T. A. and Chambers, A. F. (2006) 'Serial plasma osteopontin levels have prognostic value in metastatic breast cancer', *Clin Cancer Res,* 12(11 Pt 1), pp. 3337-43.

Brooks, P. C., Montgomery, A. M., Rosenfeld, M., Reisfeld, R. A., Hu, T., Klier, G. and Cheresh, D. A. (1994) 'Integrin alpha v beta 3 antagonists promote tumor regression by inducing apoptosis of angiogenic blood vessels', *Cell,* 79(7), pp. 1157-64.

Budczies, J., Bockmayr, M., Denkert, C., Klauschen, F., Lennerz, J. K., Györffy, B., Dietel, M., Loibl, S., Weichert, W. and Stenzinger, A. (2015) 'Classical pathology and mutational load of breast cancer - integration of two worlds', *J Pathol Clin Res,* 1(4), pp. 225-38.

Cao, G., Savani, R. C., Fehrenbach, M., Lyons, C., Zhang, L., Coukos, G. and Delisser, H. M. (2006) 'Involvement of endothelial CD44 during in vivo angiogenesis', *Am J Pathol,* 169(1), pp. 325-36.

Cavard, C., Audebourg, A., Letourneur, F., Audard, V., Beuvon, F., Cagnard, N., Radenen, B., Varlet, P., Vacher-Lavenu, M. C., Perret, C. and Terris, B. (2009) 'Gene expression profiling provides insights into the pathways involved in solid pseudopapillary neoplasm of the pancreas', *J Pathol,* 218(2), pp. 201-9.

Chakraborty, G., Jain, S., Behera, R., Ahmed, M., Sharma, P., Kumar, V. and Kundu, G. C. (2006) 'The multifaceted roles of osteopontin in cell signaling, tumor progression and angiogenesis', *Curr Mol Med,* 6(8), pp. 819-30.

Chakraborty, G., Jain, S. and Kundu, G. C. (2008) 'Osteopontin promotes vascular endothelial growth factor-dependent breast tumor growth and angiogenesis via autocrine and paracrine mechanisms', *Cancer Res,* 68(1), pp. 152-61.

Coll, M., Seidman, J. G. and Müller, C. W. (2002) 'Structure of the DNA-bound T-box domain of human TBX3, a transcription factor responsible for ulnar-mammary syndrome', *Structure,* 10(3), pp. 343-56.

Cook, A. C., Chambers, A. F., Turley, E. A. and Tuck, A. B. (2006) 'Osteopontin induction of hyaluronan synthase 2 expression promotes breast cancer malignancy', *J Biol Chem,* 281(34), pp. 24381-9.

Cook, A. C., Tuck, A. B., McCarthy, S., Turner, J. G., Irby, R. B., Bloom, G. C., Yeatman, T. J. and Chambers, A. F. (2005) 'Osteopontin induces multiple changes in gene expression that reflect the six "hallmarks of cancer" in a model of breast cancer progression', *Mol Carcinog,* 43(4), pp. 225-36.

Cui, T. G., Foster, R. R., Saleem, M., Mathieson, P. W., Gillatt, D. A., Bates, D. O. and Harper, S. J. (2004) 'Differentiated human podocytes endogenously express an inhibitory isoform of vascular endothelial growth factor (VEGF165b) mRNA and protein', *Am J Physiol Renal Physiol,* 286(4), pp. F767-73.

DeBenedittis, P. and Jiao, K. (2011) 'Alternative splicing of T-box transcription factor genes', *Biochem Biophys Res Commun,* 412(4), pp. 513-7.

Demay, F., Bilican, B., Rodriguez, M., Carreira, S., Pontecorvi, M., Ling, Y. and Goding, C. R. (2007) 'T-box factors: targeting to chromatin and interaction with the histone H3 N-terminal tail', *Pigment Cell Res,* 20(4), pp. 279-87.

Denhardt, D. T., Noda, M., O'Regan, A. W., Pavlin, D. and Berman, J. S. (2001) 'Osteopontin as a means to cope with environmental insults: regulation of inflammation, tissue remodeling, and cell survival', *J Clin Invest,* 107(9), pp. 1055-61.

El-Tanani, M., Platt-Higgins, A., Rudland, P. S. and Campbell, F. C. (2004) 'Ets gene PEA3 cooperates with beta-catenin-Lef-1 and c-Jun in regulation of osteopontin transcription', *J Biol Chem,* 279(20), pp. 20794-806.

El-Tanani, M. K., Campbell, F. C., Kurisetty, V., Jin, D., McCann, M. and Rudland, P. S. (2006) 'The regulation and role of osteopontin in malignant transformation and cancer', *Cytokine Growth Factor Rev,* 17(6), pp. 463-74.

Evanko, S. P., Tammi, M. I., Tammi, R. H. and Wight, T. N. (2007) 'Hyaluronan-dependent pericellular matrix', *Adv Drug Deliv Rev,* 59(13), pp. 1351-65.

Fan, W., Huang, X., Chen, C., Gray, J. and Huang, T. (2004) 'TBX3 and its isoform TBX3+2a are functionally distinctive in inhibition of senescence and are overexpressed in a subset of breast cancer cell lines', *Cancer Res,* 64(15), pp. 5132-9.

Griffioen, A. W., Coenen, M. J., Damen, C. A., Hellwig, S. M., van Weering, D. H., Vooys, W., Blijham, G. H. and Groenewegen, G. (1997) 'CD44 is involved in tumor angiogenesis; an activation antigen on human endothelial cells', *Blood,* 90(3), pp. 1150-9.

Gudmundsson, J., Besenbacher, S., Sulem, P., Gudbjartsson, D. F., Olafsson, I., Arinbjarnarson, S., Agnarsson, B. A., Benediktsdottir, K. R., Isaksson, H. J., Kostic, J. P., Gudjonsson, S. A., Stacey, S. N., Gylfason, A., Sigurdsson, A., Holm, H., Bjornsdottir, U. S., Eyjolfsson, G. I., Navarrete, S., Fuertes, F., Garcia-Prats, M. D., Polo, E., Checherita, I. A., Jinga, M., Badea, P., Aben, K. K., Schalken, J. A., van Oort, I. M., Sweep, F. C., Helfand, B. T., Davis, M., Donovan, J. L., Hamdy, F. C., Kristjansson, K., Gulcher, J. R., Masson, G., Kong, A., Catalona, W. J., Mayordomo, J. I., Geirsson, G., Einarsson, G. V., Barkardottir, R. B., Jonsson, E., Jinga, V., Mates, D., Kiemeney, L. A., Neal, D. E., Thorsteinsdottir, U., Rafnar, T. and Stefansson, K. (2010) 'Genetic correction of PSA values using sequence variants associated with PSA levels', *Sci Transl Med,* 2(62), pp. 62ra92.

Hanahan, D. and Weinberg, R. A. (2000) 'The hallmarks of cancer', *Cell,* 100(1), pp. 57-70.

Hirama, M., Takahashi, F., Takahashi, K., Akutagawa, S., Shimizu, K., Soma, S., Shimanuki, Y., Nishio, K. and Fukuchi, Y. (2003) 'Osteopontin overproduced by tumor cells acts as a potent angiogenic factor contributing to tumor growth', *Cancer Lett,* 198(1), pp. 107-17.

Hoogaars, W. M., Barnett, P., Rodriguez, M., Clout, D. E., Moorman, A. F., Goding, C. R. and Christoffels, V. M. (2008) 'TBX3 and its splice variant TBX3 + exon 2a are functionally similar', *Pigment Cell Melanoma Res,* 21(3), pp. 379-87.

Kim, M. S., Park, M. J., Moon, E. J., Kim, S. J., Lee, C. H., Yoo, H., Shin, S. H., Song, E. S. and Lee, S. H. (2005) 'Hyaluronic acid induces osteopontin via the phosphatidylinositol 3-kinase/Akt pathway to enhance the motility of human glioma cells', *Cancer Res,* 65(3), pp. 686-91.

Klinck, R., Bramard, A., Inkel, L., Dufresne-Martin, G., Gervais-Bird, J., Madden, R., Paquet, E. R., Koh, C., Venables, J. P., Prinos, P., Jilaveanu-Pelmus, M., Wellinger, R., Rancourt, C., Chabot, B. and Abou Elela, S. (2008) 'Multiple alternative splicing markers for ovarian cancer', *Cancer Res,* 68(3), pp. 657-63.

Koyama, H., Hibi, T., Isogai, Z., Yoneda, M., Fujimori, M., Amano, J., Kawakubo, M., Kannagi, R., Kimata, K., Taniguchi, S. and Itano, N. (2007) 'Hyperproduction of hyaluronan in neu-induced mammary tumor accelerates angiogenesis through stromal cell recruitment: possible involvement of versican/PG-M', *Am J Pathol,* 170(3), pp. 1086-99.

Krstic, M., Macmillan, C. D., Leong, H. S., Clifford, A. G., Souter, L. H., Dales, D. W., Postenka, C. O., Chambers, A. F. and Tuck, A. B. (2016) 'The transcriptional regulator TBX3 promotes progression from non-invasive to invasive breast cancer', *BMC Cancer,* 16(1), pp. 671.

Ladomery, M. R., Harper, S. J. and Bates, D. O. (2007) 'Alternative splicing in angiogenesis: the vascular endothelial growth factor paradigm', *Cancer Lett,* 249(2), pp. 133-42.

Lee, H. S., Cho, H. H., Kim, H. K., Bae, Y. C., Baik, H. S. and Jung, J. S. (2007) 'Tbx3, a transcriptional factor, involves in proliferation and osteogenic differentiation of human adipose stromal cells', *Mol Cell Biochem,* 296(1-2), pp. 129-36.

Li, H. R., Wang-Rodriguez, J., Nair, T. M., Yeakley, J. M., Kwon, Y. S., Bibikova, M., Zheng, C., Zhou, L., Zhang, K., Downs, T., Fu, X. D. and Fan, J. B. (2006) 'Two-dimensional transcriptome profiling: identification of messenger RNA isoform signatures in prostate cancer from archived paraffin-embedded cancer specimens', *Cancer Res,* 66(8), pp. 4079-88.

Li, P., Liu, Y., Wang, H., He, Y., Wang, X., Lv, F., Chen, H., Pang, X., Liu, M., Shi, T. and Yi, Z. (2015) 'PubAngioGen: a database and knowledge for angiogenesis and related diseases', *Nucleic Acids Res,* 43(Database issue), pp. D963-7.

Liu, J., Esmailpour, T., Shang, X., Gulsen, G., Liu, A. and Huang, T. (2011) 'TBX3 over-expression causes mammary gland hyperplasia and increases mammary stem-like cells in an inducible transgenic mouse model', *BMC Dev Biol,* 11, pp. 65.

Lomnytska, M., Dubrovska, A., Hellman, U., Volodko, N. and Souchelnytskyi, S. (2006) 'Increased expression of cSHMT, Tbx3 and utrophin in plasma of ovarian and breast cancer patients', *Int J Cancer,* 118(2), pp. 412-21.

Lyng, H., Brøvig, R. S., Svendsrud, D. H., Holm, R., Kaalhus, O., Knutstad, K., Oksefjell, H., Sundfør, K., Kristensen, G. B. and Stokke, T. (2006) 'Gene expressions and copy numbers associated with metastatic phenotypes of uterine cervical cancer', *BMC Genomics,* 7, pp. 268.

Miao, Z. F., Liu, X. Y., Xu, H. M., Wang, Z. N., Zhao, T. T., Song, Y. X., Xing, Y. N., Huang, J. Y., Zhang, J. Y., Xu, H. and Xu, Y. Y. (2016) 'Tbx3 overexpression in human gastric cancer is correlated with advanced tumor stage and nodal status and promotes cancer cell growth and invasion', *Virchows Arch,* 469(5), pp. 505-513.

Miller, S. A., Huang, A. C., Miazgowicz, M. M., Brassil, M. M. and Weinmann, A. S. (2008) 'Coordinated but physically separable interaction with H3K27-demethylase and H3K4-methyltransferase activities are required for T-box protein-mediated activation of developmental gene expression', *Genes Dev,* 22(21), pp. 2980-93.

Oltean, S. and Bates, D. O. (2014) 'Hallmarks of alternative splicing in cancer', *Oncogene,* 33(46), pp. 5311-8.

Pajares, M. J., Ezponda, T., Catena, R., Calvo, A., Pio, R. and Montuenga, L. M. (2007) 'Alternative splicing: an emerging topic in molecular and clinical oncology', *Lancet Oncol,* 8(4), pp. 349-57.

Peres, J., Davis, E., Mowla, S., Bennett, D. C., Li, J. A., Wansleben, S. and Prince, S. (2010) 'The Highly Homologous T-Box Transcription Factors, TBX2 and TBX3, Have Distinct Roles in the Oncogenic Process', *Genes Cancer,* 1(3), pp. 272-82.

Peres, J. and Prince, S. (2013) 'The T-box transcription factor, TBX3, is sufficient to promote melanoma formation and invasion', *Mol Cancer,* 12(1), pp. 117.

Perkhofer, L., Walter, K., Costa, I. G., Carrasco, M. C., Eiseler, T., Hafner, S., Genze, F., Zenke, M., Bergmann, W., Illing, A., Hohwieler, M., Köhntop, R., Lin, Q., Holzmann, K. H., Seufferlein, T., Wagner, M., Liebau, S., Hermann, P. C., Kleger, A. and Müller, M. (2016) 'Tbx3 fosters pancreatic cancer growth by increased angiogenesis and activin/nodal-dependent induction of stemness', *Stem Cell Res,* 17(2), pp. 367-378.

Pröls, F., Loser, B. and Marx, M. (1998) 'Differential expression of osteopontin, PC4, and CEC5, a novel mRNA species, during in vitro angiogenesis', *Exp Cell Res,* 239(1), pp. 1-10.

Rodriguez, M., Aladowicz, E., Lanfrancone, L. and Goding, C. R. (2008) 'Tbx3 represses E-cadherin expression and enhances melanoma invasiveness', *Cancer Res,* 68(19), pp. 7872-81.

Rooney, P., Kumar, S., Ponting, J. and Wang, M. (1995) 'The role of hyaluronan in tumour neovascularization (review)', *Int J Cancer,* 60(5), pp. 632-6.

Rudland, P. S., Platt-Higgins, A., El-Tanani, M., De Silva Rudland, S., Barraclough, R., Winstanley, J. H., Howitt, R. and West, C. R. (2002) 'Prognostic significance of the metastasis-associated protein osteopontin in human breast cancer', *Cancer Res,* 62(12), pp. 3417-27.

Savas, S. (2012) 'A curated database of genetic markers from the angiogenesis/VEGF pathway and their relation to clinical outcome in human cancers', *Acta Oncol,* 51(2), pp. 243-6.

Scatena, M., Almeida, M., Chaisson, M. L., Fausto, N., Nicosia, R. F. and Giachelli, C. M. (1998) 'NF-kappaB mediates alphavbeta3 integrin-induced endothelial cell survival', *J Cell Biol,* 141(4), pp. 1083-93.

Senger, D. R., Ledbetter, S. R., Claffey, K. P., Papadopoulos-Sergiou, A., Peruzzi, C. A. and Detmar, M. (1996) 'Stimulation of endothelial cell migration by vascular permeability factor/vascular endothelial growth factor through cooperative mechanisms involving the alphavbeta3 integrin, osteopontin, and thrombin', *Am J Pathol,* 149(1), pp. 293-305.

Shan, Z. Z., Yan, X. B., Yan, L. L., Tian, Y., Meng, Q. C., Qiu, W. W., Zhang, Z. and Jin, Z. M. (2015) 'Overexpression of Tbx3 is correlated with Epithelial-Mesenchymal Transition phenotype and predicts poor prognosis of colorectal cancer', *Am J Cancer Res,* 5(1), pp. 344-53.

Shen, S., Wang, Y., Wang, C., Wu, Y. N. and Xing, Y. (2016) 'SURVIV for survival analysis of mRNA isoform variation', *Nat Commun,* 7, pp. 11548.

Shijubo, N., Uede, T., Kon, S., Maeda, M., Segawa, T., Imada, A., Hirasawa, M. and Abe, S. (1999) 'Vascular endothelial growth factor and osteopontin in stage I lung adenocarcinoma', *Am J Respir Crit Care Med,* 160(4), pp. 1269-73.

Sohn, T. K., Moon, E. J., Lee, S. K., Cho, H. G. and Kim, K. W. (2002) 'AngioDB: database of angiogenesis and angiogenesis-related molecules', *Nucleic Acids Res,* 30(1), pp. 369-71.

Souter, L. H., Andrews, J. D., Zhang, G., Cook, A. C., Postenka, C. O., Al-Katib, W., Leong, H. S., Rodenhiser, D. I., Chambers, A. F. and Tuck, A. B. (2010) 'Human 21T breast epithelial cell lines mimic breast cancer progression in vivo and in vitro and show stage-specific gene expression patterns', *Lab Invest,* 90(8), pp. 1247-58.

Takahashi, F., Akutagawa, S., Fukumoto, H., Tsukiyama, S., Ohe, Y., Takahashi, K., Fukuchi, Y., Saijo, N. and Nishio, K. (2002) 'Osteopontin induces angiogenesis of murine neuroblastoma cells in mice', *Int J Cancer,* 98(5), pp. 707-12.

Takano, S., Tsuboi, K., Tomono, Y., Mitsui, Y. and Nose, T. (2000) 'Tissue factor, osteopontin, alphavbeta3 integrin expression in microvasculature of gliomas associated with vascular endothelial growth factor expression', *Br J Cancer,* 82(12), pp. 1967-73.

Tammi, R., MacCallum, D., Hascall, V. C., Pienimäki, J. P., Hyttinen, M. and Tammi, M. (1998) 'Hyaluronan bound to CD44 on keratinocytes is displaced by hyaluronan decasaccharides and not hexasaccharides', *J Biol Chem,* 273(44), pp. 28878-88.

Tammi, R. H., Kultti, A., Kosma, V. M., Pirinen, R., Auvinen, P. and Tammi, M. I. (2008) 'Hyaluronan in human tumors: pathobiological and prognostic messages from cell-associated and stromal hyaluronan', *Semin Cancer Biol,* 18(4), pp. 288-95.

Trochon, V., Mabilat, C., Bertrand, P., Legrand, Y., Smadja-Joffe, F., Soria, C., Delpech, B. and Lu, H. (1996) 'Evidence of involvement of CD44 in endothelial cell proliferation, migration and angiogenesis in vitro', *Int J Cancer,* 66(5), pp. 664-8.

Tuck, A. B., O'Malley, F. P., Singhal, H., Harris, J. F., Tonkin, K. S., Kerkvliet, N., Saad, Z., Doig, G. S. and Chambers, A. F. (1998) 'Osteopontin expression in a group of lymph node negative breast cancer patients', *Int J Cancer,* 79(5), pp. 502-8.

Veiseh, M., Kwon, D. H., Borowsky, A. D., Tolg, C., Leong, H. S., Lewis, J. D., Turley, E. A. and Bissell, M. J. (2014) 'Cellular heterogeneity profiling by hyaluronan probes reveals an invasive but slow-growing breast tumor subset', *Proc Natl Acad Sci U S A,* 111(17), pp. E1731-9.

Venables, J. P. (2004) 'Aberrant and alternative splicing in cancer', *Cancer Res,* 64(21), pp. 7647-54.

Venables, J. P., Klinck, R., Bramard, A., Inkel, L., Dufresne-Martin, G., Koh, C., Gervais-Bird, J., Lapointe, E., Froehlich, U., Durand, M., Gendron, D., Brosseau, J. P., Thibault, P., Lucier, J. F., Tremblay, K., Prinos, P., Wellinger, R. J., Chabot, B., Rancourt, C. and Elela, S. A. (2008) 'Identification of alternative splicing markers for breast cancer', *Cancer Res,* 68(22), pp. 9525-31.

Weber, G. F., Ashkar, S., Glimcher, M. J. and Cantor, H. (1996) 'Receptor-ligand interaction between CD44 and osteopontin (Eta-1)', *Science,* 271(5248), pp. 509-12.

Weigel, P. H. and DeAngelis, P. L. (2007) 'Hyaluronan synthases: a decade-plus of novel glycosyltransferases', *J Biol Chem,* 282(51), pp. 36777-81.

Willmer, T., Cooper, A., Sims, D., Govender, D. and Prince, S. (2016) 'The T-box transcription factor 3 is a promising biomarker and a key regulator of the oncogenic phenotype of a diverse range of sarcoma subtypes', *Oncogenesis,* 5, pp. e199.

Yamaguchi, A., Goi, T., Taguchi, S., Ohtaki, N., Seki, K., Hirose, K., Nakagawara, G., Urano, T. and Furukawa, K. (1998) 'Clinical significance of serum levels of CD44 variant exons 8-10 protein in colorectal cancer', *J Gastroenterol,* 33(3), pp. 349-53.

Yarosh, W., Barrientos, T., Esmailpour, T., Lin, L., Carpenter, P. M., Osann, K., Anton-Culver, H. and Huang, T. (2008) 'TBX3 is overexpressed in breast cancer and represses p14 ARF by interacting with histone deacetylases', *Cancer Res,* 68(3), pp. 693-9.

Zhang, C., Li, H. R., Fan, J. B., Wang-Rodriguez, J., Downs, T., Fu, X. D. and Zhang, M. Q. (2006) 'Profiling alternatively spliced mRNA isoforms for prostate cancer classification', *BMC Bioinformatics,* 7, pp. 202.

Chapter 5

General Discussion

5 General Discussion

Through the use of the 21T series breast cancer cell lines representing distinct stages of progression (ADH, DCIS, IDC) in the 3D Matrigel system, our lab employed array-based transcriptional profiling to identify clinically-relevant genes which may be implicated in the DCIS to IDC transition (Souter et al., 2010). TBX3 was identified as 2.8-fold up-regulated in this transition (Souter et al., 2010). Based on these preliminary findings, as well as accumulating literature implicating TBX3 in the promotion of malignancy, I focused on elucidating the role of TBX3 isoforms in breast cancer progression.

I hypothesized that the transcriptional regulatory proteins TBX3iso1 and TBX3iso2 have distinct roles in breast cancer progression, which is likely mediated by their downstream transcriptional targets. The follow-up work to address my hypothesis was organized into three main chapters, dealing with **(1)** functionality of TBX3 isoforms *in vitro*, **(2)** mechanism by which TBX3 isoforms promote EMT, and **(3)** *in vivo* differences between TBX3iso1 and TBX3iso2.

(1) CHAPTER 2 – Examination of functional and phenotypic changes associated with modulation of TBX3 levels at various stages of breast cancer progression

I have shown that overexpression of TBX3iso1 and TBX3iso2 promotes progression in an *in vitro* model of early stage breast cancer. This occurs through alteration of several cellular properties including growth, survival, invasiveness, and the acquisition of an EMT phenotype. Prominent functional and phenotypic changes initially identified with overexpression of TBX3iso1 and TBX3iso2 were identical. I therefore focused on the molecular mechanism by which TBX3 isoforms promote invasiveness and induction of EMT in the next chapter, since the acquisition of an EMT phenotype is associated with several clinical parameters including reduced survival and chemo-resistance (Polyak and Weinberg, 2009, De Craene and Berx, 2013, Nieto et al., 2016).

(2) CHAPTER 3 – TBX3 promotes progression of pre-invasive breast cancer cells by inducing EMT and directly up-regulating SLUG

In order to assess the downstream mechanisms responsible for TBX3-induced EMT, I conducted ChIP-arrays and RNA-Seq to assess the direct transcriptional targets of TBX3iso1 and TBX3iso2, focusing on genes/pathways similarly regulated by both isoforms. I found that both TBX3 isoforms regulate expression of several EMT-related genes, including SLUG (directly) and TWIST1 (indirectly). Translating these *in vitro* molecular findings to clinical samples of early-stage breast cancers, I showed that TBX3 levels are up-regulated in CCLs, with a concomitant increase in SLUG and TWIST1 expression. This is predicted to promote proliferation and plasticity of early, pre-invasive lesions. TBX3 expression is maintained in a subset of low-grade DCIS, and was associated with the degree of invasiveness of Stage I breast cancers. Pathway analysis revealed that overexpression of both TBX3 isoforms induces altered expression of several proteases and protease inhibitors, which is consistent with the ability to degrade basement membrane and prime for early invasion. These events are facilitated by TBX3-induced and SLUG-dependent expression of pro-migratory molecules such as MMP14, fibronectin, and vimentin. My proposed model of TBX3-dependent advancement of low-grade DCIS to IDC is particularly relevant in the non-high grade, ER-positive pathway of progression.

(3) CHAPTER 4 – Isoform-specific promotion of breast cancer tumorigenicity by TBX3 involves induction of angiogenesis

My last chapter deals with elucidation of relevant mechanisms responsible for increased tumorigenicity of TBX3iso1 *in vivo* in nude mouse xenograft assays. Tumors generated from non-tumorigenic cells overexpressing TBX3iso1 were invasive and highly vascular. Mining of transcriptional differences in RNA-Seq data revealed up-regulation of pro-angiogenic transcripts with overexpression of TBX3iso1; this was not observed with overexpression of TBX3iso2. Importantly, overexpression of TBX3iso1 consistently resulted in up-regulation of OPN and HAS2 across three non-tumorigenic breast cancer cell lines, and increased hyaluronan retention in 21NT transfectants. Lastly, examination of the TCGA breast cancer cohort revealed a transcriptional shift during cancer progression, with an 8.1-fold higher TBX3iso1/TBX3iso2 ratio in tumors relative to control. This ratio was also associated with tumor grade and aggressive breast cancer subtypes.

5.1 Promotion of invasiveness by TBX3

Transcriptional profiling of isogenic DCIS-like and IDC-like cells grown in 3D Matrigel was previously conducted by our laboratory, in which TBX3 was identified as significantly up-regulated in the DCIS to IDC transition (Souter et al., 2010). At that time, the focus of TBX3-related studies within the literature was characterization of functional and phenotypic changes associated with TBX3 (irrespective of isoform), along with identification of transcriptional targets and validation across cancer subtypes. Additionally, much of the existing literature focused on TBX3 in embryogenesis and development of organ systems. TBX3 transcriptional targets are likely context dependent, as studies have shown that conclusions regarding effects mediated by TBX3 are often not consistent across cancer subtypes, let alone in the process of embryogenesis vs. tumorigenesis (Willmer et al., 2016a, Zhu et al., 2016).

My initial studies required characterization of TBX3-mediated effects in breast cancer, with validation across cell lines representing different molecular subtypes. I characterized the phenotypic and functional changes associated with overexpression of TBX3iso1 and TBX3iso2 in breast cancer cell lines. Changes associated with overexpression of TBX3 isoforms included increased cell survival, proliferation and colony-forming ability, decreased apoptosis, and increased invasiveness. In contrast, shRNA-mediated knockdown of total TBX3 levels in invasive 21MT-1 cells resulted in decreased colony formation rates, along with decreased invasiveness. Throughout my studies, overexpression of either TBX3iso1 or TBX3iso2 resulted in increased invasiveness, as shown by transwell invasion assays, along with *in vitro* invadopodia formation, and *in vivo* extravasation and invadopodia formation assays within the CAM model. Use of the CAM model further aided in demonstrating changes in invasiveness between 21MT-1 transductant cells (shTBX3 21MT-1 and shLUC 21MT-1), as we were unable to use them in traditional *in vitro* migration and invasion assays due to the larger size of the cells. The inclusion of several layers of validation regarding *in vivo* invasiveness as well as several methods of detecting invadopodia formation are novel findings, further supporting the existing literature regarding TBX3-induced invasiveness across several cancer types (Rodriguez et al., 2008, Peres et al., 2010, Willmer et al., 2016a).

Initiation of invadopodia formation commences through the binding of growth factor ligands to their cognate receptor, leading to activation of Src kinase required for induction of

invadopodia-specific proteins (Murphy and Courtneidge, 2011, Burger et al., 2014). Several growth factors (i.e. TGF-ß, FGF, Wnts) are able to induce expression of TBX3 (Renard et al., 2007, Fillmore et al., 2010, Li et al., 2013). I have shown that overexpression of either TBX3iso1 or TBX3iso2 leads to up-regulation of Src at the mRNA and protein level. The activity of Src is modulated through phosphorylation at residues Y527 (inhibitory) and Y416 (activating) (Irtegun et al., 2013). Overexpression of TBX3iso1 and TBX3iso2 resulted in reduced phosphorylation at the inhibitory Y527 site suggesting increased functionality (Irtegun et al., 2013), with no change in phosphorylation at Y416. Several proteases are also enriched within invadopodia structures, including MMP2, MMP9 and MMP14 (Weaver, 2006). Importantly, both TBX3iso1 and TBX3iso2 up-regulate MMP9 and MMP14 expression, and an increase in the active MMP2 was observed by gelatin zymography, further aiding in focal ECM degradation. I have also shown that the induction of the membrane-bound protease MMP14 by TBX3 is dependent on SLUG expression. My work has therefore added to the literature in terms of characterization of functionality of TBX3 isoforms, including promotion of invadopodia formation and focal substrate degradation. TBX3 may be an important regulator of invasiveness through enhancing invadopodia formation, as TBX3 is induced by several upstream growth factors, and modulates expression of downstream effectors important for the proper functionality of invadopodia.

5.2 Transcriptional targets of TBX3 – Cell Cycle Control

While transcriptional regulation by TBX3 is not well understood and continues to focus on its repressive effects on transcription (with much of the literature focusing on direct repression of $p14^{ARF}$ by TBX3), there are a few studies in which TBX3 was shown to directly up-regulate gene transcription. This includes direct up-regulation and binding to the TBE in the promoter of jun dimerization protein 2 (*JDP2*), a histone chaperone with an important role in differentiation and senescence, along with Connexin 43 (*GJA1*) and *GATA6*, which are important regulators of heart development (Jin et al., 2002, Nakade et al., 2009, Boogerd et al., 2011, Lu et al., 2011, Yao et al., 2014).

Through integrated analysis of coupled ChIP-array and RNA-Seq data for TBX3iso1 and TBX3iso2 overexpressing cells, I observed that approximately 2/3 of TBX3iso1 and TBX3iso2-bound genes were down-regulated, and 1/3 of TBX3iso1 and TBX3iso2-bound genes were up-regulated at the mRNA level. Noteworthy genes which were bound in ChIP-

arrays and transcriptionally up-regulated by both TBX3 isoforms include cyclin D (*CCND1*), cyclin E (*CCNE1*) and cell division cycle 25 homolog A (*CDC25A*), all of which are important cell cycle regulators, as well as SLUG (*SNAI2*), an EMT-inducing transcription factor. Importantly, the aforementioned cell cycle regulators are all involved in mediating the transition from G1 to S phase. The CDC25A phosphatase removes the inhibitory phosphate groups on the cyclin D-CDK4/6 and cyclin E-CDK2 complexes (Robert, 2015). Once activated, the major role of the cyclin D-CDK4/6 and cyclin E-CDK2 complexes is phosphorylation of the Rb protein (Robert, 2015). Rb is first phosphorylated by the cyclin D-CDK4/6 complex, resulting in reduced affinity of Rb for E2F (Robert, 2015). The cyclin E-CDK2 complex further phosphorylates Rb, ensuring maximal release of E2F (Robert, 2015). Upon release from Rb, E2F activates transcription of genes involved in DNA replication (Robert, 2015).

The processes associated with G1/S phase transition are negatively regulated by inhibitors of CDKs previously described: $p16^{INK4A}$ (*inhibitor of kinases;* inhibits cyclin D-CDK4/6 complex) and $p21^{CIP1}$ (*cyclin inhibitory protein;* inhibits cyclin D-CDK4/6, cyclin E-CDK2, cyclin A-CDK2 complexes). The well-described anti-senescence effect mediated by TBX3 through direct down-regulation of $p14^{ARF}$ (Brummelkamp et al., 2002, Lingbeek et al., 2002, Yarosh et al., 2008), $p16^{INK4A}$ (Kumar P et al., 2014), and $p21^{CIP1}$ (Hoogaars et al., 2008, Willmer et al., 2016b) are therefore amplified through direct up-regulation of cyclin D1, cyclin E1, and CDC25A, all of which are required for progression from G1 to S phase.

Interestingly, cyclin D is often up-regulated in breast cancer and is strongly expressed in ER+ breast cancers resistant to hormone therapy (Kenny et al., 1999, Hui et al., 2002, Hodges et al., 2003), displaying similar expression patterns with TBX3 (Fillmore et al., 2010). Additionally, up-regulation of cyclin E and CDC25A is associated with reduced survival in breast cancer (Cangi et al., 2000, Keyomarsi et al., 2002).

The various direct mechanisms whereby TBX3 controls expression of important mediators of cell cycle progression is summarized in **Figure 5.2.1**. As highlighted above, up-regulation of CDC25A is suggestive of increased activation of G1-phase cyclin-CDK complexes which are required for G1/S phase transition (Sandhu et al., 2000). Down-regulation of $p14^{ARF}$, $p16^{INK4A}$, and $p21^{CIP1}$ results in reduced inhibitory effects on G1-phase cyclin-CDK complexes. This increased expression and potentially increased activity of cyclin

D-CDK4/6 and cyclin E-CDK2 is expected to result in accelerated cell cycle progression and increased rates of proliferation (Masamha and Benbrook, 2009). TBX3 is also required for S/G2 phase transition, as depletion of TBX3 results in accumulation in S phase; the authors suggested that this may be mediated through TBX3-dependent down-regulation of $p21^{CIP1}$ (Willmer et al., 2015). TBX3 is therefore able to promote progression through both G1/S and S/G2 phase transitions, which is associated with increased proliferation rates. Indeed, these findings are in accordance with the widely-documented pro-proliferative effect associated with up-regulation of TBX3, as well as my findings of increased proliferation and growth rates in 3D Matrigel with overexpression of TBX3iso1 and TBX3iso2 reported in Chapter 1 (Lee et al., 2007a, Platonova et al., 2007, Miao et al., 2016, Willmer et al., 2016b, Wu et al., 2017).

While binding events for *CCND1*, *CCNE1* and *CDC25A* contain significant FDR-corrected statistical values, and are transcriptionally up-regulated with overexpression of both TBX3 isoforms, further validation studies are needed to assess whether these binding events are direct and occur in breast cancer cell lines and various other cancer cell lines. Further elucidation of direct transcriptional targets of TBX3 is important in order to understand the functionality of TBX3 with regards to transcriptional regulation. This should be assessed in an isoform-specific context.

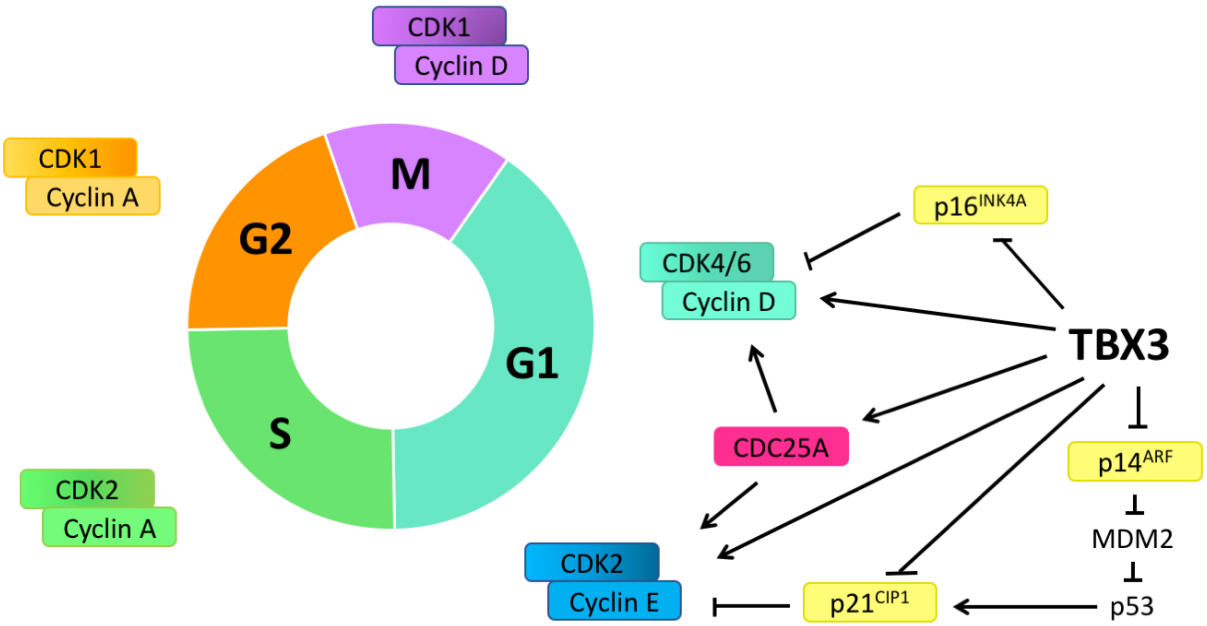

Figure 5.2.1 – Proposed model of control of cell cycle progression by TBX3.

5.3 Transcriptional targets of TBX3 – EMT Regulation

Through assessment of gene expression changes associated with overexpression of TBX3iso1 or TBX3iso2 relative to the control, there were prominent alterations in expression of EMT and invasion-associated genes. This was observed in the high-throughput RNA-Seq data, and recapitulated in the qRT-PCR arrays and through various functional assays. While the association between TBX3 and an EMT phenotype has been previously suggested through profiling of epithelial and mesenchymal markers (Humtsoe et al., 2012, Shan et al., 2015, Miao et al., 2016) along with direct down-regulation of E-cadherin (Rodriguez et al., 2008, Dong et al., 2018), direct modulation of transcription factors and inducers of EMT by TBX3 has not been reported and is therefore a novel finding.

Although several genes involved in the cell cycle were both bound by and up-regulated by both TBX3 isoforms (according to ChIP-array and RNA-Seq data, respectively), I focused on TBX3-induced up-regulation of SLUG transcript levels due to its well-documented role in EMT (Barrallo-Gimeno and Nieto, 2005, Humtsoe et al., 2012, Phillips and Kuperwasser, 2014). ChIP-array analysis showed that TBX3iso1 and TBX3iso2 bind near an intron-exon junction of the SLUG (*SNAI2*) gene. Through merging of ChIP-array data with Encyclopedia of DNA Elements (ENCODE) files, this binding site was revealed to possess a highly conserved TBE, located within the 5’ end of exon 2. This identified TBE overlaps with an RNA polymerase II (Pol II) binding site and a DNase I hypersensitivity (DHS) region. This binding has been validated by ChIP qRT-PCR, showing that overexpression of TBX3iso1 or TBX3iso2 leads to their enrichment at this genomic location. Since this binding is not located in an upstream promoter region and rather is located near an intron/exon boundary, my interpretation is that TBX3 promotes transcriptional elongation of the SLUG transcript and prevents stalling of Pol II transcriptional machinery. The effect of these proposed molecular events would lead to elevated SLUG transcript levels, as shown by RNA-Seq, and validated by qRT-PCR and western blot.

High throughput experiments utilizing Pol II ChIP-Seq (Guenther et al., 2007, Muse et al., 2007, Zeitlinger et al., 2007) and global run-on sequencing (GRO)-Seq to assess sites of active transcription (Core et al., 2008, Larschan et al., 2011, Min et al., 2011) have revealed that Pol II pausing is a widespread and critical rate-limiting step governing gene transcription (Kwak and Lis, 2013). The prolonged binding of transcription factors, along with Pol II stalling

contributes to maintenance of an open chromatin structure, and is therefore a feature of active, highly-regulated genes (Fuda et al., 2009, Gilchrist et al., 2010, Jonkers and Lis, 2015). Assessment of TBX3 binding sites across the genome has identified a significant overlap with Pol II binding sites from the ENCODE database; this may be inherent due to close associations with transcription factors and Pol II, and/or a byproduct of promoter array usage and enrichment of promoter binding sites which are also occupied by Pol II.

This identified TBX3 binding site in the *SNAI2* gene contains a DHS region, which is associated with open and transcriptionally active chromatin. DHS is often used as markers of cis-regulatory elements including promotors, enhancers, and silencers (Lewin et al., 2011). The ENCODE DNase-Seq datasets revealed a high degree of overlap of DHS regions for the TBX3 binding site across a panel of 125 diverse cell and tissue types (identified in 41/125 cell lines) (Thurman et al., 2012). This region may therefore act as an enhancer and regulate transcription of the *SNAI2* gene through binding of various co-activators and/or transcription factors such as TBX3. Enhancers are cis-regulatory elements that promote transcription of nearby gene(s) through binding of trans-activating transcription factors, and by interacting with proximal regulatory factors through chromatin looping mechanisms (Lewin et al., 2011). While enhancers play a modest role on transcriptional initiation, they are able to increase elongation efficiency (Krumm et al., 1993, Yankulov et al., 1994, Krumm et al., 1995). The process of enhanced transcriptional elongation may be mediated through 3D chromatin looping, which brings promoters and enhancers into close proximity, attracting transcription factors and promoting continuation of transcriptional elongation (Ghavi-Helm et al., 2014, Heinz et al., 2015, Jonkers and Lis, 2015). Some transcription factors (such as MYC and NF_KB) are also able to increase Pol II efficiency through recruiting elongation factors (Yankulov et al., 1994, Rahl et al., 2010, Danko et al., 2013, Diamant and Dikstein, 2013, Kwak and Lis, 2013). TBX3 may therefore regulate expression of SLUG through the promotion of transcriptional elongation of SLUG transcripts, and prevention of Pol II stalling. Further studies are needed in order to substantiate this hypothesis, as association with enhancers and non-promoter binding of TBX3 have not been reported.

TBX3 may also promote SLUG expression through indirect mechanisms as well. As degradation of SLUG is induced through binding of p53 and $p21^{CIP1}$ (Kim et al., 2014), direct down-regulation of $p21^{CIP1}$ by TBX3 may also result in reduced degradation of SLUG.

5.4 TBX3 in precursor lesions – CCLs and DCIS

My findings from Chapter 3 represent the first study to assess TBX3 expression by immunohistochemistry separately in various cell compartments, and the first in-depth TBX3 IHC study in breast cancer. Elevated expression of EMT-transcription factors, including TBX3, SLUG and TWIST1 in CCLs was an interesting and unexpected finding. CCLs, and particularly the FEA variant, are on a histological continuum with ADH, DCIS and IDC, representing the earliest morphological precursor in the LG breast cancer progression pathway (Wellings and Jensen, 1973, Wellings et al., 1975, Lee et al., 2006, Abdel-Fatah et al., 2008, Feeley and Quinn, 2008, Turashvili et al., 2008). As such, CCLs possess increased levels of genomic aberrations including low rates of allelic imbalances relative to morphologically normal breast epithelial cells (Simpson et al., 2005, Dabbs et al., 2006, Turashvili et al., 2008, Bürger et al., 2013, Bombonati and Sgroi, 2011), often coexist with both precursor lesions (ADH, DCIS) and IDC (Go et al., 2012), and are frequently detected as abnormalities on mammographically screening (Lerwill, 2008). It has been demonstrated that loss of 16q, an early mutational event associated with progression along the LG breast cancer pathway, occurs in similar rates across FEA, ADH and DCIS; the degree of genomic instability, however, increases with further progression (O'Connell et al., 1998, Moinfar et al., 2000, Simpson et al., 2005, Larson et al., 2006, Gao et al., 2009).

CCLs are typically ER+, PR+, HER2-, and prominently express increased levels of Ki67, Bcl2 and cyclin D, thereby promoting a proliferative and anti-apoptotic profile (Polosukhin, 1999, Vincent-Salomon, 2003, Tremblay et al., 2005, Simpson et al., 2005, Dabbs et al., 2006, Lee et al., 2006, Noel et al., 2006, Bombonati and Sgroi, 2011). Interestingly, previous studies have reported increased ER expression in CCLs relative to adjacent morphologically normal breast epithelial cells (Tremblay et al., 2005, Lee et al., 2006, Lee et al., 2007b, Abdel-Fatah et al., 2008). Downstream targets of ER include several genes involved in proliferation and apoptosis (Gompel et al., 2000, Anderson and Clarke, 2004), and it has therefore been suggested that the pro-proliferative and anti-apoptotic profile in CCLs may be stimulated by estrogen and mediated through ER (Wellings et al., 1975, Lee et al., 2007b). Overexpression of ER-α in breast epithelial cells of transgenic mice results in rapid development of hyperplasia and DCIS, with occasional progression to invasive carcinoma (Frech et al., 2005). These studies suggest that the effects mediated by estrogen

through ER may be partially responsible for the development of CCLs, as well as subsequent progression to more advanced lesions (Frech et al., 2005).

Our group, and others, have shown that TBX3 expression is tightly correlated with ER expression (Fan et al., 2004, Fillmore et al., 2010). It is intriguing to speculate whether ER and TBX3 are coordinately expressed to similar degrees in precursor lesions of the breast. Indeed, the TBX3 promoter possesses multiple half-estrogen response elements (Fan et al., 2004), and administration of endogenous estradiol induces expression of TBX3 (Fillmore et al., 2010). Additionally, TBX3 is required for the formation of ER+ mammary epithelial cells (Kunasegaran et al., 2014), showing reciprocal induction of gene expression between TBX3 and ER. The reported benefits of anti-estrogen therapies such as tamoxifen for patients with precursor lesions (Fisher et al., 1999, Esteva and Hortobagyi, 2004, Allred et al., 2012, Coopey et al., 2012) may work, in part, through inhibition of TBX3 expression at this early, critical stage of tumorigenesis. While this is only speculative, more work is needed in order to fully establish this link, including examination of TBX3 expression in epithelial cell compartments (FEA, ADH and DCIS) in patients who have undergone treatment with tamoxifen.

Aside from up-regulation of ER expression, there is currently limited knowledge regarding transcriptional profiles of CCLs. Through micro-dissection of histologically normal epithelial cells and CCLs, Lee et al. conducted microarray analysis in order to examine changes in gene expression profiles and associated molecular pathways altered in CCLs (Lee et al., 2007b). They reported that CCLs frequently reactivate pathways involved in embryonic development and suppress pathways involved in terminal differentiation (Lee et al., 2007b). My finding of elevated expression of EMT transcription factors, particularly the estrogen responsive transcription factor TBX3 with critical roles in development, is in agreement with the aforementioned studies. In addition to the high throughput transcriptional studies, my IHC studies have shed light on the elevated expression of EMT transcription factors in CCLs, including TBX3, SLUG and TWIST1. It is possible that TBX3 is inducing expression of SLUG and TWIST1 at this early stage of progression, as expressions of all aforementioned markers is coordinately elevated. Although associations in expression has been shown *in vitro*, this may not necessarily hold true *in vivo.* Sophisticated experiments involving temporal induction of TBX3 in mouse mammary glands, and assessment of induced

genes at various stages may be the best way to answer this experimental question. While one may obtain correlational data through assessment of expression of particular markers through IHC, one cannot conclude that direct transcriptional up-regulation of particular genes is occurring in a particular lesion *in vivo.*

The prevailing view is that activation of a single oncogene is insufficient to drive cancer progression; cooperation with other oncogenes and/or mutational events is frequently employed by EMT transcription factors in the process of malignant transformation (Ansieau et al., 2008, Smit and Peeper, 2010, Morel et al., 2012, Tran et al., 2012, Puisieux et al., 2014). For example, while TBX3 expression on its own is usually not enough to impart malignant properties to genomically stable cells, overexpression of MYC or oncogenic H-Ras^{Val17} with TBX3 (but not by themselves), protects cells from apoptosis through inhibition of p14^{ARF} (Carlson et al., 2002). Additionally, up-regulation of EMT transcription factor reduces the number of genetic events required for malignant transformation of breast epithelial cells, allowing cells to overcome onco-suppressive mechanisms (Morel et al., 2012, De Craene and Berx, 2013, Puisieux et al., 2014). Increased ER expression and downstream signaling is also permissive for the accumulation of genetic alterations (Lee et al., 2007b). The aforementioned processes, acting together and regulated by TBX3, may lead to promotion of an EMT phenotype at early stages, and allow for full progression to IDC.

Expression of TBX3, SLUG and TWIST1 is up-regulated in CCLs and maintained in some DCIS lesions, and may impart additional properties associated with induction of invasiveness. In my evaluation of DCIS lesions with and without associated invasion, there was no difference in TBX3 expression between Stage 0 and Stage I samples. I did, however, observe a strong positive correlation between TBX3 expression in the DCIS lesion and size of the invasive focus. Importantly, I showed that elevated TBX3 expression within LG DCIS was associated with larger invasive carcinomas across Stage I cancers. While TBX3 itself was not useful in predicting invasion, it may have an association with the degree of invasiveness, as observed in my IHC, functional and molecular studies. These findings suggests that there are potentially other co-factors that may be acting in concert with TBX3 in the promotion of invasiveness.

Interestingly, pathway analysis of transcripts altered by both TBX3iso1 and TBX3iso2 revealed significant enrichment of proteases and protease inhibitors. This transcriptional event is particularly important at the pre-invasive stage, as focal disruption of the basement membrane has been shown to coincide with the dissolution of the myoepithelial cell layer and progression of DCIS to IDC (Man et al., 2003, Hu et al., 2008). Proteases secreted by tumor cells are able to progressively destroy the basement membrane, which leads to dissolution of the myoepithelial cell layer (Hu et al., 2008). This is important, as additional mutations within tumor cells of DCIS are not required for progression; the loss of basement membrane, myoepithelial cell dissolution, and loss of epithelial cell organization and polarity is sufficient to promote this transition (Hu et al., 2008). Previous studies have reported that MMP14 is amongst the main regulators of the basement membrane transmigration process *in vivo* (Hotary et al., 2006), likely through activation of MMP2 (Duffy et al., 2000). Through my studies I have shown that overexpression of TBX3 isoforms results in increased MMP14 expression, and induction of MMP14 is dependent on SLUG. Additionally, I have shown that overexpression of both TBX3 isoforms is associated with increased activity of MMP2.

In conclusion, I have proposed a unique pathway in which TBX3 promotes progression through advancement of low-grade DCIS to invasive carcinoma, as depicted in **Figure 3.3.6** of Chapter 3. This model is particularly relevant in patients with ER+, non-high grade precursor lesions (CCL, DCIS), in which overexpression of TBX3 induces other molecular regulators of EMT (including SLUG and TWIST1). Additionally, TBX3 up-regulates expression of several proteases (i.e. MMP9, MMP14, uPa), and down-regulates expression of several protease inhibitors (i.e. CST6). These transcriptional changes mediated by TBX3 set the stage for basement membrane breakdown and invasion into adjacent stroma. Further studies are needed in order to assess whether TBX3 expression may provide reliable risk stratification for patients diagnosed with DCIS. This may potentially be conducted in concert with multiple biomarkers and/or multi-parameter gene expression assays in order to increase predictive and/or prognostic value.

5.5 TBX3 in IDC

I have demonstrated significant differences in tumorigenicity between the TBX3 isoforms through nude mouse xenograft experiments, which was a surprising and novel finding. Although existing literature has focused solely only one isoform of TBX3 (often the clone used is not specified), a few existing studies have suggested that the two TBX3 isoforms have differential functionality (Stennard et al., 1999, Fan et al., 2004, Lee et al., 2007a, DeBenedittis and Jiao, 2011, Zhao et al., 2014). Through mining of differences in transcriptional profiles between TBX3iso1 and TBX3iso2 overexpressing cells and conducting pathway analysis, I have reported that overexpression of TBX3iso1 is associated with a pro-angiogenic gene signature.

The effects mediated by TBX3 isoforms with regard to EMT and promotion of invasiveness were identical throughout my findings in Chapter 2 and Chapter 3. Due to these similarities, along with an absence of commercially available isoform-specific antibodies for TBX3, I focused on total TBX3 protein expression in my IHC study. While I have shown that expression of total TBX3 levels are up-regulated in early stages of breast cancer progression, the relative abundance of each isoform is unknown. As TBX3iso1 is associated with the promotion of angiogenesis, it may therefore be helpful at later stages of tumor development.

The process of angiogenesis is vital for tumor growth, since solid cancers must form a blood supply if they are to grow beyond 1-2 mm in size; tumor vascularization thus allows for acquisition of nutrients, oxygen perfusion, and systemic spread (Hanahan and Weinberg, 2000, Knowles and Selby, 2005). Indeed, the xenograft tumors formed by TBX3iso1 overexpressing cells were highly vascular, as gauged by microvascular density counts. As observed by *in vitro* tubule formation assays, pro-angiogenic soluble factors are released from cells overexpressing TBX3iso1 that are functional in activating endothelial cells. On the contrary, conditioned media from cells overexpressing TBX3iso2 had similar effects on endothelial cells as the empty vector control. Importantly, TBX3iso1 (but not TBX3iso2) is able to up-regulate expression of OPN and HAS2, and lead to increased pericellular HA retention. The aforementioned transcriptional changes were robust and observed across three cell lines, with expression of OPN and HAS2 often down-regulated with overexpression of TBX3iso2. It is well documented that elevated levels of OPN and HA within the microenvironment are able to promote angiogenesis *in vivo* through binding of OPN (via

integrins, CD44) and HA (via CD44) on endothelial cells, thereby promoting their migration, proliferation, and vascular channel formation (Brooks et al., 1994, Senger et al., 1996, Trochon et al., 1996, Griffioen et al., 1997, Arap et al., 1998, Scatena et al., 1998, Bayless et al., 2000, Savani et al., 2001). These binding and downstream signaling events leading to vascularization are permissive to tumor growth, and likely allowed for the observed exponential growth of tumors. Based on the kinetics of tumor growth which I reported in Chapter 4, as well as well as my findings of the pro-angiogenic function of TBX3iso1, the enhanced growth and tumorigenicity is likely due to the process of angiogenesis. This is in agreement with the findings of Shirinifard et al., who conducted 3D simulations of tumor growth, reporting that exponential growth of tumor cells at late stages of tumor development occurs only in vascularized tumors, whereas tumor growth in avascular tumors did not exceed linear growth values (Shirinifard et al., 2009). Further studies are required for elucidation of differential targets of TBX3iso1 and TBX3iso2, and assessment and validation of which direct targets downstream of TBX3iso1 may be responsible for up-regulation of pro-angiogenic factors and thus vascular channel formation by endothelial cells.

My mining of the TCGA breast cancer dataset has revealed a transcriptional shift in breast cancer progression, with increased TBX3iso1/TBX3iso2 expression in cancer tissues relative to normal breast tissue. This shift of increased TBX3iso1 expression was associated with several clinicopathological parameters, including high grade and more aggressive breast cancer subtypes. Interestingly, these are the opposite characteristics identified for TBX3 expression in breast cancer. I believe that this splice shift is due to changes in upstream splicing machinery, as several splice regulatory proteins are up-regulated in breast cancers (Watermann et al., 2006, Huang et al., 2007, Skotheim and Nees, 2007, Venables et al., 2008). Differences in breast cancer specific alternative splicing events have been observed between grade 1 and grade 3 breast tumors as well, with a distinct trend towards exon loss of several transcripts in ER- tumors (Venables et al., 2008). These splicing changes were not associated with differences in combined expression of alternatively spliced transcripts (and as such TBX3 expression is low in ER- tumors) (Venables et al., 2008). It has been strongly suggested that functional selection for oncogenic splice variants occurs within tumors (Venables et al., 2008), and enhanced expression of TBX3iso1 may be an adaptive oncogenic mechanism. While the splice factors which are associated with an elevated TBX3iso1/TBX3iso2 ratio are unknown, they appear to be associated with aggressive breast tumors.

5.6 Future Studies

To summarize, I have identified that the transcriptional regulator TBX3 is highly expressed in precursor lesions of the breast including CCLs and DCIS, in a manner similarly implicated in the context of other cancer types (Fan et al., 2004, Hansel et al., 2004, Lomnytska et al., 2006, Lyng et al., 2006, Rodriguez et al., 2008, Yarosh et al., 2008, Cavard et al., 2009, Gudmundsson et al., 2010, Souter et al., 2010, Witte, 2010, Begum and Papaioannou, 2011, Miao et al., 2016). TBX3 expression is elevated in ER+, PR+, low-grade breast cancers, and is significantly associated with the degree of invasiveness in Stage I breast tumors. These studies have provided critical information regarding the stages in which expression of nuclear-localized TBX3 is up-regulated in cancer cells, and may be transcriptionally active in the promotion of tumorigenesis within the breast. Based on my IHC studies, TBX3 appears to be promoting progression of precursor lesions (CCLs, DCIS) through the low-grade molecular pathway.

Further exploration of possible target genes that are regulated by and downstream of TBX3 isoforms should be conducted in order to identify and validate direct targets which are critical to cellular invasion. These gene products may themselves be potential targets for breast cancer therapy. This may include validation of identified cell-cycle proteins and/or mediators of EMT (such as SLUG) in other breast cancer cell lines, and further validation in cell lines representing other cancer subtypes. Initial validation in a breast cancer context is important, as functional effects mediated by TBX3, as well as direct transcriptional targets, are often described as context-dependent and may vary across cancer subtypes (Willmer et al., 2016a, Zhu et al., 2016, Willmer et al., 2017).

An important follow-up experiment to my findings would be micro-dissection of the DCIS cross-sections (Stage 0 and Stage I) which express high vs. low TBX3 to assess for enrichment of transcripts associated with elevated TBX3 expression and invasiveness. Importantly, elevated TBX3 expression in DCIS of Stage I breast cancer samples is associated with the degree of invasiveness. Critical information may therefore be obtained through these transcriptional profiling experiments, which may link elevated and co-ordinate expression of TBX3 and another potential co-factor with invasiveness of breast cancers.

As I have reported significant differences between TBX3 isoforms in the promotion of angiogenesis and *in vivo* tumorigenesis, high-resolution analysis of differential transcriptional targets of TBX3iso1 and TBX3iso2 is required to elucidate which genes may be responsible for mediating this phenotype, with emphasis on genes involved in facilitating up-regulation of OPN (as TBX3iso1 does not directly bind the *SPP1* gene). Additionally, as the T-box domain facilitates several protein-protein interactions (Hoogaars et al., 2008, Lu et al., 2010), there are likely differences in which proteins TBX3iso1 and TBX3iso2 interact with. This has been suggested by limited studies (Zhao et al., 2014), but would be interesting to explore further. While these studies likely do not possess immediate translatable findings, they would be important in fully understanding the functional differences between TBX3 isoforms.

In conclusion, my thesis research has established that TBX3 is an important mediator of invasiveness in early-stage breast cancers. My proposed model is particularly relevant for luminal A breast cancers, which represents approximately 70% of all breast cancer diagnoses (Howlader et al., 2014). My findings will permit further understanding of expression profiles of precursor lesions, including CCLs and DCIS. An understanding of such molecular alterations and associated transcriptional profiles is essential in order to provide prognostic and predictive information regarding the propensity to progress to IDC, thereby avoiding progression to stages associated with reduced survival. Decisions regarding clinical management should be done on a per-patient basis based on the intrinsic characteristics of the tumor. Assessment of TBX3 expression, isoform ratios, and/or downstream signaling pathways in patients with low-grade DCIS may aid in this endeavor, although validation and follow-up studies are required. The validation cohort would be very important, as the single study which assessed the natural progression of LG DCIS across a median of 31 years highlighted that the risk of invasive recurrence is greatest within the first fifteen years after diagnosis (Sanders et al., 2005). Critical information may therefore be obtained through these profiling experiments, which may link elevated and co-ordinate expression of TBX3 and another potential co-factor with invasiveness of breast cancers.

5.7 References

Abdel-Fatah, T. M., Powe, D. G., Hodi, Z., Reis-Filho, J. S., Lee, A. H. and Ellis, I. O. (2008) 'Morphologic and molecular evolutionary pathways of low nuclear grade invasive breast cancers and their putative precursor lesions: further evidence to support the concept of low nuclear grade breast neoplasia family', *Am J Surg Pathol,* 32(4), pp. 513-23.

Allred, D. C., Anderson, S. J., Paik, S., Wickerham, D. L., Nagtegaal, I. D., Swain, S. M., Mamounas, E. P., Julian, T. B., Geyer, C. E., Costantino, J. P., Land, S. R. and Wolmark, N. (2012) 'Adjuvant tamoxifen reduces subsequent breast cancer in women with estrogen receptor-positive ductal carcinoma in situ: a study based on NSABP protocol B-24', *J Clin Oncol,* 30(12), pp. 1268-73.

Anderson, E. and Clarke, R. B. (2004) 'Steroid receptors and cell cycle in normal mammary epithelium', *J Mammary Gland Biol Neoplasia,* 9(1), pp. 3-13.

Ansieau, S., Bastid, J., Doreau, A., Morel, A. P., Bouchet, B. P., Thomas, C., Fauvet, F., Puisieux, I., Doglioni, C., Piccinin, S., Maestro, R., Voeltzel, T., Selmi, A., Valsesia-Wittmann, S., Caron de Fromentel, C. and Puisieux, A. (2008) 'Induction of EMT by twist proteins as a collateral effect of tumor-promoting inactivation of premature senescence', *Cancer Cell,* 14(1), pp. 79-89.

Arap, W., Pasqualini, R. and Ruoslahti, E. (1998) 'Cancer treatment by targeted drug delivery to tumor vasculature in a mouse model', *Science,* 279(5349), pp. 377-80.

Barrallo-Gimeno, A. and Nieto, M. A. (2005) 'The Snail genes as inducers of cell movement and survival: implications in development and cancer', *Development,* 132(14), pp. 3151-61.

Bayless, K. J., Salazar, R. and Davis, G. E. (2000) 'RGD-dependent vacuolation and lumen formation observed during endothelial cell morphogenesis in three-dimensional fibrin matrices involves the alpha(v)beta(3) and alpha(5)beta(1) integrins', *Am J Pathol,* 156(5), pp. 1673-83.

Begum, S. and Papaioannou, V. E. (2011) 'Dynamic expression of Tbx2 and Tbx3 in developing mouse pancreas', *Gene Expr Patterns,* 11(8), pp. 476-83.

Bombonati, A. and Sgroi, D. C. (2011) 'The molecular pathology of breast cancer progression', *J Pathol,* 223(2), pp. 307-17.

Boogerd, C. J., Wong, L. Y., van den Boogaard, M., Bakker, M. L., Tessadori, F., Bakkers, J., 't Hoen, P. A., Moorman, A. F., Christoffels, V. M. and Barnett, P. (2011) 'Sox4 mediates Tbx3 transcriptional regulation of the gap junction protein Cx43', *Cell Mol Life Sci,* 68(23), pp. 3949-61.

Brooks, P. C., Montgomery, A. M., Rosenfeld, M., Reisfeld, R. A., Hu, T., Klier, G. and Cheresh, D. A. (1994) 'Integrin alpha v beta 3 antagonists promote tumor regression by inducing apoptosis of angiogenic blood vessels', *Cell,* 79(7), pp. 1157-64.

Brummelkamp, T. R., Kortlever, R. M., Lingbeek, M., Trettel, F., MacDonald, M. E., van Lohuizen, M. and Bernards, R. (2002) 'TBX-3, the gene mutated in Ulnar-Mammary Syndrome, is a negative regulator of p19ARF and inhibits senescence', *J Biol Chem,* 277(8), pp. 6567-72.

Bürger, H., de Boer, M., van Diest, P. J. and Korsching, E. (2013) 'Chromosome 16q loss--a genetic key to the understanding of breast carcinogenesis', *Histol Histopathol,* 28(3), pp. 311-20.

Burger, K. L., Learman, B. S., Boucherle, A. K., Sirintrapun, S. J., Isom, S., Díaz, B., Courtneidge, S. A. and Seals, D. F. (2014) 'Src-dependent Tks5 phosphorylation regulates invadopodia-associated invasion in prostate cancer cells', *Prostate,* 74(2), pp. 134-48.

Cangi, M. G., Cukor, B., Soung, P., Signoretti, S., Moreira, G., Ranashinge, M., Cady, B., Pagano, M. and Loda, M. (2000) 'Role of the Cdc25A phosphatase in human breast cancer', *J Clin Invest,* 106(6), pp. 753-61.

Carlson, H., Ota, S., Song, Y., Chen, Y. and Hurlin, P. J. (2002) 'Tbx3 impinges on the p53 pathway to suppress apoptosis, facilitate cell transformation and block myogenic differentiation', *Oncogene,* 21(24), pp. 3827-35.

Cavard, C., Audebourg, A., Letourneur, F., Audard, V., Beuvon, F., Cagnard, N., Radenen, B., Varlet, P., Vacher-Lavenu, M. C., Perret, C. and Terris, B. (2009) 'Gene expression profiling provides insights into the pathways involved in solid pseudopapillary neoplasm of the pancreas', *J Pathol,* 218(2), pp. 201-9.

Coopey, S. B., Mazzola, E., Buckley, J. M., Sharko, J., Belli, A. K., Kim, E. M., Polubriaginof, F., Parmigiani, G., Garber, J. E., Smith, B. L., Gadd, M. A., Specht, M. C., Guidi, A. J., Roche, C. A. and Hughes, K. S. (2012) 'The role of chemoprevention in modifying the risk of breast cancer in women with atypical breast lesions', *Breast Cancer Res Treat,* 136(3), pp. 627-33.

Core, L. J., Waterfall, J. J. and Lis, J. T. (2008) 'Nascent RNA sequencing reveals widespread pausing and divergent initiation at human promoters', *Science,* 322(5909), pp. 1845-8.

Dabbs, D. J., Carter, G., Fudge, M., Peng, Y., Swalsky, P. and Finkelstein, S. (2006) 'Molecular alterations in columnar cell lesions of the breast', *Mod Pathol,* 19(3), pp. 344-9.

Danko, C. G., Hah, N., Luo, X., Martins, A. L., Core, L., Lis, J. T., Siepel, A. and Kraus, W. L. (2013) 'Signaling pathways differentially affect RNA polymerase II initiation, pausing, and elongation rate in cells', *Mol Cell,* 50(2), pp. 212-22.

De Craene, B. and Berx, G. (2013) 'Regulatory networks defining EMT during cancer initiation and progression', *Nat Rev Cancer,* 13(2), pp. 97-110.

DeBenedittis, P. and Jiao, K. (2011) 'Alternative splicing of T-box transcription factor genes', *Biochem Biophys Res Commun,* 412(4), pp. 513-7.

Diamant, G. and Dikstein, R. (2013) 'Transcriptional control by NF-κB: elongation in focus', *Biochim Biophys Acta,* 1829(9), pp. 937-45.

Dong, L., Dong, Q., Chen, Y., Li, Y., Zhang, B., Zhou, F., Lyu, X., Chen, G. G., Lai, P., Kung, H. F. and He, M. L. (2018) 'Novel HDAC5-interacting motifs of Tbx3 are essential for the suppression of E-cadherin expression and for the promotion of metastasis in hepatocellular carcinoma', *Signal Transduct Target Ther,* 3, pp. 22.

Duffy, M. J., Maguire, T. M., Hill, A., McDermott, E. and O'Higgins, N. (2000) 'Metalloproteinases: role in breast carcinogenesis, invasion and metastasis', *Breast Cancer Res,* 2(4), pp. 252-7.

Esteva, F. J. and Hortobagyi, G. N. (2004) 'Prognostic molecular markers in early breast cancer', *Breast Cancer Res,* 6(3), pp. 109-18.

Fan, W., Huang, X., Chen, C., Gray, J. and Huang, T. (2004) 'TBX3 and its isoform TBX3+2a are functionally distinctive in inhibition of senescence and are overexpressed in a subset of breast cancer cell lines', *Cancer Res,* 64(15), pp. 5132-9.

Feeley, L. and Quinn, C. M. (2008) 'Columnar cell lesions of the breast', *Histopathology,* 52(1), pp. 11-9.

Fillmore, C. M., Gupta, P. B., Rudnick, J. A., Caballero, S., Keller, P. J., Lander, E. S. and Kuperwasser, C. (2010) 'Estrogen expands breast cancer stem-like cells through paracrine FGF/Tbx3 signaling', *Proc Natl Acad Sci U S A,* 107(50), pp. 21737-42.

Fisher, B., Dignam, J., Wolmark, N., Wickerham, D. L., Fisher, E. R., Mamounas, E., Smith, R., Begovic, M., Dimitrov, N. V., Margolese, R. G., Kardinal, C. G., Kavanah, M. T., Fehrenbacher, L. and Oishi, R. H. (1999) 'Tamoxifen in treatment of intraductal breast cancer: National Surgical Adjuvant Breast and Bowel Project B-24 randomised controlled trial', *Lancet,* 353(9169), pp. 1993-2000.

Frech, M. S., Halama, E. D., Tilli, M. T., Singh, B., Gunther, E. J., Chodosh, L. A., Flaws, J. A. and Furth, P. A. (2005) 'Deregulated estrogen receptor alpha expression in mammary epithelial cells of transgenic mice results in the development of ductal carcinoma in situ', *Cancer Res,* 65(3), pp. 681-5.

Fuda, N. J., Ardehali, M. B. and Lis, J. T. (2009) 'Defining mechanisms that regulate RNA polymerase II transcription in vivo', *Nature,* 461(7261), pp. 186-92.

Gao, Y., Niu, Y., Wang, X., Wei, L. and Lu, S. (2009) 'Genetic changes at specific stages of breast cancer progression detected by comparative genomic hybridization', *J Mol Med (Berl),* 87(2), pp. 145-52.

Ghavi-Helm, Y., Klein, F. A., Pakozdi, T., Ciglar, L., Noordermeer, D., Huber, W. and Furlong, E. E. (2014) 'Enhancer loops appear stable during development and are associated with paused polymerase', *Nature,* 512(7512), pp. 96-100.

Gilchrist, D. A., Dos Santos, G., Fargo, D. C., Xie, B., Gao, Y., Li, L. and Adelman, K. (2010) 'Pausing of RNA polymerase II disrupts DNA-specified nucleosome organization to enable precise gene regulation', *Cell,* 143(4), pp. 540-51.

Go, E. M., Tsang, J. Y., Ni, Y. B., Yu, A. M., Mendoza, P., Chan, S. K., Lam, C. C., Lui, P. C., Tan, P. H. and Tse, G. M. (2012) 'Relationship between columnar cell changes and low-grade carcinoma in situ of the breast--a cytogenetic study', *Hum Pathol,* 43(11), pp. 1924-31.

Gompel, A., Somaï, S., Chaouat, M., Kazem, A., Kloosterboer, H. J., Beusman, I., Forgez, P., Mimoun, M. and Rostène, W. (2000) 'Hormonal regulation of apoptosis in breast cells and tissues', *Steroids,* 65(10-11), pp. 593-8.

Griffioen, A. W., Coenen, M. J., Damen, C. A., Hellwig, S. M., van Weering, D. H., Vooys, W., Blijham, G. H. and Groenewegen, G. (1997) 'CD44 is involved in tumor angiogenesis; an activation antigen on human endothelial cells', *Blood,* 90(3), pp. 1150-9.

Gudmundsson, J., Besenbacher, S., Sulem, P., Gudbjartsson, D. F., Olafsson, I., Arinbjarnarson, S., Agnarsson, B. A., Benediktsdottir, K. R., Isaksson, H. J., Kostic, J. P., Gudjonsson, S. A., Stacey, S. N., Gylfason, A., Sigurdsson, A., Holm, H., Bjornsdottir, U. S., Eyjolfsson, G. I., Navarrete, S., Fuertes, F., Garcia-Prats, M. D., Polo, E., Checherita, I. A., Jinga, M., Badea, P., Aben, K. K., Schalken, J. A., van Oort, I. M., Sweep, F. C., Helfand, B. T., Davis, M., Donovan, J. L., Hamdy, F. C., Kristjansson, K., Gulcher, J. R., Masson, G., Kong, A., Catalona, W. J., Mayordomo, J. I., Geirsson, G., Einarsson, G. V., Barkardottir, R. B., Jonsson, E., Jinga, V., Mates, D., Kiemeney, L. A., Neal, D. E., Thorsteinsdottir, U., Rafnar, T. and Stefansson, K. (2010) 'Genetic correction of PSA values using sequence variants associated with PSA levels', *Sci Transl Med,* 2(62), pp. 62ra92.

Guenther, M. G., Levine, S. S., Boyer, L. A., Jaenisch, R. and Young, R. A. (2007) 'A chromatin landmark and transcription initiation at most promoters in human cells', *Cell,* 130(1), pp. 77-88.

Hanahan, D. and Weinberg, R. A. (2000) 'The hallmarks of cancer', *Cell,* 100(1), pp. 57-70.

Hansel, D. E., Rahman, A., House, M., Ashfaq, R., Berg, K., Yeo, C. J. and Maitra, A. (2004) 'Met proto-oncogene and insulin-like growth factor binding protein 3 overexpression correlates with metastatic ability in well-differentiated pancreatic endocrine neoplasms', *Clin Cancer Res,* 10(18 Pt 1), pp. 6152-8.

Heinz, S., Romanoski, C. E., Benner, C. and Glass, C. K. (2015) 'The selection and function of cell type-specific enhancers', *Nat Rev Mol Cell Biol,* 16(3), pp. 144-54.

Hodges, L. C., Cook, J. D., Lobenhofer, E. K., Li, L., Bennett, L., Bushel, P. R., Aldaz, C. M., Afshari, C. A. and Walker, C. L. (2003) 'Tamoxifen functions as a molecular agonist inducing cell cycle-associated genes in breast cancer cells', *Mol Cancer Res,* 1(4), pp. 300-11.

Hoogaars, W. M., Barnett, P., Rodriguez, M., Clout, D. E., Moorman, A. F., Goding, C. R. and Christoffels, V. M. (2008) 'TBX3 and its splice variant TBX3 + exon 2a are functionally similar', *Pigment Cell Melanoma Res,* 21(3), pp. 379-87.

Hotary, K., Li, X. Y., Allen, E., Stevens, S. L. and Weiss, S. J. (2006) 'A cancer cell metalloprotease triad regulates the basement membrane transmigration program', *Genes Dev,* 20(19), pp. 2673-86.

Howlader, N., Altekruse, S. F., Li, C. I., Chen, V. W., Clarke, C. A., Ries, L. A. and Cronin, K. A. (2014) 'US incidence of breast cancer subtypes defined by joint hormone receptor and HER2 status', *J Natl Cancer Inst,* 106(5).

Hu, M., Yao, J., Carroll, D. K., Weremowicz, S., Chen, H., Carrasco, D., Richardson, A., Violette, S., Nikolskaya, T., Nikolsky, Y., Bauerlein, E. L., Hahn, W. C., Gelman, R. S., Allred, C., Bissell, M. J., Schnitt, S. and Polyak, K. (2008) 'Regulation of in situ to invasive breast carcinoma transition', *Cancer Cell,* 13(5), pp. 394-406.

Huang, C. S., Shen, C. Y., Wang, H. W., Wu, P. E. and Cheng, C. W. (2007) 'Increased expression of SRp40 affecting CD44 splicing is associated with the clinical outcome of lymph node metastasis in human breast cancer', *Clin Chim Acta,* 384(1-2), pp. 69-74.

Hui, R., Finney, G. L., Carroll, J. S., Lee, C. S., Musgrove, E. A. and Sutherland, R. L. (2002) 'Constitutive overexpression of cyclin D1 but not cyclin E confers acute resistance to antiestrogens in T-47D breast cancer cells', *Cancer Res,* 62(23), pp. 6916-23.

Humtsoe, J. O., Koya, E., Pham, E., Aramoto, T., Zuo, J., Ishikawa, T. and Kramer, R. H. (2012) 'Transcriptional profiling identifies upregulated genes following induction of epithelial-mesenchymal transition in squamous carcinoma cells', *Exp Cell Res,* 318(4), pp. 379-90.

Irtegun, S., Wood, R. J., Ormsby, A. R., Mulhern, T. D. and Hatters, D. M. (2013) 'Tyrosine 416 is phosphorylated in the closed, repressed conformation of c-Src', *PLoS One,* 8(7), pp. e71035.

Jin, C., Li, H., Murata, T., Sun, K., Horikoshi, M., Chiu, R. and Yokoyama, K. K. (2002) 'JDP2, a repressor of AP-1, recruits a histone deacetylase 3 complex to inhibit the retinoic acid-induced differentiation of F9 cells', *Mol Cell Biol,* 22(13), pp. 4815-26.

Jonkers, I. and Lis, J. T. (2015) 'Getting up to speed with transcription elongation by RNA polymerase II', *Nat Rev Mol Cell Biol,* 16(3), pp. 167-77.

Kenny, F. S., Hui, R., Musgrove, E. A., Gee, J. M., Blamey, R. W., Nicholson, R. I., Sutherland, R. L. and Robertson, J. F. (1999) 'Overexpression of cyclin D1 messenger RNA predicts for poor prognosis in estrogen receptor-positive breast cancer', *Clin Cancer Res,* 5(8), pp. 2069-76.

Keyomarsi, K., Tucker, S. L., Buchholz, T. A., Callister, M., Ding, Y., Hortobagyi, G. N., Bedrosian, I., Knickerbocker, C., Toyofuku, W., Lowe, M., Herliczek, T. W. and Bacus, S. S. (2002) 'Cyclin E and survival in patients with breast cancer', *N Engl J Med,* 347(20), pp. 1566-75.

Kim, J., Bae, S., An, S., Park, J. K., Kim, E. M., Hwang, S. G., Kim, W. J. and Um, H. D. (2014) 'Cooperative actions of p21WAF1 and p53 induce Slug protein degradation and suppress cell invasion', *EMBO Rep,* 15(10), pp. 1062-8.

Knowles, M. A. and Selby, P. (2005) *Introduction to the cellular and molecular biology of cancer.* New York: Oxford University Press.

Krumm, A., Hickey, L. B. and Groudine, M. (1995) 'Promoter-proximal pausing of RNA polymerase II defines a general rate-limiting step after transcription initiation', *Genes Dev,* 9(5), pp. 559-72.

Krumm, A., Meulia, T. and Groudine, M. (1993) 'Common mechanisms for the control of eukaryotic transcriptional elongation', *Bioessays,* 15(10), pp. 659-65.

Kumar P, P., Emechebe, U., Smith, R., Franklin, S., Moore, B., Yandell, M., Lessnick, S. L. and Moon, A. M. (2014) 'Coordinated control of senescence by lncRNA and a novel T-box3 co-repressor complex', *Elife,* 3.

Kunasegaran, K., Ho, V., Chang, T. H., De Silva, D., Bakker, M. L., Christoffels, V. M. and Pietersen, A. M. (2014) 'Transcriptional repressor Tbx3 is required for the hormone-sensing cell lineage in mammary epithelium', *PLoS One,* 9(10), pp. e110191.

Kwak, H. and Lis, J. T. (2013) 'Control of transcriptional elongation', *Annu Rev Genet,* 47, pp. 483-508.

Larschan, E., Bishop, E. P., Kharchenko, P. V., Core, L. J., Lis, J. T., Park, P. J. and Kuroda, M. I. (2011) 'X chromosome dosage compensation via enhanced transcriptional elongation in Drosophila', *Nature,* 471(7336), pp. 115-8.

Larson, P. S., de las Morenas, A., Cerda, S. R., Bennett, S. R., Cupples, L. A. and Rosenberg, C. L. (2006) 'Quantitative analysis of allele imbalance supports atypical ductal hyperplasia lesions as direct breast cancer precursors', *J Pathol,* 209(3), pp. 307-16.

Lee, H. S., Cho, H. H., Kim, H. K., Bae, Y. C., Baik, H. S. and Jung, J. S. (2007a) 'Tbx3, a transcriptional factor, involves in proliferation and osteogenic differentiation of human adipose stromal cells', *Mol Cell Biochem,* 296(1-2), pp. 129-36.

Lee, S., Medina, D., Tsimelzon, A., Mohsin, S. K., Mao, S., Wu, Y. and Allred, D. C. (2007b) 'Alterations of gene expression in the development of early hyperplastic precursors of breast cancer', *Am J Pathol,* 171(1), pp. 252-62.

Lee, S., Mohsin, S. K., Mao, S., Hilsenbeck, S. G., Medina, D. and Allred, D. C. (2006) 'Hormones, receptors, and growth in hyperplastic enlarged lobular units: early potential precursors of breast cancer', *Breast Cancer Res,* 8(1), pp. R6.

Lerwill, M. F. (2008) 'Flat epithelial atypia of the breast', *Arch Pathol Lab Med,* 132(4), pp. 615-21.

Lewin, B., Krebs, J. E., Kilpatrick, S. T. and Goldstein, E. S. (2011) *Lewin's genes X.* 10th edn. Sudbury, Mass.: Jones and Bartlett.

Li, J., Weinberg, M. S., Zerbini, L. and Prince, S. (2013) 'The oncogenic TBX3 is a downstream target and mediator of the TGF-β1 signaling pathway', *Mol Biol Cell,* 24(22), pp. 3569-76.

Lingbeek, M. E., Jacobs, J. J. and van Lohuizen, M. (2002) 'The T-box repressors TBX2 and TBX3 specifically regulate the tumor suppressor gene p14ARF via a variant T-site in the initiator', *J Biol Chem,* 277(29), pp. 26120-7.

Lomnytska, M., Dubrovska, A., Hellman, U., Volodko, N. and Souchelnytskyi, S. (2006) 'Increased expression of cSHMT, Tbx3 and utrophin in plasma of ovarian and breast cancer patients', *Int J Cancer,* 118(2), pp. 412-21.

Lu, J., Li, X. P., Dong, Q., Kung, H. F. and He, M. L. (2010) 'TBX2 and TBX3: the special value for anticancer drug targets', *Biochim Biophys Acta,* 1806(2), pp. 268-74.

Lu, R., Yang, A. and Jin, Y. (2011) 'Dual functions of T-box 3 (Tbx3) in the control of self-renewal and extraembryonic endoderm differentiation in mouse embryonic stem cells', *J Biol Chem,* 286(10), pp. 8425-36.

Lyng, H., Brovig, R. S., Svendsrud, D. H., Holm, R., Kaalhus, O., Knutstad, K., Oksefjell, H., Sundfor, K., Kristensen, G. B. and Stokke, T. (2006) 'Gene expressions and copy numbers associated with metastatic phenotypes of uterine cervical cancer', *BMC Genomics,* 7, pp. 268.

Man, Y. G., Tai, L., Barner, R., Vang, R., Saenger, J. S., Shekitka, K. M., Bratthauer, G. L., Wheeler, D. T., Liang, C. Y., Vinh, T. N. and Strauss, B. L. (2003) 'Cell clusters overlying focally disrupted mammary myoepithelial cell layers and adjacent cells within the same duct display different immunohistochemical and genetic features: implications for tumor progression and invasion', *Breast Cancer Res,* 5(6), pp. R231-41.

Masamha, C. P. and Benbrook, D. M. (2009) 'Cyclin D1 degradation is sufficient to induce G1 cell cycle arrest despite constitutive expression of cyclin E2 in ovarian cancer cells', *Cancer Res,* 69(16), pp. 6565-72.

Miao, Z. F., Liu, X. Y., Xu, H. M., Wang, Z. N., Zhao, T. T., Song, Y. X., Xing, Y. N., Huang, J. Y., Zhang, J. Y., Xu, H. and Xu, Y. Y. (2016) 'Tbx3 overexpression in human gastric cancer is correlated with advanced tumor stage and nodal status and promotes cancer cell growth and invasion', *Virchows Arch,* 469(5), pp. 505-513.

Min, I. M., Waterfall, J. J., Core, L. J., Munroe, R. J., Schimenti, J. and Lis, J. T. (2011) 'Regulating RNA polymerase pausing and transcription elongation in embryonic stem cells', *Genes Dev,* 25(7), pp. 742-54.

Moinfar, F., Man, Y. G., Bratthauer, G. L., Ratschek, M. and Tavassoli, F. A. (2000) 'Genetic abnormalities in mammary ductal intraepithelial neoplasia-flat type ("clinging ductal carcinoma in situ"): a simulator of normal mammary epithelium', *Cancer,* 88(9), pp. 2072-81.

Morel, A. P., Hinkal, G. W., Thomas, C., Fauvet, F., Courtois-Cox, S., Wierinckx, A., Devouassoux-Shisheboran, M., Treilleux, I., Tissier, A., Gras, B., Pourchet, J., Puisieux, I., Browne, G. J., Spicer, D. B., Lachuer, J., Ansieau, S. and Puisieux, A. (2012) 'EMT inducers catalyze malignant transformation of mammary epithelial cells and drive tumorigenesis towards claudin-low tumors in transgenic mice', *PLoS Genet,* 8(5), pp. e1002723.

Murphy, D. A. and Courtneidge, S. A. (2011) 'The 'ins' and 'outs' of podosomes and invadopodia: characteristics, formation and function', *Nat Rev Mol Cell Biol,* 12(7), pp. 413-26.

Muse, G. W., Gilchrist, D. A., Nechaev, S., Shah, R., Parker, J. S., Grissom, S. F., Zeitlinger, J. and Adelman, K. (2007) 'RNA polymerase is poised for activation across the genome', *Nat Genet,* 39(12), pp. 1507-11.

Nakade, K., Pan, J., Yamasaki, T., Murata, T., Wasylyk, B. and Yokoyama, K. K. (2009) 'JDP2 (Jun Dimerization Protein 2)-deficient mouse embryonic fibroblasts are resistant to replicative senescence', *J Biol Chem,* 284(16), pp. 10808-17.

Nieto, M. A., Huang, R. Y., Jackson, R. A. and Thiery, J. P. (2016) 'EMT: 2016', *Cell,* 166(1), pp. 21-45.

Noel, J. C., Fayt, I., Fernandez-Aguilar, S., Buxant, F. and Boutemy, R. (2006) 'Proliferating activity in columnar cell lesions of the breast', *Virchows Arch,* 449(6), pp. 617-21.

O'Connell, P., Pekkel, V., Fuqua, S. A., Osborne, C. K., Clark, G. M. and Allred, D. C. (1998) 'Analysis of loss of heterozygosity in 399 premalignant breast lesions at 15 genetic loci', *J Natl Cancer Inst,* 90(9), pp. 697-703.

Peres, J., Davis, E., Mowla, S., Bennett, D. C., Li, J. A., Wansleben, S. and Prince, S. (2010) 'The Highly Homologous T-Box Transcription Factors, TBX2 and TBX3, Have Distinct Roles in the Oncogenic Process', *Genes Cancer,* 1(3), pp. 272-82.

Phillips, S. and Kuperwasser, C. (2014) 'SLUG: Critical regulator of epithelial cell identity in breast development and cancer', *Cell Adh Migr,* 8(6), pp. 578-87.

Platonova, N., Scotti, M., Babich, P., Bertoli, G., Mento, E., Meneghini, V., Egeo, A., Zucchi, I. and Merlo, G. R. (2007) 'TBX3, the gene mutated in ulnar-mammary syndrome, promotes growth of mammary epithelial cells via repression of p19ARF, independently of p53', *Cell Tissue Res,* 328(2), pp. 301-16.

Polosukhin, V. V. (1999) 'Ultrastructural study of the destructive and repair processes in pulmonary inflammation and following endobronchial laser therapy', *Virchows Arch,* 435(1), pp. 13-9.

Polyak, K. and Weinberg, R. A. (2009) 'Transitions between epithelial and mesenchymal states: acquisition of malignant and stem cell traits', *Nat Rev Cancer,* 9(4), pp. 265-73.

Puisieux, A., Brabletz, T. and Caramel, J. (2014) 'Oncogenic roles of EMT-inducing transcription factors', *Nat Cell Biol,* 16(6), pp. 488-94.

Rahl, P. B., Lin, C. Y., Seila, A. C., Flynn, R. A., McCuine, S., Burge, C. B., Sharp, P. A. and Young, R. A. (2010) 'c-Myc regulates transcriptional pause release', *Cell,* 141(3), pp. 432-45.

Renard, C. A., Labalette, C., Armengol, C., Cougot, D., Wei, Y., Cairo, S., Pineau, P., Neuveut, C., de Reynies, A., Dejean, A., Perret, C. and Buendia, M. A. (2007) 'Tbx3 is a downstream target of the Wnt/beta-catenin pathway and a critical mediator of beta-catenin survival functions in liver cancer', *Cancer Res,* 67(3), pp. 901-10.

Robert, J. (2015) *Textbook of Cell Signalling in Cancer*

An Educational Approach: Springer.

Rodriguez, M., Aladowicz, E., Lanfrancone, L. and Goding, C. R. (2008) 'Tbx3 represses E-cadherin expression and enhances melanoma invasiveness', *Cancer Res,* 68(19), pp. 7872-81.

Sanders, M. E., Schuyler, P. A., Dupont, W. D. and Page, D. L. (2005) 'The natural history of low-grade ductal carcinoma in situ of the breast in women treated by biopsy only revealed over 30 years of long-term follow-up', *Cancer,* 103(12), pp. 2481-4.

Sandhu, C., Donovan, J., Bhattacharya, N., Stampfer, M., Worland, P. and Slingerland, J. (2000) 'Reduction of Cdc25A contributes to cyclin E1-Cdk2 inhibition at senescence in human mammary epithelial cells', *Oncogene,* 19(47), pp. 5314-23.

Savani, R. C., Cao, G., Pooler, P. M., Zaman, A., Zhou, Z. and DeLisser, H. M. (2001) 'Differential involvement of the hyaluronan (HA) receptors CD44 and receptor for HA-mediated motility in endothelial cell function and angiogenesis', *J Biol Chem,* 276(39), pp. 36770-8.

Scatena, M., Almeida, M., Chaisson, M. L., Fausto, N., Nicosia, R. F. and Giachelli, C. M. (1998) 'NF-kappaB mediates alphavbeta3 integrin-induced endothelial cell survival', *J Cell Biol,* 141(4), pp. 1083-93.

Senger, D. R., Ledbetter, S. R., Claffey, K. P., Papadopoulos-Sergiou, A., Peruzzi, C. A. and Detmar, M. (1996) 'Stimulation of endothelial cell migration by vascular permeability factor/vascular endothelial growth factor through cooperative mechanisms involving the alphavbeta3 integrin, osteopontin, and thrombin', *Am J Pathol,* 149(1), pp. 293-305.

Shan, Z. Z., Yan, X. B., Yan, L. L., Tian, Y., Meng, Q. C., Qiu, W. W., Zhang, Z. and Jin, Z. M. (2015) 'Overexpression of Tbx3 is correlated with Epithelial-Mesenchymal Transition phenotype and predicts poor prognosis of colorectal cancer', *Am J Cancer Res,* 5(1), pp. 344-53.

Shirinifard, A., Gens, J. S., Zaitlen, B. L., Popławski, N. J., Swat, M. and Glazier, J. A. (2009) '3D multi-cell simulation of tumor growth and angiogenesis', *PLoS One,* 4(10), pp. e7190.

Simpson, P. T., Gale, T., Reis-Filho, J. S., Jones, C., Parry, S., Sloane, J. P., Hanby, A., Pinder, S. E., Lee, A. H., Humphreys, S., Ellis, I. O. and Lakhani, S. R. (2005) 'Columnar cell lesions of the breast: the missing link in breast cancer progression? A morphological and molecular analysis', *Am J Surg Pathol,* 29(6), pp. 734-46.

Skotheim, R. I. and Nees, M. (2007) 'Alternative splicing in cancer: noise, functional, or systematic?', *Int J Biochem Cell Biol,* 39(7-8), pp. 1432-49.

Smit, M. A. and Peeper, D. S. (2010) 'Epithelial-mesenchymal transition and senescence: two cancer-related processes are crossing paths', *Aging (Albany NY),* 2(10), pp. 735-41.

Souter, L. H., Andrews, J. D., Zhang, G., Cook, A. C., Postenka, C. O., Al-Katib, W., Leong, H. S., Rodenhiser, D. I., Chambers, A. F. and Tuck, A. B. (2010) 'Human 21T breast epithelial cell lines mimic breast cancer progression in vivo and in vitro and show stage-specific gene expression patterns', *Lab Invest,* 90(8), pp. 1247-58.

Stennard, F., Zorn, A. M., Ryan, K., Garrett, N. and Gurdon, J. B. (1999) 'Differential expression of VegT and Antipodean protein isoforms in Xenopus', *Mech Dev,* 86(1-2), pp. 87-98.

Thurman, R. E., Rynes, E., Humbert, R., Vierstra, J., Maurano, M. T., Haugen, E., Sheffield, N. C., Stergachis, A. B., Wang, H., Vernot, B., Garg, K., John, S., Sandstrom, R., Bates, D., Boatman, L., Canfield, T. K., Diegel, M., Dunn, D., Ebersol, A. K., Frum, T., Giste, E., Johnson, A. K., Johnson, E. M., Kutyavin, T., Lajoie, B., Lee, B. K., Lee, K., London, D., Lotakis, D., Neph, S., Neri, F., Nguyen, E. D., Qu, H., Reynolds, A. P., Roach, V., Safi, A., Sanchez, M. E., Sanyal, A., Shafer, A., Simon, J. M., Song, L., Vong, S., Weaver, M., Yan, Y., Zhang, Z., Lenhard, B., Tewari, M., Dorschner, M. O., Hansen, R. S., Navas, P. A., Stamatoyannopoulos, G., Iyer, V. R., Lieb, J. D., Sunyaev, S. R., Akey, J. M., Sabo, P. J., Kaul, R., Furey, T. S., Dekker, J., Crawford, G. E. and Stamatoyannopoulos, J. A. (2012) 'The accessible chromatin landscape of the human genome', *Nature,* 489(7414), pp. 75-82.

Tran, P. T., Shroff, E. H., Burns, T. F., Thiyagarajan, S., Das, S. T., Zabuawala, T., Chen, J., Cho, Y. J., Luong, R., Tamayo, P., Salih, T., Aziz, K., Adam, S. J., Vicent, S., Nielsen, C. H., Withofs, N., Sweet-Cordero, A., Gambhir, S. S., Rudin, C. M. and Felsher, D. W. (2012) 'Twist1 suppresses senescence programs and thereby accelerates and maintains mutant Kras-induced lung tumorigenesis', *PLoS Genet,* 8(5), pp. e1002650.

Tremblay, G., Deschênes, J., Alpert, L. and Quenneville, L. A. (2005) 'Overexpression of estrogen receptors in columnar cell change and in unfolding breast lobules', *Breast J,* 11(5), pp. 326-32.

Trochon, V., Mabilat, C., Bertrand, P., Legrand, Y., Smadja-Joffe, F., Soria, C., Delpech, B. and Lu, H. (1996) 'Evidence of involvement of CD44 in endothelial cell proliferation, migration and angiogenesis in vitro', *Int J Cancer,* 66(5), pp. 664-8.

Turashvili, G., Hayes, M., Gilks, B., Watson, P. and Aparicio, S. (2008) 'Are columnar cell lesions the earliest histologically detectable non-obligate precursor of breast cancer?', *Virchows Arch,* 452(6), pp. 589-98.

Venables, J. P., Klinck, R., Bramard, A., Inkel, L., Dufresne-Martin, G., Koh, C., Gervais-Bird, J., Lapointe, E., Froehlich, U., Durand, M., Gendron, D., Brosseau, J. P., Thibault, P., Lucier, J. F., Tremblay, K., Prinos, P., Wellinger, R. J., Chabot, B., Rancourt, C. and Elela, S. A. (2008) 'Identification of alternative splicing markers for breast cancer', *Cancer Res,* 68(22), pp. 9525-31.

Vincent-Salomon, A. (2003) '[Columnar lesions: a frequent diagnosis in breast pathology!]', *Ann Pathol,* 23(6), pp. 593-6.

Watermann, D. O., Tang, Y., Zur Hausen, A., Jäger, M., Stamm, S. and Stickeler, E. (2006) 'Splicing factor Tra2-beta1 is specifically induced in breast cancer and regulates alternative splicing of the CD44 gene', *Cancer Res,* 66(9), pp. 4774-80.

Weaver, A. M. (2006) 'Invadopodia: specialized cell structures for cancer invasion', *Clin Exp Metastasis,* 23(2), pp. 97-105.

Wellings, S. R. and Jensen, H. M. (1973) 'On the origin and progression of ductal carcinoma in the human breast', *J Natl Cancer Inst,* 50(5), pp. 1111-8.

Wellings, S. R., Jensen, H. M. and Marcum, R. G. (1975) 'An atlas of subgross pathology of the human breast with special reference to possible precancerous lesions', *J Natl Cancer Inst,* 55(2), pp. 231-73.

Willmer, T., Cooper, A., Peres, J., Omar, R. and Prince, S. (2017) 'The T-Box transcription factor 3 in development and cancer', *Biosci Trends,* 11(3), pp. 254-266.

Willmer, T., Cooper, A., Sims, D., Govender, D. and Prince, S. (2016a) 'The T-box transcription factor 3 is a promising biomarker and a key regulator of the oncogenic phenotype of a diverse range of sarcoma subtypes', *Oncogenesis,* 5, pp. e199.

Willmer, T., Hare, S., Peres, J. and Prince, S. (2016b) 'The T-box transcription factor TBX3 drives proliferation by direct repression of the p21(WAF1) cyclin-dependent kinase inhibitor', *Cell Div,* 11, pp. 6.

Willmer, T., Peres, J., Mowla, S., Abrahams, A. and Prince, S. (2015) 'The T-Box factor TBX3 is important in S-phase and is regulated by c-Myc and cyclin A-CDK2', *Cell Cycle,* 14(19), pp. 3173-83.

Witte, J. S. (2010) 'Personalized prostate cancer screening: improving PSA tests with genomic information', *Sci Transl Med,* 2(62), pp. 62ps55.

Wu, Y., Feng, J., Hu, W. and Zhang, Y. (2017) 'T-box 3 overexpression is associated with poor prognosis of non-small cell lung cancer', *Oncol Lett,* 13(5), pp. 3335-3341.

Yankulov, K., Blau, J., Purton, T., Roberts, S. and Bentley, D. L. (1994) 'Transcriptional elongation by RNA polymerase II is stimulated by transactivators', *Cell,* 77(5), pp. 749-59.

Yao, C., Yao, G. Q., Sun, B. H., Zhang, C., Tommasini, S. M. and Insogna, K. (2014) 'The transcription factor T-box 3 regulates colony-stimulating factor 1-dependent Jun dimerization protein 2 expression and plays an important role in osteoclastogenesis', *J Biol Chem,* 289(10), pp. 6775-90.

Yarosh, W., Barrientos, T., Esmailpour, T., Lin, L., Carpenter, P. M., Osann, K., Anton-Culver, H. and Huang, T. (2008) 'TBX3 is overexpressed in breast cancer and represses p14 ARF by interacting with histone deacetylases', *Cancer Res,* 68(3), pp. 693-9.

Zeitlinger, J., Stark, A., Kellis, M., Hong, J. W., Nechaev, S., Adelman, K., Levine, M. and Young, R. A. (2007) 'RNA polymerase stalling at developmental control genes in the Drosophila melanogaster embryo', *Nat Genet,* 39(12), pp. 1512-6.

Zhao, D., Wu, Y. and Chen, K. (2014) 'Tbx3 isoforms are involved in pluripotency maintaining through distinct regulation of Nanog transcriptional activity', *Biochem Biophys Res Commun,* 444(3), pp. 411-4.

Zhu, B., Zhang, M., Williams, E. M., Keller, C., Mansoor, A. and Davie, J. K. (2016) 'TBX2 represses PTEN in rhabdomyosarcoma and skeletal muscle', *Oncogene,* 35(32), pp. 4212-24.

6 Appendices

6.1 Chapter 3 – Supplementary Data

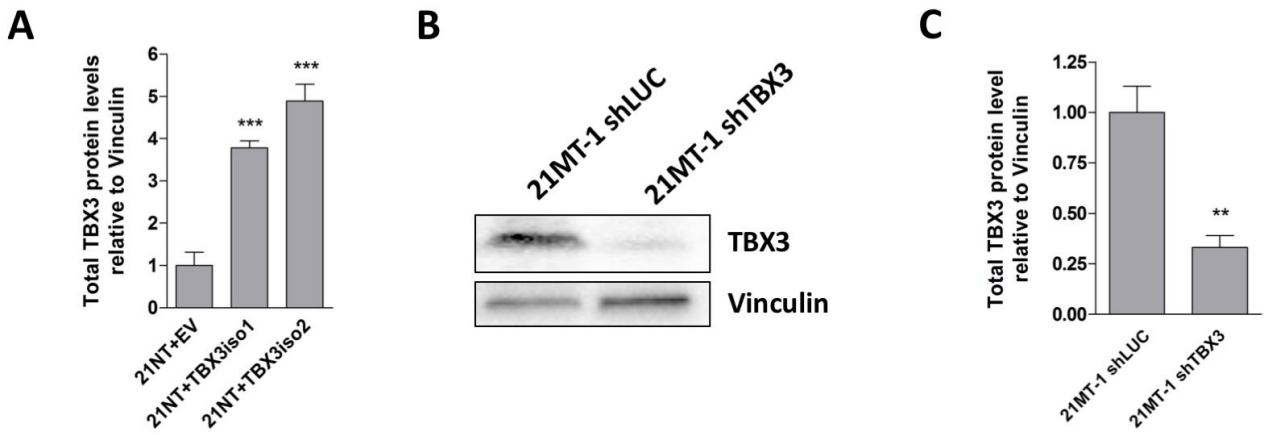

Appendix 1 – TBX3 protein expression in 21NT transfectant and 21MT-1 transductant cell lines.

(A-C) Western blot analysis showing total TBX3 protein levels in generated stable cell lines. 21NT cells were transfected to overexpress TBX3iso1 or TBX3iso2, or transfected with an empty vector (EV) control. 21MT-1 cells were transduced with either shLUC (luciferase; off-target control) or shTBX3. Protein samples were separated by 10% SDS-PAGE and quantified by densitometry. Protein levels were normalized to Vinculin, which served as the loading control.

**p<0.05, **p<0.01, ***p<0.001 by one-way ANOVA with Tukey post-hoc for comparison between three groups, and Student's t-test for comparison between two groups.*

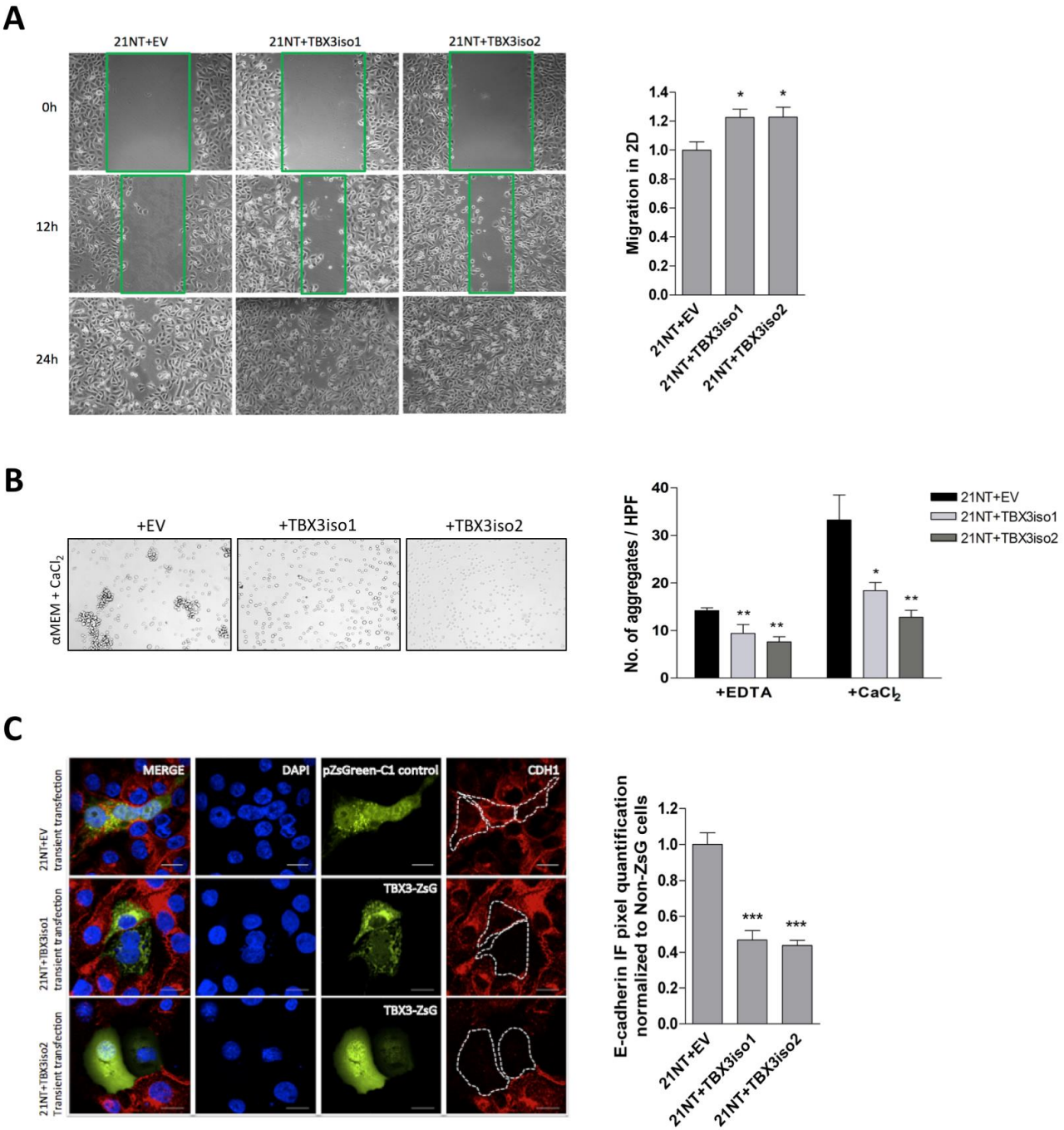
A
21NT+EV
21NT+TBX3iso1
21NT+TBX3iso2
0h
12h
24h
Migration in 2D
1.4
1.2
1.0
0.8
0.6
0.4
0.2
0.0
*
*
21NT+EV
21NT+TBX3iso1
21NT+TBX3iso2
B
+EV
+TBX3iso1
+TBX3iso2
αMEM + CaCl2
No. of aggregates / HPF
40
30
20
10
0
**
**
*
**
+EDTA
+CaCl2
21NT+EV
21NT+TBX3iso1
21NT+TBX3iso2
C
MERGE
DAPI
pZsGreen-C1 control
CDH1
21NT+EV transient transfection
21NT+TBX3iso1 transient transfection
21NT+TBX3iso2 Transient transfection
TBX3-ZsG
TBX3-ZsG
E-cadherin IF pixel quantification normalized to Non-ZsG cells
1.2
1.0
0.8
0.6
0.4
0.2
0.0
***
***
21NT+EV
21NT+TBX3iso1
21NT+TBX3iso2

Appendix 2 – Phenotypic assessment of TBX3 overexpressing cell lines.

(A) Assessment of migration in 2D in 21NT transfectant cell lines. A scratch was produced in a confluent monolayer of cells, and migration of cells into the scratch area was monitored at 0, 12 and 24 hours post-scratch. Migration was quantified as ratio of wound area filled at 0 and 12 hours, and normalized to the empty vector control. **(B)** Cell-cell adhesion assay. Cells were harvested and re-suspended in media containing either 3mM EDTA or 1mM $CaCl_2$ and incubated in a petri dish at 37ºC for 30 minutes with gentle agitation. Clusters containing over 4 cells were counted across 10 fields of view. **(C)** 21NT cells were transiently transfected with either a TBX3iso1 or TBX3iso2 plasmid containing a ZsGreen reporter, or empty vector control expressing ZsGreen. CDH1 was visualized using a red-fluorescently labeled antibody. CDH1 signal was quantified by counting pixels within the red channel of ZsGreen positive transfected cells.

**p<0.05, **p<0.01, ***p<0.001 by one-way ANOVA with Tukey post-hoc for comparison between three groups.*

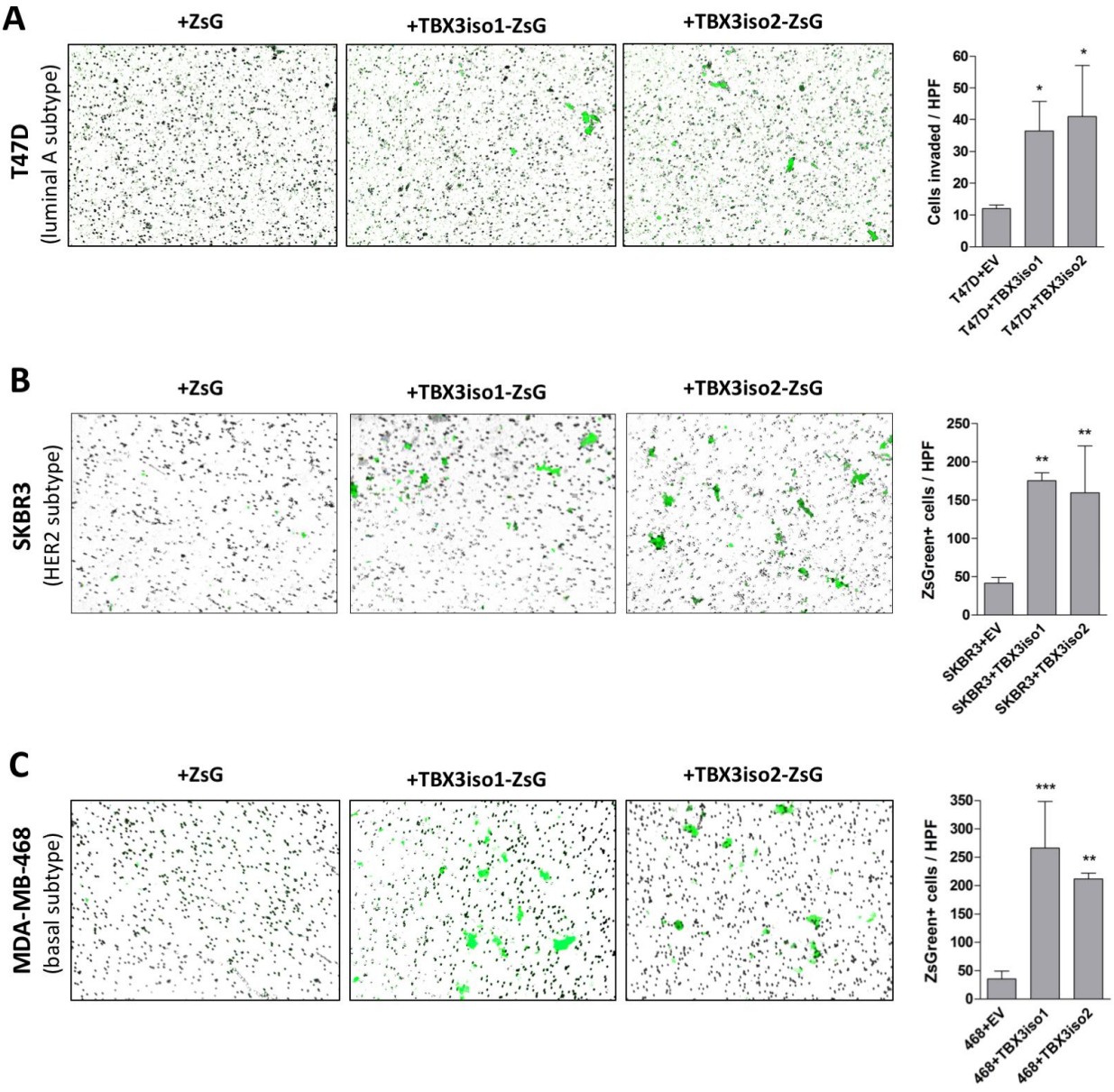

Appendix 3 - Effect of TBX3 overexpression on invasiveness in cell lines representing other breast cancer molecular subtypes.

The invasive ability of TBX3 transfectant lines was assessed using Matrigel-coated transwell inserts. **(A-C)** T-47D (luminal A), SKBR3 (HER2-enriched), and MDA-MB-468 (basal-like) cells were transfected with either an empty vector (EV), or TBX3iso1, or TBX3iso2 construct within the pZsGreen1-N1 vector containing a ZsGreen reporter. Twenty-four hours post-transfection, 50,000 cells were added to the upper chamber of an 8.0µm pore transwell insert coated with Matrigel and allowed to invade for 18 hours. The number of green cells per field of view was used in the analysis.

**p<0.05, **p<0.01, ***p<0.001 by one-way ANOVA with Tukey post-hoc for comparison between three groups.*

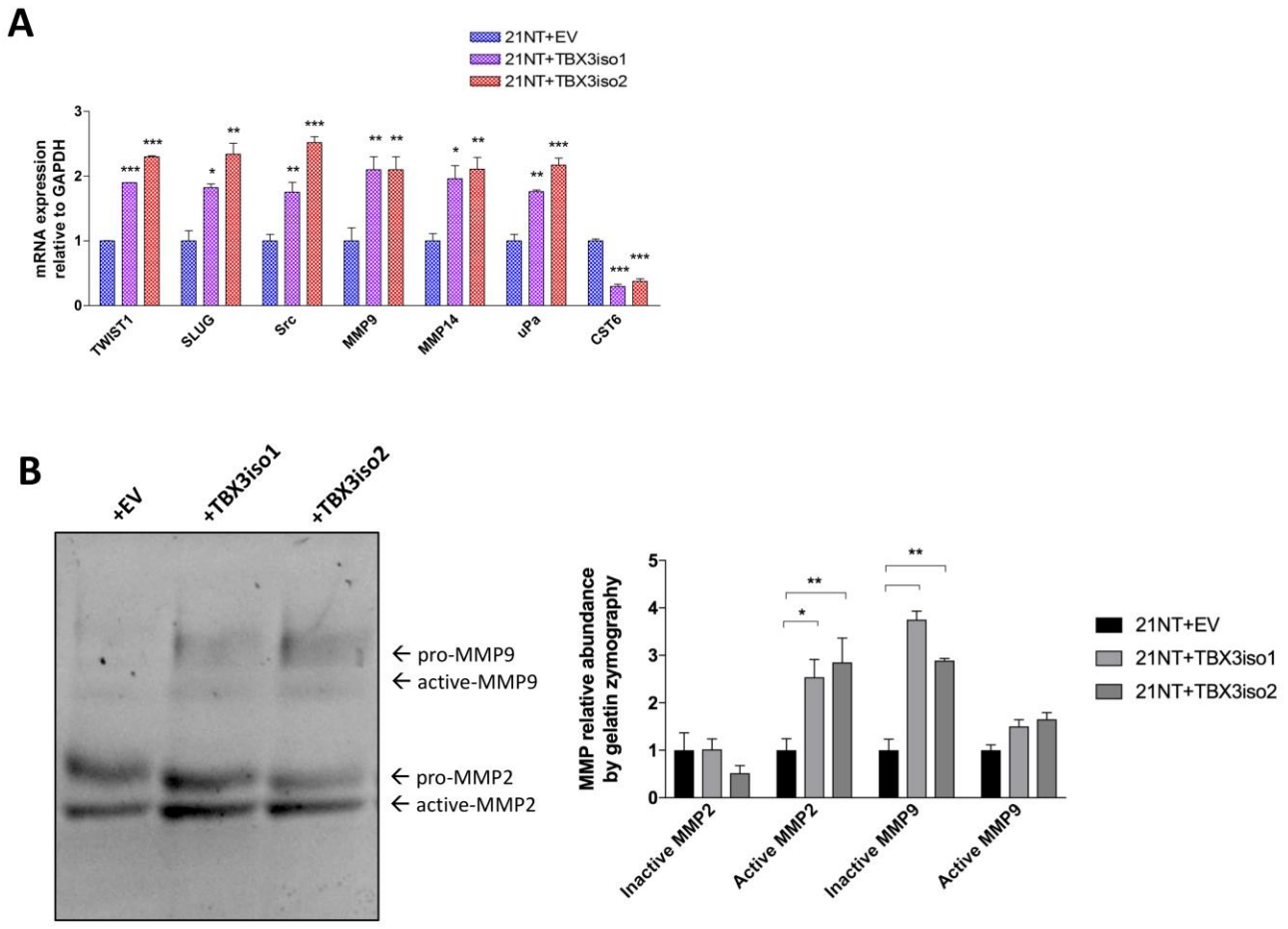

Appendix 4 – Assessment of EMT markers in TBX3 overexpressing cell lines.

(A) The mRNA expression of several EMT markers was evaluated by qRT-PCR. Expression was normalized to GAPDH expression levels, and depicted as fold change relative to the empty vector control. **(B)** Conditioned media was concentrated and resolved on a 10% zymogram gelatin gel. The gel was renatured and developed, and size of the proteolyzed bands was quantified by densitometry using the reverse image (as shown). Active (82 kDa) vs. inactive (pro-) MMP9 (92 kDa), and active (63 kDa) vs. inactive (pro-) MMP2 (72 kDa) were identified by molecular weight.

**p<0.05, **p<0.01, ***p<0.001 by one-way ANOVA with Tukey post-hoc for comparison between three groups.*

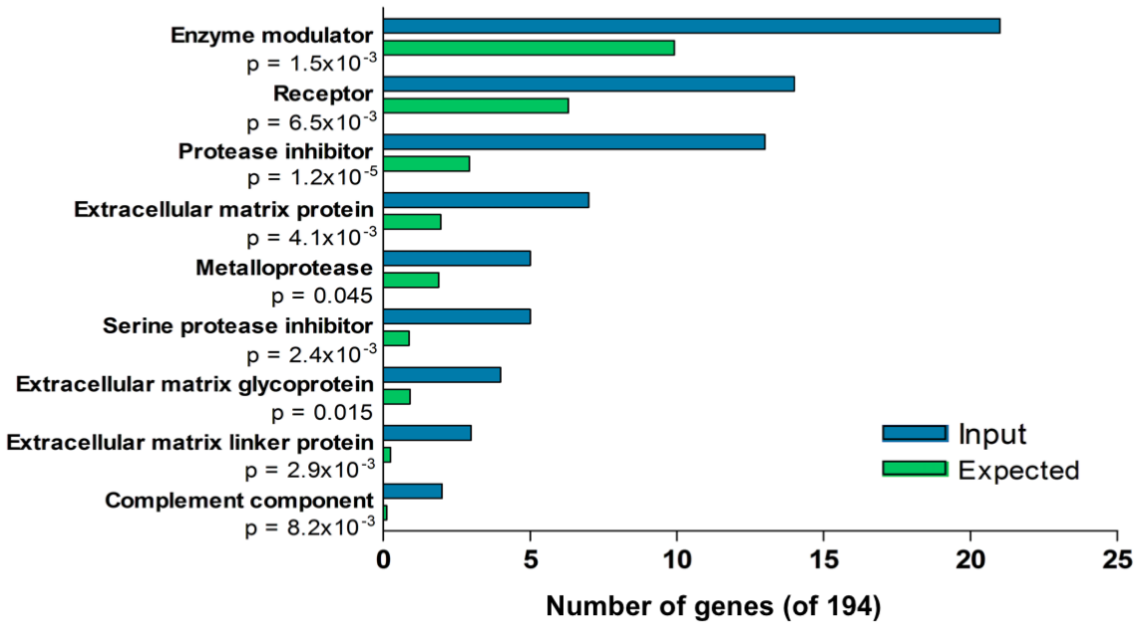

Appendix 5 – Protein class analysis of direct transcriptional targets of TBX3.

The 194 genes directly bound by both TBX3 isoforms in ChIP-array data and whose transcript levels were significantly altered in expression by RNA-Seq (>1.5 fold up or down, FDR<0.05) were analyzed using the PANTHER database, conducting over-representation analysis and focusing on protein class. Protein classes with the lowest p-values are shown. P-values were calculated by comparing expected numbers compared to input numbers in the gene list.

6.2 Chapter 3 – Immunohistochemistry Quality Control

As shown in Appendix 6-9, stringent quality control measures were used for all IHC-based quantifications. For TBX3 expression specifically, I conducted cell fractionation experiments through isolation of cytoplasmic and nuclear fractions by ultracentrifugation, followed by immunoblotting cellular fractions of 21PT and 21NT transfectants, and 21MT-1 transductants (Appendix 6). Although these examples represent isogenic cell lines and cellular fractionation was not conducted on other cell lines representing different molecular subtypes from different patients, we observed exclusive nuclear localization of TBX3 in cell fractionation experiments as well as in IHC. While TBX3 is a transcription factor and is expected to be located to the nucleus, a few studies have reported cytoplasmic expression of TBX3 by IHC in colorectal cancer, pancreatic cancer, and HNSCC (Burgucu et al., 2012, Shan et al., 2015, Wang et al., 2015). Lomnytska et al. reported elevated levels of truncated TBX3 protein in the plasma of breast cancer and ovarian cancer patients, in which they suggested that TBX3 is mis-localized in cancer tissues and leaks out of cells and into plasma (Lomnytska et al., 2006).

One of the most important aspects of reliable IHC staining is antibody selection, requiring new optimization depending on each new batch or clone, and selecting conditions that offers the highest contrast of true positive signal over background (Yaziji and Barry, 2006, Matos et al., 2010). We have conducted thorough optimization of TBX3 IHC protocols, utilizing several commercially-available antibodies (Abcam, ab99302, rabbit polyclonal (used for study); Abcam, 154828, rabbit monoclonal; Invitrogen, 42-4800, rabbit polyclonal; Sigma, HPA005799, rabbit polyclonal). Several parameters have been considered, including antigen retrieval time and buffer components, antibody and concentration, blocking steps, etc. until a clean staining pattern with minimal background was achieved. Unfortunately, IHC staining patterns observed are a direct result of the staining optimization process, and improper localization can be observed without thorough optimization and proper positive and negative controls (Matos et al., 2010). Several of the aforementioned conditions (and remaining antibodies) gave high levels of background staining along with a consistent brown ‘blush’ in carcinoma cells, the extent which I believe is artifactual. It is a common rule that when the subcellular and micro-anatomical location of the protein of interest is known, the immunoreactivity pattern obtained for IHC studies should follow this distribution (Seidal et al., 2001). While I cannot exclude that cytoplasmic TBX3 expression is not associated with any

clinicopathological parameters, we focused exclusively on nuclear-localized TBX3 for quantification purposes, as this is where TBX3 is active in regulating transcription. SLUG and TWIST1 IHC optimization and quantification of expression was conducted in the same manner as TBX3.

Expression of TBX3, SLUG and TWIST1 was assessed in the same area across serial sections in a control slide (Appendix 7, Appendix 8), and expression was assessed for each run to ensure reproducible results and therefore eliminate potential confounding variables (Appendix 9). For each of the markers, I quantified expression in benign non-columnar epithelial cells, CCLs, DCIS, and in the invasive carcinoma. This mode of assessment is particularly strong and enhances our understanding of distribution of markers in a cell-specific context. Additionally, the use of full slides allows for observation of expression patterns along a larger area and therefore minimizes sampling bias associated with tumor heterogeneity which is inherent in the use of tissue microarrays (Rubin et al., 2002, Besusparis et al., 2016). Lastly, I used semi-automated computer-assisted image analysis for my quantification of biomarker expression due to the ease and efficiency of use, as well as its documented association with increased accuracy and reproducibility when compared to manual quantification methods (Cross, 2001, Lehr et al., 2001, Umemura et al., 2004, Diaz and Sneige, 2005, Matos et al., 2010).

Section 6.2 REFERENCES

Besusparis, J., Plancoulaine, B., Rasmusson, A., Augulis, R., Green, A. R., Ellis, I. O., Laurinaviciene, A., Herlin, P. and Laurinavicius, A. (2016) 'Impact of tissue sampling on accuracy of Ki67 immunohistochemistry evaluation in breast cancer', *Diagn Pathol,* 11(1), pp. 82.

Burgucu, D., Guney, K., Sahinturk, D., Ozbudak, I. H., Ozel, D., Ozbilim, G. and Yavuzer, U. (2012) 'Tbx3 represses PTEN and is over-expressed in head and neck squamous cell carcinoma', *BMC Cancer,* 12, pp. 481.

Cross, S. S. (2001) 'Observer accuracy in estimating proportions in images: implications for the semiquantitative assessment of staining reactions and a proposal for a new system', *J Clin Pathol,* 54(5), pp. 385-90.

Lomnytska, M., Dubrovska, A., Hellman, U., Volodko, N. and Souchelnytskyi, S. (2006) 'Increased expression of cSHMT, Tbx3 and utrophin in plasma of ovarian and breast cancer patients', *Int J Cancer,* 118(2), pp. 412-21.

Matos, L. L., Trufelli, D. C., de Matos, M. G. and da Silva Pinhal, M. A. (2010) 'Immunohistochemistry as an important tool in biomarkers detection and clinical practice', *Biomark Insights,* 5, pp. 9-20.

Rubin, M. A., Dunn, R., Strawderman, M. and Pienta, K. J. (2002) 'Tissue microarray sampling strategy for prostate cancer biomarker analysis', *Am J Surg Pathol,* 26(3), pp. 312-9.

Seidal, T., Balaton, A. J. and Battifora, H. (2001) 'Interpretation and quantification of immunostains', *Am J Surg Pathol,* 25(9), pp. 1204-7.

Shan, Z. Z., Yan, X. B., Yan, L. L., Tian, Y., Meng, Q. C., Qiu, W. W., Zhang, Z. and Jin, Z. M. (2015) 'Overexpression of Tbx3 is correlated with Epithelial-Mesenchymal Transition phenotype and predicts poor prognosis of colorectal cancer', *Am J Cancer Res,* 5(1), pp. 344-53.

Umemura, S., Itoh, J., Itoh, H., Serizawa, A., Saito, Y., Suzuki, Y., Tokuda, Y., Tajima, T. and Osamura, R. Y. (2004) 'Immunohistochemical evaluation of hormone receptors in breast cancer: which scoring system is suitable for highly sensitive procedures?', *Appl Immunohistochem Mol Morphol,* 12(1), pp. 8-13.

Wang, H. C., Meng, Q. C., Shan, Z. Z., Yuan, Z. and Huang, X. Y. (2015) 'Overexpression of Tbx3 predicts poor prognosis of patients with resectable pancreatic carcinoma', *Asian Pac J Cancer Prev,* 16(4), pp. 1397-401.

Yaziji, H. and Barry, T. (2006) 'Diagnostic Immunohistochemistry: what can go wrong?', *Adv Anat Pathol,* 13(5), pp. 238-46.

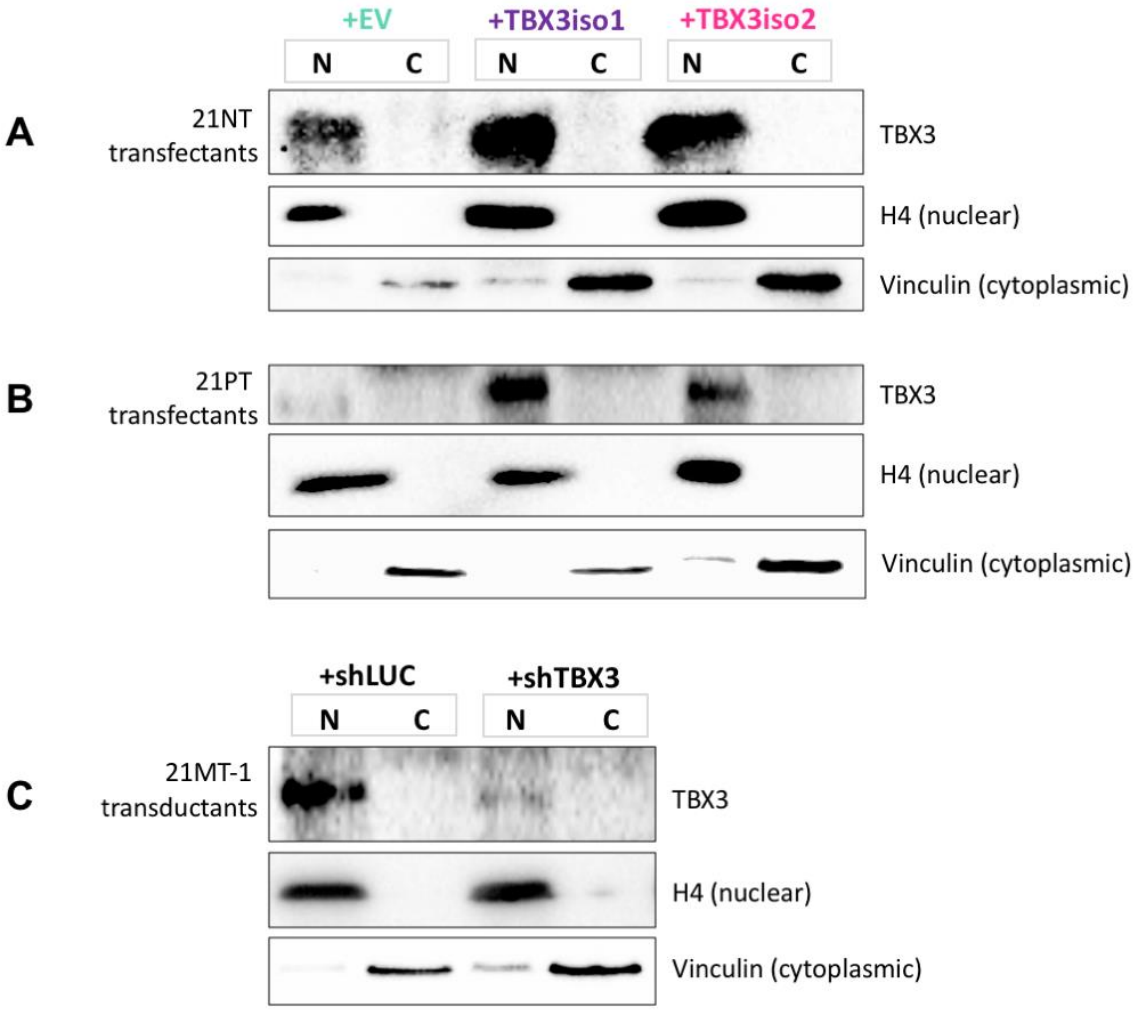

Appendix 6 – TBX3 expression in nuclear and cytoplasmic fractions of 21T cells.

Cellular fractionation and analysis of TBX3 expression in nuclear and cytoplasmic compartments of **(A)** 21PT, **(B)** 21NT, and **(C)** MT-1 cell lines. The 21PT and 21NT cell lines were stably transfected with either an empty vector (EV), TBX3iso1 or TBX3iso2 overexpressing plasmid. Total TBX3 expression was knocked down in 21MT-1 transductants; the shTBX3 clone with highest knockdown is shown. Nuclear fractions are shown by histone H4 expression, and cytoplasmic fractions are shown by vinculin.

Benign breast epithelium, TBX3 stain

Columnar Cell Lesions, TBX3 stain

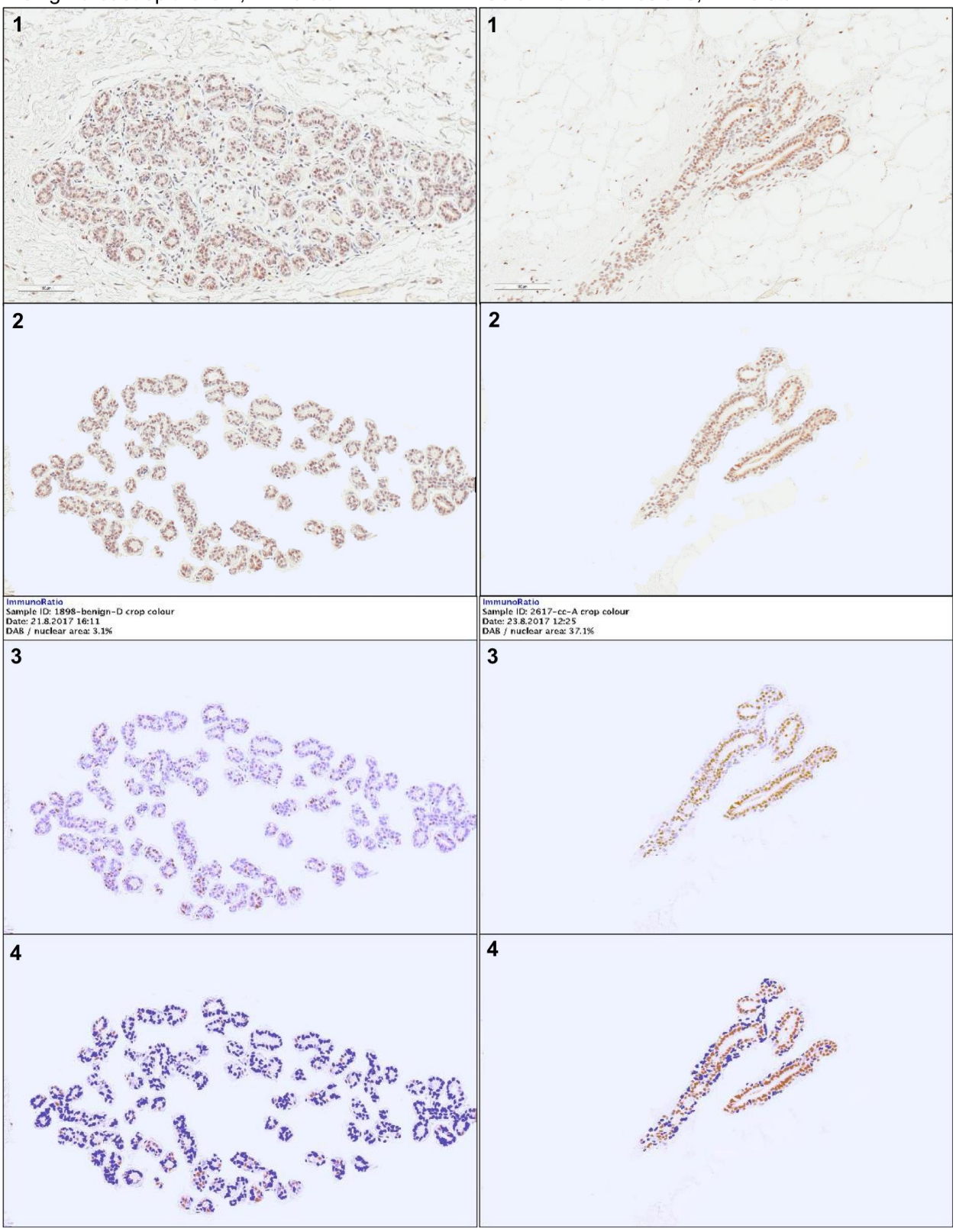

Appendix 7 – ImmunoRatio analysis of TBX3 expression in benign and columnar breast epithelium.

Scanned digital slides of TBX3, SLUG and TWIST1 immunohistochemically stained slides were quantified for nuclear expression of each marker using ImmunoRatio. TBX3 expression by IHC in benign and columnar breast epithelial cells, and the associated quantification process is shown. The process consisted of four major steps: **(1)** Images of tissue compartments were acquired, and included benign non-columnar cells, benign columnar cell lesions (CCLs; includes columnar cell change, columnar cell hyperplasia or flat epithelial atypia), DCIS and invasive cancer. **(2)** Stromal cells, necrotic areas, and cells outside of the compartment in question were cropped out using ImageJ in order to solely analyze expression of markers in the cell type of interest. **(3)** The faint background signal was removed using ImageJ in order to bring out blue hematoxylin stain of negative nuclei. **(4)** The ImmunoRatio plugin for ImageJ was used to quantify percentage of nuclei positive for each marker. A control slide representing serial sections was included for each run (with quantification and statistical analysis) to ensure identical and reproducible staining for each run.

DCIS, TBX3 stain

Invasive Mammary Carcinoma, TBX3

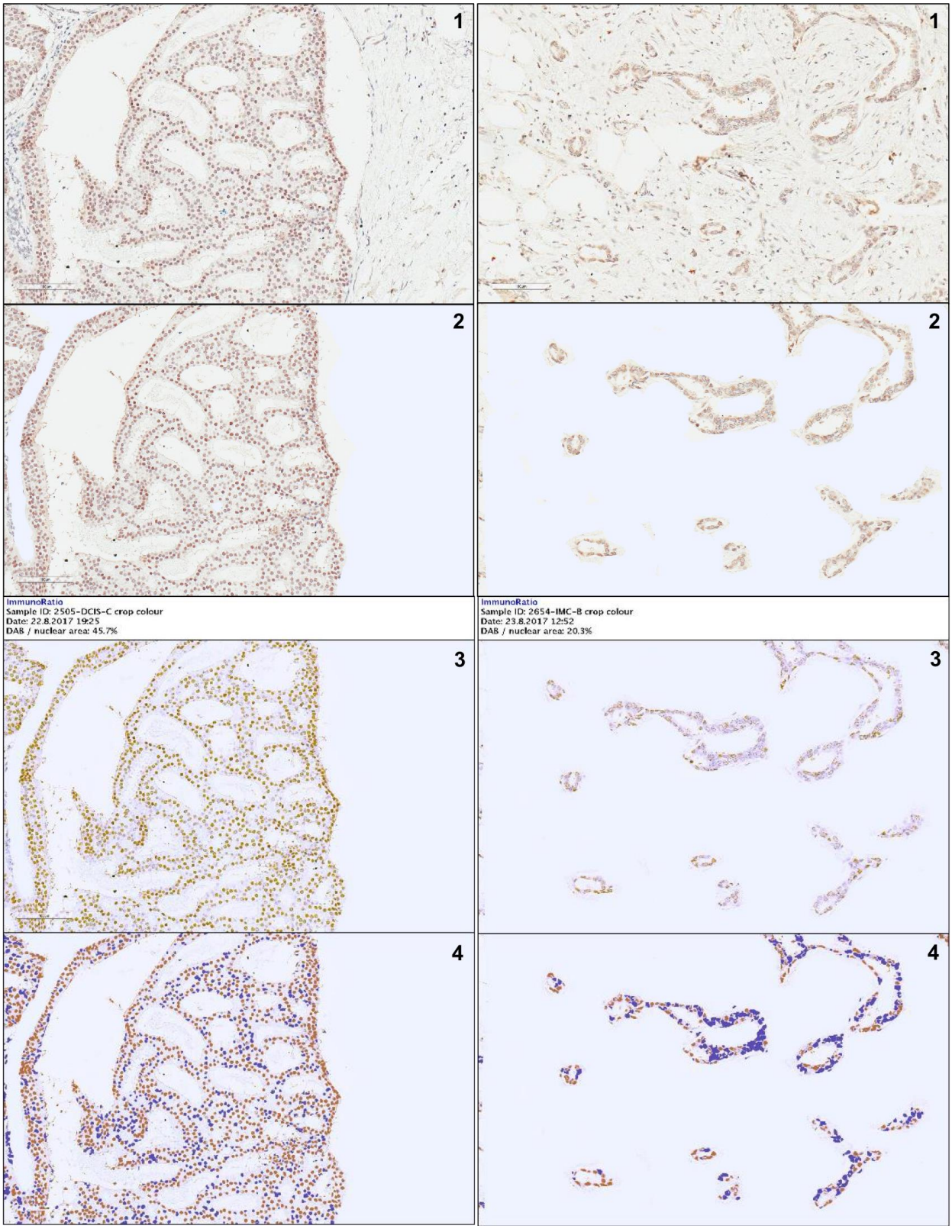

Appendix 8 – ImmunoRatio analysis of TBX3 expression in DCIS and IDC.

Scanned digital slides of TBX3, SLUG and TWIST1 immunohistochemically stained slides were quantified for nuclear expression of each marker using ImmunoRatio. TBX3 expression by IHC in DCIS and IDC, and the associated quantification process is shown. The process consisted of four major steps: **(1)** Images of tissue compartments were acquired, and included benign non-columnar cells, benign columnar cell lesions (CCLs; includes columnar cell change, columnar cell hyperplasia or flat epithelial atypia), DCIS and invasive cancer. **(2)** Stromal cells, necrotic areas, and cells outside of the compartment in question were cropped out using ImageJ in order to solely analyze expression of markers in the cell type of interest. **(3)** Faint background signal was removed using ImageJ in order to bring out blue hematoxylin stain of negative nuclei. **(4)** The ImmunoRatio plugin for ImageJ was used to quantify percentage of nuclei positive for each marker. A control slide representing serial sections was included for each run (with quantification and statistical analysis) to ensure identical and reproducible staining for each run.

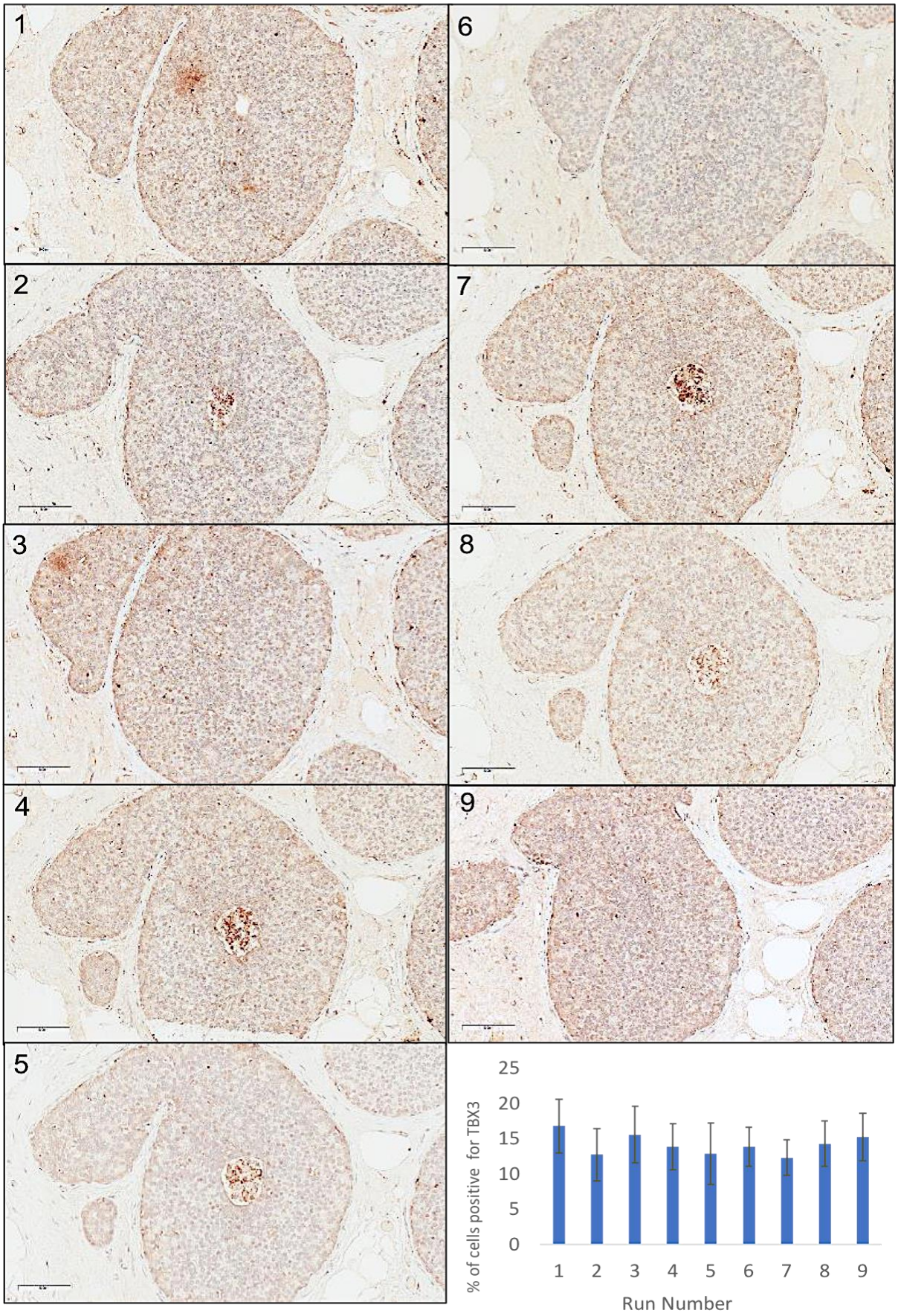
1
6
2
7
3
8
4
9
5
25
20
15
10
5
0
% of cells positive for TBX3
1
2
3
4
5
6
7
8
9
Run Number

Appendix 9 – Quality control of TBX3 staining by immunohistochemistry.

A control slide representing serial sections was included for each IHC run. Images were acquired of the same DCIS across serial section, and quantification was conducted as described in Materials and Methods (Chapter 3) and shown in Appendix 8. Expression of markers was graphed, and statistical analysis were conducted in order to ensure identical and reproducible staining for each run. If expression of markers was statistically different in the control slide, quantification was not conducted, and the batch of slides was re-stained until a similar staining pattern was observed.

6.3 Chapter 4 – Supplementary Data

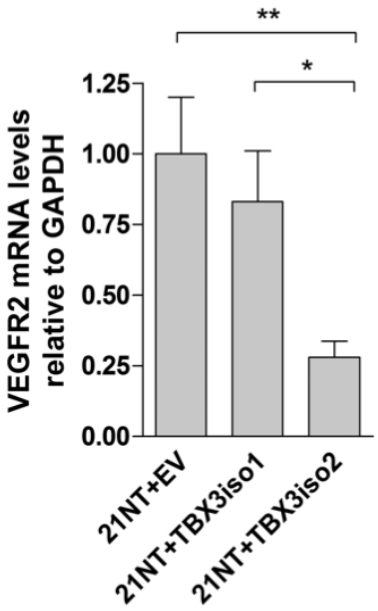

Appendix 10 – Expression of VEGFR2 by qRT-PCR.

The mRNA expression of VEGFR2 was assessed across 21NT transfectant cell lines by qRT-PCR, normalized to GAPDH expression levels, and depicted as fold change relative to the empty vector control.

**p<0.05, **p<0.01, ***p<0.001 by one way ANOVA with Tukey post-hoc for comparison between three groups. Error bars represent standard deviation.*

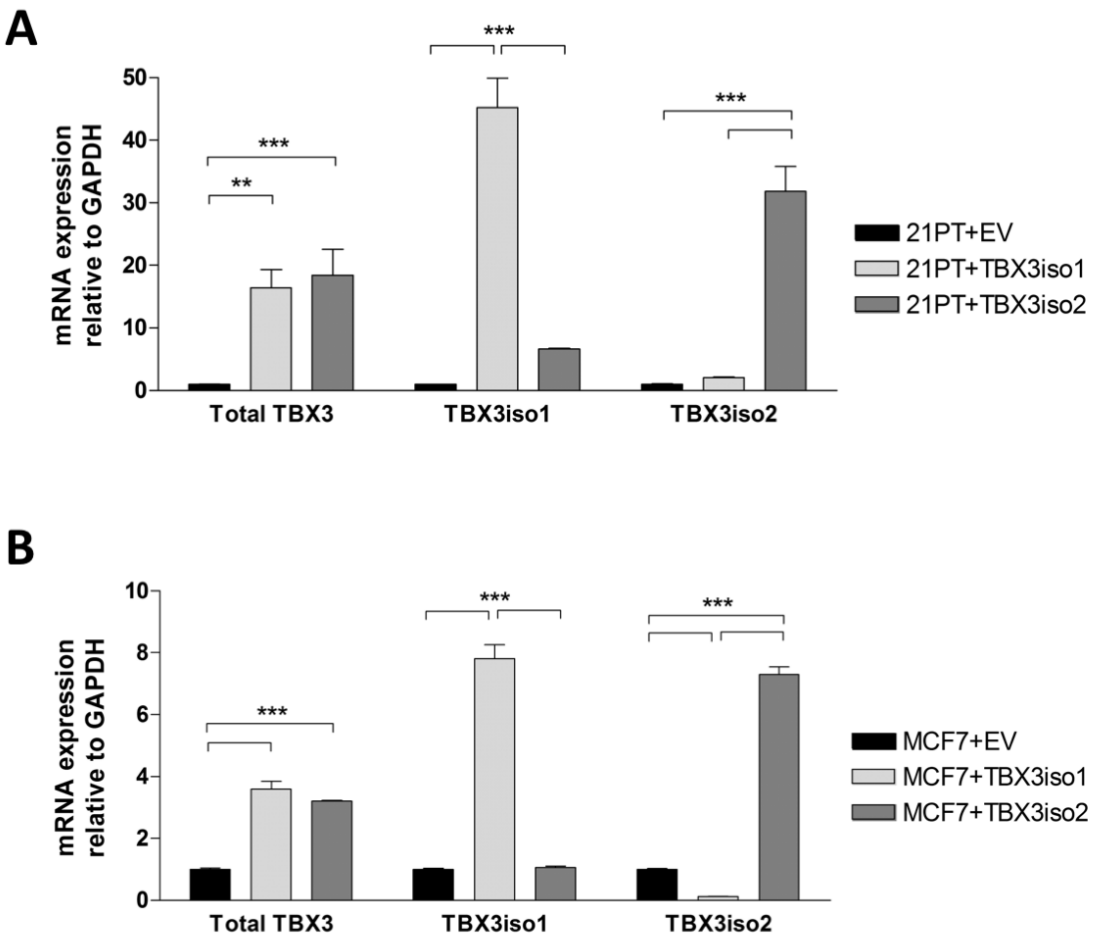

Appendix 11 – TBX3 expression in stable transfectant cell lines.

(A) Total TBX3, TBX3iso1 and TBX3iso2 expression was assessed by qRT-PCR in 21PT stable transfectant cell lines, normalized to GAPDH expression levels, and depicted as fold change relative to the empty vector control. **(B)** Total TBX3, TBX3iso1 and TBX3iso2 expression was assessed by qRT-PCR in MCF7 stable transfectant cell lines, normalized to GAPDH expression levels, and depicted as fold change relative to the empty vector control.

**p<0.05, **p<0.01, ***p<0.001 by one way ANOVA with Tukey post-hoc for comparison between three groups. Error bars represent standard deviation.*

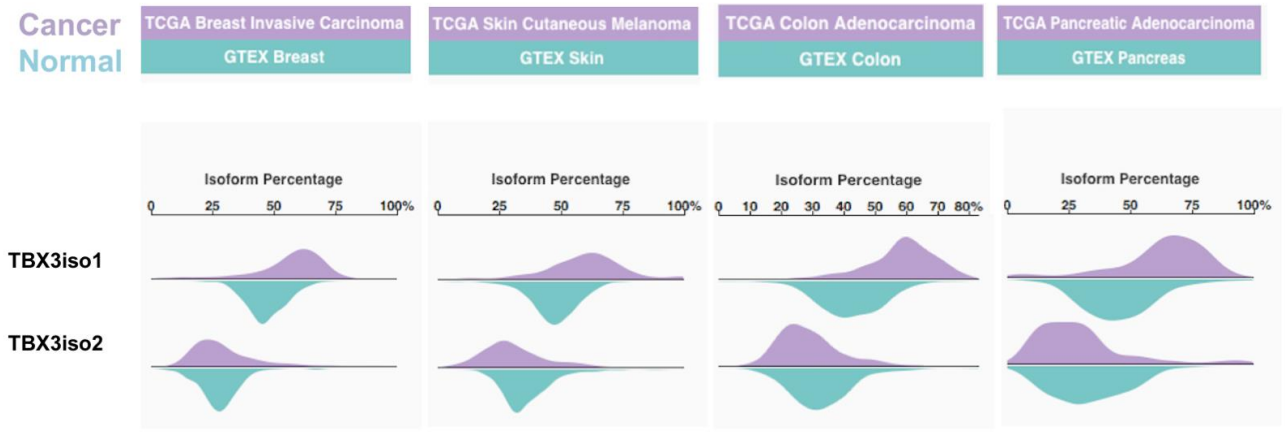

Appendix 12 – Assessment of TBX3 isoform expression in TCGA and GTEx datasets.

TBX3iso1 and TBX3iso2 expression levels were assessed across tumor types in which TBX3 overexpression has been documented (breast cancer, melanoma, colon, and pancreatic cancer). Isoform percentage is shown along the top axis, with TBX3 isoform expression shown in tumors (The Cancer Genome Atlas, TCGA; purple hills) and normal tissues (Genotype Tissue Expression Project, GTEx; blue hills). Data was assessed using XenaBrowser (www.xenabrowser.net).

Curriculum Vitae

Name: Milica Krstic

2013 – 2018 **Doctor of Philosophy**
Department of Pathology and Laboratory Medicine,
Schulich School of Medicine and Dentistry
Western University, London, ON

Project: The role of transcriptional regulator TBX3 in early breast cancer progression.

Supervisors: Dr. Alan Tuck, Dr. Ann Chambers

2009 – 2013 **Honours Bachelor of Science in Biology and Biotechnology**
University of Windsor, Windsor, ON

HONOURS AND AWARDS

- **Translational Breast Cancer (TBCRU) Studentship from the London Regional Cancer Program, funded in part by the Breast Cancer Society of Canada**
  Western University; Sept. 2013 – Dec. 2018 (applied for annually)

- **Ontario Graduate Scholarship (OGS)**
  External Funding at Western University; Sept. 2015 – Aug. 2016; May 2017 – April 2018

- **Cameron Wallace Graduate Student Award in Pathology**
  Western University; April 2018

- **European Molecular Biology Laboratory (EMBL) Advanced Training Fellowship**
  EMBL, Sept. 2017

- **Dutkevich Memorial Foundation Travel Award**
  Western University; Nov. 2017

- **Dr. Frederick Winnett Luney Graduate Research Award**
  Western University, April 2017

- **CIHR Strategic Training Program in Cancer Research and Technology Transfer (CIHR STP CaRTT)**
  Western University; Sept. 2014 – Aug. 2015

- **Presentation Awards:**

- Top Poster Presentation Award, **Oncology Research and Education Day** Western University; June 2018
- Best Basic Science Poster Presentation Award, **Pathology Research Day** Western University; April 2018
- CIHR Silver Award, **Canadian Student Health Research Forum (CSHRF)** University of Manitoba; June 2017
- Oral Presentation Award, **London Health Research Day** Western University; March 2017
- Oral Presentation Award, **Oncology Research & Education Day** Western University; June 2016
- M. Daria Haust Award for Best Basic Science Oral Presentation, **Pathology Research Day,** Western University – March 2015
- Best Basic Science Poster Presentation Award, **Pathology Research Day** Western University – March 2014

PUBLICATIONS

1. "The transcriptional regulator TBX3 promotes progression from non-invasive to invasive breast cancer", **Krstic M**, MacMillan CD, Leong HS, Clifford AG, Souter LH, Dales DW, Postenka CO, Chambers AF, Tuck AB. *BMC Cancer*. 2016;16(1):671. PMID: 27553211

2. "Genome-wide analysis reveals a role for TDG in estrogen receptor-mediated enhancer RNA transcription and 3-dimensional reorganization", Kolendowski B, Hassan H, **Krstic M**, Isovic M, Thillainadesan G, Chambers A, Tuck A, Torchia J. *Epigenetics and Chromatin*. 2018;11(5). PMID: 29378668

3. "TBX3 promotes progression of pre-invasive breast cancer cells by inducing EMT and directly up-regulating SLUG", **Krstic M**, Kolendowski B, Cecchini M, Postenka CO, Hassan HM, Andrews J, Leong HS, Torchia J, Chambers AF, Tuck AB. *(Manuscript in review)*

4. "Promotion of angiogenesis by TBX3iso1 through selective up-regulation of cancer-associated cytokines", **Krstic M**, Hassan H, Kolendowski B, Hague N, Anborgh P, Postenka CO, Torchia J, Chambers AF, Tuck AB. (*Manuscript in preparation)*

RELATED WORK EXPERIENCE

- ***Western Pathology Association (WPA) – Academic Vice President***
  Sept. 2014 – Sept. 2018
- ***Western University, Pathology 3240 (Understanding Disease) Teaching Assistant***
  Sept. 2014 – Dec. 2014, Sept. 2015 – Dec. 2015, Sept. 2016 – Dec. 2016
- ***University of Windsor, Research Assistant***
  Department of Chemistry and Biochemistry; May 2013 – Aug. 2013